The use of remote sensing and GIS for modelling aquaculture site suitability in relation to changing climate

A thesis submitted to the University of Stirling for the degree of Doctor of Philosophy

by

Neil Handisyde

Institute of Aquaculture

University of Stirling

December 2014.

Declaration

I declare that this thesis is an original piece of work conducted independently by myself and the work contained here has not been submitted for any other degree. All research material and sources of information have been duly acknowledged and cited.

Signature of Candidate

_____

Neil Handisyde

ABSTRACT

Globally fish production has continued to increase during recent years at a rate exceeding that of human population growth. However the contribution from capture fisheries has remained largely static since the late 1980s with the increase in production being accounted for by dramatic growth in the aquaculture sector. As of 2012 aquaculture accounted for approximately 42% of total fisheries production and 78% of inland fish production. In view of these figures it is unsurprising that for a number of regions aquaculture represents an important source of both food security and income.

The use of Geographical Information Systems (GIS) and spatial data have seen substantial developments in recent years with the help of increasingly affordable computing capacity. From an aquaculture perspective the use of GIS has shown significant potential as a means of combining varied data sources, including those acquired via remote sensing, into models to provide decision support in relation to site selection. A common theme amongst site suitability assessments is the incorporation of climate variables relating to temperature and water availability. These factors in turn can have a significant influence on aquaculture in terms of water availability and quality, and temperature modulated growth performance.

There is now a strong consensus that during the 20th century, and especially during recent decades, the earth has experienced a significant warming trend. There is also strong agreement that this warming trend is at least partially a consequence of anthropogenic greenhouse gas emissions and that some degree of further warming is inevitable. While global warming is typically discussed in terms of degrees centigrade of average global temperature increase the full effects in terms of climate changes will be varied both in terms of location and season.

The current project focuses on site suitability for aquaculture in relation to changing climate conditions. Significant use is made of GIS and a range of spatial data including remotely sensed data and output from a series of climate models. The project consists of a number of key components:

1. Vulnerability of aquaculture related livelihoods to climate change was assessed at the global scale based on the concept of vulnerability to climate related impacts as a function of sensitivity to climate change, exposure to climate change, and adaptive capacity. Use was

made of national level statistics along with gridded climate and population data. Climate change scenarios were supplied using the MAGICC/SCENGEN climate modelling tools. Analysis was conducted for aquaculture in freshwater, brackish, and marine environments with outputs represented as a series of raster images. A number of Asian countries (Vietnam, Bangladesh, Laos, and China) were indicated as most vulnerable to impacts on freshwater production. Vietnam, Thailand, Egypt and Ecuador stood out in terms of brackish water production. Norway and Chile were considered most vulnerable to impacts on Marine production while a number of Asian countries (China, Vietnam, and the Philippines) also ranked highly.

2. Site suitability for pond-based aquaculture was modelled at the global scale using a 10 arcsecond grid. Data from an ensemble of 13 climate models was used to model pond temperature and water availability for rain fed ponds under late 20th century conditions and for a 2°C global warming scenario. Two methods are demonstrated for combining data with a focus on the culture of warm water species. Results suggest both positive and negative impacts in relation to the 2°C warming scenario depending on location and season. Some areas are projected to see negative effects from maximum temperatures during the warmest parts of the year while for many regions there are likely to be potential increases in growth performance during colder months with possible expansion into previously unsuitable areas.
3. Methods for detecting surface water using remotely sensed data were investigated for Bangladesh. Use was made of data from the Moderate-resolution Imaging Spectroradiometer (MODIS) and Landsat ETM+ instruments with accuracy assessed against ground truth data collected in the field. A time series was constructed using all available MODIS data (approximately 13 years with an 8 day temporal resolution) to show areas of: surface water, land, and mixed land and water. The time series was then analysed to produce a layer showing the percentage of the total time series where surface water is indicated thus providing a spatial representation of flood prevalence.
4. A land cover data set was produced using 9 Landsat ETM+ scenes to cover the majority of Bangladesh. 10 different classification routines were evaluated including a decision tree approach unique to the current study. Classification results were assessed against two sets of ground control points produced: one based on field collected ground truth data and the other using a stratified random sampling procedure in association with visual analysis of high

resolution true colour satellite images and ETM+ composites. The most accurate classifications were provided by the decision tree method developed for the current study and a Multi-Layer Perceptron (MLP) neural network based classifier.

5. Site suitability for pond-based aquaculture within Bangladesh was assessed using a GIS in combination with the ETM+ based land cover data, the MODIS based surface water time series, and components of the global site suitability assessment including modelled pond temperature data. Assessments were made based on late 20th century conditions and a 2°C global warming scenario. The MODIS surface water time series was also used to show the effects of storm surge flooding in relation to cyclone Aila that struck Bangladesh on 25th May 2009. The south and east of the country were considered most suitable for aquaculture due to more favourable cold season temperatures and higher water balance values. The north west of the country was considered least favourable due to higher maximum modelled pond temperatures and lower water balance values. The effect of the 2°C warming scenario was to enhance these trends.

To date the potential spatial implications of changing climate for aquaculture has been significantly under researched. In this respect the current study provides a highly useful indication of where aquaculture related livelihoods may be vulnerable. In addition valuable and unique insights are provided into the distribution of areas of both potential increased, as well as decreased, suitability for existing aquaculture and further aquaculture development.

ACKNOWLEDGEMENTS

Firstly I would like to give very special thanks to my main supervisor Professor Lindsay Ross for his valuable support, help and advice over the years. I would also very much like to thank my second supervisor Dr Trevor Telfer for all his help.

I would like to thank Dr. Md. Abdus Salam and the students at Bangladesh Agricultural University, Mymensingh for their valuable inputs and help when visiting Bangladesh.

I would also like to thank Lynne Falconer for her valuable help and for generally being a good laugh. I also want to thank all the other friends and colleagues who have kept me entertained and offered support over the years. In no particular order: Ben Perry, Alfredo Tello, Lynn Munro, Richard Newton, Victor Peredo Alvarez aka coach P, Victro, Donna-Claire Hunter, Joly Ghanawi, Juan Navas, Fani Lamprianidou, Supat Khongpuang, and Vietnam's funniest man Long Pham. Anyone I've forgotten I'm sorry.

I must give very special thanks to my parents for their support and essentially making this possible. I also want to thank Marjorie Cates for her financial support.

Above all, I want to thank Margit for her constant love, support and understanding through what has been a long and often difficult process.

Contents

LIST OF FIGURES

LIST OF TABLES

1 INTRODUCTION

Globally, fish production has increased steadily over the last five decades at a rate exceeding that of human population growth so that as of 2012 mean world *per capita* fish consumption is estimated at 19.2kg compared with 9.9kg in the 1960s (FAO, 2014). This increase is generally seen as beneficial from a health perspective with fish consumption providing an important source of quality protein, fatty acids and micronutrients (Kawarazuka, 2010). In many poorer regions where fish represents a significant portion of consumed animal protein, and where diet in general may lack diversity, then fishes contribution to overall nutrition may be especially significant (Belton et al., 2014, Thilsted, 2013). While total global fish production has continued to increase, the proportion supplied by capture fisheries has remained largely static since the late 80s onwards with increased production accounted for by the dramatic growth in the aquaculture sector (FAO, 2014). Table 1-1 outlines global capture fisheries and aquaculture production from 2007 - 2012 and highlights the points made above. It is also important to note the significance of inland aquaculture both in terms of greater overall production than the marine sector, and also in terms of more rapid growth meaning that as of 2012 inland aquaculture production accounts for approximately 62.9% of total aquaculture production and 26.5% of total global fish production.

Table 1-1: Global capture fisheries and aquaculture production (FAO, 2014).

	2007	2008	2009	2010	2011	2012
			Million tonnes			
Capture fisheries production						
Inland	10.1	10.3	10.5	11.3	11.1	11.6
Marine	80.7	79.9	79.6	77.8	82.6	79.7
Total capture	90.8	90.1	90.1	89.1	93.7	91.3
Aquaculture production						
Inland	29.9	32.4	34.3	36.8	38.7	41.9
Marine	20	20.5	21.4	22.3	23.3	24.7
Total aquaculture	49.9	52.9	55.7	59	62	66.6
Total fish production	140.7	143.1	145.8	148.1	155.7	158
Utilisation						
Human consumption	117.3	120.9	123.7	128.2	131.2	136.2
Non-food uses	23.4	22.2	22.1	19.9	24.5	21.7
Population (billions)	6.7	6.8	6.8	6.9	7	7.1
Per capita food fish supply (kg)	17.6	17.9	18.1	18.5	18.7	19.2

Figure 1-1 shows aquaculture production quantities from fresh and brackish water aquaculture for the year 2012 while Figure 1-2 shows average annual growth rate of fresh and brackish water aquaculture for the years 2007-2012. Viewed together Figures 1-1 and 1-2 show that China followed by a number of other Asian countries currently dominate production but that inland aquaculture production is seeing significant growth in a number of African countries and throughout much of Latin America.

As well as being an important source of food, aquaculture makes significant economic contributions in many regions (see Figure 3-2 for an indication of aquaculture's contribution to national GDP) and represents a significant source of income and employment either directly or through the supply of associated goods and services (FAO, 2012).

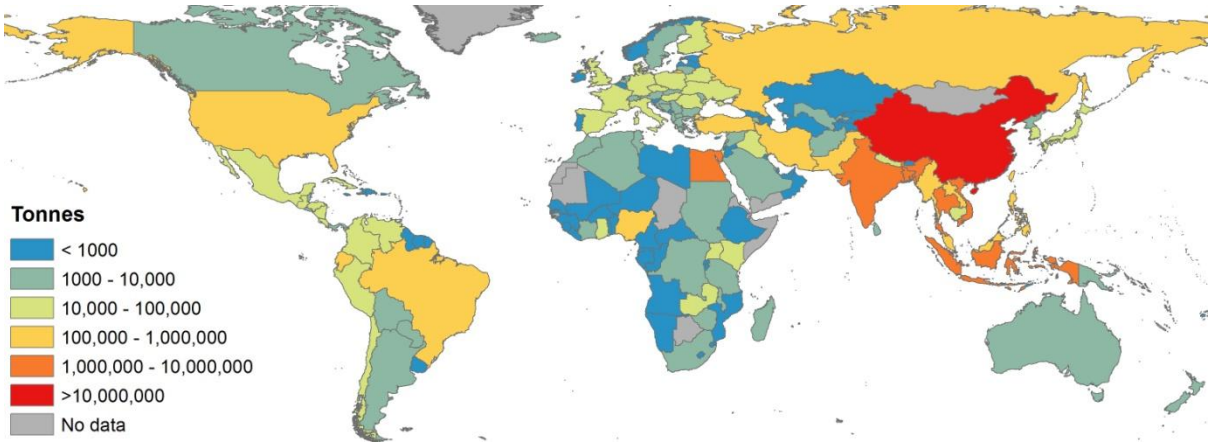

Figure 1-1: Aquaculture production (tonnes) from fresh and brackish water environments for the year 2012 (FishStatJ, 2014).

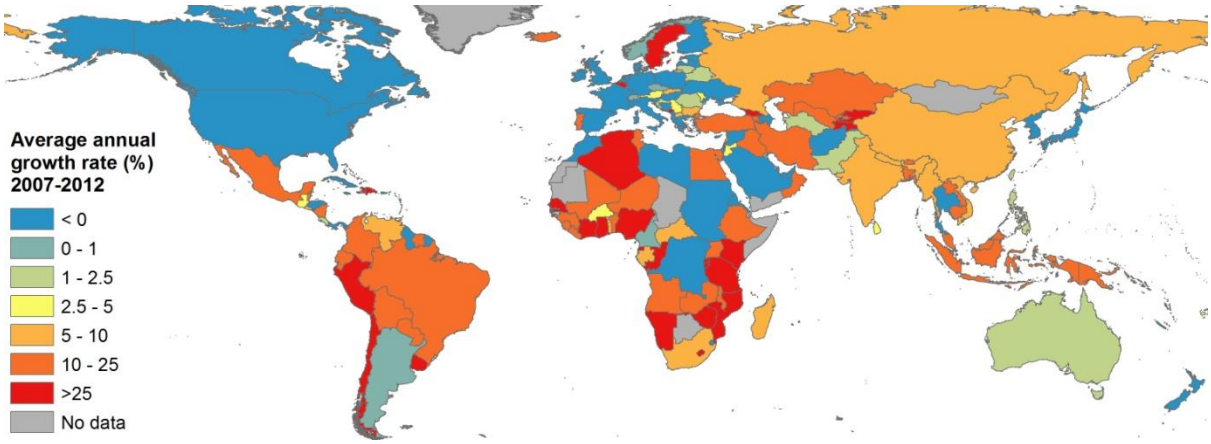

Figure 1-2: Average annual growth rate of aquaculture production quantities from fresh and brackish water environments for the years 2007 - 2012 (FishStatJ, 2014).

Inland aquaculture methods are diverse and include: ponds, tanks and raceways, sophisticated recalculating systems, and cages. Globally, pond culture represents the most significant source of production (Dugan et al., 2007) and can vary considerably in intensity from extensive systems with little in the way of additional inputs and low levels of stock, to highly stocked monocultures that make use of commercial formulated feeds and other management strategies such as mechanical aeration. While aquaculture systems and species are extremely varied, the location of successful aquaculture will depend of a broad range of geographic, environmental, socio-economic, demographic and climatic variables (Ross et al., 2009). For those concerned with aquaculture promotion and development this essentially represent a series of site selection questions with the aim of matching

appropriate methods and species to locations where they can achieve greatest success, often in areas where natural resources are facing increasing pressure in line with a growing human population (Ross et al., 2013).

The use of Geographical Information Systems (GIS) has seen rapid development in recent years, paralleled by increasingly affordable hardware, as a means to approach spatial management questions (Ross et al., 2009). At a very basic level representing individual variables spatially in the form of maps can be extremely useful in terms of visualisation of data. GIS is also commonly used to answer spatial question relating to individual variables with operations involving distance, area, and proximity being especially common. However the real power of GIS is in its ability to combine multiple and varied data sources into models with the aim of addressing complex spatial questions and thus providing a highly useful means of decision support (Nath et al., 2000, Ross et al., 2009).

GIS is dependent on input data represented spatially as a series of raster grids or vector files with associated databases. While the collection of data using traditional survey methods as well as the digitisation of existing paper maps provide potential inputs, recent decades have also seen significant increases in the quantity, quality, and availability of remotely sensed (RS) data (Campbell and Wynne, 2011). RS data have the potential to be processed and classified to represent ground cover which in turn can be especially useful in areas where traditional mapping may be limited. Another substantial benefit of remotely sensed data is that it can be obtained from multiple time points and is therefore very useful in examining environmental change (e.g. Dewan and Yamaguchi, 2009a, Rahman et al., 2013).

While the uptake of GIS, and especially remote sensing, to address spatial questions for aquaculture has to date been moderate, its use has been actively promoted and investigated over the last 15 to 20 years (Ross et al., 2009). Studies focussing on optimal site selection have ranged in scale from localised assessments (e.g. Giap et al., 2005, Ross et al., 2011, Salam et al., 2005), to those operating at the continental level (e.g. Aguilar-Manjarrez and Nath, 1998, Kapetsky, 1994, Kapetsky and Nath, 1997).

While the variables used in GIS-based site suitability work for aquaculture have been varied depending on requirements and data availability, the incorporation of climate-related variables is common. Although aquaculture systems are to varied extents managed and controlled, with the

possible exception of indoor recirculating systems they are dependent on local environmental and climate conditions to dictate temperature regimes and water availability, which in turn exert an extremely strong influence on productivity (Kapetsky, 2000).

There is now a very strong consensus that the earth has experienced a significant warming trend during the 20th century, especially the second half, continuing to the present time, with an average global temperature increase in the region of 0.72°C for the period 1951-2012 (IPCC, 2013). There is also strong agreement that this trend is at least partly a result of human driven increases in greenhouse gas concentrations (Cook et al., 2013, IPCC, 2013). It is likely that we are committed to at least some further warming as a function of the thermal inertia of the oceans and ice sheets (IPCC, 2013), and as the green house gas concentrations continue to increase steadily (Figure 1-3), some degree of additional warming seems inevitable. It is important to note that while warming is often discussed as a global average, change is not evenly distributed spatially. In general there is a tendency for greater than average warming over land areas (Figure 2-3) with considerable variability both regionally and seasonally (IPCC, 2013). While there is less agreement among the current generation of climate models over precipitation regimes compared with those for temperature, patterns of precipitation are also projected to change with some areas becoming dryer while others become wetter (IPCC, 2013).

Potential relationships between climate and aquaculture are summarised in Table 1-2 (and discussed in more detail in later sections). To date there has been a relatively small amount of work investigating climate interactions with aquaculture. Most work has taken the form of general overviews of potential issues (De Silva and Soto, 2009, Handisyde et al., 2006), or has focussed on specific areas, species and culture scenarios (e.g. Nguyen et al., 2014, Hanson and Peterson, 2014). When assessing potential effects of climate change on a given area there is often a tendency to focus on adverse impacts, and while such work is valuable it is important to remember that not all climate related impacts on aquaculture will be negative, and that while some areas may become less favourable for a given species and culture system other areas may stand to benefit through changes in temperature regimes and/or water availability. Rather than selecting specific systems and locations and then asking the question of how will these be affected, a GIS and spatial modelling approach essentially turns the question around and asks which areas are most and least suitable, and in a climate change context how this distribution will change.

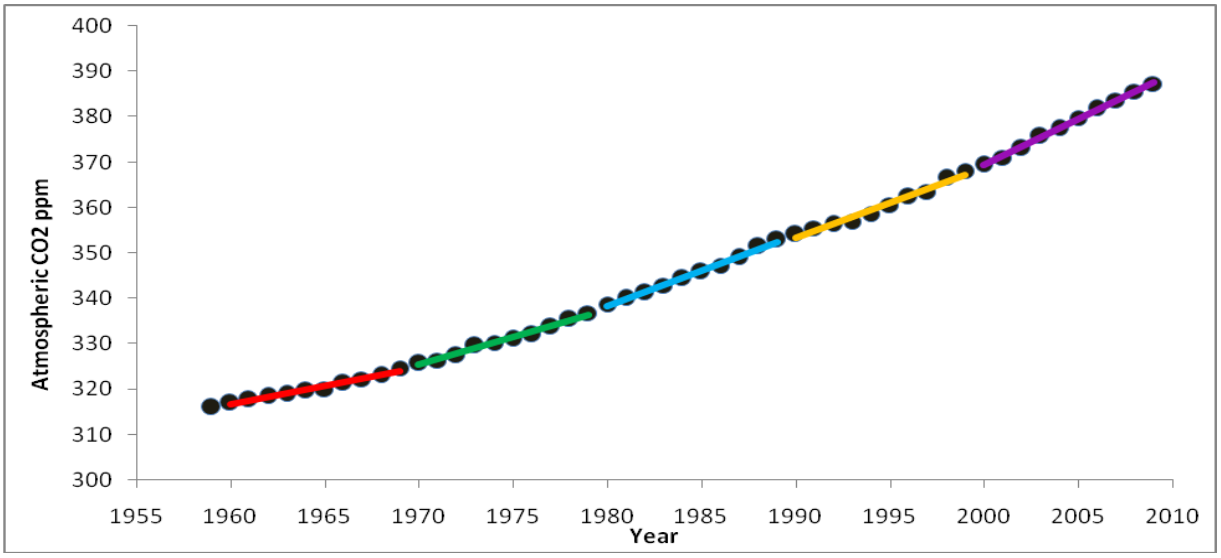

60s 0.81ppm per year

70s 1.23ppm per year

80s 1.58ppm per year

90s 1.56ppm per year

00s 2.04ppm per year

Figure 1-3: Annual mean atmospheric CO2 concentrations (Tans and Keeling, 2014).

Table 1-2: Potential Impacts of climate change on aquaculture systems and production. (Source: Handisyde et al., 2006).

Drivers of change	Impacts on culture systems	Operational impacts
Sea surface temperature changes	• Increase in harmful algal blooms that release toxins in the water and produce fish kills • Decreased dissolved oxygen • Increased incidents of disease and parasites • Enhanced growing seasons • Change in the location and/or size of the suitable range for a given species • Lower natural winter mortality • Enhanced growth rates and feed conversions (metabolic rate) • Enhanced primary productivity (photosynthetic activity) to benefit production of filter-feeders • Altered local ecosystems - competitors and predators • Competition, parasitism and predation from exotic and invasive species	• Changes in infrastructure and operation costs • Increased infestation of fouling organisms, pests, nuisance species and/or predators • Expanded geographic distribution and range of aquatic species for culture • Changes in production levels
	• Damage to coral reefs that may have helped protect shore from wave action – may combine with sea level rise to further increase exposure	• Increased chance of damage to infrastructure from waves or flooding of inland coastal areas due to storm surges
Change in other oceanographic variables (variations in wind velocity, currents and wave action)	• Decreased flushing rate that can affect food availability to shellfish • Alterations in water exchanges and waste dispersal • Change in abundance and/or range of capture fishery species used in the production of fishmeal and fish oil	• Accumulation of waste under pens • Increased operational costs
Seal level rise	• Loss of areas available for aquaculture • Loss of areas such as mangroves that may provide protection from waves/surges and act as nursery areas that supply aquaculture seed • Sea level rise combined with storm surges may create more severe flooding. • Salt intrusion into ground water	• Damage to infrastructure • Changes in aquaculture zoning • Competition for space with ecosystems providing costal defence services (i.e. mangroves) • Increased insurance costs • Reduced freshwater availability

Increase in frequency and/or intensity of storms	• Large waves • Storm surges • Flooding from intense precipitation • Structural damage • Salinity changes • Introduction of disease or predators during flood episodes	• Loss of stock • Damage to facilities • Higher capital costs, need to design cages moorings, jetties etc. that can withstand events • Negative effect on pond walls and defences • Increased insurance costs
Higher inland water temperatures (Possible causes: changes in air temperature, intensity of solar radiation and wind speed	• Reduced water quality especially in terms of dissolved oxygen • Increased incidents of disease and parasites • Enhanced primary productivity may benefit production • Change in the location and/or size of the suitable range for a given species • Increased metabolic rate leading to increased feeding rate, improved food conversion ratio and growth provided water quality and dissolved oxygen levels are adequate otherwise feeding and growth performance may be reduced	• Changes in level of production • Changes in operating costs • Increase in capital costs e.g. aeration, deeper ponds • Change of culture species
Floods due to changes in precipitation (intensity, frequency, seasonality, variability)	• Salinity changes • Introduction of disease or predators • Structural damage • Escape of stock	• Loss of stock • Damage to facilities • Higher capital costs involved in engineering flood resistance • Higher insurance costs
Drought (as an extreme event (shock), as opposed to a gradual reduction in water availability)	• Salinity changes • Reduced water quality • Limited water volume	• Loss of stock • Loss of opportunity – limited production (probably hard to insure against)
Water stress (as a gradual reduction in water availability (trend) due to increasing evaporation rates and decreasing rainfall)	• Decrease water quality leading to increased diseases • Reduce pond levels • Altered and reduced freshwater supplies – greater risk of impact by drought if operating close to the limit in terms of water supply	• Costs of maintaining pond levels artificially • Conflict with other water user • Loss of stock • Reduced production capacity • Increased per unit production costs • Change of culture species

The current work focuses on site suitability modelling determined using GIS models while making significant use of remotely sensed data. Data from historic climate data sets are incorporated along with projections from a series of climate models to allow for the investigation of the potential impacts of climate change on spatial suitability factors for aquaculture. Specific research objectives are as follows:

1. To develop a global scale model of vulnerability to address the question; assuming that climate related change results in negative impacts for aquaculture then where would the greatest impacts on aquaculture related livelihoods occur? Use is made of national level statistics in combination with data representing current climate and projections from an ensemble of climate models via the MAGICC/SCENGEN application to assess vulnerability of aquaculture to changes in climate at the national scale.
2. To Develop a model of site suitability for pond-based aquaculture of warm water species at the global scale using high resolution gridded data, and investigate how patterns of suitability may change under future climate conditions? A GIS is used in association with a series of gridded data sets with a maximum resolution of 10 arcseconds (approximately 300m at the equator). Data representing current climate as well as that from a series of climate models is used to model pond temperature and water availability for rain fed ponds under late 20th century conditions and for a 2°C average global warming scenario.
3. To investigate the use of remotely sensed Moderate Resolution Imaging Spectroradiometer (MODIS) data as a means of observing surface water distribution in Bangladesh and select a method to be used to construct a time series to explore seasonal flood patterns and durations. Use was made of data from both the Moderate-resolution Imaging Spectroradiometer (MODIS) and Landsat ETM+ instruments to access classification routines with accuracy assessed against ground truth data collected in the field. A time series was then constructed using the MODIS data with land cover classified as either: water, mixed or land. The time series was analysed to show proportion or total time series where surface water was present thus giving an indication of flood patterns and duration throughout Bangladesh.
4. To develop a land cover data set for Bangladesh based on Landsat ETM+ data. Nine ETM+ plus scenes were used to cover the majority of the country. Acquisition dates for the data corresponded closely to that of field visits and ground truth data collection. Ten classification

methods were evaluated including one developed for the current study. Accuracy was assessed against two sets of ground control points: one based on ground truth data collected in the field while the other made use of a stratified random sampling procedure in association with visual analysis of high resolution true colour satellite images and ETM+ composites.

5. To use Bangladesh as a case study that incorporates the MODIS surface water time series along with the ETM+ based land cover data (see 3 and 4 above) and other data sources including modelled pond temperature, to develop a model of site suitability for pond-based aquaculture in under current and future climate conditions to gain an understanding of how patterns of suitability in the country may change.
6. To use the data from the MODIS based surface water time series to illustrate the effects of storm surge flooding on coastal Bangladesh with specific attention paid to the impact of cyclone Aila.

2 VULNERABILITY OF AQUACULTURE TO CHANGING CLIMATE AT THE GLOBAL SCALE

2.1 Introduction

Globally the aquaculture sector has shown significant growth over recent decades and continues to expand. This contrasts with capture fishery production that when viewed as a global average has remained fairly static during recent years (Bostock et al., 2010, FAO, 2012). In 2011 global aquaculture production was approximately 63.6 million tonnes while total fisheries production from both aquaculture and capture sources equalled approximately 154 million tonnes of which 130.8 million tonnes was used for human consumption. This compares to a figure of 137.3 million tonnes for the year 2006. It is worth noting that virtually all the increase seen during the 2006 to 2011 time period came as a result of increased aquaculture production (FAO, 2012).

Aquaculture provides a source of income and employment for an increasingly large number of people with estimates of around 16.5 million people involved in aquaculture worldwide, with approximately 16 million of these in Asia (FAO, 2012). As well as those directly involved in aquaculture production there will be many more individuals whose livelihoods are at least partially connected to the aquaculture sector via the supply of goods and services such as: transportation, ice making, feed production and marketing. It is estimated that more than 100 million people depend on aquaculture for a living, either as employees in the production and support sectors or as their dependants (FAO, 2012).

Fish products represent a high quality source of protein and in some areas make important contributions in terms of food security. In countries such as China, Vietnam, India, Indonesia and Bangladesh aquaculture of low trophic level species are significant in that they reduce dependence on high protein feeds (FAO, 2012). In many areas fish represent a “cash crop” that is sold as a means to afford cheaper food items (Sugiyama et al., 2004).

Since 1850 when accurate record keeping began there has been a notable increase in average global temperature of $0.76^{o}C \pm 0.19\ ^{\circ}C$ (Houghton, 2009). Use of proxy temperature records suggests that the spatial extent and duration of warming during the middle to end of the twentieth century in the northern hemisphere makes it the most significant climate anomaly of the last 1200 years (Osborn

and Briffa, 2006). There is now a general consensus that this warming trend is at least partially a result of human activity in the form of increased green house gas emissions and thus atmospheric concentrations (Cook et al., 2013, IPCC, 2007b) and at the current time green house gas levels are continuing to rise with an average annual increase in atmospheric carbon dioxide of 2.03ppm over the last 10 years (Thoning et al., 2013). While international debate about how to tackle this trend continues, at the current time considerable uncertainty remains about future greenhouse gas concentrations and ultimately their effect on global warming (IPCC, 2007b). It is also worth noting that even if greenhouse gas levels stopped increasing now it is likely that global temperature will continue to rise for some time as a result of the high heat capacity and thus thermal inertia of the oceans (Wigley et al., 2009).

Associated with increasing average global temperatures are changes in climate. There is considerable spatial variability associated with climate change meaning that average temperatures will increase more in some areas than others and some areas will become wetter while others will become increasingly dry (IPCC, 2007b). Changes in climate will effect short-term weather patterns and while there are uncertainties about the relationship between changing climate and extreme events such as droughts, floods and cyclones, it is probable that they will become increasingly significant in some areas due to increases in intensity and /or frequency (IPCC, 2007b).

Changes in climate can affect aquaculture directly though impacts on the production process or indirectly via impacts on price and availability of aquaculture inputs and / or products being produced. For example, impacts on capture fisheries could affect the availability of feed ingredients such as fishmeal and fish oil or the availability of wild-caught fish that compete directly with aquaculture products in the marketplace.

Climate related drivers of change for aquaculture systems can largely be considered as: changes in temperature of inland water or sea surface waters, changes in oceanographic variables such as currents and waves, changing sea levels, changes in solar radiation, changes in the availability of fresh water, and changes in the frequency and / or intensity of extreme events (Handisyde et al., 2006). Another potentially significant driver that is related directly to increasing atmospheric carbon dioxide levels rather than changing climate is ocean acidification (Doney et al., 2009). These changes can have physiological impacts via changes in growth, development, reproduction and disease, ecological impacts through changes to organic and inorganic cycles, predation, ecosystem services, and

operation impacts such as species selection, site selection, sea cage technology etc. (Handisyde et al., 2006).

The ability to predict future changes in climate is improving in association with a better understanding of the climate system along with increases in computing power, and an increasing number of more sophisticated climate models, resulting in a larger number of simulations and experiments being conducted. This said, considerable uncertainty remains in relation to the modelling process itself, the climate system and potential feedback mechanisms, and future human development and associated greenhouse gas emissions and concentrations (IPCC, 2007b).

In an effort to address this uncertainty a number of potential scenarios are frequently considered. In recent years this has often meant the range of scenarios developed for the Intergovernmental Panel on Climate Change (IPCC) Special Report on Emission Scenarios (SRES) which form the basis of much climate modelling work and consider a range of differing assumptions relating to human activity such as economic and population growth, energy production and technological change (Nakicenovic and Swart, 2000). Best estimates of average global temperature increase between the periods 1980-1999 and 2090-2099 range from 1.8°C under the conservative B1 scenario to 4°C under the A1F1 scenario. There has been some criticism of SRES scenarios. For example Schiermeier (2006) suggests that many economists view the scenarios as flawed and based on outdated economic theory with doubts about assumptions regarding the speed at which the economies of developing countries will develop and converge with nations that are currently more developed. There was also concern over how projected economic development is linked with technological development and energy use.

Climate models vary considerably in terms of sensitivity, and hence degree of warming, to increasing greenhouse gas concentrations. The 23 Atmosphere-Ocean General Circulation Models AOGCMs used in the 3rd phase of the Coupled Model Intercomparison Project (CMIP3) (Meehl et al., 2007) that formed the basis of projections for the 4th IPCC assessment report (IPCC, 2007b) had a range of equilibrium climate sensitivities where a doubling of atmospheric CO_2 resulted in projected average global temperature increases ranging from 2.1°C to 4.4°C with a mean value of 3.2°C (IPCC, 2007b). It has been suggested that a large part of this variation can be attributed to uncertainties about feedbacks within the climate system such as cloud density (Dufresne and Bony, 2008, Webb et al., 2006, Williams and Webb, 2009).

Given the range of potential emission scenarios and the variability in response between climate models to any given scenario the message for those concerned with impact assessment and / or adaptation strategy development would seem to be that considerable uncertainty remains and at very least a wide range of future scenarios would need to be considered if the aim is to try and quantify impacts.

Assessments of vulnerability range in scale from single points or small areas, typically at a high spatial resolution, to global assessments where resolution may be at the scale of countries or features such as drainage basins. Vulnerability analyses also range in scope and specificity both in terms of drivers of vulnerability and what is potentially being impacted. Given the uncertainties about future development and data limitations, broad-scale more generalised assessments of vulnerability often aim to rank areas (show relative differences between them in terms of vulnerability) rather than trying to quantify results. As well as providing useful tools for decision makers in their own right, broad assessments of vulnerability may also provide useful starting points for guiding further and more detailed research in specific areas.

The Human Development Index (HDI) (Malik, 2013) provides an example of a simple composite of indicators used to rank countries in terms of general human wellbeing. The Predictive Indicator of Vulnerability (PIV) (Adger et al., 2004) can be viewed as more focused and provides another example of a global indicator that operates at the resolution of whole countries with the aim of addressing social vulnerability to climate change. The PIV uses a larger number of variables than the HDI (46 compared with 4) and thus is conceptually more complex. Adger et al. (2004) suggest that aggregating large numbers of variables into a single index should be done with caution and that disaggregated indicators can give more information on the structure of vulnerability. Doubleday et al. (2013) provides an example of a regional vulnerability assessment that is focused specifically on the aquaculture industry and used a two stage assessment process to rank 7 aquaculture species in terms of climate change related risk for south-eastern Australia. The process involved the use of experts to first compile species profiles and then assign scores to 9 different attributes of vulnerability whilst following a specified framework. More complex ecosystem and / or production models are often highly specific in focus and aim to quantify change and thus potential impacts and vulnerability. Ferreira et al. (2008) made use of ShellSim (Hawkins et al., 2002) to model blue mussel (*Mytilus edulis*) and Pacific oyster (*Crassostrea gigas*) production in Strangford Lough, Northern Ireland.

Results suggested a significant decrease in mussel production of 50% in response to a1°C temperature increase and a 70% decrease for a 4°C increase. Oysters were predicted to be less severely affected with modelled decreases of less than 8% under both temperature scenarios.

To date there have been few attempts to compare vulnerability among regions at the global scale in relation to the fisheries sector. Handisyde et al. (2006) used a GIS to conduct an assessment for aquaculture dependant livelihoods whilst also incorporating climate data at the sub-national level. Allison et al. (2005) and Allison et al. (2009) used a range of indicators to rank nations in terms of vulnerability of capture fisheries dependant livelihoods to climate change. The current study aims to produce a more focused evaluation of relative vulnerability of aquaculture-related livelihoods between regions at the global scale by incorporating data at varying resolutions within a GIS.

2.1.1 Materials and methods

Vulnerability (V) of aquaculture and associated livelihoods in relation to climate change are considered in the current study as a function of exposure to climate change (E), sensitivity to climate change (S) and adaptive capacity (AC), based on the following equation:

$V = f(E, S, AC)$ [equation1]

This working method of assessing vulnerability in relation to climate change was implemented in the Intergovernmental Panel on Climate Change third assessment report (McCarty et al., 2001) with similar approaches being applied in a range of vulnerability studies (e.g. Allison et al., 2005, Metzger et al., 2005, o'Brien et al., 2004, Schröter et al., 2005).

Rather than representing data using only a simple numerical index the current study makes use of a geographic information system (GIS) to represent and combine data spatially using a series of raster grids. Along with easily allowing for visual interpretation of results and intermediate stages of the modelling process, the use of gridded data within a GIS also allows for the combination of data that is available at varied resolutions while maintaining as much detail as possible.

2.1.2 Study extent and data selection

The study area was global in extent with spatial data represented on a latitude-longitude grid at 10 arcminute resolution (one arcminute equals approximately 1.86km at the equator). A priority when selecting data were that it is available and consistent across as many countries as possible. In practical terms this limited selection to those data sets that are already available with global coverage. Such data is often available at limited spatial resolution which in many cases means at the national level. A second priority for data selection and the modelling process was that it should be as focused as possible with a moderate number of relevant indicators. Global indexes of vulnerability have received criticism for lacking such focus (Füssel, 2010, Gall, 2007) and while use of a very large number of broad ranging indicators may seem attractive in terms of inclusivity and give the impression of a more 'sophisticated' modelling process, it is worth considering that as the number and scope of indicators is increased their individual power and focus is typically reduced.

While the data used to indicate sensitivity and adaptive capacity were available at the national level the data used to represent climate variables (exposure) were available in grid format at a range of resolutions between 2.5 degrees and 10 arcminutes. This raises the issue of how to combine data at differing resolutions. One approach is to work at the lowest resolution where higher resolution data is averaged over the lower resolution spatial units before combination within a model. This approach doesn't rely on assumptions of even distribution within spatial units and is easily defensible in terms of methodology. The main drawback of working at the lowest resolution is that valuable information contained within the higher resolution data may be lost. A hypothetical example of this would be a large country where a decrease in precipitation is predicted over half the country while an increase is predicted over the other half. While these changes may be significant in terms of factors such as water availability, floods and droughts, if they are considered as an average over the entire country they may largely cancel each other out resulting in very little or no change being indicated. The process of averaging climate variables within a country could be refined by using gridded moderately high resolution data for topographic variables such as land cover, elevation and slope to indicate regions within a county where aquaculture has the potential to take place and then average climate changes over only these areas. While this may make the analysis more appropriate for aquaculture the problems of averaging over potentially climatically diverse areas within larger countries remain. Another option would be to assign a climate exposure risk score to the country as a whole based on a consensus of expert opinion and what is known about likely climate issues and aquaculture within the

region. Notable problems with this approach include differences in the amount of information and knowledge available between countries, which is likely to be particularly low in some cases, along with a general high level of subjectivity. The approach taken in the current study is to represent all data, including that only available at the national level, on raster grids at a common resolution of 10 arcminutes which can then be combined within the model using a series of weighted combinations. The practice of converting low resolution polygon data to a higher resolution grid for modelling purposes is in agreement with other global modelling work (e.g. Handisyde et al., 2006, Vörösmarty et al., 2010) and the view is taken here that for the reasons outlined above the benefits of this approach outweigh those of working at the lowest resolution or with more complex combined systems.

Apart from projected changes for temperature, data representing current conditions was used meaning that current aquaculture-related vulnerabilities were assessed in relation to potential future climate changes. For more specific and localised assessments of vulnerability with access to a greater range of high quality data it may be possible to produce future projections for a wider range of indicators. In the case of the current study, and notably in relation to aquaculture trends and to a large extent adaptive capacity, the view was taken that attempting to extrapolate future scenarios over a time period relevant to climate change is likely to introduce considerable inaccuracies into the modelling process and that the use of current indicators in association with future climate scenarios provides the best proxy when comparing vulnerability at a broad scale (Adger and Kelly, 1999, Vincent, 2004).

2.1.3 Details of data used

Details of all data sets used in the current study are provided in Table 2-1.

Table 2-1: Data used in the current study.

Variable (units)	Data format (original resolution)	Source (reference)
Aquaculture production quantities (tonnes)	National level production statistics	FAO FishstatJ (FishStatJ, 2013)
Aquaculture production value (USD)	National level production statistics	FAO FishstatJ (FishStatJ, 2013)
Population density (persons per km^2)	Grid (30 arcseconds)	LandScan 2008 data (Landscan, 2008)
Actual evapotranspiration (mm per year)	Grid (30 arcminutes)	(Fisher et al., 2008)
Precipitation (mm per year)	Grid (10 arcminutes)	CRU CL2 (New et al., 2002)
Projected change in local temperatures under global warming(^oC)	Grid (2.5 degrees)	MAGICC/SCENGEN version 5.3 (Wigley, 2008)
Projected change in local precipitation under global warming (percent)	Grid (2.5 degrees)	MAGICC/SCENGEN version 5.3 (Wigley, 2008)
Flood frequency based on historic data	Vector Polygon	Aqueduct Global Maps 2.0 (Gassert et al., 2013)
Drought frequency based on historic data	Vector Polygon	Aqueduct Global Maps 2.0 (Gassert et al., 2013)
Cyclone frequency based on historic data	Vector line	International Best Track Archive for Climate Stewardship (IBTrACS) (Knapp et al., 2010)
Human development index (HDI)	Online database (national)	HDI 2012 (Malik, 2013)
Country borders polygons	Vector Polygon	TM_WORLD_BORDERS-0.3 (thematicmapping.org, 2013)
Marine Exclusive Economic Zones (EEZ) polygons	Vector Polygon	World EEZ v7 (Marine_Regions, 2013)

National population estimates (total population)	Data table	United Nations Population Division (UN_Population, 2013)
National GDP estimates (USD)	Data table	World Bank GDP data (World_Bank, 2013)

2.1.4 Overview of model structure

The model followed a hierarchical structure where a range of indicators were combined to represent the sensitivity, exposure and adaptive capacity components (described elsewhere in this document as sub-models) which were then combined to indicate vulnerability. A schematic overview of the model structure and potential inputs is provided in Figure 2-1. It should be noted that not all inputs are necessarily used at any one time with the choice of inputs and weightings (level of influence within the model) varying depending on what is being evaluated e.g. fresh, brackish or marine aquaculture environments. Full details of layer combinations and weightings are provided in Tables 2-3 (freshwater aquaculture), 2-4 (brackish water aquaculture), 2-5 (fresh and brackish water aquaculture combined), and 2-6 (marine aquaculture).

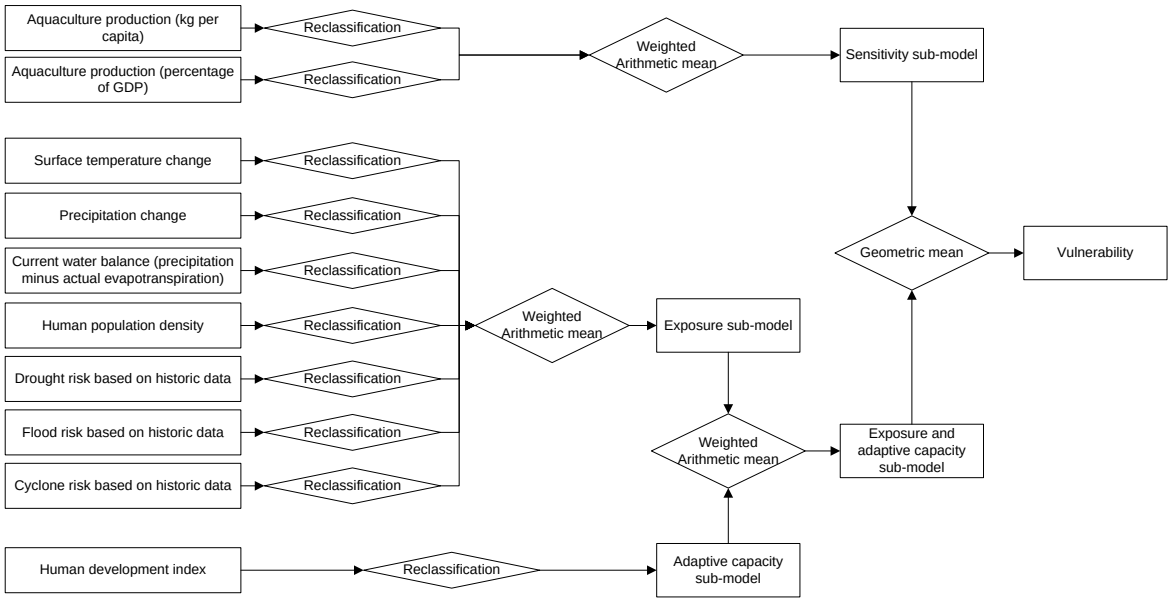

Figure 2-1: Schematic representation of model used in current study.

2.1.5 Data standardisation

In order for different indicators to be combined they need to be transformed to a common scoring system. For the current study the majority of the input data sets were in the form of a continuous numeric series, for example increase in temperature in degrees centigrade. All data were standardised on a continuous scale from 0-1 with higher numbers representing greater vulnerability, lower adaptive capacity, greater exposure, or greater sensitivity. In terms of the modelling process and interpretation of results this effectively represents a continuous series as opposed to a number of distinct classes. Details of how data were standardised for all variables used are given in Table 2-2.

Table 2-2: Details of data standardisation to a common 0 – 1 scoring system.

Variable	Standardisation details
Aquaculture production quantity (kg per capita)	Aquaculture production data were standardised to values ranging from 0 to 1 using a linear relationship where 0 represents areas with no aquaculture production and 1 equates to the area with highest production. The one exception was for mariculture where the Faroe islands which are the largest per capita producers of mariculture products were excluded as complete data needed for other areas of the model were not available.
Aquaculture production value (percentage of GDP)	As above
Human Development Index (HDI)	All values were standardised over the range 0 to 1 using an inverse relationship so that the country with the lowest HDI value receives a new value of 1 and the one with the highest HDI value receives a new value of 0.
Population density	Population density data were standardised using a linear relationship so that areas averaging more than 1000 people per square km were given a value of 1 and areas indicated as have no population were given a value of 0.
Projected temperature change	Temperature change data were standardised to values ranging from 0 to 1 based on a linear relationship between 3 standard deviations below and above the mean increase. For the fresh and brackish water models the mean value was derived from all land areas between 60^{o}S and 60^{o}N. For the marine model the average increase was obtained using a 20km buffer around all land areas between 60^{o}S and 60^{o}N. The 60^{o} north and south cut off was applied to exclude high latitude areas that are projected to warm significantly more than other areas but are generally insignificant in aquaculture terms.
Projected precipitation change	Projected precipitation change data were standardised to values ranging from 0 to 1 based on a linear relationship between 3 standard deviations above and below the mean value that was calculated over all land areas used in the study. This results in areas with the greatest projected decrease in precipitation being given the highest score and thus making the greatest contribution to vulnerability.
Cyclone risk	International Best Track Archive for Climate Stewardship (IBTrACS) data describing the number of cyclones that have occurred in a given area over the last 40 years were standardised to values ranging from 0 to 1 using a linear

	relationship with a value of 0 being assigned to areas with no recorded cyclones and 1 being assigned to the area with the highest number of recorded cyclones.
Flood risk	The Aqueduct Global Maps 2.0 flood occurrence data were already scaled from 0 to 5 with 5 representing areas with highest occurrence of flood events. The data were rescaled using a linear relationship over the range 0 to 1.
Drought risk	As above.
Water balance	Water balance was calculated as precipitation minus actual evaporation. Water balance values were standardised using a linear relationship so that areas with a water balance of 0mm per year receive a score of 1 while areas with 1000mm or more per year received a value of 0.

2.1.6 Sub-model construction

2.1.6.1 Sensitivity

Sensitivity in the current model is represented at the country scale. The aim is to indicate the significance of aquaculture to people within a country and thus how sensitive their livelihoods may be to impacts on the aquaculture sector. Aquaculture production is considered on a per capita basis and thus total population size of countries does not influence the analysis.

Two metrics are included in the sensitivity sub-model: aquaculture production quantity (kilograms per capita excluding aquatic plants) and aquaculture production as a percentage of GDP (again excluding aquatic plants). Quantity of aquaculture products *per capita* aims to represent the physical size of the aquaculture sector within a country. While the type, scale, and intensity of aquaculture operations will be significant it is assumed that, in general, nations with a high per capita production of aquaculture products are likely to have a greater percentage of their population whose livelihoods' are either directly linked to aquaculture production, or indirectly linked through the supply of goods and services to the aquaculture industry. Viewing aquaculture production as a percentage of GDP gives an indication of aquaculture's importance to the economy. Aquaculture's contribution to the economy will not only be dependent on the scale of aquaculture production within a country in terms of physical quantity but also on the relative value of aquaculture products being produced and the overall size of the country's economy. In richer countries it seems likely that not only will aquaculture make a smaller contribution to wealth, but people are more likely to have economic alternatives and

thus be more able to adapt to potential impacts and change. This issue is addressed within the adaptive capacity sub-model in the current study in terms of per capita GDP.

National level statistics for aquaculture production quantities (weight) and values (US dollars) were obtained from the United Nations Fisheries and Agriculture Organisation (FAO) via its FishStat database (FishStatJ, 2013). Data for all aquatic animals were combined while aquatic plants where excluded. Data were also sorted by culture environment which are defined by the FAO as: freshwater, brackish or marine. For both quantity and value statistics data for the three most recent years available (2008 to 2010) were averaged with the aim of reducing the effect of the inter-annual fluctuation that is seen in the statistics, especially in countries with lower levels of production. Figures for GDP for the same 2008 to 2010 period were obtained from the World Bank (World_Bank, 2013) while population data for the same period were obtained via the United Nations population division (UN_Population, 2013). Figure 2-2 shows the global distribution of production quantity and value statistics for freshwater, brackish water and marine culture environments.

Aquaculture production quantity (kg per capita) from freshwater, brackish water, and marine systems.

Aquaculture production value (percentage of GDP) from freshwater, brackish water, and marine systems.

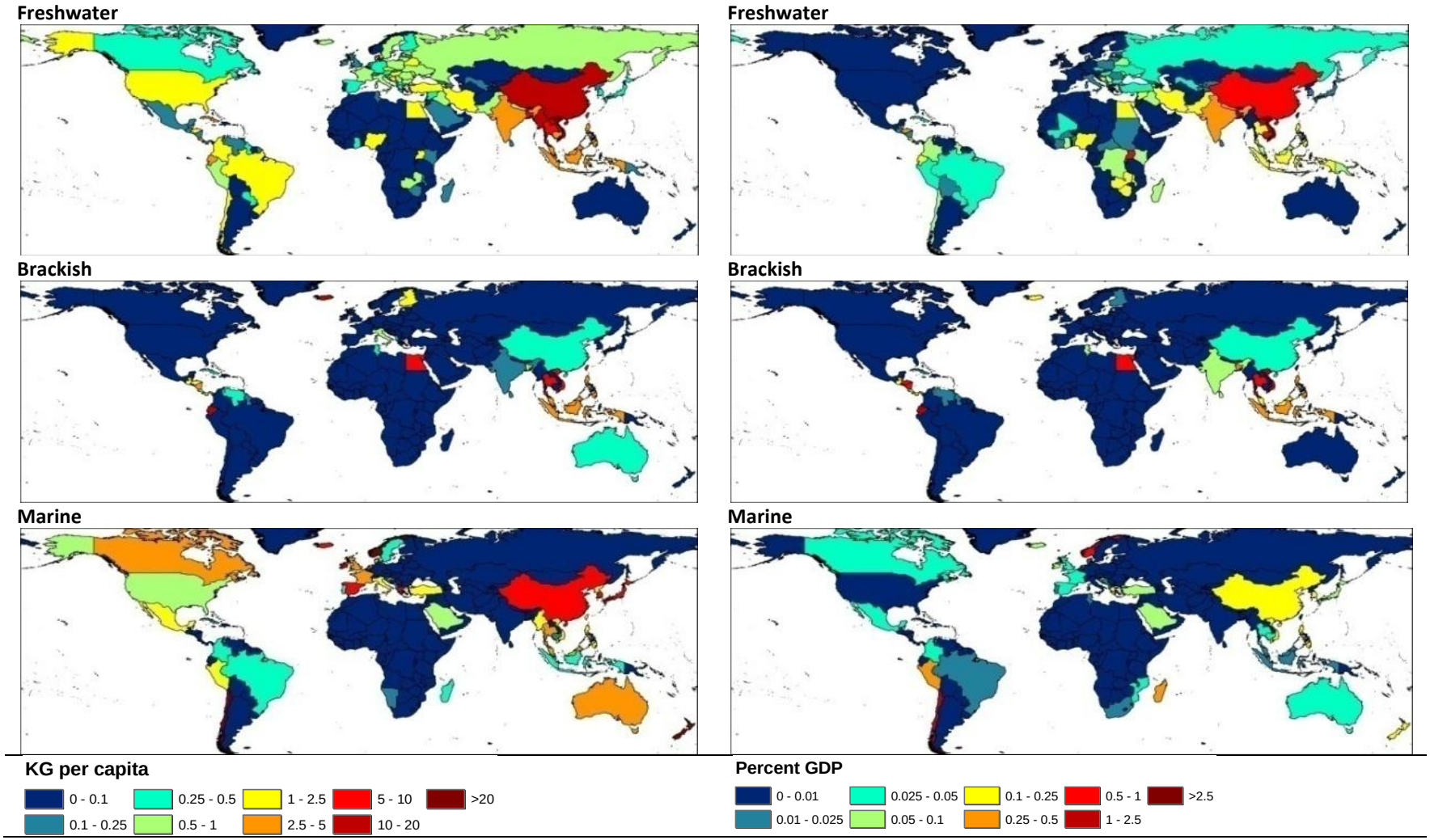

Figure 2-2: Aquaculture production statistics (average of years 2008 to 2010).

2.1.6.2 Exposure

Exposure to climate change in the context of the current study can be viewed as the relative extent of change between locations rather than an attempt to quantify actual changes. Future changes in annual mean temperature and precipitation are considered in relation to current water availability. Water balance (precipitation minus actual evaporation) is used as a proxy for current water availability. Population density is also included in the exposure sub-model based on the assumption that in areas with higher population densities the potential impacts of climate change may be increased through mechanisms such as increased requirements for resources such as water, and greater environmental pressure e.g. through increased pollution.

The frequency of past climate extremes in the form of cyclones, drought and flood events is used in the exposure sub-model as a proxy for future risk from such events based on the assumption that any increases in the intensity or frequency of these extremes is likely to be significant in areas where they are already common (Handisyde et al., 2006, Islam and Sado, 2000b).

Significant improvements in climate modelling are being made (IPCC, 2007b) with coupled Atmosphere and Ocean General Circulation Models representing the most sophisticated attempts to project future patterns of climate change. However significant variability remains between the outputs from different models and to a lesser extent different implementations of the same model. Climate models are often evaluated based on their skill at reproducing a historic climate scenario (e.g. that of the 20th century). In this respect the combined results from an ensemble of climate models normally show greater skill in reproducing the spatial details of climate when compared to a single model (IPCC, 2007b, Pierce et al., 2009). With this in mind it is common for impact assessments to make use of results from multiple climate models where possible.

For the current assessment gridded global data for projected changes in annual mean temperature and precipitation levels were obtained at 2.5 degree resolution using MAGICC/SCENGEN (version 5.3.v2) (Wigley, 2008). MAGICC is a software package that integrates a number of coupled gas-cycle, climate and ice-melt models. It allows for the exploration of projections for: average global surface air temperature, greenhouse gas concentrations and average global sea level change under a wide range of green house gas emission scenarios. The global average warming scenarios generated by MAGICC

are fed into SCENGEN where libraries of observed climate data are used along with the CMIP3 (Meehl et al., 2007) data base of climate model outputs generated for the IPCCs forth assessment report (IPCC, 2007b) to generate spatially explicit change scenarios. The advantage of using the MAGICC/SCENGEN package to generate gridded temperature and precipitation projections is that as well as allowing for quick and easy adjustment of emission scenarios and choice of Atmosphere and Ocean General Circulation Models (AOGCMs), it removes the influence that differences in sensitivity between AOGCMs would have when constructing patterns of change. This is achieved by averaging results from multiple models based on a fixed degree of warming for each model, an approach that contrasts with the approach of averaging results from multiple AOGCMs based on a future time point. This benefit can be illustrated using a simple theoretical ensemble of two climate models. If one of the models responds to a green house gas scenario for a future time period with a mean global warming of $1^{o}C$ and the other with a mean global warming of $2^{o}C$ then one model can effectively be viewed as being twice as sensitive as the other. If it is assumed that the extent of spatial changes in climate simulated in models is at least partly related to overall global warming then an equally weighted averaging of the results of the two models in question would mean that the more sensitive model would have a greater influence on the spatial variability of climate in the result.

While the CMIP3 ensemble of AOGCM results contain outputs from 24 models only 20 of these are available for selection in SCENGEN due to the availability of necessary variables. For the current study all 20 AOGCMS were selected in SCENGEN for the pattern scaling process. The global mean warming used to drive SCENGEN was $2^{o}C$ based on a year 1990 base point. Multiple warming scenarios were not considered in the current study as the aim is to show relative differences between global areas and results from SCENGEN change in a largely linear way in relation to overall mean temperature change. The MAGICC/SCENGEN derived projected changes in surface air temperature and precipitation used in the current study are shown in Figures 2-3 and 2-4.

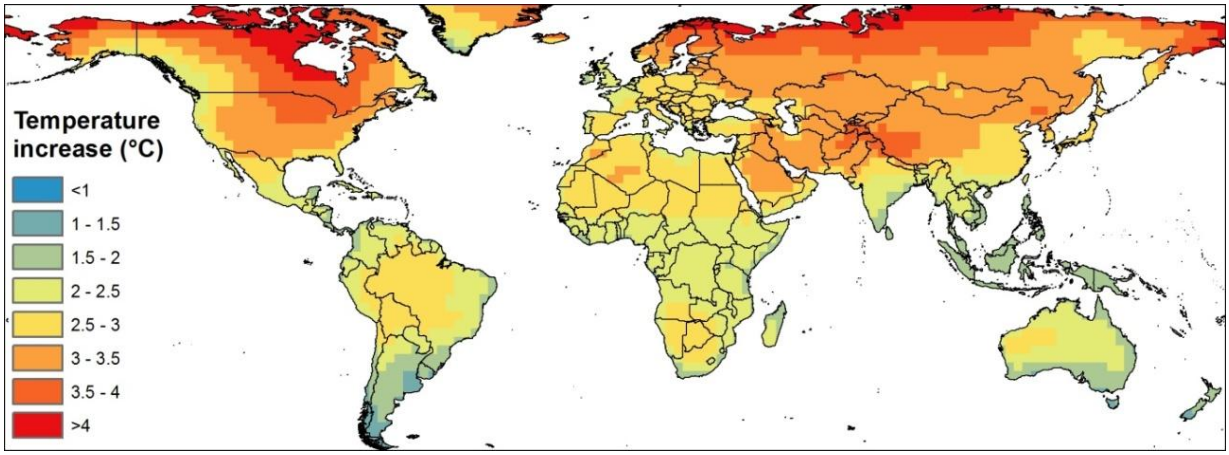

Figure 2-3: Change in average annual surface air temperature under 2°C global warming.

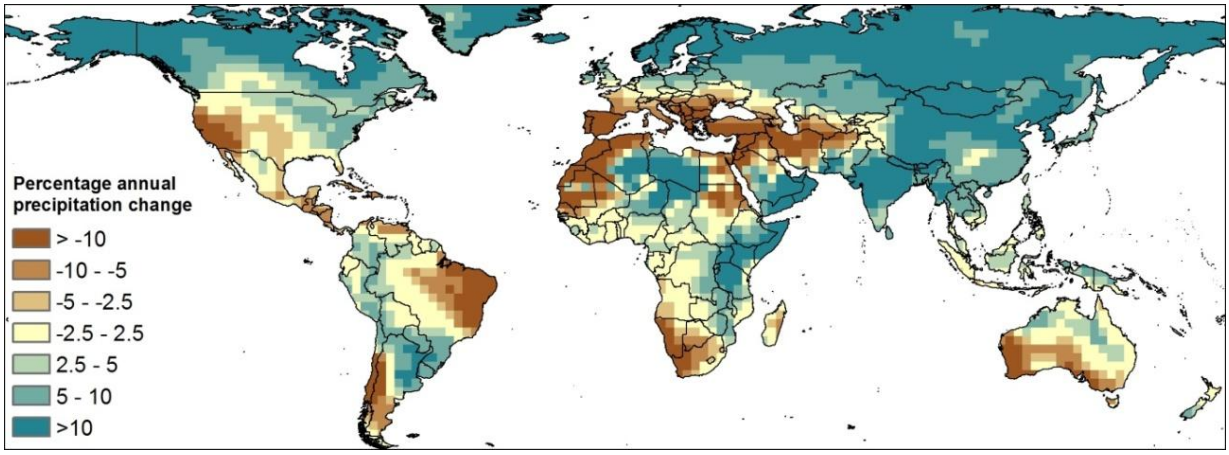

Figure 2-4: Percentage change in average annual precipitation under 2°C global warming.

Current water balance was calculated by subtracting annual average actual evapotranspiration from precipitation. Precipitation data were obtained from the Climate Data Research unit (CRU) as part of the CL2.0 data set (New et al., 2002). This data set represents a number of climate variables as monthly climatologies on a 10 arcminute global grid based on the period 1961-1990 and were constructed via the careful interpolation of data from 27075 meteorological stations in the case of precipitation. CRU CL2.0 is widely used in the literature either directly as a source of average climate or as base period with which future climate projections can be compared (Ramirez-Villegas et al., 2013, van Wart et al., 2013).

Data for modelled actual evapotranspiration data were obtained as a set of 0.5 degree resolution global grids representing actual evapotranspiration on a monthly basis over a 10 year period. The

data for each year were combined to produce a set of annual totals which were then averaged to produce a single layer. The modelled actual evapotranspiration data were produced by Fisher et al. (2008) by adapting the Priestly-Taylor method (Priestley and Taylor, 1972) and using a range of remotely sensed data to supply the required inputs (net radiation, normalized difference vegetation index, soil adjusted vegetation index, maximum air temperature, and water vapour pressure)

While it would be feasible to construct future precipitation scenarios using projected changes from SCENGEN to adjust values from the CRU CL2.0 data set, attempting to model future actual evapotranspiration would be far more problematic due to availability and quality or future projections for the necessary inputs for such an exercise. The view is taken here that any benefits that the current model could gain from the inclusion of future water balance scenarios would likely be overshadowed due to the potential introduction of largely unquantifiable inaccuracies.

Cyclone risk was estimated using the International Best Track Archive for Climate Stewardship (IBTrACS) database (Knapp et al., 2010). IBTrACS contains an archive of data relating to recorded cyclone tracks and aims to synthesis data from multiple agencies into a single product that is then freely disseminated. For the current project all cyclone tracks for a 40 year period ranging from 1973 to 2012 were included giving a total of 4549 storms in total. Storm track data were downloaded in vector line file format. A 200km buffer was applied based on average cyclone size (Australian_Bureau_of_Meteorology, 2013) giving each storm track total width of 400km. Polygons were merged to give a single polygon for each storm and then the resulting vector file was spatially joined to a 0.5 degree grid with a count being made for the number of storms at each grid cell. The resulting storm frequency grid is shown in Figure 2-5.

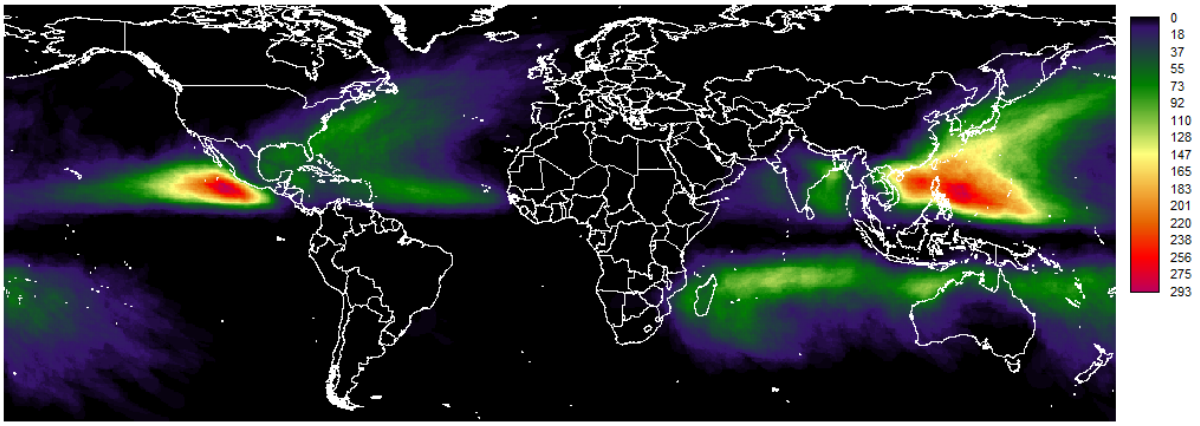

Figure 2-5: Cyclone frequency based on all storms recorded in the IBTrACS database for a 40 year period (1973-2012).

Data used to represent risk of flood and drought were obtained from the Aqueduct Global Maps 2.0 database (Gassert et al., 2013). Data were downloaded as polygon files showing: flood occurrence (number of floods recorded from 1985 to 2011), and drought severity (the average length of drought times and the dryness of the droughts from 1901 to 2008. Drought is defined as a contiguous period when soil moisture remains below the 20th percentile).

Gridded population density data (number of individuals per square kilometre) were obtained at 30 arcsecond resolution for the year 2008 from the LandScan data set (Landscan, 2008). Before it could be used in the current model the data were aggregated to 10 arcminute resolution to show average population density for each cell on the lower resolution grid. LandScan is a modelled dataset that makes use of multiple data inputs including: census information, administrative boundaries, land cover, elevation and slope. Landscan also represents the highest resolution global population data set currently available and although direct comparisons between global population data sets are limited it has been shown to outperform other global data sets when evaluated over an area of Sweden (Hall et al., 2012).

2.1.6.3 Adaptive capacity

Adaptive capacity in the current model was based on the United Nation Human Development Index (HDI) (Malik, 2013). The HDI represents a globally complete and consistent data set that is based on the combination of: health (life expectancy at birth), education (combination of mean years of schooling and expected years of schooling) and living standards (gross national income per capita). All components within the HDI are transformed to a 0-1 scale before being combined by calculating the geometric mean of the three components. Füssel (2010) cites (Gall, 2007) who undertook an evaluation of global indices in relation to social vulnerability. While generally critical of many of the indices, Gall (2007) concludes that the HDI outperforms the others examined. It is worth noting that this is despite containing a smaller number of variables than the other indices in question. HDI scores for the year 2012 are shown in Figure 2-6.

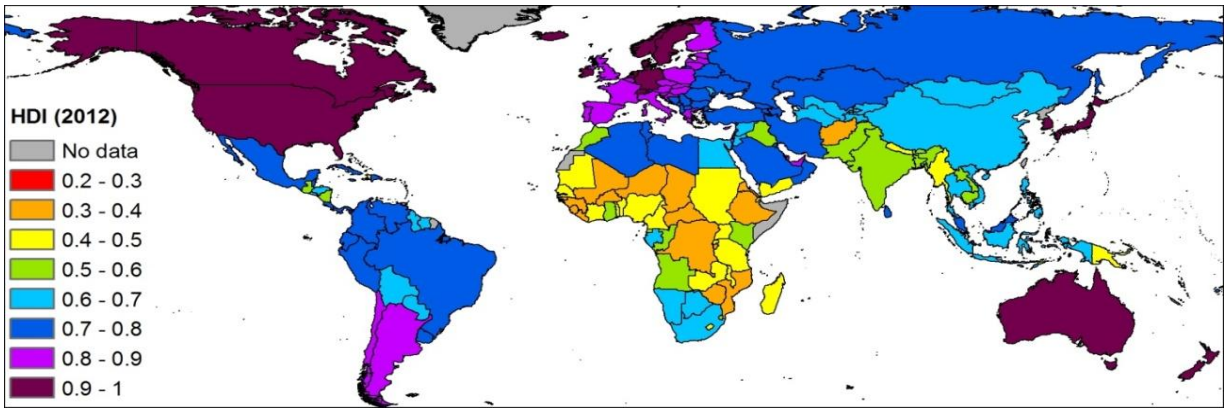

Figure 2-6: HDI values for the year 2012.

2.1.7 Layer combinations and weightings

All weightings were assigned by the author after consultation with a range of aquaculture experts. Details of weightings used for the freshwater, brackish water, combined fresh and brackish water, and marine assessment are given in Tables 2-3, 2-4, 2-5, and 2-6. The use of a geometric mean for the final combination means that very low values exert a greater influence on the final result. In practice this means that countries where aquaculture production is very low are indicated as being significantly less vulnerable. This approach is considered appropriate here based on the assumption that higher levels of aquaculture production within a region are likely to be at least partially associated with a greater number of livelihoods being either directly or indirectly linked to the sector and/or greater levels of dependence for both food and income.

Table 2-3: Weightings used for combining indicators in the vulnerability assessment for freshwater aquaculture systems.

Inputs	Weight (arithmetic mean)	Sub-model	Weight (arithmetic mean)	Sub-model	Weight (geometric mean)	Output
Temperature change	0.175	Exposure sub-model	0.333	Exposure and adaptive capacity sub-model	0.5	Vulnerability
Water balance	0.175					
Population density	0.175					
Precipitation change	0.175					
Flood risk	0.125					
Drought risk	0.125					
Cyclone risk	0.05					
Human development index	→	Adaptive capacity sub-model	0.666			
Aquaculture production (kg per capita)	0.666	→	→	Sensitivity sub-model	0.5	
Aquaculture value (percent GDP)	0.333					

Table 2-4: Weightings used for combining indicators in the vulnerability assessment for brackish water aquaculture systems.

Inputs	Weight (arithmetic mean)	Sub-model	Weight (arithmetic mean)	Sub-model	Weight (geometric mean)	Output
Temperature change	0.175	Exposure sub-model	0.333	Exposure and adaptive capacity sub-model	0.5	Vulnerability
Water balance	0.175					
Population density	0.175					
Precipitation change	0.175					
Flood risk	0.05					
Drought risk	0.05					
Cyclone risk	0.2					
Human development index	→	Adaptive capacity sub-model	0.666			
Aquaculture production (kg per capita)	0.666	→	→	Sensitivity sub-model	0.5	
Aquaculture value (percent GDP)	0.333					

Table 2-5: Weightings used for combining indicators in the vulnerability assessment for combined fresh and brackish water aquaculture systems.

Inputs	Weight (arithmetic mean)	Sub-model	Weight (arithmetic mean)	Sub-model	Weight (geometric mean)	Output
Temperature change	0.175	Exposure sub-model	0.333	Exposure and adaptive capacity sub-model	0.5	Vulnerability
Water balance	0.175					
Population density	0.175					
Precipitation change	0.175					
Flood risk	0.1					
Drought risk	0.1					
Cyclone risk	0.1					
Human development index	→	Adaptive capacity sub-model	0.666			
Aquaculture production (kg per capita)	0.666	→	→	Sensitivity sub-model	0.5	
Aquaculture value (percent GDP)	0.333					

Table 2-6: Weightings used for combining indicators in the vulnerability assessment for marine aquaculture systems.

<table>
<tr><th>Inputs</th><th>Weight (arithmetic mean)</th><th>Sub-model</th><th>Weight (arithmetic mean)</th><th>Sub-model</th><th>Weight (geometric mean)</th><th>Output</th></tr>
<tr><td>Temperature change</td><td>0.6</td><td rowspan="2">Exposure sub-model</td><td rowspan="2">0.333</td><td rowspan="3">Exposure and adaptive capacity sub-model</td><td rowspan="3">0.5</td><td rowspan="4">Vulnerability</td></tr>
<tr><td>Cyclone risk</td><td>0.4</td></tr>
<tr><td>Human development index</td><td>→</td><td>Adaptive capacity sub-model</td><td>0.666</td></tr>
<tr><td>Aquaculture production (kg per capita)</td><td>0.666</td><td rowspan="2">→</td><td rowspan="2">→</td><td rowspan="2">Sensitivity sub-model</td><td rowspan="2">0.5</td></tr>
<tr><td>Aquaculture value (percent GDP)</td><td>0.333</td></tr>
</table>

2.2 Results

Vulnerability model outputs are shown here as a set of raster images with vulnerability indicated using a continuous colour range. As is the case with other modelling exercises where a composite of multiple indicators are used, the results should be interpreted with care. The aim is not to provide an exact quantification of vulnerability and relative positions over the vulnerability range should not be interpreted in such a way. With this in mind no attempt is made to display numeric values derived from the modelling process for countries or regions, or to place results into classes with definitive labels suggesting a level of vulnerability. The best way to view the results, and the modelling process behind them, is as a means of comparing regions as being more or less vulnerable than each other.

The level of vulnerability indicated in the model outputs is strongly dependent on the per capita aquaculture production within a country based on the assumption that higher production will be related to a greater overall importance of the sector to livelihoods within a region. Images representing the combined indicators for exposure and adaptive capacity are also provided with the aim of giving an indication of vulnerability that is independent of the scale of a regions aquaculture production. Such information is useful when considering nations where aquaculture production is currently low as a national average but where an indication of vulnerability is wanted for those who are involved in the sector. It may also be possible that countries where aquaculture is less significant will be less able, or prepared, to invest in adapting to impacts on production.

Figures 2-7, 2-9, 2-11, and 2-13 show modelled vulnerability for aquaculture in freshwater, brackish water, combined fresh and brackish water, and marine systems respectively while Figures 2-8, 2-10, 2-12, and 2-14 show the results for the combined exposure and adaptive capacity sub-models excluding the effects of aquaculture industry size (sensitivity).

2.2.1 Freshwater

In terms of vulnerability related to freshwater aquaculture, Asia with its large aquaculture sector features strongly with Vietnam indicated as the most vulnerable country followed by Bangladesh, Laos, and China. Uganda is indicated as the most vulnerable country in Africa followed by Nigeria and Egypt. It is worth noting that while African countries are ranked quite low in the overall vulnerability assessment due to relatively low levels of aquaculture production, many score highly when just exposure and adaptive capacity are considered. Within the Americas Belize, Honduras, Costa Rica and Ecuador appear most vulnerable.

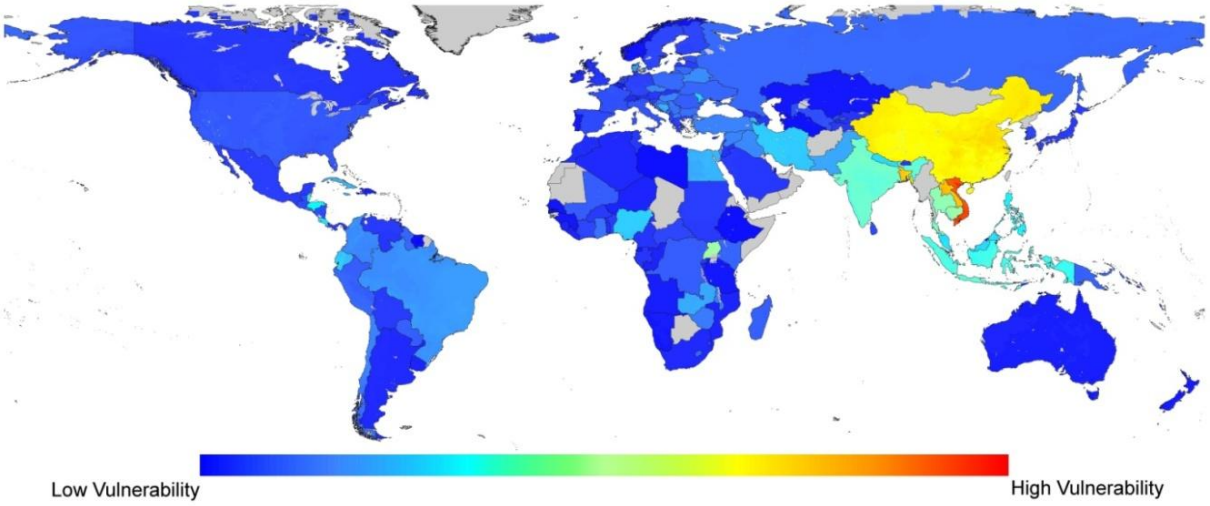

Figure 2-7: Vulnerability based on aquaculture production in freshwater systems.

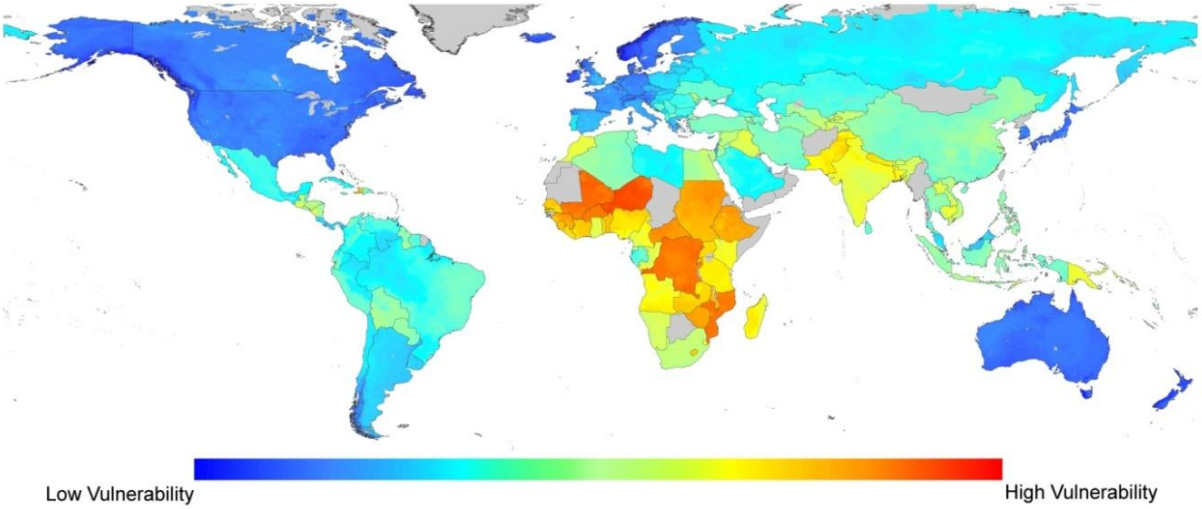

Figure 2-8: Results of the combined exposure and adaptive capacity sub-models used when assessing vulnerability for aquaculture in freshwater systems.

2.2.2 Brackish water

For brackish water production Vietnam again scores highly as does Ecuador. Egypt with its aquaculture production within the Nile delta and Thailand with its significant brackish water production of crustaceans also feature strongly.

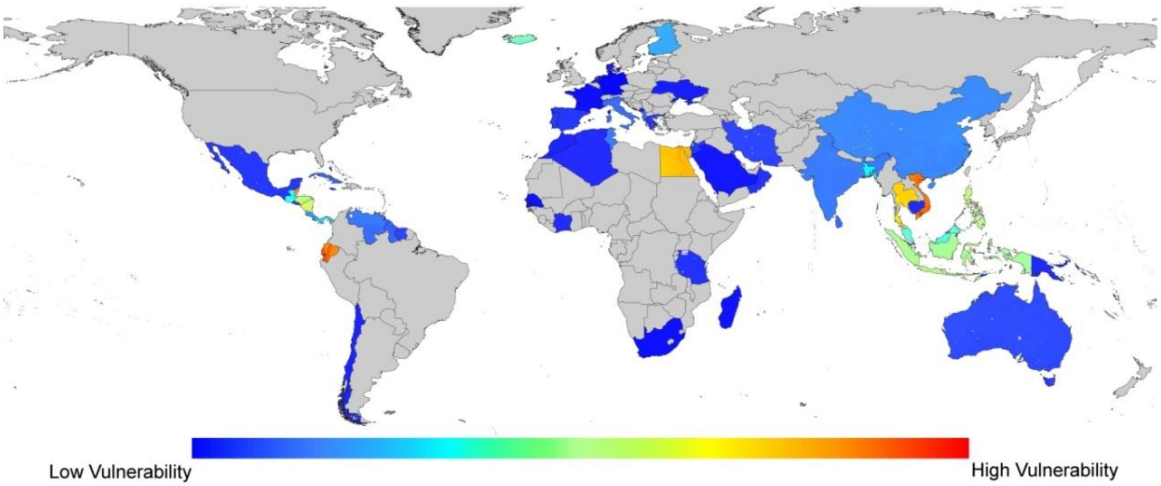

Figure 2-9: Vulnerability based on aquaculture production in brackish water systems.

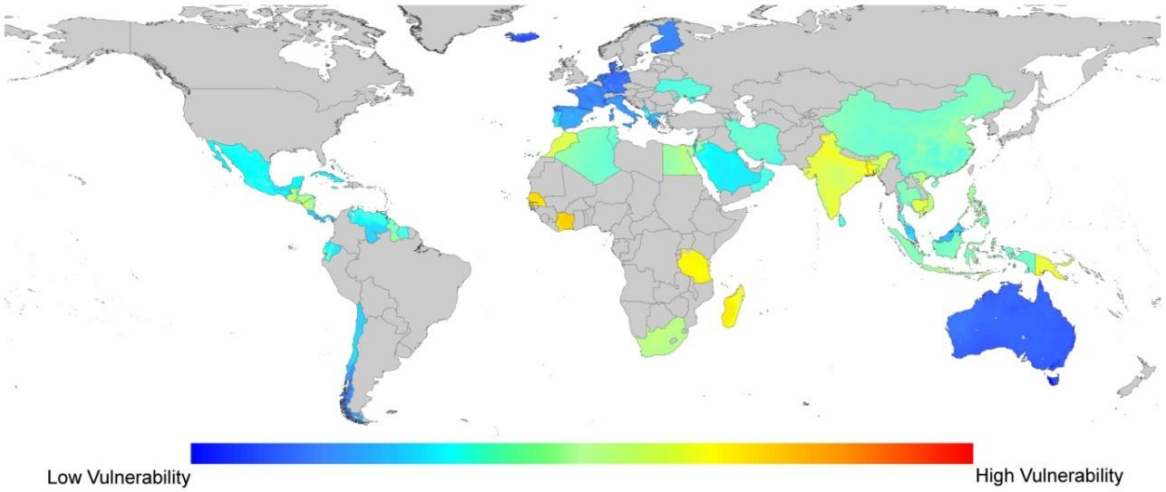

Figure 2-10: Results of the combined exposure and adaptive capacity sub-models used when assessing vulnerability for aquaculture in brackish water systems.

Vulnerability based on aquaculture production in brackish water systems.

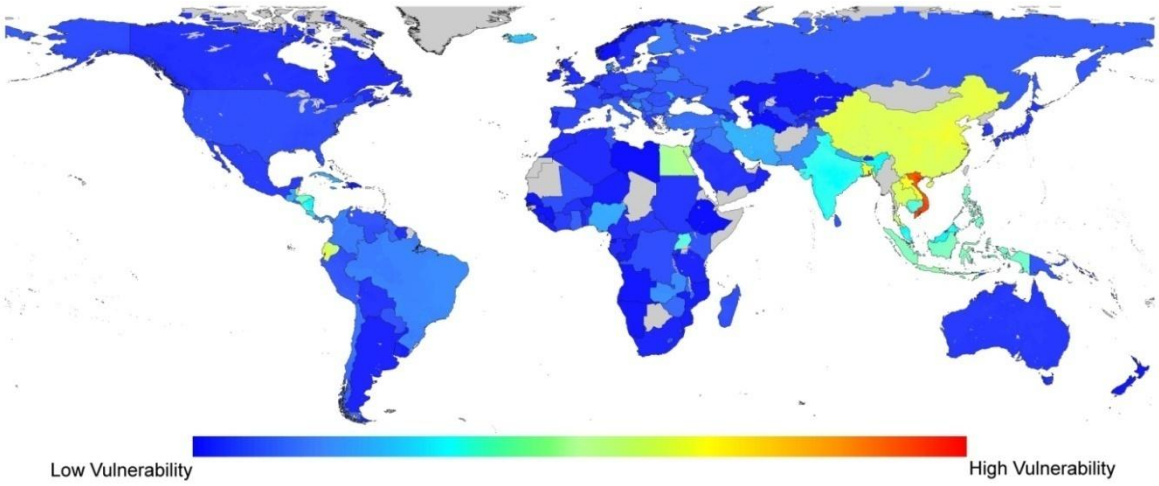

Figure 2-11: Vulnerability based on aquaculture production in both fresh and brackish water systems.

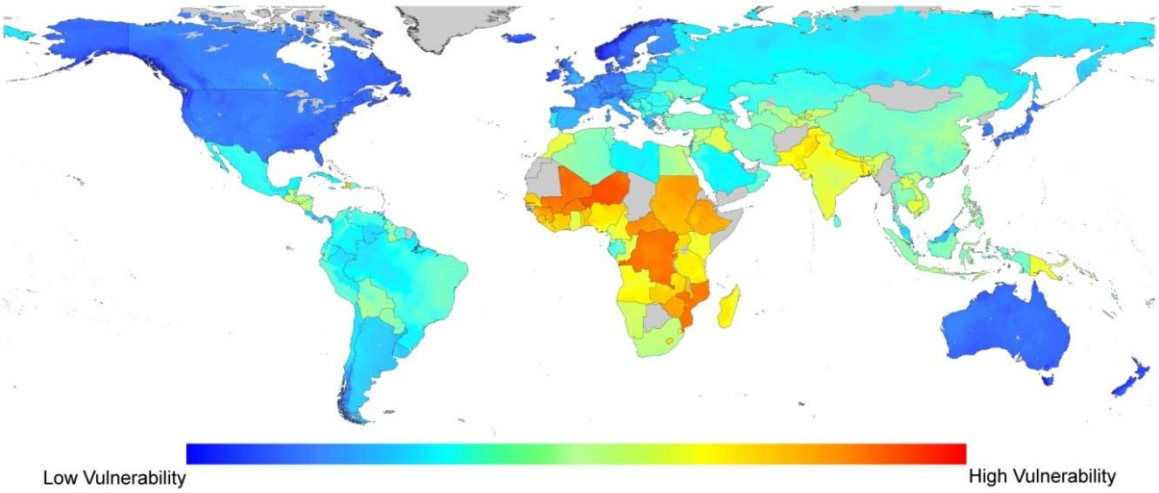

Figure 2-12: Results of the combined exposure and adaptive capacity sub-models used when assessing vulnerability for aquaculture in both fresh and brackish water systems.

2.2.3 Marine

Norway and Chile are indicated most strongly in terms of vulnerability in relation to marine aquaculture. It is worth noting that in terms of per capita aquaculture production and contribution to GDP the Faroe Islands are significantly above Norway and Chile and must be considered strongly dependent on the aquaculture sector. The Faroe Islands were not included in the current study as not all of the required data were available. Within Asia China is indicated as most vulnerable in terms of mariculture production followed by Vietnam and the Philippines. Madagascar is the African country indicated as most vulnerable while in the Americas Peru is emerges most strongly after Chile.

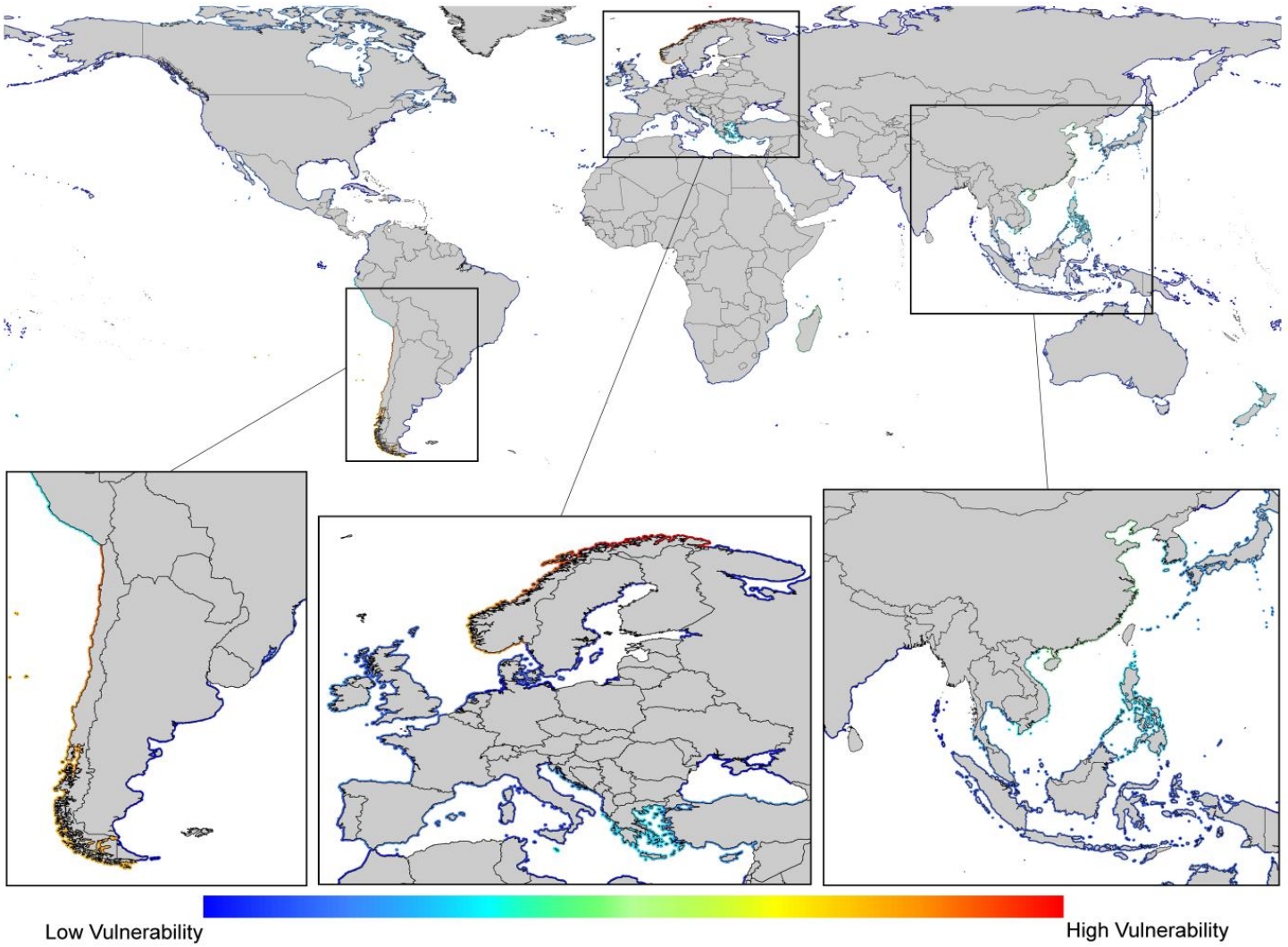

Figure 2-13: Vulnerability based on aquaculture production in marine systems.

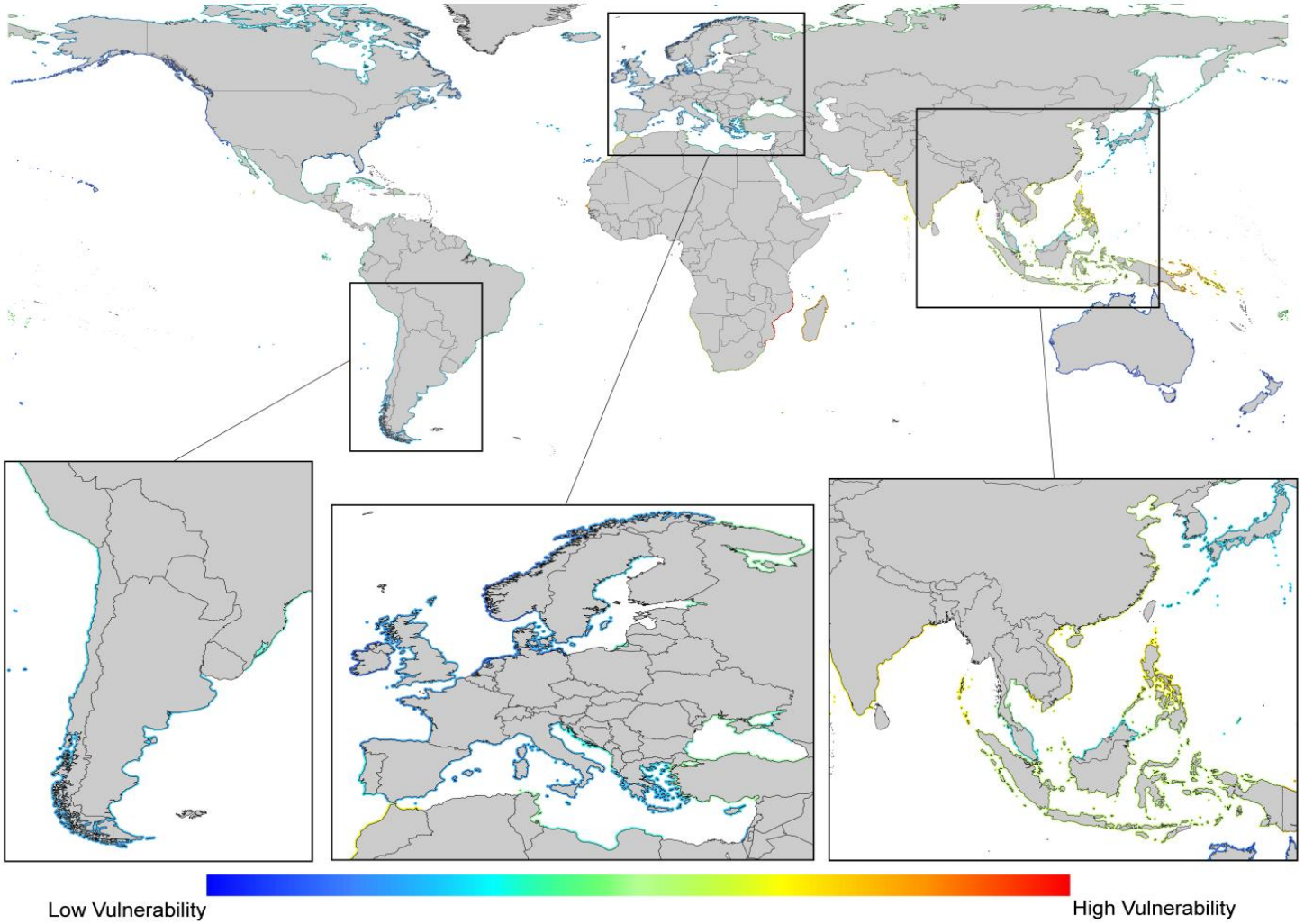

Figure 2-14: Results of the combined exposure and adaptive capacity sub-models used when assessing vulnerability for aquaculture in marine systems.

2.3 Discussion and summary

There is often a desire amongst policy makers and other users of modelling tools to have outputs that give definitive, even binary, answers that can be more or less followed without question when it comes to decision making. In reality this approach is hardly ever realistic and is often not how modelled data is intended to be used, or how it can provide most benefit. Modelling with spatial data within a GIS environment is often best considered as a means of providing decision support as part of an expert system where it is used in association with other information by individuals who have an understanding of the issues in question (Nath et al., 2000). When viewed in this context the approach demonstrated in the current study along with associated outputs can be seen as a valuable tool for informing decision makers and guiding future research.

Another way in which modelling within a GIS environment can be beneficial is that once a database and modelling approach is established and verified it is generally a fairly quick and easy task to add new data sources that may become available as well as manipulate the way in which data is classified and/or weightings (levels of significance) applied to data within the model. This process can allow different questions to be asked of the data and different scenarios to be considered. The graphical output typically associated with the use of spatial data within a GIS allows for high quality visual interpretation of results which in itself can be useful when multiple scenarios are being considered.

(Handisyde et al. (2006)) conducted an evaluation of global aquaculture vulnerability to climate change that incorporated spatial data and was also based on the concept that vulnerability is a function of sensitivity, exposure, and adaptive capacity. The authors used weighted arithmetic means to combine data and the resulting sensitivity, exposure, and adaptive capacity sub-models. A similar approach was taken by Allison et al. (2009) for capture fisheries although in this case all variables had even weightings. One potential drawback of averaging a large number of variables is that the power of each individual variable is reduced. In terms of assessing aquaculture vulnerability using mostly national level statistics a key issue is a lack of distinction between areas producing very little and large amounts of aquaculture products. In the case of Handisyde et al. (2006) this resulted in some areas with small amounts of aquaculture production being indicated as vulnerable. If the aim is to evaluate where any aquaculture-related livelihoods may be at risk then this is not an issue but if the aim is to highlight areas where greatest overall impact on livelihoods is likely when they are viewed as a whole

then there are limitations. Ultimately these issues can largely be viewed as a consequence of reducing multiple variables to a single output.

The current assessment aimed to address the issues highlighted above. Considerable emphasis was placed on the sensitivity component based on kg per capita production of aquatic species and contribution to GDP. The adaptive capacity and exposure sub-models were combined and this result was further combined with the output of the sensitivity sub-model using a geometric mean to allow areas with low values in either input to exert a greater influence on the final output. In practice this means that countries where aquaculture production is very low are indicated as being significantly less vulnerable. This approach is considered appropriate here based on the assumption that higher levels of aquaculture production within a region are likely to be at least partially associated with a greater number of livelihoods being either directly or indirectly linked to the sector and/or greater levels of dependence for both food and income. When considering aquaculture-related livelihoods that may be vulnerable in nations where overall production is low the sensitivity component of the model becomes much less relevant, if at all. The results of the combination of the exposure and adaptive capacity sub-models are provided in the current study and help shed light on this question and in doing so provide a good example of how viewing the outputs from sub-sections of the model can provide useful insights in their own right. Another area of potential improvement in the current assessment when compared with Handisyde et al. (2006) is the use of a continuous scale (0 to 1), rather than 5 discreet classes, that allows for greater differentiation between areas in terms of vulnerability and its contributing components.

Allison et al. (2005) and Allison et al. (2009) conducted a global assessment of livelihood vulnerability to climate change impacts on capture fisheries using a range of indicators available at the national scale. As in the present study vulnerability was assumed to be a function of sensitivity, exposure and adaptive capacity. The sensitivity component included: fisheries export value as a percentage of total export value, proportion of economically active population involved in the fisheries sector, total fisheries landings (tonnes), and fish protein as a percentage of total animal protein consumed. The authors point out that these data sets relate to total fisheries production from all environments i.e. inland and marine and acknowledge that these different environments are likely to be affected in different ways by changing climate. For example changes in precipitation are likely to be relevant for

inland situations while sea surface temperature may be more significant for the marine environment. Allison et al. (2009) go on to suggest that future studies should consider separating inland and marine fisheries.

Taking the above into consideration the environment field in the FAO FishStat (FishStatJ, 2014) database that allows aquaculture production data to be sorted into freshwater, brackish and marine categories was used and each of these environments was addressed in the current model separately. However distinctions between these categories are not always clear and decisions taken by those reporting on production will have an influence, especially in the case of fresh and brackish water where there is a continuum between the two environments. With this in mind a combined fresh and brackish water assessment was included in the current study along with distinct fresh and brackish scenarios. It is worth noting however that the bulk of production listed as taking place in brackish water is of crustaceans while for fresh water it is of cyprinids suggesting that the environmental distinctions are likely giving a reasonable indication of the type of aquaculture taking place in many cases. While there are likely to be situations where both inland and coastal ponds could be affected by changes in temperature and precipitation leading to water quality and availability issues, the effects of cyclones and associated storm surges are most likely to affect coastal regions and as such are most likely to pose a threat to brackish and marine aquaculture.

It is also worth noting that the accuracy of reporting of aquaculture production is likely to vary between countries with both over and under reporting being a potential issue. For potential future vulnerability assessment being conducted at the national, or particularly sub-national level, it may be practical to pursue other data sources although errors in reporting at the farm level would be difficult to address in anything other than extremely detailed and localised investigations. For a global assessment such as the current one the view is taken here that aquaculture production data available via FAO FishStat (FishStatJ, 2013) provides the most complete and consistent source, and as such can still be viewed as a useful indicator.

Allison et al. (2009) used a single metric to assess exposure to climate change, when ranking vulnerability of capture fisheries based livelihoods, in the form of mean surface air temperature change projected by the UK Hadley Centre climate model (HadCM3). The authors accepted the limitations of this approach stating “Choosing an indicator of exposure to climate change for a global analysis is fraught with constraints and assumptions” but suggest that temperature change is also the

most readily available and best understood indicator. Handisyde et al. (2006) used a greater number of metrics to represent exposure to climate change by including projected precipitation change as well as historic data for extreme events in the form of floods, drought and cyclones. By representing data for climate variables as a global grid rather than national averages the authors also reduced the potential loss of information that is likely to occur, especially in the case of large countries. The current study also uses multiple indicators for exposure but includes the use of gridded actual evapotranspiration data as well as a larger database of recorded storms in order to represent cyclone risk. Another significant improvement in the current assessment compared to Handisyde et al. (2006) is the use of an ensemble of AOGCMs via the MAGICC/SCENGEN application rather than from a single climate model which should result in a better representation of future change. This said, there is still much room for improvement in terms of climate modelling especially in relation to patterns of precipitation change where agreement between models tends to be less strong than seen for temperature. With this in mind updating of the database and model as new and improved climate projections become available should be considered.

Output from MAGICC/SCENGEN suggests that there will be greater warming over large land areas compared with oceans and there is also a notable trend for increased warming at high latitudes. For tropical areas of central and south-east Asia where much aquaculture takes place projected warming over land is in line with or only slightly above the global average with greater increases projected as one extends further north into China.

Higher average temperatures will result in an increasing number of very hot days or heat waves when compared to current conditions. This in turn may result in direct thermal stress of cultured animals especially where they are near the limits of their range. While average higher temperatures may not be fatal for species nearing the upper limits of their ideal temperature range they may reduce profits via changes in bioenergetics performance and feed conversion ratios (Handisyde et al., 2006). Increased risk of disease for aquaculture species may also be an issues associated with increasing temperatures in some areas (e.g. Callaway et al., 2012, De Silva and Soto, 2009, Handisyde et al., 2006) along with potential unknown ecological effects that may have an influence on aquaculture. While the current model associates vulnerability with increasing temperatures, an approach that has been adopted by previous studies (Allison et al., 2009, Handisyde et al., 2006), there will also be situations where increasing temperatures enhance production of certain species through mechanisms

such as: improved growth rates, longer growing seasons, and increased primary productivity. In the case of the current model where the aim is to investigate non-specific climate-related vulnerability of all aquaculture, it is suggested here that relating temperature increase to vulnerability is still the best use of the data. However for future studies with a narrower focus in terms of geographic range and culture species, there may be opportunity to consider both positive and negative impacts on aquaculture performance.

The AOGCM ensemble suggests a general trend for increased precipitation over central Asia and China while very little change or slight increases are projected for south East Asia. East Africa is expected to see increased precipitation while a decrease is projected for the Mediterranean, North Africa and Southern Europe. Decreases in precipitation are also projected for Central America and Eastern Brazil. Decreasing water availability has the potential to negatively affect aquaculture through mechanisms such as: reduced water quality leading to increased levels of stress in culture organisms and potentially disease, greater competition for water use from other sectors, changes in salinity, and reduced water levels in ponds potentially resulting in increased sensitivity to short-term drought and / or temperature fluctuations (Handisyde et al., 2006, Ross et al., 2009). It was noticeable that during a series of informal interviews conducted by the author with fish and shrimp pond farmers in Bangladesh that high temperature and drought where viewed as a single problem with the reasoning that when water is scarce temperatures tend to be high and that it is reduced water levels in ponds that allow temperature to have an impact on cultured organisms as there is little chance for them to move to cooler deeper water.

The current study associates reduced water availability, in terms of precipitation change and current water balance, with vulnerability for inland aquaculture. An accepted limitation of the model is that these variables are considered on a per grid square basis with no mechanism for lateral flow between cells and thus flow accumulation within water courses. Parish et al. (2012) has argued that the use of a simple per grid cell approach to water availability as opposed to more complex routed runoff models can be a valid method as it allows for the use of easily available data sources such as runoff values taken directly from AOGCMs. A similar point of view is adopted here in terms of the use of MAGICC/SCENGEN where only precipitation, temperature, and air pressure data are available. It is suggested here that the use of a multi model ensemble may provide benefits in terms of projection accuracy that may not be possible with the limited range of data that would be available for more

complex runoff modelling. It is also worth considering that while a significant amount of aquaculture will rely on ground and surface water that will be involved in inter cell drainage there is also much, quite possibly belonging to poorer smaller scale aquaculture producers, that is at least partially dependant on localised runoff and rainfall.

The range of indicators of exposure to climate change for marine aquaculture were more limited with only temperature change and cyclone data being used. There has been suggestion of a number of potential negative impacts on aquaculture in association with increasing sea temperatures such as harmful algae blooms, increased incidence of disease and parasites, changing feed conversion ratios, and changes in the size or location of suitable ranges of culture species (Callaway et al., 2012, De Silva and Soto, 2009, Handisyde et al., 2006, Ross et al., 2009).

While in the current model increasing temperature is associated with greater vulnerability in marine systems there will be situations where increasing temperatures result in positive changes for production, for example by improved growth performance (Lorentzen, 2008). Changes in primary productivity may also become significant with positive as well as negative consequences depending on area, current patterns, and local ecosystems (e.g. Blanchard et al., 2012, Brown et al., 2010, Chassot et al., 2010). With this in mind areas indicated as being most vulnerable should be viewed as high priorities for more detailed investigation where it is possible that both positive and negative implications for aquaculture may be found depending on the species and culture system being considered. Accurate modelling of potential impacts on marine systems may need to take place at a more localised scale using high resolution data to try to account for variables such as local variation in current, temperature, and primary productivity. In some areas there are significant inter-annual variations associated with processes such as El Niño/La Niña–Southern Oscillation which will also need to be considered by extending investigations over longer time periods and / or for a range of scenarios.

A further significant potential impact for marine aquaculture related directly to increasing atmospheric carbon dioxide levels as opposed to associated warming is ocean acidification where from an aquaculture perspective the most obvious threat is to growth and survival rates for species forming calcareous structures such as the shells of bivalve molluscs (Gazeau et al., 2007, Narita et al., 2012). Cooley et al. (2012) assessed vulnerability of nations to ocean acidification impacts on mollusc production, both wild and aquacultured, based on: contributions to the economy and dietary protein

(sensitivity), time till a modelled transient decade where water conditions are significantly altered so that currently levels of mollusc harvest cannot be guaranteed (exposure), and adaptive capacity. While not addressed specifically in the current model ocean acidification is a global issue where the extent of impacts for aquaculture will be strongly related to culture species as well as localised ecosystems and water conditions. Future research could potentially apply the approach used in the current study but with the sensitivity component adjusted to focus on species most likely to be affected by lowered pH and the exposure component adjusted to indicate areas where pH is already lower.

In summary the current assessment provides a valuable indicator of areas where livelihoods may be vulnerable to climate change related impacts on aquaculture. As previously mentioned it is best to view the information as a useful starting point for decision makers where it should be used in conjunction with expert opinion as a decision support tool. The use of spatial data in conjunction with a GIS in the current study provides an efficient way of handing and analysing varied data sources at a range of resolutions. There are numerous examples of GIS being used to model site suitability for aquaculture. These incorporate a broad range of topographical, demographic, socio-economic, and environmental variables including those relating to present climate such as water availability (e.g. Giap et al., 2005, Hossain et al., 2007, Hossain et al., 2009, Longdill et al., 2008, Ross et al., 2011, Salam et al., 2005, Salam et al., 2003).

The current work also provides a strong starting point for future research with the focus on specific species and culture practices in at-risk areas. As well as highlighting areas of risk an important goal for future detailed assessments will be to highlight areas where the potential for a given type of aquaculture may improve. With possible work such as this in mind it can be assumed that the use of GIS and modelling with spatial data have significant possibilities in terms of helping aquaculture adapt to climate change by assisting in decision making that allows appropriate species and culture practices to be matched to locations in relation to changing climatic and environmental conditions.

3 GLOBAL HIGH RESOLUTION MODELLING OF POND AQUACULTURE SITE SUITABILITY WITH REFERENCE TO FUTURE CLIMATE SCENARIOS

3.1 Introduction

Fish remains a popular food item and its consumption is being promoted in many areas as part of a healthy lifestyle. In some developing regions where overall food availability may be limited by supply and/or cost the production of cheap freshwater fish species represents an important source of quality protein, essential fatty acids, and micronutrients and thus represents an important commodity in terms of food security (Beveridge et al., 2013). With this in mind and in line with a growing human population and increasing levels of development in many areas the demand for aquaculture products is growing. To meet this demand globally aquaculture continues to expand while capture fisheries remain fairly static. In 2011 total aquaculture production, excluding aquatic plants, was approximately 63.6 million tonnes. Of this 63.6 million tonnes 44.3 was produced by inland aquaculture. Figure 3-1 shows total inland fisheries production for the years 2006 to 2011 along with the contributions made by both capture fisheries and aquaculture. In terms of inland fisheries production the graph clearly emphasises that: a) aquaculture accounts for the majority of total production, and b) aquaculture production has increased rapidly with an average annual rate of 7.2% for the 2006 - 2011 period compared with 3.27 percent for inland capture fisheries (FAO, 2012).

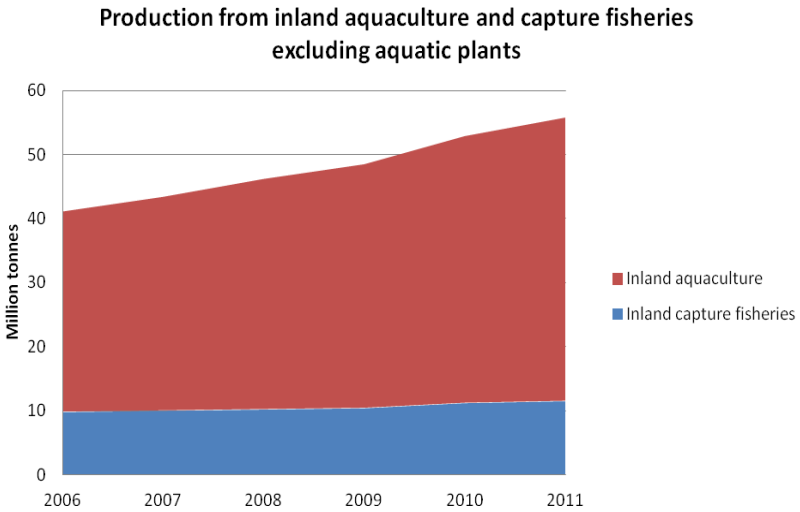

Figure 3-1: Global inland fish production.

FAO (2012) noted that freshwater fish farming provides a relatively easy entry point for small scale producers wanting to practice aquaculture in developing countries and with this and recent production increases in mind it is expected that the freshwater aquaculture sector will continue to grow during the 2010s. Brackish water aquaculture, that typically takes place in ponds, also continues to grow with an estimated average annual increase in production quantity for 7.23 % for the 2005 – 2010 period (FishStatJ, 2013). While total brackish water aquaculture production quantities are low when compared to freshwater systems they are significant in many areas and often involve high values species such as marine shrimp.

Pond-based aquaculture systems are diverse in terms of culture organisms and methods. Systems vary significantly in terms of both size and intensity ranging from small ponds that have little in the way of additional inputs and produce a relatively small number of fish that provide an additional source of food and perhaps a small amount of income for the pond owners, to large commercial operations employing densely stocked monocultures that rely heavily on commercial feeds and the use of technologies such as aeration devices.

The contribution of inland aquaculture to economies is significant, especially in a number of Asian countries. This point is illustrated in Figure 3-2 that shows aquaculture contribution to GDP from aquaculture production in fresh and brackish water environments (excluding aquatic plants) using an average of the years 2008 to 2010. Given the value of the sector it is unsurprising that aquaculture provides an important income source for an increasing number of people either directly through the production of aquatic organisms or though supporting industries such as: production of feeds, processing, and marketing. Globally it is estimated that over 100 million people are dependent on aquaculture as an income source, either directly as employees in the production or support sectors or as a dependant of such a person (FAO, 2012). While detailed estimates of the number of livelihoods related to inland pond culture are lacking, the number of individuals involved is likely to be high due to the overall extent of pond production. It is worth noting that aquaculture promotion has been shown to increase both income and food security among the extreme poor where even landless members of society were shown to benefit from aquaculture promotion through associated activities such as pond netting and fish trading (Pant et al., 2014).

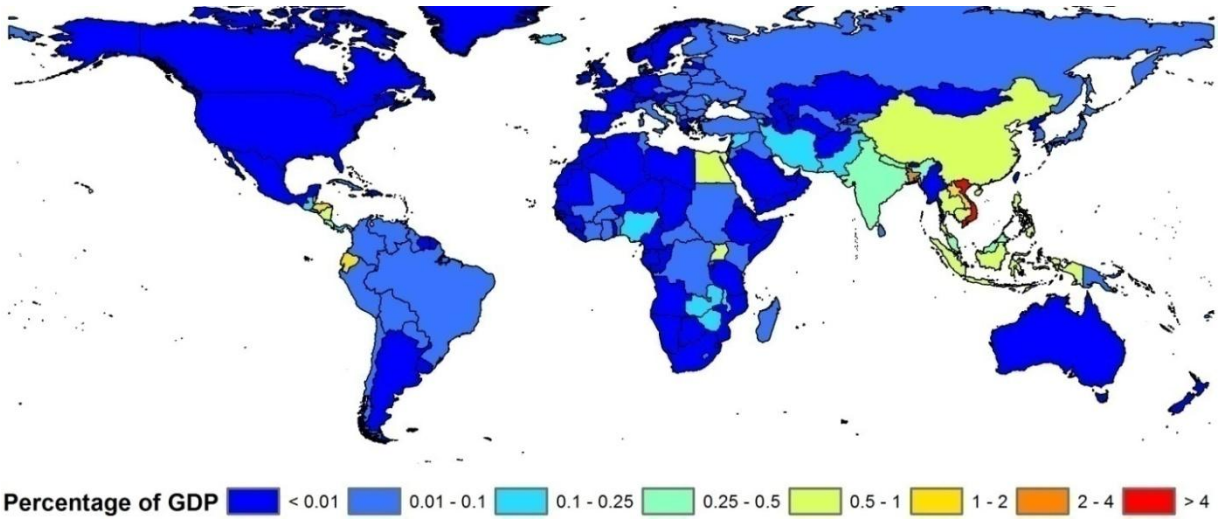

Figure 3-2: Aquaculture contribution to GDP based on average figures for the period 2008-2010.

During the 20th century, especially the latter half, and continuing to the present day the earth has experienced a significant warming trend with more pronounced warming over land areas compared to oceans (Hansen et al., 2012, Houghton, 2009, IPCC, 2007b, Jones et al., 2012, Kennedy et al., 2011a, Kennedy et al., 2011b, Morice et al., 2012, Rohde et al., 2013). This warming trend is illustrated in Figure 3-3 for land areas, oceans and combined land and ocean with a significant increase in temperatures seen from the 1970s onwards. There is now a strong consensus that this warming trend is at least partly a result of increases in atmospheric greenhouse gas levels as a result of anthropogenic emissions and that this warming trend is set to continue as greenhouse gas levels continue to increase (Cook et al., 2013, IPCC, 2007b). The ability to model future climate is continually improving in association with increased understanding of climate processes and computing power. Another key component in the ability to model climate change is the increasingly large number of climate experiments that are being conducted and combined to produce ensembles of data such as the World Climate Research Programme's (WCRP's) Coupled Model Intercomparison Project phase 3 (CMIP3) multi-model dataset used for the IPCC fourth assessment report (IPCC, 2007b). Current estimates suggest that that in association with this overall trend for global warming there will be changes in climate patterns with different areas seeing varied amounts of warming along with trends for increased wet or dryness in association with precipitation, humidity and cloud cover changes (Houghton, 2009, IPCC, 2007b).

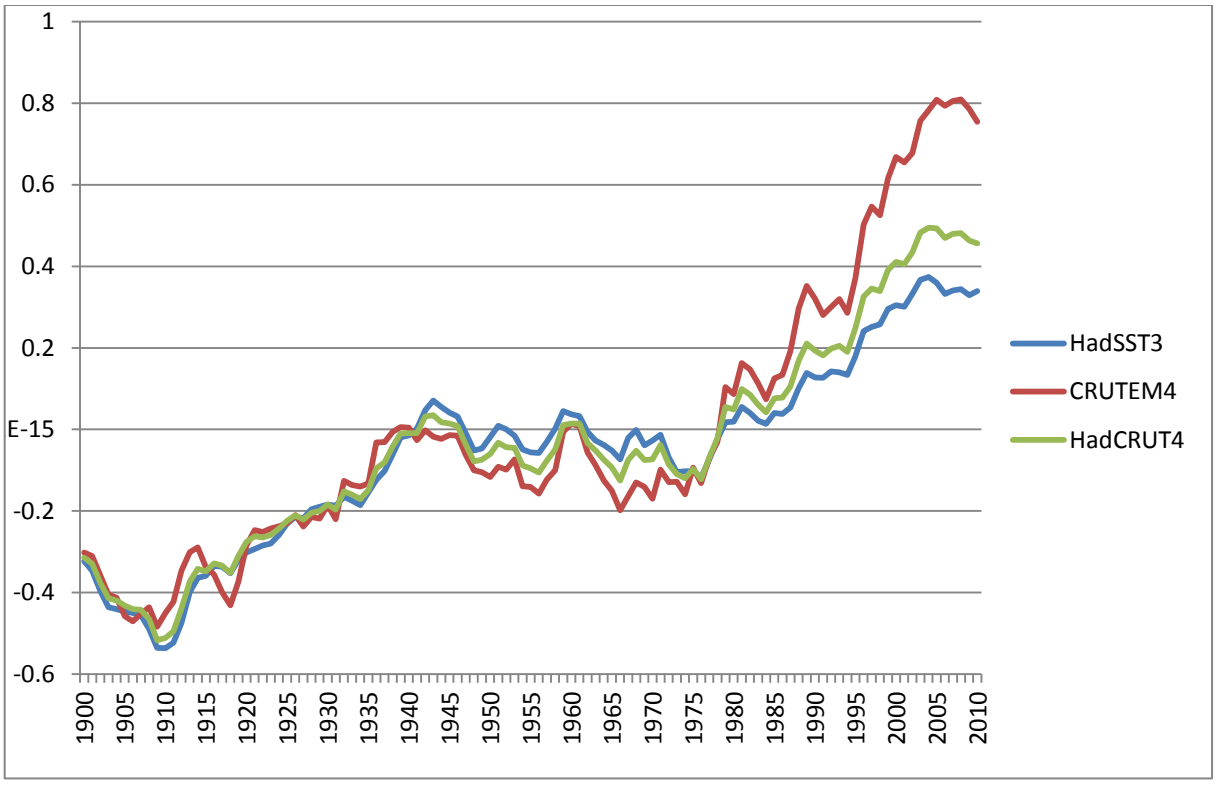

Figure 3-3: Five-year running mean of global observed temperature change over land areas (CRUTEM4) (Jones et al., 2012), Sea surface temperature (HadSST3) (Kennedy et al., 2011a; Kennedy et al., 2011b), and combined land and ocean (HadCRUT4) (Morice et al., 2012).

Pond-based aquaculture represents semi controlled systems where aquaculturists exert influence to a greater or lesser extent on factors such as species composition, feeding, and water quality. This said, pond systems are still strongly linked to the environment around them. In this respect changes in air temperature, cloud cover, wind speed, humidity, and precipitation have the potential to directly influence aquaculture through changes in water temperature, water availability, and the impacts of extreme weather events (Kapetsky, 2000).

Increased water temperature has the potential for both positive and negative impacts on aquaculture systems. For example; provided sufficient nutrients are available primary productivity may increase in relation to temperature providing an overall increase in production in systems that are less dependent on supplementary foods (Handisyde et al., 2006). Warmer conditions will result in an increase in the metabolic rate of the culture organisms. For species that were originally at the lower end of their temperature range there may be potential benefits in terms of food conversion and

growth performance provided adequate water conditions and feeding can be maintained (De Silva and Soto, 2009, Handisyde et al., 2006). However in extreme cases increased temperatures may result in direct loss of stock as temperatures move outside of their tolerated range and / or water quality and dissolved oxygen levels are reduced (De Silva and Soto, 2009, Ficke et al., 2007, Handisyde et al., 2006). For species cultured in areas where they are nearer the upper end of their temperature range there may be reductions in performance related to reduced feed intake and conversion. Ultimately such changes may result in a shift in the suitable range of a given species. For example the optimum range for culture of channel catfish (*Ictalurus punctatus*) is expected to shift north within the United States in relation to increasing temperatures with a suggested figure of 240km for every 1°C increase in average temperature (Ficke et al., 2007, McCauley and Beitinger, 1992). McCauley and Beitinger (1992) point out that growth rates and thus unit area production will increase with increasing temperature but once a level of about 30°C is reached feeding rate and therefore growth rate is reduced.

Changes in precipitation along with evaporation rates may impact on water availability for aquaculture systems. Reduced water availability may result in water quality issues, salinity changes, and reduced water volume (De Silva and Soto, 2009, Handisyde et al., 2006, Kapetsky, 2000). In the case of pond aquaculture reduced water levels combined with high temperatures may be especially problematic as the shallow water will warm up more quickly and there will be a reduced capacity for stratification and cooler conditions lower in the water column. Alternatively, areas of increasing water availability may become more suitable for aquaculture practices that would previously have been impractical or too expensive to implement.

Climate related variables are obviously not the only consideration in relation to successful aquaculture operations and ultimately there is a need to match aquaculture species and culture methods with a wide variety of climatic, environmental, topographic, socio-economic, and demographic variables. This process can essentially be viewed as a spatial problem where appropriate site selection becomes important if aquaculture is to succeed. The use of Geographic information systems (GIS) has shown great potential for use in site suitability modelling for Aquaculture in a range of marine and inland environments by allowing multiple, and varied, data types to be represented within a spatial database that can then be queried to answer specific question in relation to site suitability. Beyond this the use of GIS allows for the construction of more complex site suitability

models for aquaculture that allow for the inclusion of multiple variables through the use of approaches such as decision trees and multi criteria evaluation (Giap et al., 2005, Hossain et al., 2007, Hossain et al., 2009, Longdill et al., 2008, Nath et al., 2000, Ross et al., 2011, Salam et al., 2005, Salam et al., 2003).

Previous GIS-based aquaculture site selection work has been conducted at a range of scales and resolutions and has typically been based on the use of raster grids to represent data. For example Hossain et al. (2007) and Hossain and Das (2010) used a multi criteria evaluation approach to evaluate site suitability for tilapia and prawn (Macrobrachium *rosenbergii*) production within specific regions of Bangladesh. The authors made use of ASTER satellite imagery to evaluate land cover and consequently used a resolution of 15m. In contrast Aguilar-Manjarrez and Nath (1998) assessed site suitability for the African continent but using a lower resolution of 3 arcminutes (approximately 5.5km at the equator). Kapetsky and Nath (1997) conducted a similar exercise for Latin America at a resolution of 5 arcminutes (approximately 9km at the equator).

The current study aims to model site suitability for pond aquaculture at the global scale, using a resolution of 10 arcseconds, based on a range of gridded topographic and population data. The outputs from this site suitability assessment are then combined with estimates for water availability in rain fed ponds and daily pond temperatures modelled using climate data representing late 20th century conditions and those found in a 2°C warmer world as projected by 13 Atmosphere and Ocean General Circulation Models (AOGCMs).

3.2 Methods and data

The modelling approach adopted in the current study consists of three key components or sub-models: 1) land suitability, 2) pond temperature, and 3) water availability for rain fed ponds. Both the pond temperature and water availability sub-models make use of observed climate data and are used in association with climate model projections to compare scenarios for a late 20th century base period with that for a world with a mean temperature increase of 2°C. Each of these sub-models are described individually along with examples of their combined use.

3.2.1 Land suitability

3.2.1.1 Overview of data and model structure

Variables such as land cover, topography, soil properties, and population density have a significant effect on an areas suitability for pond aquaculture. There are a number of examples in the literature of variables such as these being included in assessments of aquaculture site suitability through incorporation into spatial models within a GIS (e.g. Aguilar-Manjarrez and Nath, 1998, Giap et al., 2005, Hossain et al., 2007, Hossain et al., 2009, Hossain and Das, 2010, Kapetsky and Nath, 1997, Salam et al., 2005, Salam and Ross, 2000).

For the current study data describing soil properties (clay content, organic carbon content, and pH), slope, land cover, and population density are represented as a series of raster grids and combined within a GIS using weighted linear combination to indicate relative land suitability. Figure 3-4 provides a schematic overview of the land suitability sub-model structure.

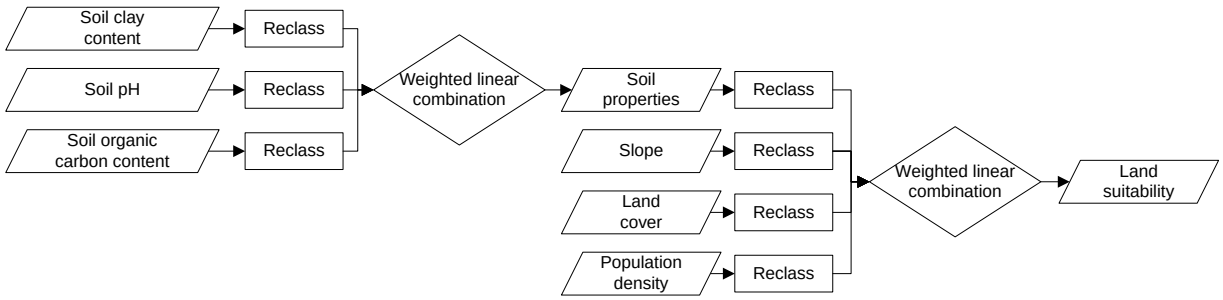

Figure 3-4: Land suitability sub-model structure.

3.2.1.2 Data standardisation

To allow differing data sets to be combined within the land suitability sub-model there is a need to reclassify or standardise the data to a common scoring system. This can be done either by reclassifying data to a number of discrete classes or by transforming data to a continuous series (e.g. between 0 and 1) (Eastman, 2012). A potential disadvantage of working with a small number of classes with inputs and outputs in integer format is that once data are combined less information is retained in the final output due to rounding. The current study makes use of a continuous range of integer values between 0 – 255 which in practical terms for site selection modelling purposes

achieves a similar result to a continuous series of floating point numbers (0 – 1) but has the advantage of allowing data to be stored in 8-bit format thus reducing storage and processing requirements for the large raster data layers involved (Drobne and Lisec, 2009).

In cases where data is represented over a continuous range (e.g. temperature) then points within the range are chosen that represent highest and lowest suitability. A continuous range of intermediate scores were then assigned using a fuzzy classification procedure. In cases where data is already in discrete classes such as in the case of land cover then classes were designated as ether: highly suitable, moderately suitable, or unsuitable and given scores of 255, 128, or 0 respectively to allow compatibility with the rest of the data and the modelling process.

A constraint class was applied in the case of variables where it was considered that certain conditions would make pond aquaculture practically impossible (e.g. pixels designated as urban areas in the case of land cover data). Constraint layers are applied throughout the model meaning that when all data layers are combined a single constraint class in one data layer will exclude that area regardless of suitability values in all other data layers.

3.2.1.3 Overview of soil properties for aquaculture ponds

The structure and composition of soil can influence it's suitability for forming aquaculture ponds. The main areas of interest in relation to pond construction are: the physical properties of the soil in relation to ease of working and ability to form structurally sound and watertight ponds, and the composition of the soil in relation to how it will influence water quality (Boyd et al., 2002, Boyd, 1990, New, 2002).

Boyd (1990) reviews soil suitability in relation to aquaculture ponds and defines a set of soil characteristic thresholds that can be used to place soils into one of three classes that are defined as having: slight, moderate or severe limitations for aquaculture. This set of basic classifications is further repeated in Hajek and Boyd (1994), Yoo and Boyd (1994), and Boyd (1995). The classification scheme originally provided by Boyd (1990) has been used as the basis for soil suitability classification in a number of GIS based studies of site suitability for pond aquaculture. These, along with other studies that have made use of reclassification of soil properties as part of GIS based models of aquaculture site suitability are detailed in Table 3-1.

Table 3-1: Overview of soil and slope suitability classification in a number of GIS based assessments of site suitability for pond aquaculture. Relevant parameters from Boyd (1990) are also included.

Study where soil and/or slope data have been used in relation to site selection for aquaculture	Parameters	Soil suitability classes used with values given in brackets	References cited in relation to classification of soil parameters in listed studies
Boyd (1990). Water Quality in Ponds for Aquaculture. Alabama Agricultural Experiment Station, Auburn University, AL, USA.	Clay content %	Slight limitation (>35), Moderate limitation (18-35), severe limitation (<18)	
	pH of bottom layer	Slight limitation (>5.5), Moderate limitation (4.5-5.5), severe limitation (<4.5)	
	Decomposed organic matter (soils <60% clay content)	Slight limitation (<4), Moderate limitation (4-12), severe limitation (>12)	
	Decomposed organic matter (soils >60% clay content)	Slight limitation (<8), Moderate limitation (8-18), severe limitation (>18)	
	Slope %	Slight limitation (<2), Moderate limitation (2-5), severe limitation (>5)	
Kapetsky (1994). A strategic assessment of warm water fish farming potential in Africa.	Soil texture	Seven soil classes defined by ESRI (1984) have been reduced to four suitability classes: Very suitable (>75% fine, 50-75% fine), moderately suitable (>75% medium, 50-75% medium), Marginally suitable (50-75% coarse, <50% all), Unsuitable (>75% coarse)	(ESRI, 1984) (ICLARM_and_GTZ, 1991)
	Slope %	Slope was taken from the FAO Soil Map of Africa where there are only three slope classes (0-8, 8-30, and >30 %). These classes reflect averages and are not the same as slope values calculated from a good quality DEM or contour map. The 0-8% slope areas were considered suitable for larger (1–5 ha) ponds, if slope is 1–2% and for 0.01–0.05 ha ponds, if slope is up to 5%. 8-30% areas where considered “mainly too steep for ponds, except in valley bottoms”. >30% areas were considered unsuitable.	

Aguilar-Manjarrez & Nath (1998). A strategic reassessment of fish farming potential in Africa.	Slope % Presence of a sulfidic layer, thickness of organic soil material, soil acidity, soil texture, depth and risk of flooding and soil depth	< 2% Most suitable, 2-5% Suitable, minor limitations can be overcome, 5-8% Moderate limitations that may be overcome via special design, construction, management or maintenance, >8% Unfit for use. These factors were considered based on guidance from Hajek and Boyd (1990). The exact methodology used to classify them in terms of soil suitability is unclear.	(Hajek and Boyd, 1994)
Kapetsky & Nath (1997). A strategic assessment of the potential for freshwater fish farming in Latin America.	Slope Effective soil depth (cm) Gravel and stones % Soil texture Salinity (dS/m) pH (H_2O) Catclays (sulphate toxic, very acid) Gypsum	Very suitable (0-2), Suitable to moderately suitable (2-8), Unsuitable (>8) Very suitable (>150), Suitable to moderately suitable (75-150), Unsuitable (<75) Very suitable (<40), Suitable to moderately suitable (40-80), Unsuitable (>80) Very suitable and suitable to moderately suitable (Loamy or clayey without swell-shrink, and not organic), Unsuitable (Sandy, or clayey with swell-shrink, or organic) Very suitable (<4), Suitable to moderately suitable (4-8), Unsuitable (>8) Very suitable (7.2-8.5), Suitable to moderately suitable (5.5-7.2), Unsuitable (<5.5, >8.5) Very suitable (Not present), Suitable to moderately suitable (Not present), Unsuitable (Present) Very suitable (Not present), Suitable to moderately suitable (Not present), Unsuitable (Present)	(Yoo and Boyd, 1994)

Hossain et al (2007). Multi-criteria evaluation approach to GIS-based land suitability classification for tilapia farming in Bangladesh	pH Salinity ppt Organic matter % C Soil Texture Slope %	Most suitable (6-8), Moderately suitable (4-6, 8-9), Not suitable (<4, >9) Most suitable (<2), Moderately suitable (2-4), Not suitable (>4) Most suitable (<1), Moderately suitable (1-2), Not suitable (>2) Most suitable (clay loam), Moderately suitable (sandy clay), Not suitable (loam, sand) Most suitable (<5), Moderately suitable (5-15), Not suitable (>15)	(FAO, 1976) (Hossain et al., 2003a) (Hossain et al., 2003b)
Hossain et al (2009). Integration of GIS and multicriteria decision analysis for urban aquaculture development in Bangladesh.	Slope % Soil Texture Soil pH Organic matter	Most suitable (<2), Moderately suitable (2-5), Not suitable (>5) Most suitable (clay loam), Moderately suitable (sandy clay), Not suitable (loam, sand) Most suitable (6-8), Moderately suitable (4-6, 8-9), Not suitable (<4, >9) Most suitable (<1), Moderately suitable (1-2), Not suitable (>2)	(FAO, 1976) (Hossain et al., 2003a) (Hossain et al., 2003b)
Salam & Ross (2000) Optimizing sites selection for development of shrimp (*Penaeus monodon*) and mud crab (*Scylla serrata*) culture in South western Bangladesh.	pH Salinity ppt Soil texture	Very suitable (6.5-9), moderately suitable (5.5-6.6), Marginally suitable (4.5-5.5), Unsuitable (<4.5, >9) Very suitable (8-26), moderately suitable (5-8, 26-32), Marginally suitable (4-5, 32-37), Unsuitable (<4.5, >9) Based on Kapetsky (1994). Seven soil classes defined by ESRI (1984) have been reduced to four suitability classes: Very suitable (>75% fine, 50-75% fine), moderately suitable (>75% medium, 50-75% medium), Marginally suitable (50-75% coarse, <50% all), Unsuitable (>75% coarse)	(Coche, 1985) (Kapetsky, 1994)

Hossain & Das (2010). GIS-based multi-criteria evaluation to land suitability modelling for giant prawn (*Macrobrachium rosenbergii*) farming in Companigonj Upazila of Noakhali, Bangladesh.	Slope % pH Organic matter % Organic carbon % Nitirte-N mg/l Phosphate-P mg/l Soil texture	Most suitable (<5), Moderately suitable (5-15), Not suitable (15) Most suitable (6-8), Moderately suitable (4-6, 8-9), Not suitable (<4, >9) Most suitable (<2), Moderately suitable (2-4), Not suitable (>4) Most suitable (<1), Moderately suitable (1-2), Not suitable (>2) Most suitable (<0.1), Moderately suitable (0.1-0.2), Not suitable (>0.2) Most suitable (<0.1), Moderately suitable (0.1-0.2), Not suitable (>0.2) Most suitable (clay loam), Moderately suitable (sandy clay), Not suitable (loam, sand)	(Hossain and Lin, 2001) (Hossain et al., 2003b) (New, 2002)
Giap, Yi & Yakupitiyage (2005). GIS for land evaluation for shrimp farming in Haiphong of Vietnam.	Slope Soil thickness (m) Soil type Soil pH Soil texture (% clay)	Highly suitable (<2), Suitable (2-5), Marginally suitable (5-10), Not suitable (>10) Highly suitable (>1), Suitable (0.5-1), Marginally suitable (<0.5), Not suitable (-) Highly suitable (Gley fluvisols), Suitable (Eutric fluvisols), Marginally suitable (Gleyic solonchaks, gleyic arenosols), Not suitable (Haplic calcisols) Highly suitable (6-7), Suitable (5-6), Marginally suitable (4-5,7-8), Not suitable (<4, >8) Highly suitable (>1), Suitable (0.5-1), Marginally suitable (<0.5), Not suitable (-)	(Hajek and Boyd, 1994)
Ragbirsingh & de Souza (2005). Site suitability for aquaculture development on the Caroni River Basin, Trinidad West Indies, using GIS.	Slope (deg) Clay %	Optimal (0-3), suitable (3-6), marginal (6-9), unsuitable (>9) Optimal (>30), suitable (20-30), marginal (20), unsuitable (<20)	(Aguilar-Manjarrez and Nath, 1998) (Kapetsky, 1994)

The soil classification guidelines originally provided by Boyd (1990) suggest a relatively high clay content is desirable in order for ponds to have good water retention properties. This view has been supported by a number of subsequent authors who have applied it in a range of site selection studies (see Table 3-1 for references). It is worth noting however that in Boyd et al. (2002) the authors suggests that previous recommendations (e.g. Boyd and J.R., 1997, Hajek and Boyd, 1994) for the use of soils with a high clay content should be reconsidered and potentially disregarded. It is suggested that heavy clay soils can be difficult to work with from an engineering point of view, proving difficult to spread in layers and compact, and may result in erodible and potentially unstable embankments with poor load bearing capacity. Boyd et al. (2002) cites McCarty (1998) who suggests that provided a good mixture of particle sizes are present then soils with a clay content of 5 to 10% may be preferable to high clay content soils when constructing embankments. Tucker and Hargreaves (2008) suggest that high clay content soils may be difficult to work and that a clay content of 15% is preferable with a content as low as 5-10% being suitable for embankments if soil is well graded. New (2002) suggests that soils that consist of silt or clay have good water retention properties although soil with clay content higher than 60% is prone to cracking when dried. It is also possible that priorities will vary between aquaculture systems in relation to size, construction methods and water supply. For example it seems likely that a large scale aquaculture development with access to a permanent water supply may have different priorities to smaller scale ponds that are dependent on more intermittent water supplies or rainfall. The current study aims to be relevant to as broad a range of pond culture scenarios as possible. That said, the requirements of smaller scale producers with limited capital investment and perhaps greater dependence on rainfall and / or intermittent water sources are considered here as especially relevant in terms of potential susceptibility to climate related changes. With all of the above in mind it was decided to assign highest suitability to soils with moderate clay content while those very high or low values were considered less suitable.

Water in ponds with acidic soils tends to have low total alkalinity as a result of low levels of bicarbonates and carbonates. The result is a reduced ability to buffer falling pH values associated with the breakdown of organic matter in aquaculture ponds. The addition of limestone to aquaculture pond soils has the effect of increasing soil ph and raising alkalinity levels in pond water thus buffering pH against potential decreases and large diurnal fluctuations in association with photosynthetic activity and dissolved carbon dioxide concentrations. The addition of lime also has the potentially beneficial effects of increasing total hardness in association with an increased concentration of

calcium ions, and providing a source of inorganic carbon that can help support photosynthesis. Selecting areas for pond development where soils naturally have a higher pH will reduce the need for additional liming and are thus considered more suitable (Boyd et al., 2002).

Soils with a high organic matter content are generally considered of low suitability for aquaculture pond construction. Egna and Boyd (1997) suggest that while a small amount of organic matter may be beneficial in increasing the cation exchange capacity of the soil, the decomposition of excess organic matter can result in anaerobic conditions at the soil-water interface with the potential for the release of reduced substances such as (NO_2, NH_3 and H_2S). The authors also suggest that soils with a high organic matter content are prone to excessive settling and thus have poor physical properties for pond construction.

3.2.1.4 Soil data choice and classification

The current study makes use of the Harmonized World Soil Database (HWSD) version 1.2 (FAO/IIASA/ISRIC/ISS-CAS/JRC, 2012) which represents a combination of a number of regional and national soil databases with the FAO-UNESCO Digital Soil Map of the World and as such provides the most complete source of soil data at the global scale. There were a few areas within the HWSD where no data values are given. Where possible these gaps were filled using a data from the World Soil Information(ISRIC) World Inventory of Soil Emission Potentials (WISE) data set (Batjes, 2009). There were a few remaining areas where data were not available from either data set. These areas were typically in desert regions and it is possible that they contain little in the way of useable soil and are generally in areas that are unlikely to be suitable for aquaculture. However, because no absolute constraints against aquaculture development were derived from soil data in the current study, the decision was taken to fill any gaps using mean values derived from the surrounding area.

Not all soil variables described by Boyd (1990) are found within the HWSD and thus available at the global scale. The current study makes use of data for soil clay content, pH, and organic carbon content. Suitability scores were assigned to these variables based on the points discussed in the soil properties section along with review of the classification system suggested by Boyd (1990) and a number of previous GIS based assessments of aquaculture site suitability that are summarised in Table 3-1 while details of suitability scores used for soil properties in the current assessment are given

in Table 3-2. In the case of soil no areas were considered as constraints based on the rationale that: a) the spatial representation of the soil database in many areas takes the form of large polygons with often distinct changes between neighbouring polygons. In reality there will be a more or less gradual shift between soil types when moving from one area to the next while at the same time there may well be local variations within polygons with regards to suitability. b) Many issues with soil can be overcome via engineering solutions meaning while making soil suitable for aquaculture in some areas may be more difficult and expensive it does not represent a constraint in the same way that large water bodies or heavily urbanised areas might.

Table 3-2: Values used for fuzzy classification of soil data .

Soil or terrain variable	High suitability	Medium suitability	Low suitability	Graphical representation
Ph	6	5	<4.5	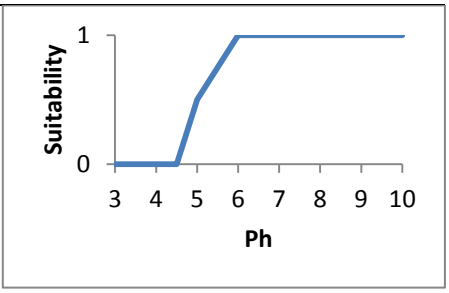
Clay content %	20 to 40	15 and 50	10 and 60	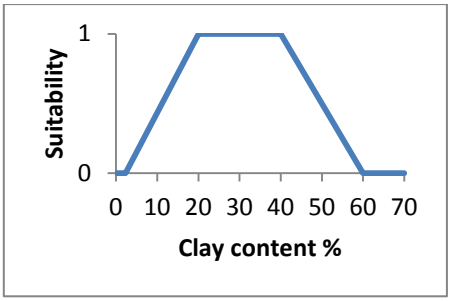
Organic Carbon %	< 2.3	4.65	7	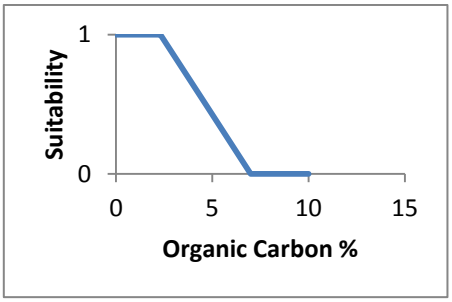

3.2.1.5 Slope - data choice and classification

Sloped terrain will generally increase the costs of aquaculture pond construction meaning that relatively flat areas are seen as preferable (Aguilar-Manjarrez and Nath, 1998). Slope values can be computed from elevation data (digital elevation model or DEM) within a GIS and have been used in previous aquaculture site suitability exercises (See Table 3-1). Currently the highest resolution globally available and consistent source of elevation data that is useable comes from the Shuttle Radar Topography Mission (SRTM) (Jarvis et al., 2008). SRTM data is available globally at 3 arc-second resolution (approximately 90m at the equator) with global coverage between 60 degrees latitude north and south. ASTER GDEM is a global DEM with a 1 arcsecond resolution which initially looks extremely promising. However inspection of the data finds it to be heavily contaminated with noise and artefacts making it a poor choice in relation to SRTM, a view that has been supported by other reviewers (e.g. Guth, 2010).

It is worth noting that the resulting slope, when calculated from a DEM, can be significantly affected by the resolution of the elevation data with lower resolutions resulting in reduced slope values. This effect is demonstrated in Figure 3-5 where 3 arcsecond SRTM data is used to compute slope values using the IDRISI GIS package. Images are also provided that show slope values for the same area but at the lower resolutions of 10 and 30 arcseconds. For each of the lower resolutions two images are given. One is produced by resampling the 3 arcsecond slope values to 10 and 30 arcseconds, while the other is produced by resampling the 3 arcsecond DEM to 10 and 30 arcseconds and then using these lower resolution DEMs to compute slope values. Through visual inspection of the images it can be seen that by reducing the resolution of the DEM there is an overall tendency for lower slope values to be produced. Along with this there is a notable loss of detail, especially in the case of the 30 arcsecond resolution examples . With the above in mind slope values for the current study were calculated at 3 arcsecond resolution and the results were then aggregated to a 10 arcsecond grid in common with other model components.

Reclassification of slope data into a common scoring system was guided by a number of previous studies (see Table 3-1 for details) while details of values used to guide fuzzy assignment of suitability scores are provided in Table 3-3.

Table 3-3: Slope values used to guide suitability classification in the current study.

Soil or terrain variable	High suitability	Medium suitability	Low suitability	Constraint
Slope %	<2	5	8	>15

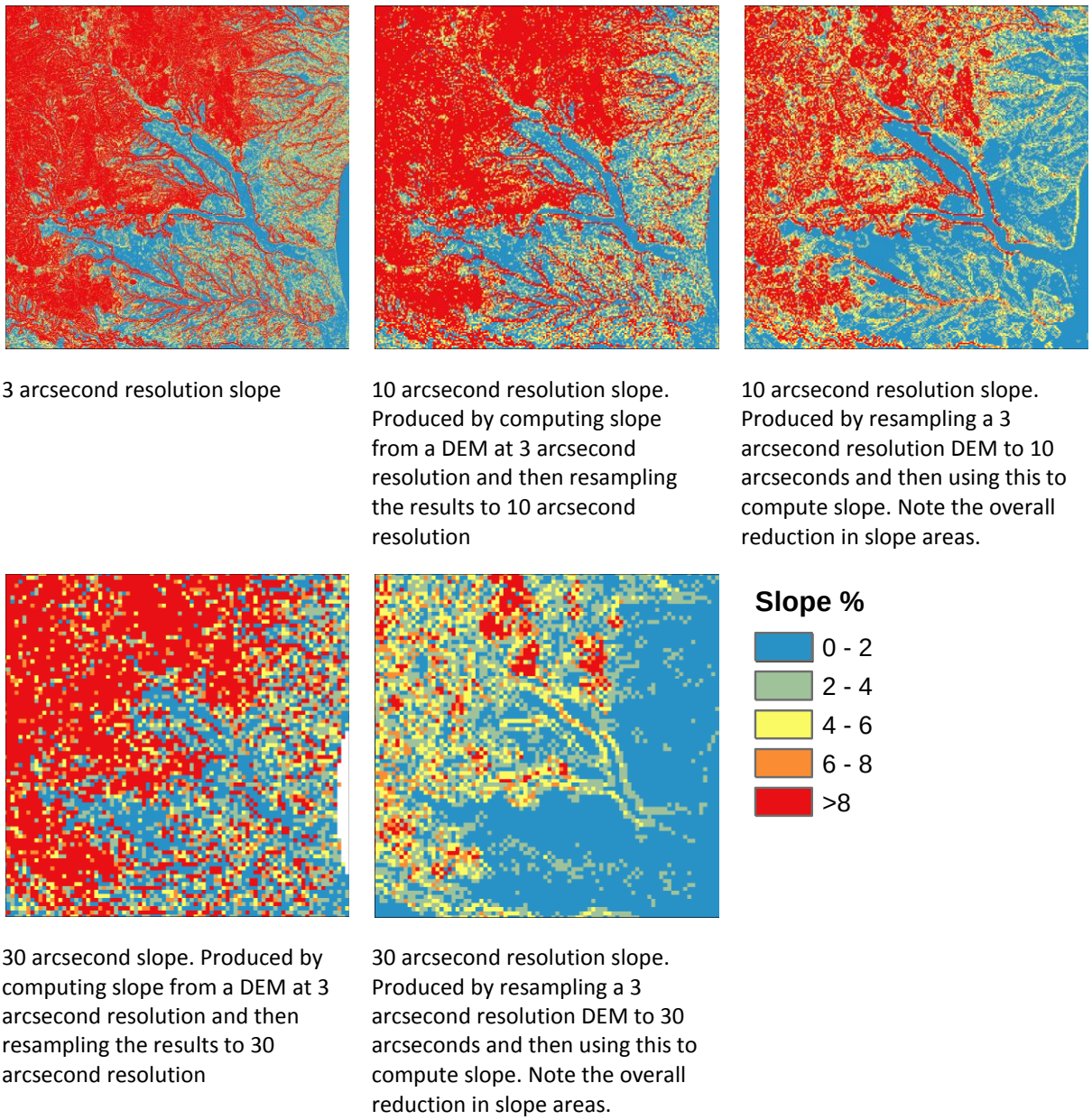

3 arcsecond resolution slope

10 arcsecond resolution slope. Produced by computing slope from a DEM at 3 arcsecond resolution and then resampling the results to 10 arcsecond resolution

10 arcsecond resolution slope. Produced by resampling a 3 arcsecond resolution DEM to 10 arcseconds and then using this to compute slope. Note the overall reduction in slope areas.

30 arcsecond slope. Produced by computing slope from a DEM at 3 arcsecond resolution and then resampling the results to 30 arcsecond resolution

30 arcsecond resolution slope. Produced by resampling a 3 arcsecond resolution DEM to 30 arcseconds and then using this to compute slope. Note the overall reduction in slope areas.

Figure 3-5: Illustration of the effect of differing resolution DEM resolution and resampling sequence on resulting slope values.

3.2.1.6 Land cover

Land cover plays a significant role in determining site suitability for aquaculture. For example areas that are currently used for crop production can often be converted relatively easily while forested areas will require more effort and in some areas are perhaps likely to raise more concern in terms of environmental impacts. Dense urban areas are likely to be completely unsuitable and can be considered as constraints to aquaculture pond development.

Detailed mapping produced through traditional survey methods is available for some regions of the world although in many cases such data would need significant processing before it could be used within a GIS. Along with processing constraints another major limitation when considering using maps based on traditional survey methods is that such data will be incomplete, inconsistent, and/or inaccessible when viewed at the global scale. An alternative, and increasingly acceptable, option is the use of remotely sensed data.

Over recent decades the use of remotely sensed data derived from satellite observations has played an increasingly significant role with regard to estimating land cover at a range of scales and resolutions. The use of remotely sensed imagery and it's classification into useful land cover maps is well established with most classification based around the use of multispectral images where surface reflectance values at multiple points within the electromagnetic spectrum are related to known values for land cover types based on ground observation of random sample points (Jensen, 2006). Classification can be based on a sample from a single time period or from a time series of images where the extra dimension of time may help in image classification such as in the case of seasonal vegetation types (Brown et al., 2013, Mingwei et al., 2008, Van Niel and McVicar, 2004, Wardlow and Egbert, 2008, Wardlow et al., 2007, Zhang et al., 2008) as well as allowing for the study of seasonal events such as flooding (e.g. Handisyde et al., 2014, Islam et al., 2010, Sakamoto et al., 2007).

The quantity and quality of remotely sensed data have increased considerably during recent years with sensors such as GoeEye-1, Pléiades, and WorldView-1 offering sub metre resolution imagery in the panchromatic band, with multispectral images at two metres or less. While high resolution imagery offers many advantages for land cover classification, such as reduced likelihood of individual pixels containing more than one land cover type, it is impractical when working with large areas, i.e.

globally due to potential processing and storage requirements as well as cost of obtaining the data itself.

A number of freely available global land cover products exist based on a range of remotely sensed data with moderate resolutions between approximately 1km and 300m at the equator. As well as differing resolutions there are considerable differences between currently available global land cover datasets in terms data acquisition dates, sensors, classification schemes and methods, and methods of verification and accuracy assessment. The key attributes of currently available data sets are detailed in Table 3-4 along with references to key documents that detail the development and verification of the datasets. Along with these developer produced descriptions there have been a number of independent efforts to compare global land cover products (Fritz et al., 2011, Hansen and Reed, 2000, Herold et al., 2008, Kaptué Tchuenté et al., 2011, Nakaegawa, 2011), and assess their quality in relation to control points (Fritz et al., 2011). For a comparison between datasets to be made there is generally a need to translate land cover classes to a single legend (Fritz et al., 2011, Herold et al., 2008, Kaptué Tchuenté et al., 2011, Nakaegawa, 2011). The fact that data is represented on grids of differing resolutions and projections represents an additional challenge when comparing land cover datasets and an approach of reconciling data to a common grid is often taken. For example Fritz et al. (2011) used an aggregation approach that considered the minimum and maximum of the class percentage as well as spatial coverage within new grid cells to reconcile GLC-2000, GlobCover, and MODIS v5 to a common geographic (latitude longitude) grid with a 0.125^{o} resolution in order to examine agreement and accuracy of cropland and forest representation between the three datasets. For accuracy assessment Fritz et al. (2011) used validation data published in Mayaux et al. (2006), Friedl et al. (2010) and Bicheron et al. (2008). Fritz et al (2011) conclude that considerable differences exist between land cover datasets, especially in relation to cropland representation with a total area of 360Mha considered as cropland in GlobCover that is designated as non cropland in MODIS v.5, an area that represents around 20% of total global cropland. (Fritz et al., 2011) also suggest that thematic accuracy of the newer higher resolution data sets (MODIS v.5 and GlobCover) is no better than CLC-2000 and in the case of GlobCover is actually worse when considering the classification of cropland and forests (see Table 3-5).

Table 3-4: Details of freely available global land cover products derived from satellite data.

Land cover product	Sensor - spatial resolution	Year of data collection	Number of classes and nomenclature	Classification method	Reference
UMD	AVHRR - 1/100°	1992-1993	14 simplified IGBP	Global - Supervised classification decision tree	Hansen et al., (2000)
IGBP-DISCover	AVHRR - 1/100°	1992-1993	17 IGBP	Continent-by-continent - unsupervised clustering with post classification refinement	Loveland et al. 2000
GLC2000	VGT-1 - 1/112°	2000	22 LCCS	Regional - Flexible based on local expertise	Mayaux et al. (2004)
MODIS v5	MODIS - 1/240°	2005	17 IGBP	Global - Supervised classification using decision tree	Friedl et al. (2010)
GLOBCOVER	MERIS - 1/360°	2004-2006	22 LCCS	Regional - Flexible based on local expertise	Arino et al. (2008)

Table 3-5: Results of accuracy assessment of MODIS, GlobCover, and CLC2000 in predicting forest and cropland cover. Adapted from Fritz et al (2011).

Dataset	Overall accuracy assessment %	
	Forest	Cropland
CLC2000	81	76
MODIS v.5	80	77
GlobCover	60	57.6

Herold et al. (2008) compared four 1km resolution global land cover data sets (GLCC, GLCF, MODIS 1k, and GLC2000). The authors standardised the different data sets to 13 common classes based on LCCS definitions. The paper reviews previous attempts to assess the accuracy of the data sets and proposes average global accuracy figures of: 66.9% (GLCC), 68.6% (GLC2000), and 78.3% (MODIS). However the authors go on to caution against assuming that MODIS is necessarily superior to the other data sets as

the validation methods used vary as does the number of classes and thus detail of the legends. Herold et al. (2008) go on to evaluate class specific accuracy by aggregating error matrix data for GLC2000 (Mayaux et al., 2006), MODIS 1k (MODIS_land_cover_team, 2003), and GLCC (Scepan, 1999) to 13 common classes. The results suggest that different data sets perform better for certain classes and that in many cases spatial agreement between the three data sets examined is low with values ranging from 23.4 to 83.1 percent dependant on class. Herold et al. (2008) also suggest that all datasets have low accuracy when attempting to represent areas of mixed trees, shrublands, and herbaceous vegetation as there is often a mixture of life forms within each pixel. This contrasts to more "pure" categories such as snow, bare ground and evergreen broadleaf forests. The authors suggest that there is potential for improvement through better definition of mixed classes and the use of higher resolution remotely sensed data.

Kaptué Tchuenté et al. (2011) compared landcover data for Africa from four data sets: ECOCLIMAP-II, GLC2000, MODIS LC-I, and GLOBCOVER. All the data sets were aggregated to 7 common classes representing: Forest/mixed forest, Woodland/shrubland, Cropland, Grassland, Bare land, Inland water, and Urban and built-up areas. Figure 3-6 (from: Kaptué Tchuenté et al., 2011) shows the areas represented by each aggregated class for the four data sets. While the urban, bare land, and inland water classes are fairly consistent in the extent of their coverage there are large discrepancies in the other classes, especially in the case of woodland/shrubland. The Authors also examined agreement between the four products by using each map as a reference and seeing how well the others represent it. While there is considerable variability between classes overall accuracies ranged from 56.25 to 68.76 percent. Kaptué Tchuenté et al. (2011) conclude that even though there may have been some change in land cover between the acquisition dates of the remotely sensed data used by the four products it cannot account for the considerable variation seen. The authors also highlight the difficulties of accurately representing land cover using moderate resolution imagery when several land cover types are present and suggest that higher resolution imagery could be of benefit.

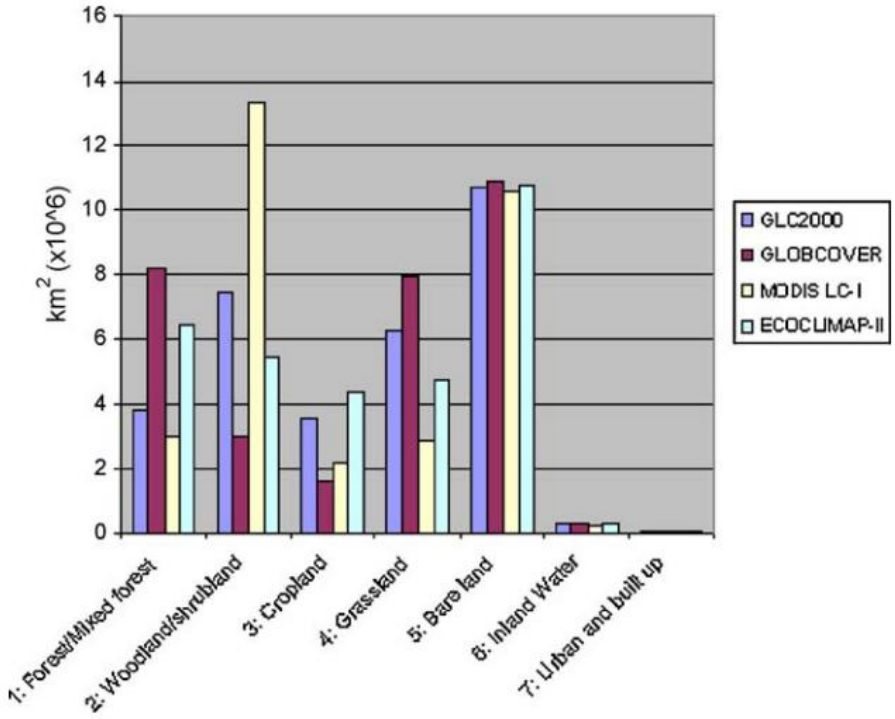

Figure 3-6: Differences between land cover products in representing land cover over the African continent (from: Kaptué Tchuenté et al., 2011).

In cases of mixed cover within a pixel the sensor receives an average surface reflectance value for the different land cover types for each spectral band being recorded. The studies outlined above suggest that while attempts are often made to classify 'mixed' pixels, doing so with a high degree of accuracy can prove very difficult with potential for mixed pixel inaccuracies increasing in relation to pixel size. As a result existing global land cover data sets derived from moderate resolution remotely sensed data tend to be better at representing larger homogenous areas rather than areas where land cover is mixed over relatively small spatial scales. Friedl et al. (2010) describe version 5 of the MODIS land cover product which is available at an equatorial resolution of approximately 500m compared with 1km for the previous version. The authors suggest that for fragmented land cover types such as urban areas the higher resolution found in the MODIS version 5 products provides a significantly better representation of land cover. In many developing regions, where pond-based aquaculture is significant, land use patterns are often intricate with stakeholders being concerned with relatively small parcels of land. It seems likely that higher resolution land cover data sets will provide

advantages in such areas despite not necessarily showing improved performance globally compared to lower resolution data sets when aggregated to a common lower resolution grid.

Given the potential benefits of higher resolution data along with the more recent acquisition of surface reflectance data used in the MODIS version 5 and GlobCover products the decision was taken to use these to describe land cover within the current model. Due to the differences between the two data sets and the categorical nature of the data they contain it was decided that the best approach was to run the model twice, once for each data set. This generates two separate outcomes where the only difference in inputs is the land cover data used. Land cover data makes a considerable difference to the final model output in some areas both in terms of suitability values and through the use of constraint classes. This combined with a lack of evidence suggesting superiority of one data set over supports the use of this two outcome approach. MODIS data were resampled from 15 arcsecond to 10 arcsecond resolution based on nearest neighbour values to match the resolution of GlobCover and the SRTM derived slope data within the model.

3.2.1.6.1 Reclassification of land cover data sets

A number of previous studies have used land cover data within a GIS to help guide site selection for aquaculture. For example Hossain et al. (2007) used land cover as part of a multicriteria evaluation approach to model site suitability for tilapia farming in Bangladesh while Hossain and Das (2010) conducted a similar study with the aim of modelling site suitability for *Macrobrachium rosenbergii* production. In both studies land was classified as: existing aquaculture and grasslands are considered 'most suitable', Paddy cultivation areas are considered 'moderately suitable and mixed orchard and seasonal vegetable cultivation areas are considered 'not suitable'. Giap et al. (2005) used land cover within a GIS based model of site suitability for shrimp farming in Haiphong, Vietnam. Areas of current aquaculture pond were classified as 'highly suitable', rangeland and salt farm were classified as 'suitable', agricultural land as 'marginally suitable', and mangroves, villages and mixed orchards and 'not suitable'. In an evaluation of site suitability for small semi-intensive pond culture of *Tilapia sp., Hoplosternum littorale* and *Macrobrachium rosenbergii,* Ragbirsingh and De Souza (2005) list Forest reserve, Industry, Institution, Quarry, Recreation, Residential, and Swamp as unsuitable land use criteria while Agriculture and Mixed Forest are considered suitable with no distinction made between the two despite the modelling process allowing for three different levels of suitability.

As land cover data is categorical rather than continuous it is not possible to standardise the data over a continuous range of numbers in the same ways as were done for soil properties and slope values. Instead all land cover classes were reclassified as having high, medium, or low suitability, or as a constraint class. The high, medium and low suitability classes were assigned values of 0, 128, and 255-255 and as such fit with the continuous values used for other data within the modelling process.

One approach to using both GlobCover and MODIS data would be to first standardise the data set to a common set of classes as done by authors wishing to compare land cover data sets (e.g. Bai, 2010, Herold et al., 2008, Kaptué Tchuenté et al., 2011), and then assign suitability classes to these. As has already been discussed the current study aims to generate two separate outcomes, one for MODIS and the other for GlobCover data. With this in mind, and as the aim is to evaluate suitability for aquaculture rather than assess differences between land use data sets *per se*, the view was taken that rather than using the middle step of transforming both data sets to a common set of classes before assigning suitability the best approach was to assign suitability ratings to the data set as they stand. This also reduces the chance of aquaculture relevant details getting lost in the translation process. Details of the classes found in the GlobCover and MODIS data sets and their reclassification can be found in Table 3-6 while an example of the two resulting classification outcomes is shown for the Ghana area in Figure 3-7.

Table 3-6: Details of MODIS and GlobCover classes and their reclassification for use in the current study.

MODIS IGBP	MODIS details	GlobCover LCCS classes
0 Water bodies	Oceans, seas, lakes, reservoirs, and rivers. Can be either fresh or salt– water bodies.	210 Water bodies
1 evergreen needleleaf forest	Lands dominated by needleleaf woody vegetation with a percent cover >60% and height exceeding 2 m. Almost all trees remain green all year. Canopy is never without green foliage.	70 Closed (>40%) needleleaved evergreen forest (>5m)
2 Evergreen broadleaf forest	Lands dominated by broadleaf woody vegetation with a percent cover >60% and height exceeding 2 m. Almost all trees and shrubs remain green year round. Canopy is never without green foliage.	40 Closed to open (>15%) broadleaved evergreen and/or semi-deciduous forest (>5m) 160 Closed (>40%) broadleaved forest regularly flooded - Fresh water 170 Closed (>40%) broadleaved semi-deciduous and/or evergreen forest regularly flooded – Saline water
3 Deciduous needleleaf forest	Lands dominated by woody vegetation with a percent cover >60% and height exceeding 2 m. Consists of seasonal needleleaf tree communities with an annual cycle of leaf-on and leaf-off periods.	90 Open (15-40%) needleleaved deciduous or evergreen forest (>5m)
4 Deciduous broadleaf forest	Lands dominated by woody vegetation with a percent cover >60% and height exceeding 2 m. Consists of broadleaf tree communities with an annual cycle of leaf-on and leaf-off periods.	50 Closed (>40%) broadleaved deciduous forest (>5m)
5 Mixed forests	Lands dominated by trees with a percent cover >60% and height exceeding 2 m. Consists of tree communities with interspersed mixtures or mosaics of the other four forest types. None of the forest types exceeds 60% of landscape.	100 Closed to open (>15%) mixed broadleaved and needleleaved forest (>5m)
6 Closed shrublands	Lands with woody vegetation less than 2 m tall and with shrub canopy cover >60%. The shrub foliage can be either evergreen or deciduous.	110 Mosaic Forest/Shrubland (50-70%) / Grassland (20-50%)
7 Open shrublands	Lands with woody vegetation less than 2 m tall and with shrub canopy cover between 10% and 60%. The shrub foliage can be either evergreen or deciduous.	150 Sparse (>15%) vegetation (woody vegetation, shrubs, grassland)

8 Woody savannas	Lands with herbaceous and other understory systems, and with forest canopy cover between 30% and 60%. The forest cover height exceeds 2 m.	60 Open (15-40%) broadleaved deciduous forest (>5m)
9 Savannas	Lands with herbaceous and other understory systems, and with forest canopy cover between 10% and 30%. The forest cover height exceeds 2 m.	120 Mosaic Grassland (50-70%) / Forest/Shrubland (20-50%) 130 Closed to open (>15%) shrubland (<5m)
10 Grasslands	Lands with herbaceous types of cover. Tree and shrub cover is less than 10%.	140 Closed to open (>15%) grassland
11 Permanent wetlands	Lands with a permanent mixture of water and herbaceous or woody vegetation. The vegetation can be present either in salt, brackish, or fresh water.	180 Closed to open (>15%) vegetation (grassland, shrubland, woody vegetation) on regularly flooded or waterlogged soil - Fresh, brackish or saline water
12 Croplands	Lands covered with temporary crops followed by harvest and a bare soil period (e.g., single and multiple cropping systems). Note that perennial woody crops will be classified as the appropriate forest or shrub land cover type.	11 Post-flooding or irrigated croplands 14 Rain-fed croplands
13 Urban and built up	Land covered by buildings and other man-made structures.	190 Artificial surfaces and associated areas (urban areas >50%)
14 Croplands/natural vegetation	Lands with a mosaic of croplands, forests, shrubland, and grasslands in which no one component comprises more than 60% of the landscape.	20 Mosaic Cropland (50-70%) / Vegetation (grassland, shrubland, forest) (20-50%)
		30 Mosaic Vegetation (grassland, shrubland, forest) (50-70%) / Cropland (20-50%)
15 Snow and ice	Lands under snow/ice cover throughout the year.	220 Permanent snow and ice
16 Barren or sparsely vegetated	Lands with exposed soil, sand, rocks, or snow and never have more than 10% vegetated cover during any time of the year.	200 Bare areas

High suitability: green shading	Medium suitability: yellow shading	Low suitability: Pink shading	Constraint areas: grey shading

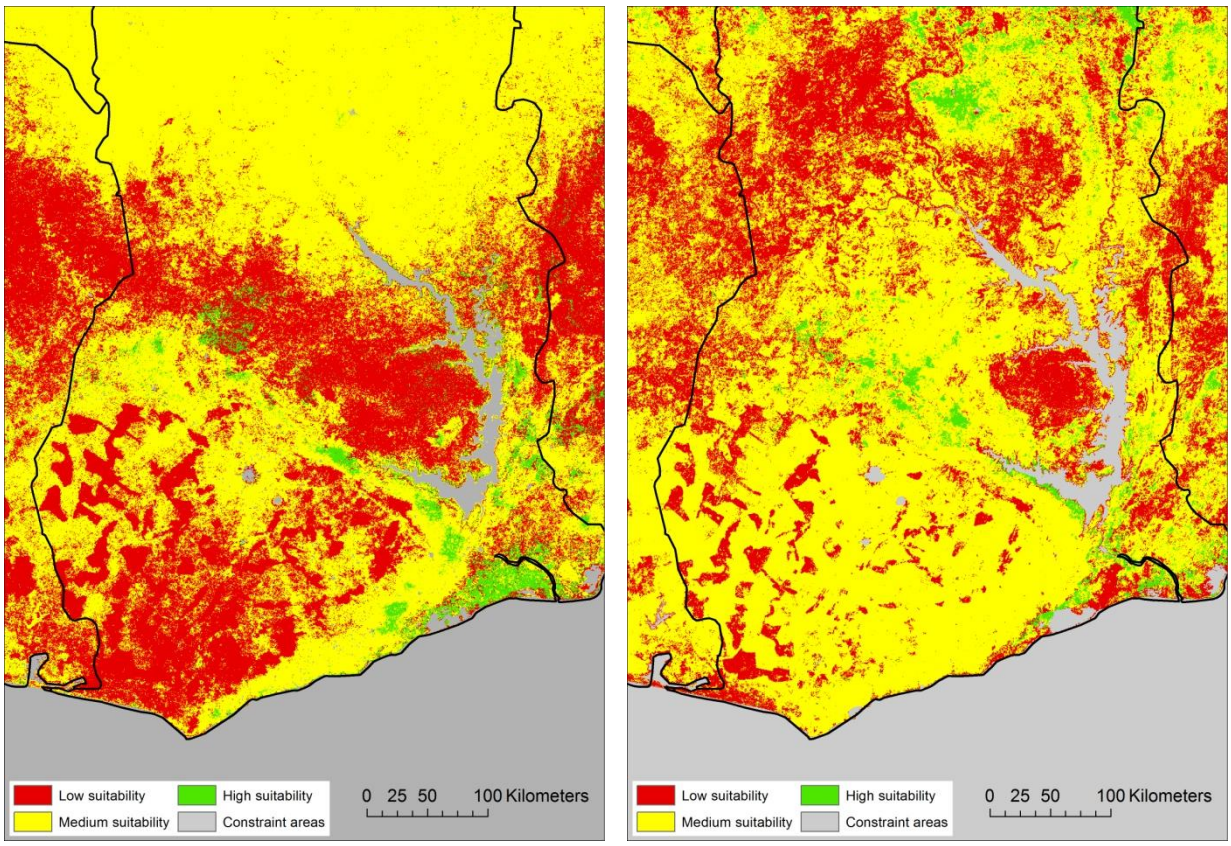

Reclassification of MODIS land cover data Reclassification of GlobCover data

Figure 3-7: Reclassification to MODIS and GLobCover global land cover data sets based on the classification scheme outlined in Table 3-6.

3.2.1.7 Population density

The use of population density data within site selection models for aquaculture production is common and acts as indicators of labour availability (Hossain et al., 2009, Hossain and Das, 2010), potential pollution and/or other negative impacts associated with high population densities and (Giap et al., 2005), competing uses for land, and market potential (Aguilar-Manjarrez and Nath, 1998, Salam et al., 2003).

3.2.1.7.1 Data choice

A number of global gridded population density data sets are available and these are summarised in Table 3-7 while sample regions are displayed in Figure 3-8. The Gridded population of the World (GPW) data uses the original census units meaning that while data is represented on a 2.5 arcminute grid in practical terms the data is represented by polygons of varying size which for many areas

means that the effective resolution is low. The Global Rural-Urban Mapping Project (GRUMP) data set is represented on a 30 arcsecond grid and is essentially the same as the GPW data set in its use of census units. The differences are: the increased resolution, that it is only available up until the year 2000, and it includes a minimal modelling component that considers urban areas based on night time light data. The LandScan data set also uses a 30 arcsecond resolution but differs from GRUMP in that it is a highly modelled data set using a greater number of input data sources. It is also more up to date compared to GRUMP providing estimates for the year 2008 as opposed to 2000 for GRUMP. There have been very few attempts to evaluate and compare gridded global population density data sets. Tatem et al. (2011) investigated the effect of spatial population data set choice when estimating disease risk and noted that the choice of data set makes a considerable difference to the outcome. Hall et al. (2012) compare population grids from Landscan, GPW, GRUMP, and the population density grid of the EU-27+ data set (Gallego, 2010) for an area of Sweden. The authors conclude that, while considerable differences occur between the data sets, statistically LandScan performs best. They also note that, surprisingly, the EU-27+ and GRUMP data sets showed significant inaccuracies in their estimates of total population for the study region.

LandScan 2008 data is chosen over the other gridded global population data sets as it appears to provide advantages in terms of resolution (both actual grid and ability to disaggregate census polygons), up to date representation, and potentially accuracy.

Table 3-7: comparison of gridded global population density data products.

Dataset	Time periods represented	Spatial resolution	Input data used	Reference
LandScan	2008	30 arcseconds	Census (CIA), land cover, elevation, slope, roads, populated areas/points	(Landscan, 2008)
Gridded Population of the World (GPW)	1990, 1995, 2000, 2005, 2010, 2015	2.5 arcminutes	Census (UNPD), water bodies.	(SEDAC/CIESIN, n.d.)
Global Rural Urban Mapping Project (GRUMP)	1990, 1995, 2000	30 arcseconds	Census (UNPD), populated areas, water bodies.	(CIESIN, n.d.)

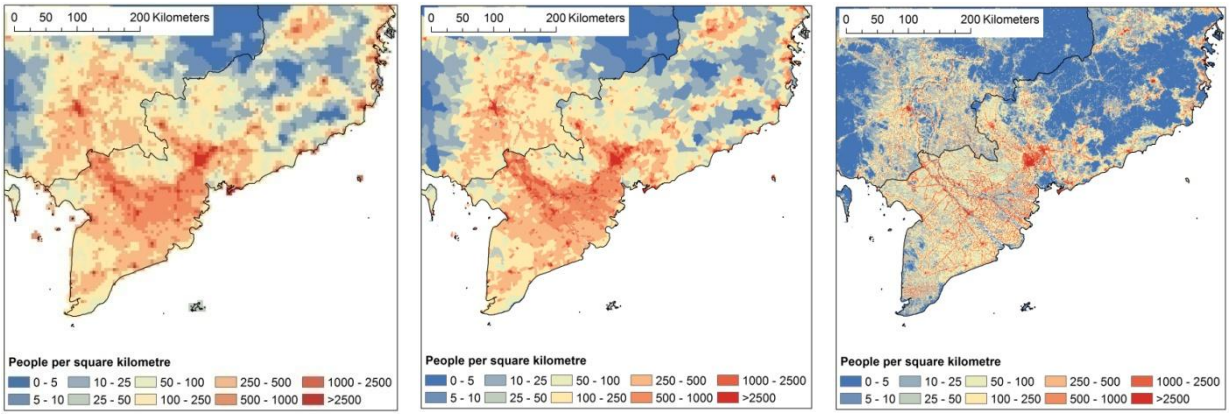

GPW GRUMP LandScan

Figure 3-8: Examples of outputs from currently available gridded global population density datasets.

3.2.1.7.2 Population density data - processing and classification

A review of existing literature shows considerable diversity in terms of reclassifying population density data in relation to site suitability for aquaculture (Table 3-8). It seems likely that the average population density over the study areas within the reviewed literature has played a role in influencing views of what constitutes high and low population densities and thus thresholds of high and low suitability for aquaculture. What can be concluded when the literature is viewed as a whole is that areas of very high or very low population densities are less favourable and in extreme cases may be considered as constraints.

Table 3-8: Use of population density data in relation to aquaculture site suitability.

Reference	Use of population density data	Notes
(Hossain et al., 2009)	3 classes under the heading of 'labour availability' (individuals per km2): Most suitable >100, moderately suitable (50-100), not suitable (<50).	Investigates site suitability for carp farming in urban water bodies in Chittagong, Bangladesh. Uses an MCE approach.
(van Brakel and Ross, 2011)	Classes based on people per km2: <1 = remote, 1-10 = sparsely populated, 10-100 = rural low density, 100-500 = rural high density, 500-5000 = peri-urban, >5000 = urban.	Investigates potential market access for poor people involved with aquaculture. Uses Bayesian model.
(Hossain and Das, 2010)	3 classes under the heading of 'labour availability' (individuals per km2): Most suitable >100, moderately suitable (50-100), not suitable (<50).	Models prawn farming potential. Gives New (2002) and Hossain et al. (2007,2009) as sources for this classification.
(Hossain et al., 2007)	3 classes for population density: <1000 = suitable, 1000-1500 = moderately suitable, >1500 = not suitable. N.B. there is a constraint layer for areas where aquaculture would not be allowed.	There isn't any obvious information about why or how the population density was classified. Giap et al (2005) is given as a reference.
(Giap et al., 2005)	4 classes for population density: <500 = highly suitable, 500-1000 = suitable, 1000-2000 = marginally suitable, >2000 = unsuitable.	Some reference in the results section to how high population areas can impact on shrimp farming via domestic wastes.

For the current study a single data layer was created with the aim of expressing site suitability in relation to population density using a continuous scale of 0 to 255 with 255 being most suitable by using the following methodology.

Landscan 2008 population density data were reclassified on a linear scale of suitability (255 – 0) with a population density (people per km^2) of 100 equalling 255 and 2000 or greater equalling 0. Higher suitability is attributed to lower population density areas as here competition for land and potential pollution impacts are likely to be less. Areas with population densities of less than 100 people per km^2 are considered to be sparsely populated with a potential lack of human resources required for aquaculture production. As the LandScan population density data is represented on a grid with individual cells representing an area of less than one square kilometre it is necessary to consider the population density of nearby cells from which potential labour sources may be available. With this in mind for areas with a population density of less than 100 people per km^2 for each cell an average

value was calculated for all cells within a 5 cell radius. The result was reclassified on a linear scale ranging from a maximum (most suitable) value of 255 for values of 100 or greater down to 0 for values of 10 or less.

A constraint class was applied very sparingly for areas with extremely low and high population densities using focal statistics and a series of Boolean intersections, and based on the assumption that availability of potential fish farm workers along with other goods and services is likely to be limited in unpopulated areas while extremely dense populations will typically represent urban areas where competition for space is likely to be high along with potential pollution risks. Details of how the population density constraint layer was constructed are given in Figure 3-9. The mean value from the 25 pixel radius filter is aimed at identifying extremely sparsely populated regions while the mean value from the 5 pixel radius filter is aimed at identifying small population centres that may be present as single pixels whose surrounding area may be suitable for aquaculture production.

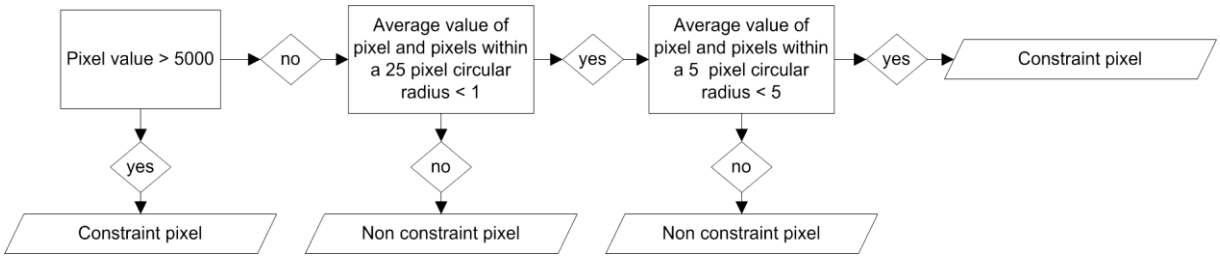

Figure 3-9: Designation of constraint pixels when classifying LandScan population density data. All values represent people per km^2.

3.2.1.8 Layer combination

In order to combine data within the land suitability sub-model all layers were resampled to a common 10 arcsecond resolution grid based on nearest neighbour values. Combination of data layers followed a hierarchical structure and made use of weighted linear combinations (Drobne and Lisec, 2009, Eastman, 2012), essentially as series of weighted averages, to allow for varying levels of significance to be assigned to specific variables, an approach that has been used at the global scale (Vörösmarty et al., 2010) as well as for a number of regional aquaculture assessments (Giap et al., 2005, Hossain and Das, 2010). Weightings were assigned by the author after consultation with a range of experts within the Institute of Aquaculture, Stirling. An overview of the concepts behind GIS based multi-

criteria decision analysis can be found in Drobne and Lisec (2009) and Eastman (1999), and specifically in relation to aquaculture in Nath et al. (2000). A schematic overview of how data layers were combined in the current study is shown in Figure 3-10 while details of weightings used are provided in Table 3-9.

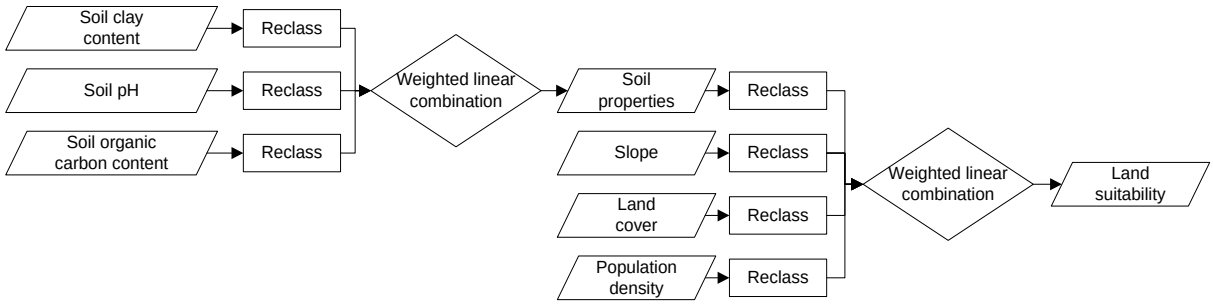

Figure 3-10: Land suitability sub-model structure.

Table 3-9: Weighting used when combining criteria in the land suitability sub-model.

Inputs	weight	Inputs	weight	Output
Soil clay content	0.55 →	Soil suitability	0.15 →	Land suitability MODIS OR Land suitability GlobCover
Soil pH	0.3 →			
Soil organic matter content	0.15 →			
		Slope	0.35 →	
		Land cover (MODIS) OR Land cover (GlobCover)	0.2 →	
		Population density	0.3 →	
		Constraint (MODIS land cover)	→	
		Constraint slope	→	
		Constraint population density	→	

3.2.2 Pond temperature sub-model

3.2.2.1 Introduction

Temperature ranges in aquaculture ponds are of key importance, affecting choice of species and strongly influencing growth performance. As such being able to estimate pond temperatures under a given set of climate variables is crucial if the potential for aquaculture under future climate is to be modelled.

Direct field measurements of temperature have been used by some authors to inform GIS based site selection for aquaculture. For example Hossain and Das (2010), when assessing site suitability for freshwater prawn farming in Bangladesh, used temperature measurements taken at 14 sample sites within the sample area although the methods used, actual number of samples taken, and over what time period is not stated. In a similar study Hossain et al. (2007) uses water temperature when assessing site suitability for tilapia production although in this instance no details are given with regards to data acquisition or structure.

An alternative approach to relying on measured temperatures, and one that allows for much greater spatial and temporal scope, including future projections, is the use of modelled pond temperatures derived from climate and weather data. Attempts at estimating temperatures based on climatic and environmental factors have been undertaken for a wide variety of waterbodies including lakes (Livingstone and Lotter, 1998, Sharma et al., 2008), streams (Flint and Flint, 2008, Koch and Grünewald, 2010, Mohseni and Stefan, 1999, Morrill et al., 2005, Neumann et al., 2003), cooling ponds (Ryan et al., 1974), and algae ponds Béchet et al. (2011). The rapid global growth of pond-based aquaculture has encouraged attempts to model the temperatures of aquaculture ponds either as a subject in its own right (Cathcart and Wheaton, 1987, Culberson and Piedrahita, 1996, Klemetson and Rogers, 1985, Losordo and Piedrahita, 1991) or as part of broader studies often concerned with site suitability for culture of specific species (Aguilar-Manjarrez and Nath, 1998, Kapetsky and Nath, 1997). At their simplest, estimates have been based on linear regression between air temperature and water temperature. For example Kapetsky (1994) used a linear relationship between mean monthly daytime air temperature and water temperature as part of a GIS based assessment of pond-based aquaculture potential in Africa. Data used for the regression came from three ponds at a research station near Harare, Zimbabwe. The Author notes that one of the limitations of this

approach is the potential for considerable variability between mean monthly and mean daily water temperatures with a variability of -6.8 and +6.6C seen in one of the sample ponds. It is also worth considering that in this case data for the regression came from a single area with the results being applied at the continental scale where varying ranges of solar radiation, humidity and wind speed will also be relevant.

Cathcart and Wheaton (1987) described a model designed to predict the vertical temperature profile in a turbid aquaculture pond. The model consisted of three parts that aimed to account for the absorption of solar radiation, thermal convection, and mixing of heat down through the water column as a result of wind action. The model assumes pond surface temperatures are known and a method of estimating hourly surface temperatures from daily maximum and minimums is also given. Another model designed to simulate thermal stratification in shallow aquaculture ponds has been described by Losordo and Piedrahita (1991). The model simulates discrete fully horizontally mixed layers with a depth of 10cm for the surface element and 20cm for those below. A key feature of the two models mentioned above is the need for a wide range of data inputs at relatively small time steps in order to simulate a diurnal temperature cycle and associated stratification processes. In the case of Losordo and Piedrahita (1991): Solar irradiance, wind speed, wind vector magnitude, air temperature, and relative humidity were used at 0.33 hourly intervals while the model also required photosynthetically active solar radiation (PAR) at 5 and 20cm depths, initial pond temperature, and Julian day to be provided at daily intervals while site latitude, pond length and width, and anemometer height are considered as constants. While such models have the potential for simulating pond temperatures with a good degree of accuracy the significant data requirements limit their potential use over large areas where a more limited range of inputs are available.

Aguilar-Manjarrez and Nath (1998) used a pond temperature model originally developed by Nath (1996) to estimate pond temperatures for Africa. The model makes the assumption of a fully mixed water column and is based on modelling heat exchange at the water surface while potential heat transfer to and from the pond sediment are not included. Assuming there is no regular flow of water in and out of the pond then required variables for the model are: air temperature, relative humidity, wind speed, solar radiation, cloud cover and elevation. Nath (1996) undertook verification for the model at two sites in Thailand that represent a warm humid low elevation tropical environment, one site in Honduras representing a dryer tropical environment, and a site in Rwanda representing a high

elevation area with lower air temperatures. Daily pond temperatures were recorded as an average of twice daily measurements at multiple depths throughout the water column. Nath (1996) states that for all four sites predicted temperatures based on daily means and recorded water temperatures were not significantly different ($p > 0.05$). Nath (1996) also points out that water and air temperature profiles tend to have similar profiles at all of the four sites.

While the model described by Nath (1996) lacks some of the sensitivity of small time step stratified pond models (Losordo and Piedrahita, 1991) it has the advantage of being verified across a range of sites and importantly is based on the use of daily mean climate variables and as such is more appropriate for use at the global scale with currently available global climate data sets.

3.2.2.2 Pond temperature model

The model described by Nath (1996) (equation 1) was applied within the current study to model water temperature in a hypothetical two metre deep pond at daily interval for two 10 year time series, one representing late 20th century conditions and the other a 2°C average global temperature increase.

$\phi_{net} = \phi_{sn} + \phi_{an} - \phi_{ws} - \phi_e \pm \phi_c$ [Equation 1]

where:

ϕ_{sn} = Short-wave solar radiation

ϕ_{an} = Net long-wave atmospheric radiation

ϕ_{ws} = Water surface radiation

ϕ_e = Evaporative heat loss

ϕ_c = Conductive heat exchange

and $\phi_{sn} = \phi_s(1 - A_s)$ [Equation 2] (Henderson-Sellers, 1984 cited in Nath, 1996)

Where ϕ_s = short wave radiation and A_s = short wave reflectivity. For the current study it was assumed that $A_s = 0.06$ based on recommendation by Henderson-Sellers (1984) cited in Nath (1996).

$\phi_{an} = (1-r)\varepsilon_a \sigma T_{ak}^4$ [Equation 3] (Henderson-Sellers, 1984 cited in Nath, 1996)

Where r = water surface reflectance to long wave-wave radiation which is assumed to be 0.03 (Henderson-Sellers, 1984; Losordo and Piedrahita, 1991 cited in Nath 1996), σ = Stefan-Boltzmann constant (4.896×10^{-6} kJ m^{-2} d^{-1} K^{-4}), and T^{ak} = absolute air temperature (^oK). ε_a was calculated using the $\varepsilon_a = 0.937 \times 10^{-5} \times T_{ak}^2(1 + 0.17C_c^2)$ where C_c represents cloud cover as a decimal fraction (Swinbank, 1963, modified by Wunderlich, 1972, and cited in Nath, 1996).

$\phi_{ws} = \varepsilon_w \sigma T_{wk}^4$ [Equation 4] (Henderson-Sellers, 1984 cited in Nath, 1996)

Where ε_w = emissivity of water (estimated as 0.97), and T_{wk} = absolute water temperature (^oK).

$\phi_e = (e_s - e_a)[\lambda(T_{wv} - T^{av})^{1/3} + b_0 u_2]$ [Equation 5] (Ryan et al., 1974 cited in Nath, 1996)

Where e_s = saturated vapour pressure (mm Hg) at the current water temperature and e_a = water vapour pressure immediately above the ponds surface (mm Hg). T_{wv} is the virtual water temperature (^oK) and T_{av} is the virtual air temperature (^oK). λ and b_0 are constants: λ = 311.02 KJ m^{-2} d^{-1} $mmHG^{-1}$ $K^{-1/3}$, and b_o = 368.61 KJ m^{-2} d^{-1} $mmHG^{-1}$ $(m\ s^{-1})^{-1}$. u_2 represents wind velocity (m s^{-1}) at 2 metres above the water surface.

Saturated vapour pressure and water vapour pressure can be estimated based on equations by Troxler and Thackston (1977) cited in Nath (1996):

$e_s = 25.37\exp[17.62-(5271/T_{wk})]$ [Equation 5]

$e_a = R_h \times 25.37\exp[17.62-(5271/T_{ak})]$ [Equation 6]

Where R_h is relative humidity as a decimal fraction.

Virtual water temperature is defined as:

$T_{wv} = T_{wk}/[1 –(0.378x (e_s/P))]$ [Equation 7]

Virtual air temperature is defined as:

$T_{av} = T_{ak}/[1 –(0.378x (e_a/P))]$ [Equation 8]

Where P = barometric pressure (mm Hg) which can be estimated from altitude using the following formula (Colt, 1984 cited in Nath, 1996):

$P = 760/10^{z\backslash 19748.2}$ [Equation 9]

Where z = altitude (m).

$\phi_c = \phi_e \times 0.61 \times 10^{-3} P \times ((T_{wk} – T_{ak})/(e_s – e_a))$ [Equation 10]

3.2.2.3 Data choice and use

The current study made use of four main data sources. The CRU CL2 (New et al., 2002) climatology data set, and the NASA solar radiation (NASA_SSE_6.0, n.d.) data set were used to represent average monthly climate conditions for the late 20th century at a reasonably high resolution of 10 arcminutes. Data from 13 Atmosphere Ocean General Circulation Models (AOGCMs) that were used to inform the IPCC 4th assessment report were obtained from the Coupled Model Intercomparison Project (CMIP3) archive and used to adjust the CRU CL2 base data to create a second set of climatology data that represents conditions in a 2°C warmer world. Finally, data from the Japanese 25-year Reanalysis Project (JRA-25) (Onogi et al., 2007) were used to create a set of daily climate anomalies that where applied to the higher resolution base climatology data sets to produce two 10 year series of daily climate conditions that represents late 20th century conditions as well as those for a 2°C warmer world. The daily time series data were then used to model pond temperature.

3.2.2.3.1 Base climatology data

Global data sets representing historic climate values are typically produced through the interpolation of data from meteorological stations (Hijmans et al., 2005, New et al., 2002, UDel_AirT_Precip, n.d.), or through reanalysis where past weather is modelled with models being informed by recorded meteorological data (e.g. JRA25, ERA40, NCEP/NCAR). There are also a number of projects aiming to provide climate related data such as temperature and rainfall through the use of remotely sensed data. Examples include the Tropical Rainfall Measuring Mission (TRMM) for precipitation and the Moderate Resolution Imaging Spectroradiometer (MODIS) land surface temperature and emissivity product (MOD11A1) for temperature. The use of remotely sensed data is attractive in that it is effectively sampling all areas of the earth's surface and thus not relying on interpolation or weather modelling to fill in gaps between meteorological stations which can be large in some areas of the world. This said, remote sensing projects typically focus on single variables (e.g. temperature) and there may also be potential concerns over accuracy of estimates with factors such as cloud cover potentially impacting results (Wan, 2008). There are also the issues of return period, or sampling frequency, and the length of time for which the data set is available which in many cases may not be long enough to allow for the extraction of reliable climate averages.

The CRU CL2.0 data set (New et al., 2002) provides data for a range of climate variables as global gridded data with a 10 arcminute resolution. The data represent monthly climatological means calculated over a 30 year period (1961-1990) based on the interpolation of data from a large number of meteorological stations (e.g. 27075 for precipitation and 12783 for mean temperature). The CRU CL2.0 data is widely used in the literature as a source of average climate conditions for representing current or recent conditions, or acting as a base period for comparing future scenarios with (e.g. Blanchet et al., 2014, Buisson et al., 2013).

The CRU CL2.0 data set (New et al., 2002) was selected for use in the current project as it was viewed as offering high quality data at a reasonable resolution. Another key factor is that with the exception of solar radiation and cloud cover the CRU CL2.0 data set supplied all of the variables needed for the pond temperature modelling process (air temperature, wind speed, relative humidity, and elevation). Mean monthly data for solar radiation were obtained via the NASA Surface meteorology and Solar Energy (NASA_SSE_6.0, n.d.) database at one degree resolution and regridded using bilinear

interpolation to a 10 arcminute resolution consistent with the CRU CL 2.0 data. Cloud cover data were taken directly from the JRA25 reanalysis data set.

3.2.2.3.2 AOGCM data

The ability to model future climate change scenarios is improving (IPCC, 2007b) with coupled Atmosphere and Ocean General Circulation Models (AOGCMs) representing the most sophisticated efforts to project future climate patterns. Historically, results from GCM experiments have been limited in number and climate change impact studies have made do with outputs from a single model (e.g. Jones and Thornton, 2003). Others (e.g. Berry et al., 2006, Tuck et al., 2006) have used outputs from a number of GCMs but applied them individually within in an impact modelling process resulting in an overall output for each climate model and thus a range of change scenarios to consider. In recent years coordinated efforts have been made between climate modelling centres to run a set of standardised experiments, such as those designed to contribute to the Intergovernmental Panel on Climate Change (IPCC) fourth assessment report (AR4) thus allowing for averages from multiple models to be used in impact assessments (IPCC, 2007b, IPCC, 2007a).

There is still significant variation between outputs from different models and to some extent different runs of the same model. The ability of AOGCMs to reproduce details of past climate is often used as a means to evaluate models performance in relation to each other. While some models appear to show greater skill than others in this respect it has been noted that when viewed globally a combined ensemble of multiple climate models will generally outperform individual models in terms of skill at reproducing the spatial details of past climate variability (Fordham et al., 2011, IPCC, 2007b, Pierce et al., 2009, Reichler and Kim, 2008).

When using output from climate models it is common to use monthly or yearly climatologies over a future 20 or 30 year time period and compare these to recent conditions, again using average values over a similar 20 or 30 year period. There is often considerable variation between the outputs of different climate models as a result of differing algorithms as well as assumptions about processes that drive weather and climate. For those concerned with impact studies and the effects of climate change the variability between climate models can be viewed as consisting of: a) spatial variability of patterns of change e.g. location of areas predicted to see increases or decreases in precipitation, and

b) overall model sensitivity i.e. the predicted average global temperature increase in relation to a set increase in green house gas concentrations.

An issue that is often overlooked when combining data from an ensemble of climate models is the varying sensitivities of the models used. The 23 GCMs that contribute to the 4th IPCC assessment report have a range of equilibrium climate sensitivities where a doubling of atmospheric CO_2 results in average global temperature increases ranging from 2.1°C to 4.4°C with a mean value of 3.2°C (IPCC, 2007b). This means that if an average value is derived from the ensemble of models for a given point in the future or green house gas increase then those models with higher sensitivities will exert a greater influence on the spatial distribution of climate variables (Fordham et al., 2011). An alternative strategy, and the approach adopted in the current study, is to use degrees of average global warming rather than fixed levels of CO_2 increase relating to future time periods under emissions scenarios.

Data necessary for pond temperature and evaporation modelling were available from 13 general circulation models (GCMs) forced using the AIB emission scenario. For each model a monthly climatology was established based on a 31 year mean where the centre point (i.e. 15 years each side) corresponded to a 2°C temperature increase compared to the 1961-1990 base period when comparing global annual average temperatures. The base period data (1961-1990) were taken from control runs for each climate model that aim to replicate 20th century conditions. Details of GCM data used time periods representing a 2°C temperature increase over base conditions for each model are given in Table 3-10. The data from the 13 GCMs were combined using an equally weighted average to give two ensembles: one representing late 20th century conditions and the other a 2°C warmer world. The relative difference (i.e. percentage change) between these data sets for: relative humidity, wind speed, and solar radiation, as well as the actual difference (°C) were applied to the CRU-CL2 data to produce a new data based on CRU-CL2 that represents a 2°C global warming scenario.

Table 3-10: Climate models used to supply data.

Originating Group(s)	Country	CMIP3 I.D.	Date where global mean temperature reaches 2°C more than 1961-1990 base period under SRES scenario A1B
Bjerknes Centre for Climate Research	Norway	BCCR-BCM2.0	2064
Canadian Centre for Climate Modelling & Analysis	Canada	CGCM3.1(T47)	2056
Canadian Centre for Climate Modelling & Analysis	Canada	CGCM3.1(T63)	2044
Météo-France / Centre National de Recherches Météorologiques	France	CNRM-CM3	2056
LASG / Institute of Atmospheric Physics	China	FGOALS-g1.0	2063
NASA / Goddard Institute for Space Studies	USA	GISS-AOM	2085
NASA / Goddard Institute for Space Studies	USA	GISS-EH	2078
NASA / Goddard Institute for Space Studies	USA	GISS-ER	2077
Institute for Numerical Mathematics	Russia	INM-CM3.0	2052
Institut Pierre Simon Laplace	France	IPSL-CM4	2050
Center for Climate System Research (The University of Tokyo), National Institute for Environmental Studies, and Frontier Research Center for Global Change (JAMSTEC)	Japan	MIROC3.2(hires)	2035
Center for Climate System Research (The University of Tokyo), National Institute for Environmental Studies, and Frontier Research Center for Global Change (JAMSTEC)	Japan	MIROC3.2(medres)	2053
Meteorological Research Institute	Japan	MRI-CGCM2.3.2	2069

3.2.2.3.3 Construction of daily climate time series for pond temperature modelling

Daily values for: air temperature, wind speed, relative humidity, solar radiation, and cloud cover were obtained via the Japanese 25-year Reanalysis Project (JRA-25) data set at a grid resolution of 1.125 degrees for a 10 year period (1991-2000). The JRA-25 data set was chosen over the other weather

reanalysis data sets that are freely available (NCEP/NCAR Reanalysis 1, NCEP-DOE Reanalysis 2, and ERA40) as it was freely available at a higher resolution.

Monthly climatological means for the same variables were also obtained from the JRA-25 database and relative differences between JRA-25 climatological monthly means and daily values were calculated for wind speed, solar radiation, relative humidity to produce a set of daily anomalies. A set of daily anomalies were also produced for the air temperature data but as actual differences in degrees centigrade. This daily anomaly data were regridded using bilinear interpolation to a 10 arcminute resolution consistent with the CRU CL 2.0 data set. The daily anomalies were then applied to the CRU CL 2.0 and NASA SSE 6.0 monthly climatologies to produce a time series of plausible daily values for air temperature, wind speed, relative humidity, and solar radiation at 10 arcminute resolution over a 10 year period that was then be fed into the pond temperature model. A second 10 year time series of daily values were created that represented a 2°C warmer world. This was achieved by applying the daily anomalies to CRU CL 2.0 and NASA SSE 6.0 data that had previously been adjusted using monthly anomalies obtained from the ensemble of GCM data.

The benefits of using daily anomaly data is that it allows for the investigation of potential extremes that will not be present in the monthly climatologically averages. The decision to apply anomalies from the JRA-25 data set to the CRU CL 2.0 data set rather than using them directly is based on two main factors. Firstly the CRU CL 2.0 data is at a considerably higher resolution that allows for much better representation of local variation, especially in relation to elevation. Secondly the CRU CL2 data set is derived from a large number of observations, as opposed to being derived from reanalysis modelling of past climate and as such can be assumed to provide a reasonably accurate representation of recent global climate variables.

3.2.3 Water availability for rain fed ponds

3.2.3.1 Introduction

Inland aquaculture has an obvious dependence on fresh water resources. The source of water and the way in which it is supplied to an aquaculture operation will be dependent on the type of system and its location. That said, water sources can generally be considered as: existing surface water bodies

(e.g. lakes, rivers, canals etc.), ground water, and direct rainfall and runoff from the area immediately surrounding the ponds.

Water is lost from aquaculture systems via: deliberate water exchange, evaporation, and leaks/seepage. For rain fed pond systems the concept of water balance (rainfall minus evaporation minus seepage) dictates the availability of water within the system. The rate of evaporation from a pond surface is influenced by a number of climatic variables, notably: temperature, humidity, intensity of solar radiation, and wind speed. These variables along with the extent and timing of precipitation can all be considered as aspects of climate that are potentially subject to change in relation to global warming meaning that with the exception of seepage from the pond base, water availability within a rain fed pond is entirely dependent on climate.

The current study aims to investigate water balance and the likelihood that rain fed ponds will contain water on a monthly basis throughout the year. Modelling was conducted for late 20th century conditions (1961-1990) as well as a similar 30 year time series representing a 2°C warmer world.

3.2.3.2 Methods and data

3.2.3.2.1 Potential evaporation calculation

There has been a considerable amount of work aimed at estimating potential evaporation based on climate and weather data. Much of this work has been concerned with evapotranspiration from crops where there are significant issues for agriculture in relation to water availability. The FAO has suggested the Penman-Monteith equation as a standard for establishing reference evapotranspiration values (Allen et al., 1998). Aguilar-Manjarrez and Nath (1998) used the Penman-Monteith equation to establish potential evapotranspiration values as part of a GIS based assessment of fish farming potential in Africa. The authors then used an adjustment factor based on the difference between pan evaporation and reference evapotranspiration to establish estimates of evaporation from an open water surface. Winter et al. (1995) found that the Penman equation fared well in an evaluation of 11 equations used for calculating evaporation from a small lake in the United States by comparing results to those obtained using an energy budget method (Sturrock et al., 1992). Mosner and Aulenbach (2003) suggest that the Penman equation fared poorly as part of an assessment of four methods of calculating evaporation from a lake in the south eastern United States

when compared to energy budget estimates of evaporation. However the results of the Penman equation seem much better when compared to those published by the Georgia Automated Environmental Monitoring Network that are also given in the same study.

Linacre (1993) described a simplified version of the Penman equation for estimating lake evaporation where the required inputs are: mean daytime temperature, dewpoint temperature, solar irradiance, wind speed, and altitude. Linacre (1993) goes on to describe two methods for estimating values for solar radiation in areas where such data are unavailable.

The current study makes use of the equation described by Linacre (1993) which can be expressed as:

E_o (mm day $^{-1}$) = $(0.015 + 0.00042T + 10^{-6}z)[0.8R_s – 40 + 2.5Fu(T - T_d)$ [Equation 11]

where:

E_o = evaporation rate (mm per day)

T = mean daily temperature (°C)

T_d = dew point temperature (°C)

z = elevation (m)

u = wind speed at 2m (metres per second)

R_s = solar irradiance (watts per square metre)

$F = (1 – 8.7 \times 10^{-5} z)$

3.2.3.2.2 Data used for calculating potential evaporation and water balance

For many parts of the world rainfall is seasonal with distinct wet and dry seasons. There is also a tendency in many regions for evaporation rates, and in particular precipitation quantities, to vary on a year to year basis. For rain fed aquaculture this can be significant in terms of growing season length and potential risk of water shortage. In order to take account of inter-annual variation it is necessary to use a time series of data that accounts for variability. The 10 year daily series of climate data constructed for modelling pond temperatures within the current study would provide one potential solution, however water availability issues tend to operate over longer time scales than fluctuations

in temperature and are likely to be best served by a longer time series without the need for such frequent data points.

The CRU TS3.10 (Harris et al., 2014) data set represents a gridded time series, with half degree resolution, of monthly means for a range of climate variables running from 1901-2009 that is based on interpolation of observed weather data. This data set was used to supply temperature, dew point temperature as well as elevation data used to calculate potential evaporation rates, with the same data set also used to provide precipitation data for determining water balance. Wind speed and solar radiation data were not available as part of CRU TS3.10. Instead, average values for each month were obtained from the CRU CL2.0 data set for wind speed, and from NASA (SSE 6.0) for solar radiation. Figure 3-11 shows average daily water balance (precipitation minus potential evaporation from a water surface) for late 20th century conditions (1961-1990) while Figure 3-12 shows relative change to these values under 2°C global warming.

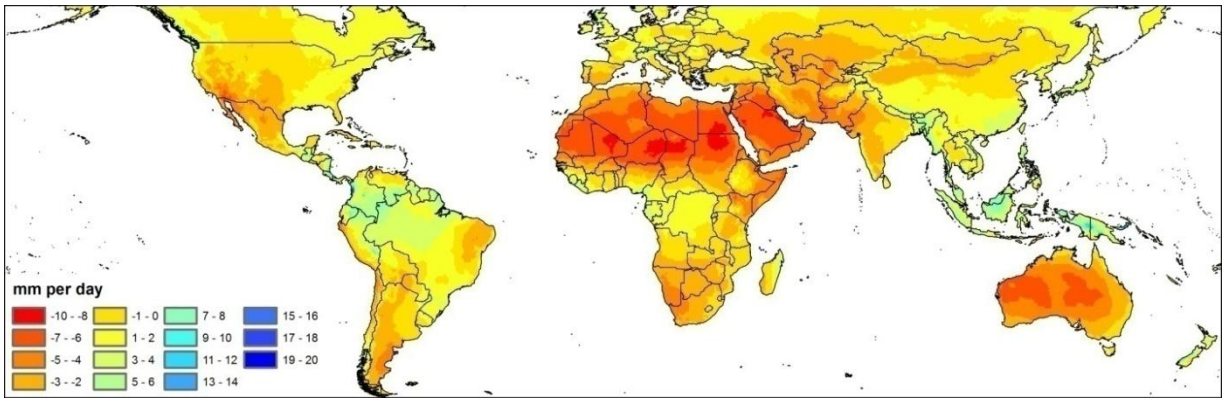

Figure 3-11: Average daily water balance (precipitation minus potential evaporation from a water surface) for late 20th century conditions (1961-1990).

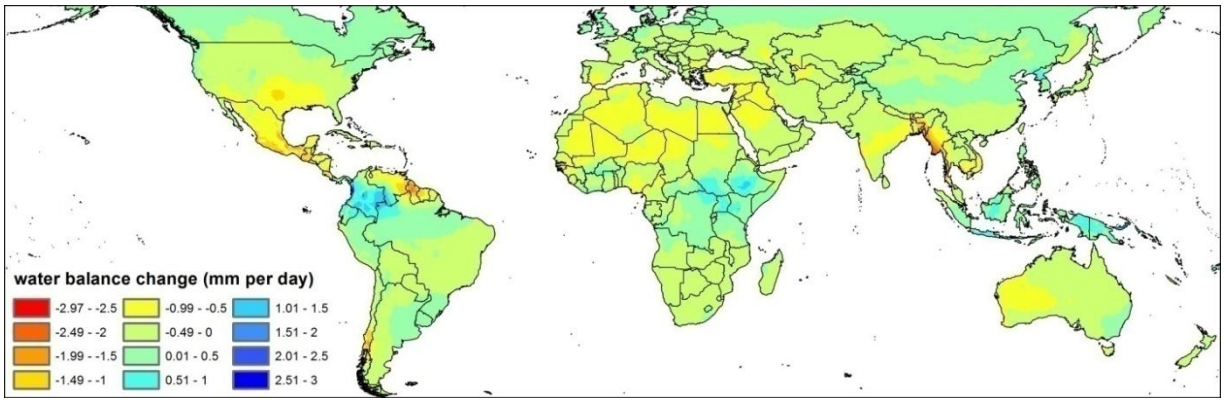

Figure 3-12: Change in average daily water balance in relation to 2°C average global temperature increase.

3.2.3.2.3 Seepage rates

The rate of seepage through pond sediments plays a role in the water balance of aquaculture ponds and for areas where the water table is below the level of the pond bottom may be the largest cause of water loss exceeding evaporation rates in many cases (Boyd, 1987). The rate of seepage will depend on water depth and temperature but is largely dictated by the physical properties of the pond base where soils with a high clay content are generally less permeable. As well as permeable soils Yoo and Boyd (1994) suggest that other causes of increased seepage include: shallow soils over fractured bedrock, soils with a high gypsum content which leaves spaces as the gypsum dissolves, and poor construction methods such as insufficient compaction of soils or inadequate spread of soil over exposed rock areas.

Seepage is often calculated by recording reduction in water depth and subtracting that lost through evaporation which may be estimated using methods such as recorded pan evaporation, seepage meters, and capped pipes driven into the pond substrate (Stone and Boyd, 1989). The amount of water lost to seepage varies considerably. Examples of recorded seepage rates in a number of ponds settings are given by Boyd and Tucker (1998) and are summarised here in Table 3-11. Boyd and Tucker (1998) also note that seepage rates vary seasonally with warmer temperatures resulting in faster seepage, and that seepage can vary considerably between ponds found in the same area. This point can be illustrated using the example of Boyd (1982) who noted that the seepage rates among 51 small ponds at the Auburn University Fisheries Research Unit varied from 1.2 to 20.5 mm per day.

Table 3-11: Summary of recorded pond seepage rates given by Boyd and Tucker (1998).

Pond details	Seepage (mm per day)	Original source
Coastal Plain soils, Alabama	3.81	(Parsons, 1949).
Piedmont Plateau, Alabama	10.9	(Parsons, 1949).
Blackbelt Prairie, Alabama (heavy clay soil)	1.5	(Parsons, 1949).
Small natural ponds in Minnesota	1	(Allred et al., 1971, Manson et al., 1968)
Piedmont Plateau, Alabama	8.9	(Boyd and Shelton, 1984)
12 ponds at Gualaca Panama	19 - 58	(Teichert-Coddington et al., 1988)
Comayagua, Honduras	7.75	(Green and Boyd, 1995)

Attempts to incorporate values for seepage and thus water availability for rain fed ponds as part of broader site suitability assessment for aquaculture have been limited. Kapetsky and Nath (1997) and Aguilar-Manjarrez and Nath (1998) both cited seepage rate definitions provided by Yoo and Boyd (1994) (low = <4.83 mm/day, moderate 4.83 – 9.91 mm/day, high = 9.91 – 14.99 mm/day, extreme = >14.99mm/day). Ultimately both sets of authors settled for a single low seepage rate of 2.77 mm/day (100cm/year).

3.2.3.2.4 Calculating water balance

As well as rainfall landing directly on the pond water surface there will be a certain amount of runoff from the sides of the pond meaning that the ponds actual capture area is somewhat larger than the water surface its self. Kapetsky and Nath (1997) and Aguilar-Manjarrez and Nath (1998) addressed this issue by multiplying precipitation values by the constant 1.1 suggesting a total capture area of 110% of the actual water surface. In reality the capture area will depend on the size of the pond and its surroundings with smaller ponds likely to have a greater total drainage area relative to their actual surface area meaning that when total drainage area is considered water balance can be described as:

Water balance = (precipication x (total drainage area/water surface area)) – seepage

Another way in which the pond water availability question could be viewed would be to ask what size of drainage area is needed for a given precipitation and seepage rate in order for a pond to contain water at a certain time of year. Given that variable time series data is being used and values from one month feed into the next, the calculation of exact drainage areas for a given depth isn't feasible. In order to try and address some of this uncertainty and gain a better understanding of what different seepage rates and relative drainage areas would mean for ponds globally a range of possible scenarios are considered in the current study with drainage areas representing 1.1, 1.5 and 2 times pond surface area, and seepage rates of 2.41, 7.37, and 12.45 mm per day. These seepage rates represent the mid points of the low, medium, and high seepage ranges given by Yoo and Boyd (1994).

3.2.3.2.5 Likelihood of ponds containing water

Water depth was modelled for a theoretical 2 metre deep pond on a monthly basis using water balance values derived from CRU TS3.00, CRU CL2, and NASA solar radiation data. Details of how pond water depth was calculated are given in Text box 3-1. An initial starting depth of 1000mm (half full) was specified for all areas and the model was run from the beginning of the time series (January 1901) allowing pond depths to stabilise before reaching the main analysis period (1961-1990). This process was repeated for the different seepage and runoff scenarios, and for a second time series of data where all variables had been adjusted to represent a 2°C global warming scenario. This was done using anomalies from the combined output from the 13 GCMs that were described in the pond temperature modelling section. Figure 3-13 gives an example of modelled water depths showing the average depth for the month of June for 1961-1990 time period and for a 30 year time period adjusted to represent a 2°C warmer world.

Once monthly pond water depths were established the following processes were applied to all months representing the same 30 year period (1961-1990) used when modelling pond temperatures.

1. Boolean classification was applied to all data within the 1961-1990 period so that all areas where ponds are at least half full (>1000mm) are identified.
2. For each month the probability that ponds would be at least half full during the 30 year period (1961-1990) was established.
3. The number of consecutive months where there is at least a 90 percent (27 out of 30 years) probability of ponds being half full was established. This is significant for aquaculture in that it essentially controls growing season length for rain fed ponds.

Water depth from previous month + (precipitation - evaporation - seepage) = result
If result > than 2000mm then water depth = 2000mm
If result < than 0mm then water depth = 0mm
If result >0 and <2000 then water depth = result

Text box 3-1: Method used to calculate monthly pond water depth from time series data.

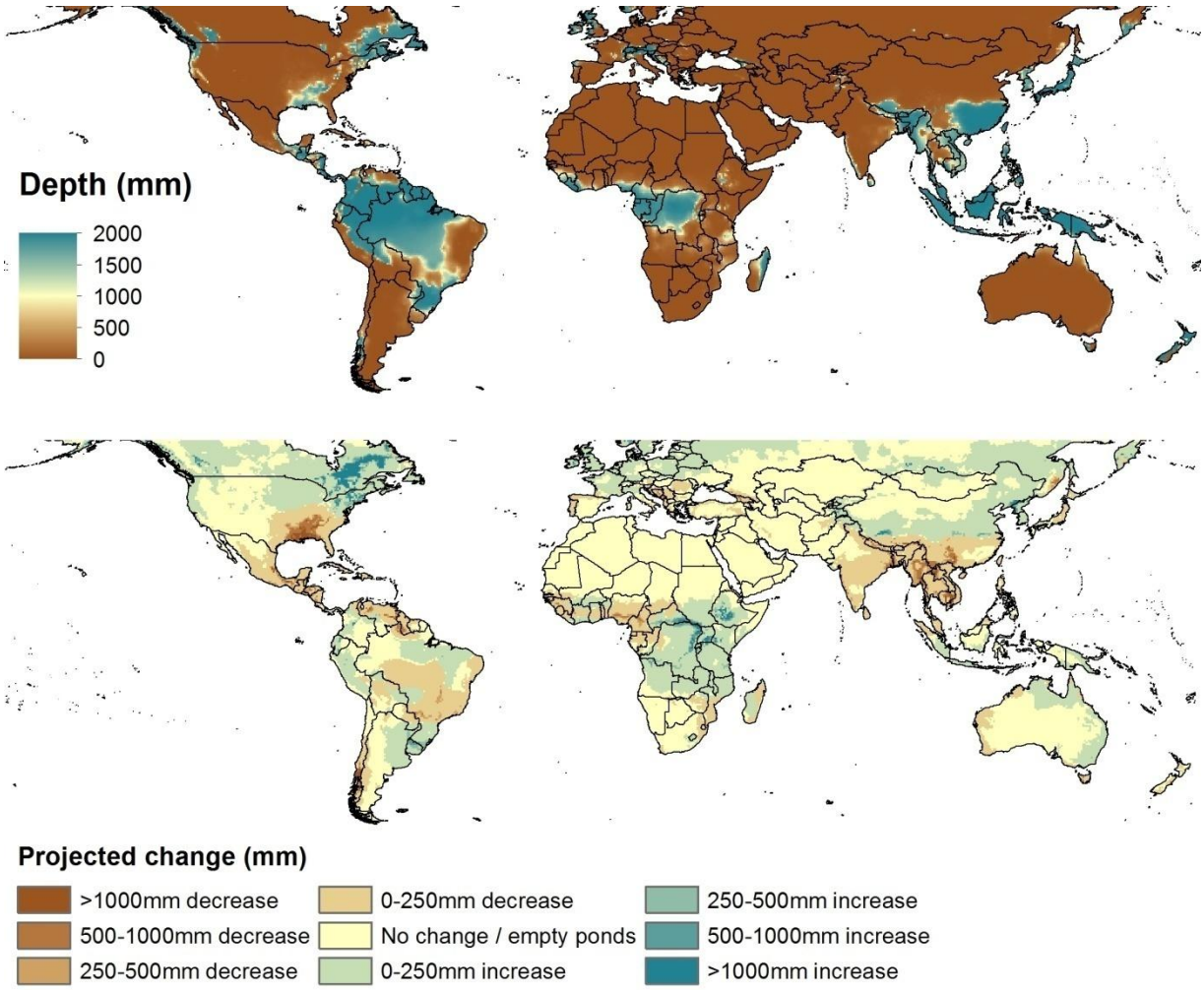

Figure 3-13: Average modelled June water depth for the period 1961-1990 (top) and projected change in water depth under the 2°C average global warming (bottom).

3.2.4 Combination of sub-model outputs

Viewing the individual outputs generated by the land suitability, water temperature, and rain fed pond water availability sub-models provides a range of useful information in relation to site suitability. However a key strength of representing spatial data within a GIS is the ability to combine multiple data sources in a variety of structured ways to help guide decision making. The reclassification of varied data sources to a common scale and their combination using a series of linear weighted averages (Eastman, 2012) has already been discussed in relation to the land suitability sub-model. Such an approach can be extremely useful as it effectively allows a large number of factors to be considered simultaneously while at the same time allowing different levels of

significance to be assigned to factors in the form of weightings. The weighted linear combination (WLC) process is relatively easy to conceptualise which is potentially beneficial when eliciting expert opinion with regards to weightings, a process that can often be helped by first ranking factors in order of significance.

A potential limitation of WLC is that the number of factors increases there is an increasing chance of them cancelling each other out (Drobne and Lisec, 2009). As a simplified example if it is assumed there are three factors and for a given pixel two have a suitability score of 100 (maximum suitability) and the third has a score of zero (minimum suitability) then an equally weighted WLC would result in a score of 66.6 which is likely to represent a moderately good level of suitability despite one factor being classified as highly unsuitable. Whether this situation is reasonable will depend on the nature of the data and the reasons for combining it. One possible solution is the use of constraints in the form of Boolean intersections that represent a logical AND operation. In GIS terms this often means multiplying the results of a process such as WLC with a raster grid containing pixels classed as zero or one (Drobne and Lisec, 2009, Eastman, 2012, Nath et al., 2000). This was done in the current study for the land suitability sub-model where areas with extreme values for slope and/or population density were excluded from the final output regardless of overall suitability score. This Boolean approach can be extended and combined with other operations to form complex decision trees where a series of questions are asked of the spatial database (Nath et al., 2000). This approach contrasts to that of using simple weighted averages and can be useful, especially in relation to quantitative data sources, where more definitive rather than indicative results are required.

Another way to address the problem of trade off between factors is the use of ordered weighted averaging (OWA) instead of WLC. Like WLC, OWA also uses factor weights that influence the trade off between factors. The key difference is that OWA also uses a second set of weightings (order weights) that are applied at each location (raster pixel) in relation to the rank order of factors at the location. The order weights effectively provide a means of influencing the amount of trade off between criteria as well as offering a way of controlling the risk of low scoring criteria being "lost" in the averaging process (Drobne and Lisec, 2009, Eastman, 1999, Eastman, 2012). For example using the same three equally weighted factors described previously, if order weights of 1, 0, 0 were specified then full weighting would be given the lowest scoring factor meaning its value would be represented to the exclusion of the others, a zero trade off scenario with zero risk of low scores being under

represented. More moderate use e.g. 0.6, 0.25, 0.15 would allow factor weights to come into play with moderate amounts of trade off and moderately strong influence given to the lower scoring factors at each location. Specifying equal order weights results in full trade off of factor weights resulting in the same output as a WLC. Reversing the example above (i.e. 0.15, 0.25, 0.6) results in greater influence being given to the highest scoring factor at each location in what can essentially be viewed as an optimistic versus pessimistic modelling approach (Drobne and Lisec, 2009).

The way in which data is classified and combined for aquaculture site selection will vary depending upon species, culture systems, and priorities of the decision makers. It is worth noting that once a spatial database is established within a GIS along with a modelling approach it is normally relatively quick and easy to adapt it in relation to different questions and scenarios.

Two examples are given in the current study based on tilapia (*Oreochromis niloticus*) a warm water species commonly cultured in ponds with a global distribution. The first example uses a OWA approach to combine outputs from the land suitability sub-model in association with Fuzzy classified results from the pond temperature model. In this instance water availability for rain fed ponds is not included in the OWA as the intention was to assess suitability for all areas and assume that water may be available from other surface or ground sources. It would be relatively easy to compare results with the Boolean outputs from the water availability sub-model to indicate which areas considered suitable in terms of land suitability and temperature would also potentially be able to function with rain fed ponds under the different scenarios. The second example queries the pond temperature and water availability sub-models and uses these to specify useable areas. Output from the land suitability sub-model can then be used within these areas to further assess site suitability in relation to what is on the ground.

3.2.4.1 Combination of land suitability and temperature using an OWA

For each month modelled mean pond temperature was reclassified using fuzzy points for maximum suitability between 27°C and 32°C and for minimum suitability below 18°C and above 36°C (see Figure 3-14). Nile tilapia can survive temperatures considerably outside of this range (Philippart and Ruwet, 1982, Sifa et al., 2002), however they show a temperature preferendum of around 30°C, depending on acclimation temperature (Chervinski, 1982), with maximum swimming performance obtained

between 28 and 32°C. There is also a suggestion from experimental studies that as temperatures reach the mid thirties (°C) then growth performance is negatively affected. Xie et al. (2011) examined the growth performance of Nile tilapia at 25, 28, 31, 34, and 37°C and found that overall growth performance were best in the 28, 31, and 34°C groups while optimum growth temperature was estimated at 30.1°C with maximum protein retention at 28°C. At 37°C growth performance and protein retention were worse than all other treatments. Workagegn (2012) conducted similar research with temperatures of 24, 26, 28, 30, 32, and 34°C. The best temperatures in terms of specific growth rate and feed conversion ratio were 32 followed by 30°C, with lower performance seen in the 34°C treatment. When reclassifying the temperature it was also considered that temperatures would likely vary around the mean modelled value and some degree of safety margin was considered appropriate (see model outputs section for modelled pond temperatures for further discussion).

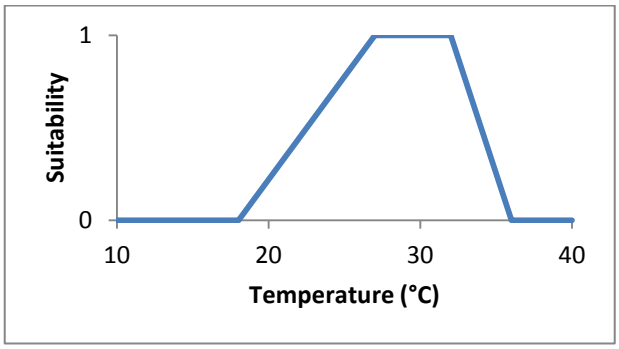

Figure 3-14: Fuzzy reclassification of modelled pond temperature values for combination with land.

For the land suitability layer an average value of the layers generated using MODIS and GlobCover land cover data were used.

Equal factor weights were applied to both land suitability and reclassified pond temperature layers as they were both considered highly important in determining site suitability. Order weights of 0.66 and 0.33 were assigned meaning that for each pixel the lowest ranking factor would be represented twice as strongly. This allowed for greater distinction of areas where either of the input factors were low and placed increased emphasis on areas where both factors ranked strongly.

3.2.4.2 Selection of areas with specific temperature and water availability values

For this example the following criteria were specified for each month:

1. Modelled mean average daily pond temperature between 27 and 32°C
2. Modelled maximum average daily pond temperature less than 36°C
3. Modelled minimum average daily pond temperature more than 14°C
4. Rain fed pond predicted to be containing water based on low seepage rates and precipitation over an area representing 150% of the pond surface.
5. The number of consecutive months meeting these conditions was calculated and a set of Boolean layers representing 6, 9, and 12 consecutive months per year were created.
6. The Boolean masks were applied to outputs from the land suitability sub-model where suitability scores had been reduced from a scale of 0-255 to 5 equal interval classes plus one showing constraint areas. These masks were then used to extract area statistics as well as allow for visual inspection of results.
7. Steps 1-6 above were repeated for both late 20th century conditions and the 2°C average global warming scenario and applied to land suitability based on both MODIS and GlobCover land cover data.

3.3 Model outputs and related discussion

Outputs from each of the sub-models are presented here separately along with those obtained from the combined sub-models. In each case findings and the modelling process are discussed and, where appropriate, suggestions of potential further research are considered.

3.3.1 Land suitability sub-model - outputs and discussion

Example output from the land suitability sub-model using MODIS land cover data is provided in Figure 3-15 while the difference between the results when using MODIS and GlobCover as inputs are shown in Figure 3-16. An indication of the differences between constraint areas of the classified MODIS and GlobCover data is given in Figure 3-17 using southern Vietnam as an example. It is worth noting that when viewing the images at full resolution within a GIS environment it is possible to see small areas

of suitability in many parts of the world that are not obvious when viewing a global image. The magnified areas in Figures 3-15 and 3-16 showing parts of Ghana and Vietnam help give an indication of the level of spatial detail provided by the model as well as helping to highlight differences between the MODIS and GlobCover based outputs.

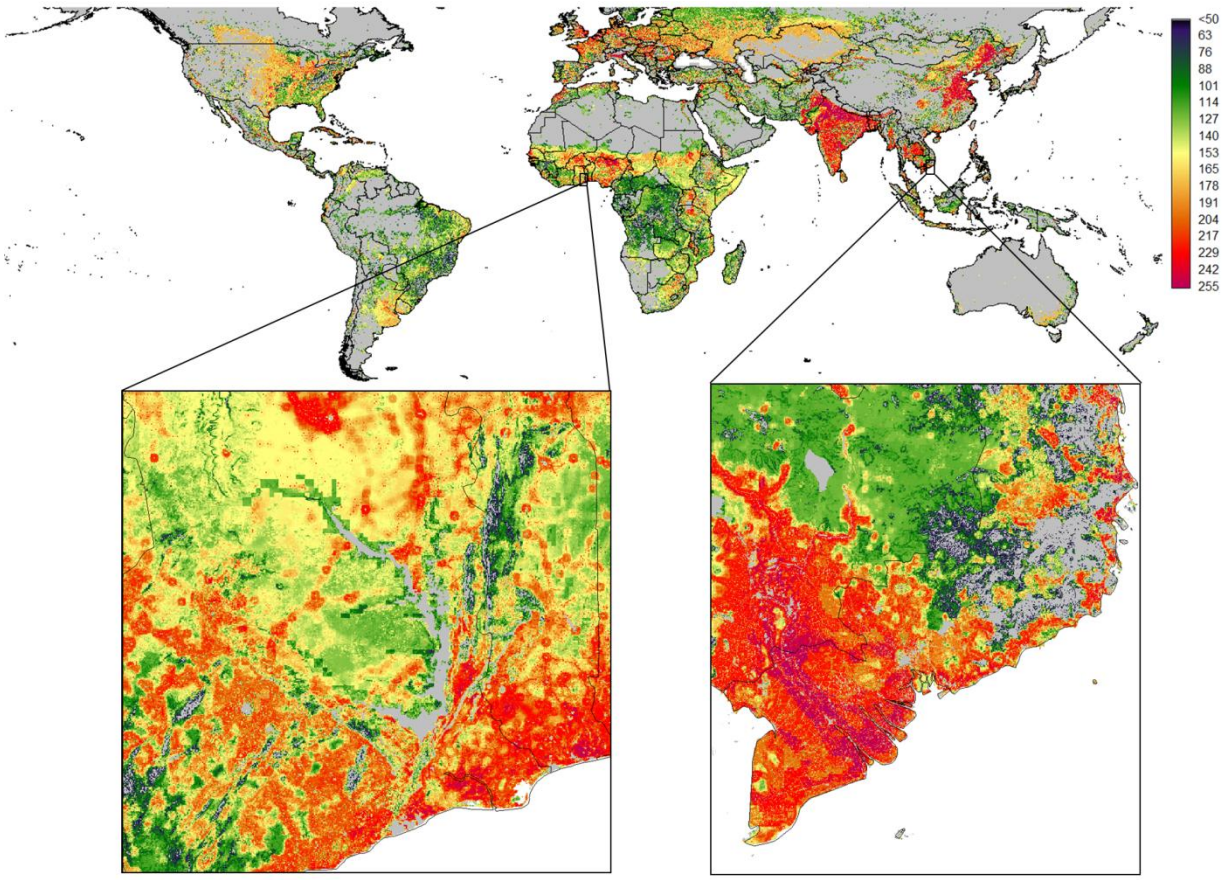

Figure 3-15: Output from land suitability sub-model using the MODIS land cover dataset. Constraint areas shown as grey.

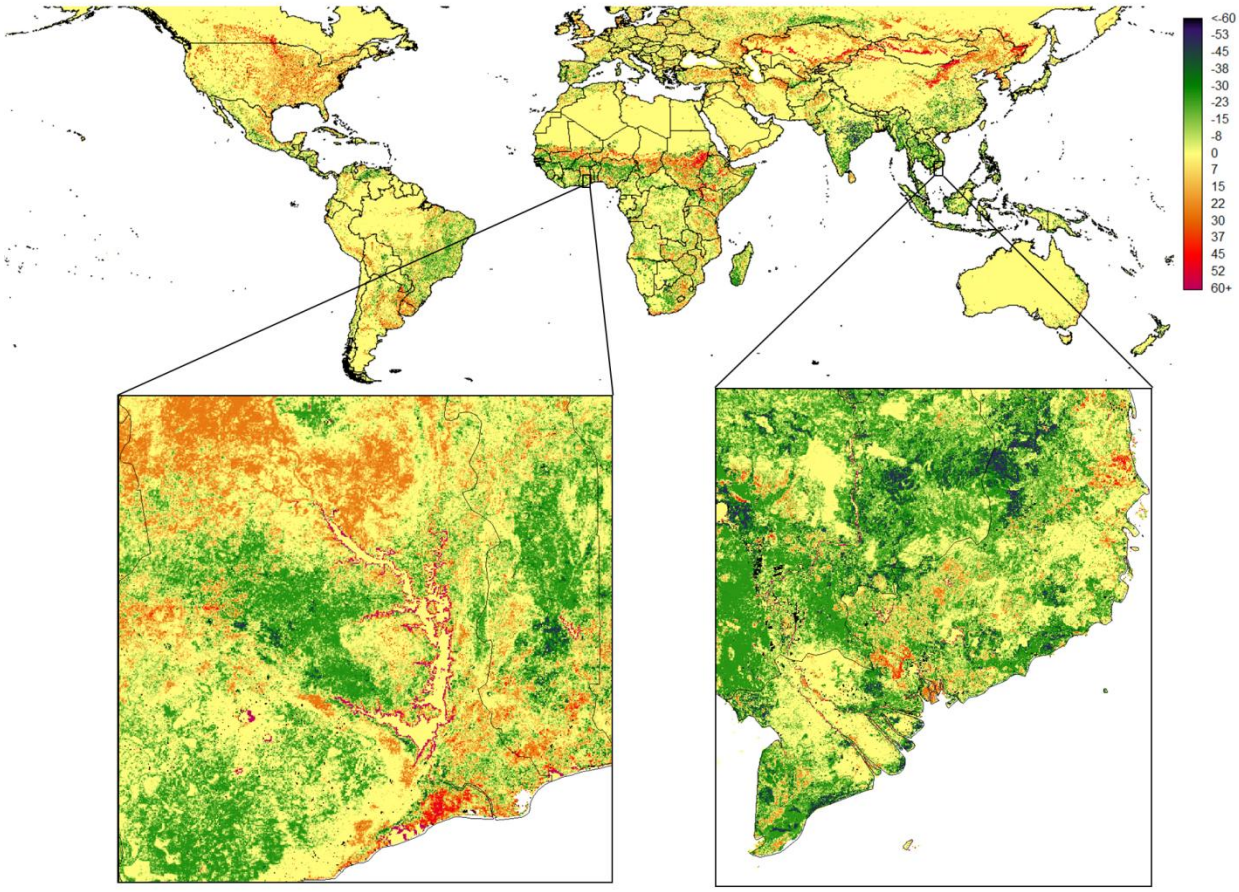

Figure 3-16: Difference between the land suitability sub-model outputs depending on whether MODIS or GlobCover were used to represent land cover. Positive numbers represent a higher score for MODIS, negative numbers for GlobCover.

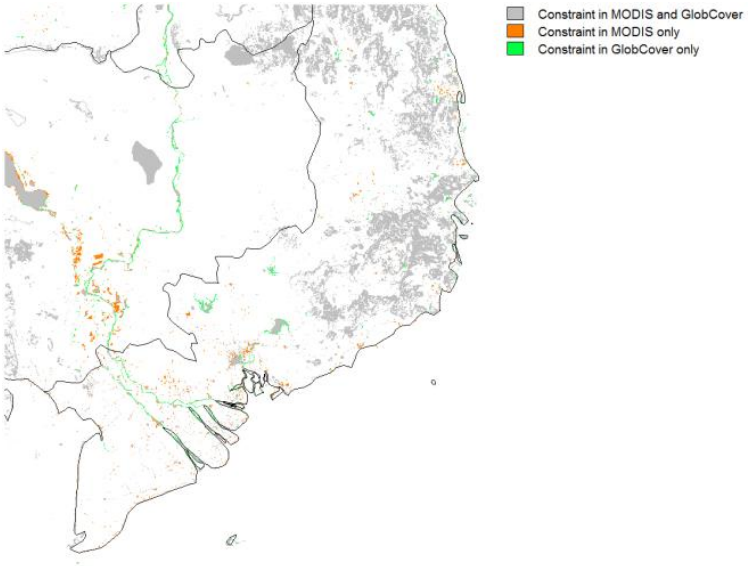

Figure 3-17: Constraint areas after classifying the MODIS and GlobCover land cover products.

When considered at the continental scale Asia stands out as having large areas of land with high suitability scores. India and Bangladesh are especially notable while China, Thailand and Vietnam also have large areas indicated as highly suitable. Much of the suitability in these areas is a result of cropland being indicated by the land cover data which under the current classification scheme is considered potentially available for conversion to aquaculture ponds. The fact that such areas are often flat and in the case of many Asian countries moderately populated also contribute to their suitability. Rice in particular has been combined with aquaculture in many areas either in the form of deep water areas around paddy fields or as part of a seasonal pattern where fields effectively become fish ponds for part of the year (Ahmed and Garnett, 2011).

While remotely sensed land cover data is invaluable for assessments such as the current one, the considerable differences seen between MODIS and GlobCover along with broadness of classes (e.g. different types of cropland are not specified) highlights the limitations of currently available products. As previously discussed part of the problem lies in the relatively low resolution of the sensors used and resulting mixture of land cover types that may be present in a single pixel. With this and continued improvements in computing capacity in mind the development of higher resolution global land cover products would seem to be potentially beneficial.

The next big step in terms of a global land cover product would seem to be a move to using data of around 30m resolution derived from sensors such as Landsat ETM+. Sexton et al. (2013) demonstrated the rescaling of MODIS data to 30m resolution using Landsat images while Gong et al. (2013) published preliminary results for a Landsat based global land cover product. Figure 3-18 shows an example of the 30m land cover product described by Gong et al. (2013) covering Bangladesh. The edges of the individual Landsat scenes within the area displayed are fairly obvious with sudden shifts from one land cover type to another. It is also notable that much of Bangladesh is classified as bareland or forest in what is an extremely densely populated and cultivated country. Despite these limitations the desire to develop such a product should be encouraged as if it can be improved it could become highly useful under a wide range of applications.

The slope values used in the current assessment were calculated from SRTM data at 3 arcsecond resolution and then aggregated to a 10 arcsecond grid to match the resolution of the GlobCover land cover data. It is possible that maintaining the entire database at 3 arcsecond resolution may have yielded slight improvements in terms of terrain slope information although given the lower resolution

of the other data sets any overall benefits would likely be minimal. It is also worth noting that the storage and processing requirements for data sets of such a high resolution would be beyond the capabilities of the current project.

Being a modelled data set the LandScan population density data is also a potential source of inaccuracy. Careful visual inspection in relation to high resolution imagery such as that seen in Google earth suggests that it seems to do a good job of linking higher population densities to areas with obvious urbanisation on the ground. There did appear to be some false positives especially in areas with an overall low population density where the LandScan data would suggest a single more densely populated pixel that did not correspond to any obvious human development. A newer version of LandScan is currently available but at a cost that was prohibitive for the current project. It maybe that an improved algorithm in association with more detailed input data would yield a slightly better, though largely unverifiable, result. This said, the LandScan product used in the current study would seem to offer a significant advantage over the other globally available gridded data sets which are largely derived from a set of variably sized polygons.

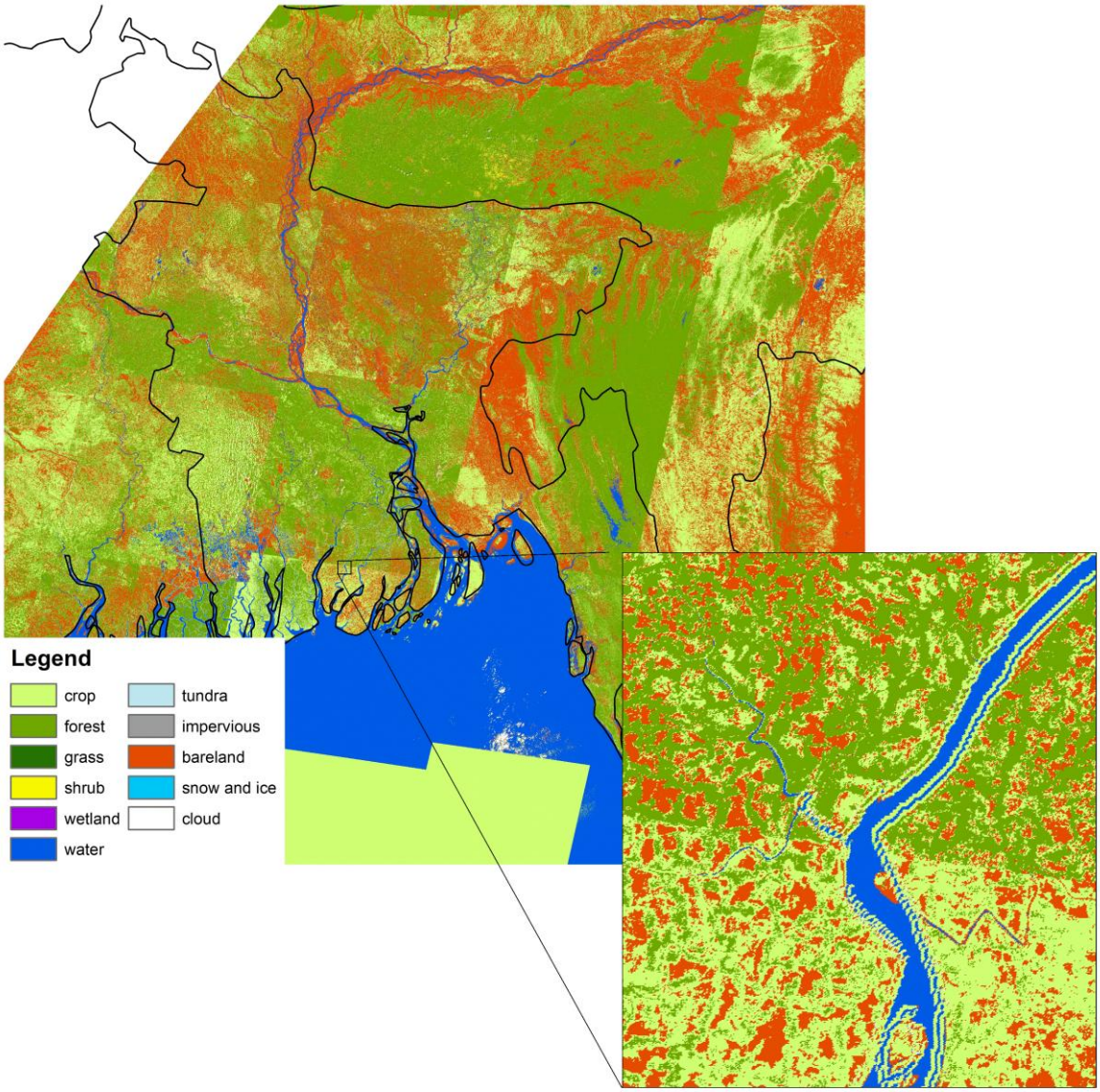

Figure 3-18: A section of the 30m land cover data set for Bangladesh (Gong et al., 2014).

3.3.2 Pond temperature sub-model - outputs and discussion

Examples of pond temperature modelling results (Figure 3-19), show the modelled mean pond temperature for the month of June under late 20th century conditions and for a 2°C global warming scenario along with the difference between the two scenarios. Figure 3-20 shows minimum and maximum modelled temperatures for the same month. Images representing results for all other months can be found in Appendix 1.

Temperature extremes experienced during periods of especially hot or cold weather can be of concern to aquaculturists. The effects of climate change on these extremes has been suggested as a mechanism for direct impacts on aquaculture production through loss of stock due to either directly exceeding the thermal limits of the species, or in relation to stress related disease events (De Silva and Soto, 2009, Ficke et al., 2007). Figure 3-21 gives a more detailed view of modelled maximum temperatures for the months of June and July over much of Asia where a significant amount of the worlds inland aquaculture takes place. Under the 2°C warming scenario there are quite a few areas where temperatures are in the mid thirties or even slightly above. While such temperatures may not exceed the lab based critical thermal maxima of the majority of warm water culture species, under typical culture conditions they may represent a significant source of stress with potential impacts on growth and survival (De Silva and Soto, 2009). It is also worth considering that the climate data used to predict pond temperature represents daily mean values and therefore modelled pond temperature are also in the form of daily means and thus do not account for diurnal temperature fluctuations which could potentially result in higher day time temperatures.

Along with long term modelling using daily means Nath (1996) modelled the diurnal temperature cycle for ponds in Thailand, Honduras, and Rwanda. Nath (1996) provides graphs for each site indicating that modelled water temperatures during the course of a day are consistent with observations at all four locations. Actual daily water temperature fluctuations shown in the graphs are in the region of 2 to 4°C depending on location. Losordo and Piedrahita (1991) modelled temperature variation and thermal stratification in shallow aquaculture ponds. The authors simulated fully wind mixed water column diurnal temperature ranges as well as thermal stratification for Californian catfish ponds and provided a number of graphs suggesting diurnal temperature ranges of up to 6°C for the mixed ponds. Losordo and Piedrahita (1991) also show results for two simulations of temperatures in stratified ponds where surface temperatures range from approximately 27 - 36°C over a 24 hour period while at depths of 60 and 80cm modelled temperatures ranged between approximately 27 and 30°C, and 27 and 32°C. Culberson and Piedrahita (1996) modelled temperature at a range of depths for ponds in Thailand, Rwanda, and Honduras with depths ranging from 80 to 116cm. Measured temperatures for surface layers varied by approximately 4 or 5°C during a 24 hour period while temperatures for the bottom layer only fluctuated by a around 1°C for two of the sites and approximately 2°C for the other.

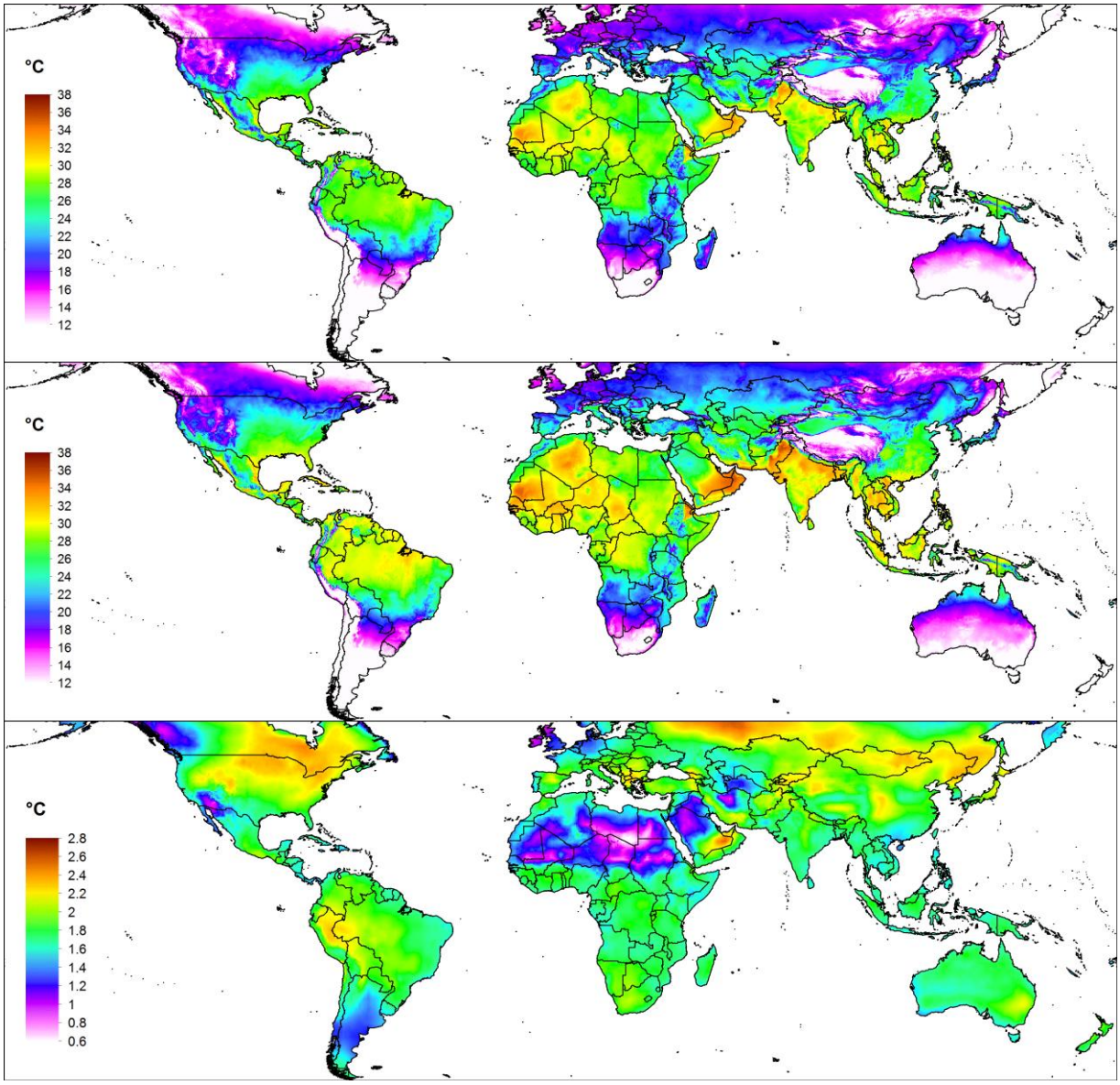

Figure 3-19: Examples of modelled June pond temperatures. Top image show late 20th century conditions, middle image shows 2°C average global warming conditions and the bottom image show the difference between the late 20th century and 2°C warming scenarios.

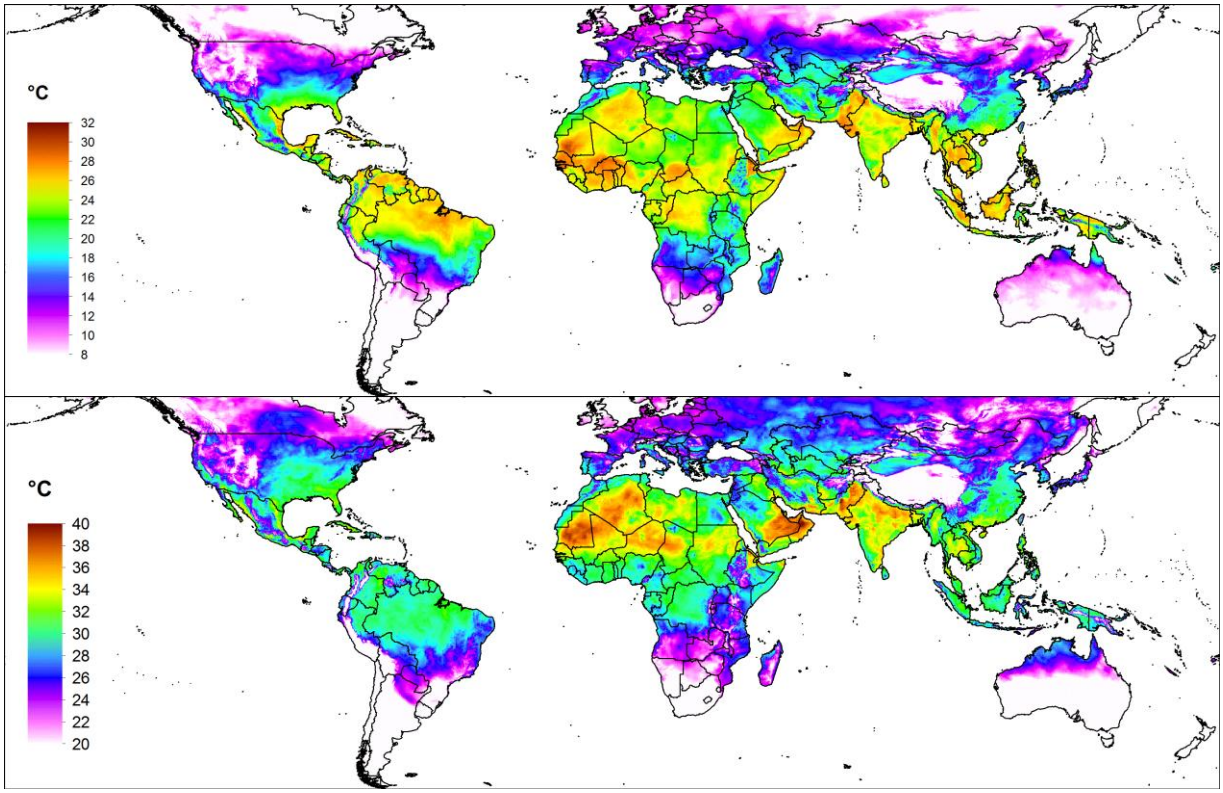

Figure 3-20: Modelled daily average minimum temperature (top), and maximum temperature (bottom) for the month of June under late 20th century conditions.

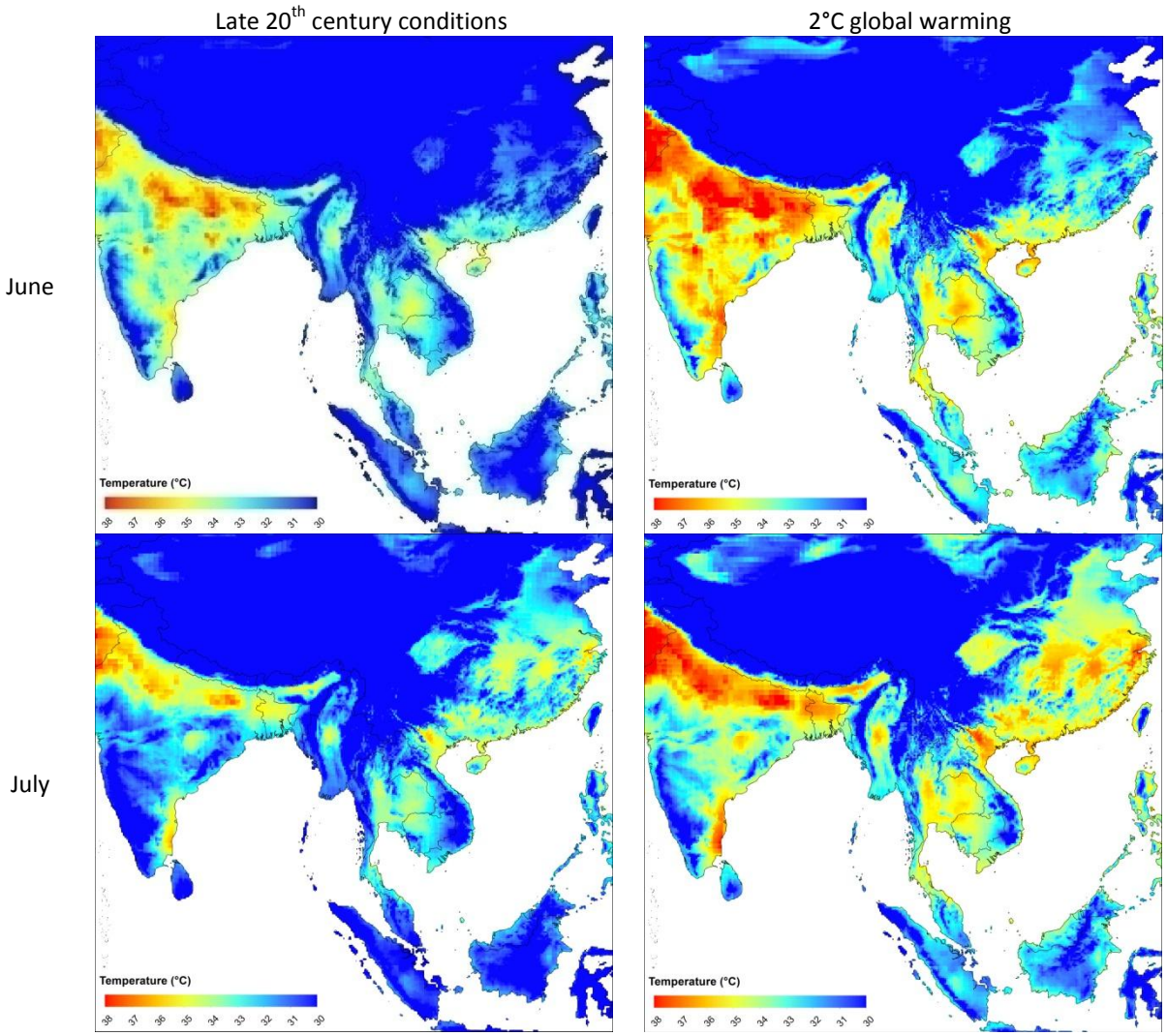

Figure 3-21: Modelled maximum pond temperature for south Asia during June and July under late 20th century conditions and 2°C global warming.

Weekly temperature records with readings taken at 6am and 6pm where obtained from Bangladesh Agricultural University (BAU) for two experimental aquaculture ponds for a four month period (April to July, 2006). The highest recorded temperature from the data set was 36.47°C while the lowest recorded temperature was 22.73°C. The maximum variation between AM and PM temperatures recorded during a single day was 7.67°C and the lowest was 0.3°C. The differences in daily temperature variation recorded during the observation period illustrate again that pond temperatures can vary considerably during the course of a day. The average daily temperature for both ponds over the four month period was 29.4°C, while the minimum and maximum daily average temperatures were 24.64°C and 33.11°C. While a four month time series from a single year is

insufficient to draw any significant conclusions and precise details of how temperatures were taken and at what depth were not available, it is still encouraging to note the recorded average temperature and minimum and maximum average daily temperatures fit well with modelled temperatures from the current study for the same location and time period of: 29.68°C (mean), 25.56°C (minimum), and 33.26°C (maximum).

In terms of the current study it seems likely that diurnal fluctuations in pond temperatures may result in temperatures beyond the maximum and minimum daily mean values obtained. Another factor to consider is that the temperature modelling was conducted for relatively deep ponds (2 metres) meaning day to day variability may be less, potentially resulting in less extreme minima and maxima than may be seen in a significantly shallower pond. That said, the model used in the current study assumes a fully mixed water column but as discussed in the previous paragraph significant stratification tends to take place in aquaculture ponds, especially during warmer daytime hours. The degree of stratification can be significant, for example Losordo and Piedrahita (1991) cite Losordo (1998) and state that vertical temperature gradients of up to 12°C have been recorded from catfish ponds in southern California. With the above in mind it seems probable that in areas where high modelled pond temperatures are predicted, and where there is a notable diurnal fluctuation in air temperature, then water temperatures may exceed the modelled values. Unless the pond is very shallow or artificially mixed then stratification is likely to result in the surface layers of the pond becoming considerably warmer while the lower layers remain more stable. This may be significant for aquaculture as culture organisms will be able to avoid potential extremes of temperature.

It was noted that modelled pond temperatures would show significant variability from one day to the next. This was especially true in the case of temperature reduction where there was a substantial reduction in surface air temperature from one day to the next, particularly when higher wind speeds and lower humidity levels were involved. Under these conditions the large reductions in water temperature within the model are largely the result of heat lost to evaporative cooling where water temperatures are significantly higher than surface air temperatures. These results would seem to be influenced to some degree by the model being run with 24 hour time steps and the use of daily mean weather values. For example, on a day where the average surface air temperature is substantially lower than the previous day the water temperature derived from the previous days calculation is going to be considerably higher than the air temperature. As the model calculates an energy budget

for each time step it is essentially assuming these temperature differences apply over the whole 24h period giving rise to an exaggerated temperature change when the next time step results are calculated. This effect was mitigated in the current study to some extent by specifying relatively deep, and thus more stable, model ponds. It is also worth noting that when evaluating the model using daily average values for climate Nath (1996) found the model to be reliable. That said this aspect of the model and its potential to accurately predict extreme minimum and maximum temperatures could be worthy of future investigation if validation pond temperature data of sufficient quantity, quality and temporal resolution could be obtained for a variety of climate areas. In reality, air temperatures and other climate variables along with pond temperatures will change gradually and continuously. In modelling terms this would be the equivalent of an infinite number of time steps. Reducing the length of the time steps within the model may be one way in which issues of excessive temperature swings as well as diurnal temperature variations could be addressed although in practice the level of temporal detail possible will currently be limited when working at a global scale by the temporal resolution of climate data sets as well as computing capacity.

In association with an increase in time step frequency the implementation of stratified pond models such as those described by Culberson and Piedrahita (1996) and Losordo and Piedrahita (1991) may be worthy of further investigation. To date such models have focused on individual locations and data requirements tend to be extensive. Research that focuses on simplifying and validating such models in order to make use of available spatial data at a broader scale could be potentially valuable.

The reasons for using GCM data to adjust 20th century climate data sets in the current study rather than using GCM output directly have been covered in the methodology section dealing with pond temperature modelling. This methodology makes the assumption that climate variability under future warming conditions will be the same as those under late 20th century conditions and that there will just be a shift in the mean. In impact terms increasing variability around the mean would result in higher and lower extremes in temperature than would be expected using the current method. While it is often assumed that temperature variability will increase in association with global warming recent evidence suggests that this may not be the case. Huntingford et al. (2013) suggest that while there have been increases in variability recorded in some areas evidence suggests this is now decreasing and that the standard deviation of globally averaged temperature anomalies has remained stable over time. The authors also examine outputs from an ensemble of recent climate models

(CMIP5) that predict a decrease in global average temperature standard deviation during the 21st century in association with increasing greenhouse gas concentrations.

Local factors that cannot realistically be incorporated into large scale models may also influence pond temperature to some extent and may need consideration at the individual farm or pond level. Wind speed at the ponds surface may vary from average wind speed in relation to surrounding vegetation and other structures, this in turn may increase or decrease evaporative heat loss and conductive heat exchange between the pond surface and air. Turbidity of ponds will affect the absorption of solar radiation (Kutty, 1987) although in aquaculture scenarios turbidity is likely to be fairly high in most ponds. There is also potential for reduction in solar radiation reaching ponds through shading provided either deliberately or as a result of pond surroundings.

Nath (1996) conducted a sensitivity analysis when developing the model applied in the current study and found that for simulations of daily average water temperature mean air temperature had the greatest effect on outcome followed by relative humidity, short-wave solar radiation, cloud cover, and wind speed. Nath (1996) suggests that the sensitivity analysis results point to daily mean water temperatures being closely linked to evaporative heat flux which is in turn a function of ambient air temperature, relative humidity and wind speed. Nath (1996) also notes that the fairly low significance of solar radiation in the model outcome is surprising and notes that other pond water temperature models such as those developed by: Fritz et al. (1980), Krant et al. (1982), and Losordo (1998) are more sensitive to solar radiation.

Results of linear regression of annual mean 20th century air temperature data used in the current study (independent variable) with annual mean modelled 20th century pond temperatures (dependant variable) are shown in Figure 3-22. Regressions were conducted over areas with land suitability scores of at least 128 out of 255 and where average annual temperatures are over 5, 10, 15, and 20°C. While the fit of the regression becomes less good as minimum air temperature used increases it is noticeable that that the slope of the regression line becomes less steep and the intercept increases. This trend would fit with the observations of Nath (1996) in that evaporative heat flux plays a significant role in the model results at higher temperatures. Ultimately this means that the current model suggests that on average pond temperatures will decrease somewhat less than air temperatures. Taking an average over areas where annual average air temperatures are over 10°C and where land suitability scores are in the upper half of the range gives an increase in air

temperature of 2.4°C and in increase in modelled pond temperature of 1.8°C under 2°C of average global warming. This trend is further highlighted in Figures 3-23 and 3-24.

Temperature data is more easily measured and tends to be more readily available than data for other climate variables. Also, air temperature is typically simulated with a good degree of accuracy by climate models. Given this and the above discussion, the further investigation of the relationship between air temperatures and pond temperature would seem a good area for potential further investigation. While a straight forward linear relationship between air and water temperature that can be applied over wide ranging areas and climate conditions for aquaculture is unrealistic, more regional relationships such as those developed by Wax and Pote (1990) may be useful in providing 'quick and easy' means of assessing site suitability and potential impacts of temperature change.

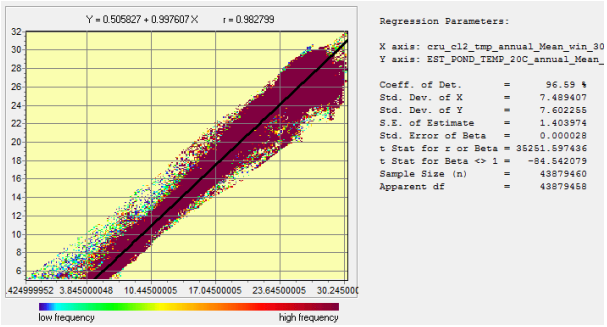

Regression area = land suitability score ≥ 128 and mean air temperature ≥ 5C

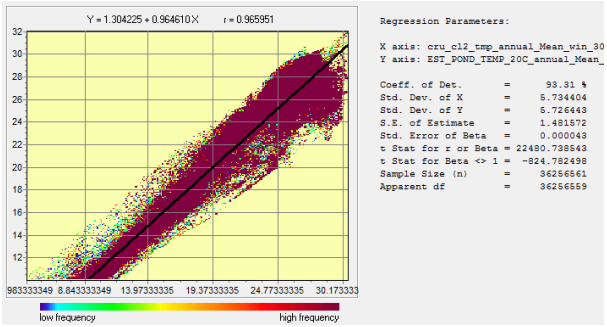

Regression area = land suitability score ≥ 128 and mean air temperature ≥ 10C

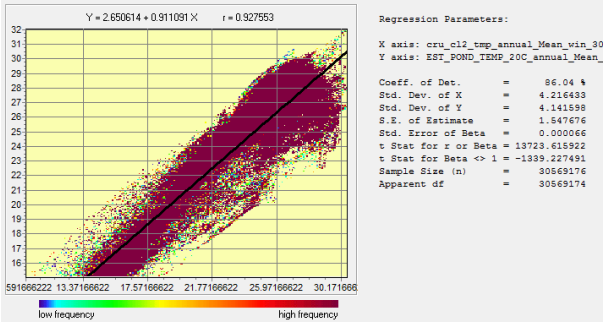

Regression area = land suitability score ≥ 128 and mean air temperature ≥ 15C

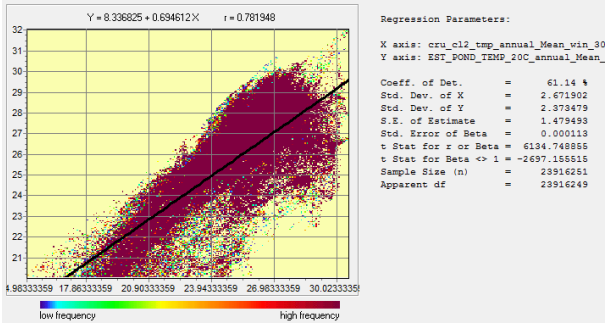

Regression area = land suitability score ≥ 128 and mean air temperature ≥ 20C

Figure 3-22: Regression of annual mean 20th century air temperature (x axis) with modelled annual mean 20th century pond temperature (y axis). Regressions were conducted over areas with land suitability scores of at least 128 out of 255 and where average annual temperatures where over 5, 10, 15, and 20°C.

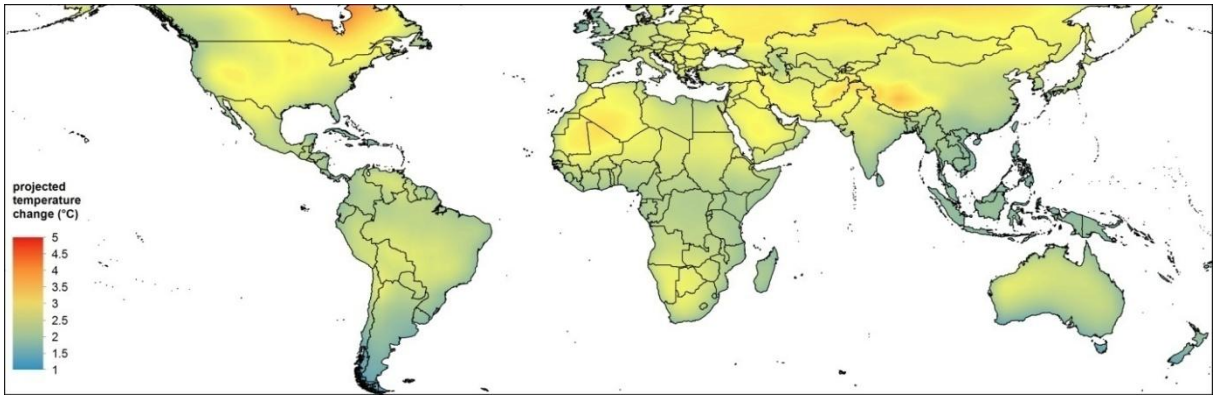

Figure 3-23: Estimated mean annual surface air temperature change under a 2°C warming scenario.

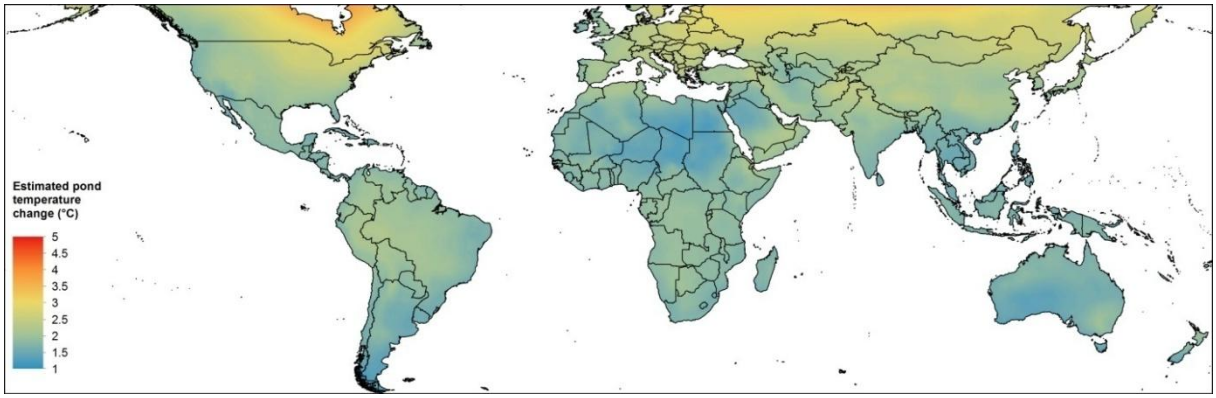

Figure 3-24: Estimated mean annual pond temperature change under a 2°C warming scenario.

3.3.3 Water availability for rain fed ponds - outputs and discussion

Figure 3-25 shows an overview of results from modelling water availability in rain fed ponds for a number of seepage and runoff scenarios under late 20th century conditions and for a 2°C mean global warming scenario. Highlighted areas show where water is predicted for more than 6, 9, and for 12 consecutive months per year based on at least a 90 percent probability of a 2 metre deep pond being at least half full. In the case of the high seepage rate results are only shown for the maximum precipitation runoff scenario (200% of pond area) as there were very few areas indicated when small runoff quantities were used.

Table 3-12 shows the areas (km^2) for the results shown in Figure 3-25. The relative change between the late 20th century and 2°C global warming scenarios are also given. In general, a warmer world will mean increased evaporation rates although this may be offset in some areas by increasing precipitation (IPCC, 2007b). Overall, the figures displayed in Table 3-12 suggest an overall increase in area where rain fed ponds maybe expected to contain water. The large increases in area seen under the medium and high seepage scenarios can at least partially be accounted for by the small overall areas predicted to have water in association with the relatively low resolution (0.5 degree) of the CRU TS3.0 time series data used, meaning that a change in a small number of pixels accounts for a relatively large increase in percentage terms.

Figure 3-26 shows the relative change in precipitation under 2°C average global warming as predicted by the 13 GCMs used in the current study. A notable drying trend is projected over the Mediterranean area with decreases also projected over southern Africa and Mexico. An increase is predicted over Eastern Africa while the picture over much of Asia is rather mixed. It is important to note that unlike temperature where agreement between climate models on patterns of change is generally strong, considerable uncertainty remains in relation to precipitation with different climate models predicting both increases and decreases for precipitation over the same areas. This point is further illustrated here in Figure 3-27 which shows out of 21 climate that contributed to the IPCCs 4th assessment report, the number that project an increase in precipitation over Asia. Given these considerations it is difficult to draw any firm conclusions from the data presented in terms of climate change effects on rain fed aquaculture. The results presented are probably best viewed in relation to current conditions with cautious indications where rain fed water availability patterns may be subject to change. It is also worth noting that the amount of seepage specified made a considerable

difference to model outcomes suggesting that appropriate pond construction may play an important role in feasibility of rain fed aquaculture in marginal water availability areas.

For many areas water supply for aquaculture ponds extends beyond direct rainfall. In some very low lying swampy areas a high water table may maintain water in ponds (Sharma et al., 2013) while other ponds may depend on surface water from lakes, rivers, streams, springs and canals, or groundwater from wells (Kelly and Kohler, 1997). Various studies have attempted to model global changes in water supply under climate change scenarios (e.g. Islam et al., 2007, Murray et al., 2012). While potentially useful in highlighting future water resource issues, such studies are concerned with regional changes and operate at low resolutions (e.g. 0.5 degrees). In reality water resources that dictate site selection for aquaculture will typically be highly localised and complex with a very limited ability to be incorporated into broad-scale site selection models such as the current one.

One interesting area where there may be scope for further development in locating surface water sources over large areas is the use of remotely sensed data. For example, MODIS data have been used to indicate the presence of surface water in relation to flood events (Handisyde et al., 2014, Islam et al., 2010, Sakamoto et al., 2007) and while MODIS operates at a relatively low resolution (250-500m), similar approaches could potentially be taken with high resolution sensors. While cloud cover is a problem for many regions in theory if multiple images can be obtained representing different times of year then it may also be possible to gain some insight into the seasonal nature of surface water supplies.

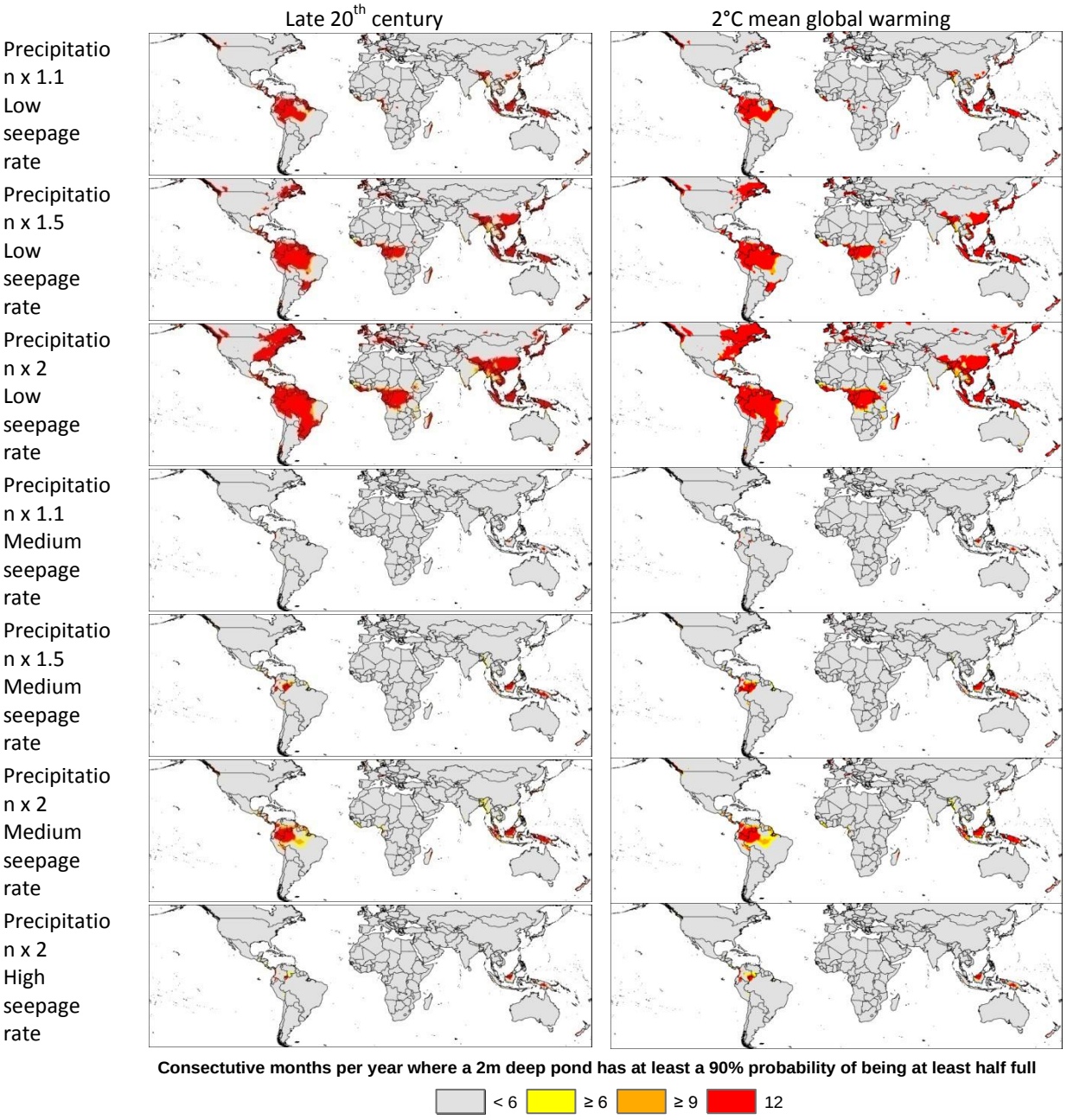

Figure 3-25: Number of consecutive months per year where a model rain fed pond has at least a 90% probability of being half full under a range of runoff and seepage scenarios.

Table 3-12: Areas (km2) of model outputs shown in Figure 25.

Seepage scenario	Runoff scenario (percentage of pond area)	Consecutive months per year pond is at least half full	Area (km^2) under late 20^{th} century conditions	Area (km^2) 2°C mean global warming	2°C warming area as a percentage of 20^{th} century
Low	110%	6	12,985,222	12,471,338	96.04
		9	12,286,294	11,767,006	95.77
		12	11,288,853	10,985,716	97.31
	150%	6	25,519,070	25,474,825	99.83
		9	24,485,203	24,490,161	100.02
		12	22,572,093	22,679,503	100.48
	200%	6	39,782,011	40,899,093	102.81
		9	38,167,792	39,132,288	102.53
		12	35,105,297	36,019,513	102.60
Medium	110%	6	441,536	670,769	151.92
		9	367,823	579,666	157.59
		12	289,807	466,639	161.02
	150%	6	3,209,949	3,752,914	116.92
		9	2,470,716	3,109,322	125.85
		12	1,951,437	2,565,078	131.45
	200%	6	10,198,978	10,066,509	98.70
		9	7,495,995	7,639,839	101.92
		12	5,484,890	5,583,307	101.79
High	110%	6	41,951	63,468	151.29
		9	32,980	51,424	155.93
		12	29,907	45,277	151.39
	150%	6	191,133	270,256	141.40
		9	161,166	204,250	126.73
		12	118,378	170,552	144.07
	200%	6	1,469,138	1,859,296	126.56
		9	1,065,717	1,511,807	141.86
		12	828,391	1,164,318	140.55

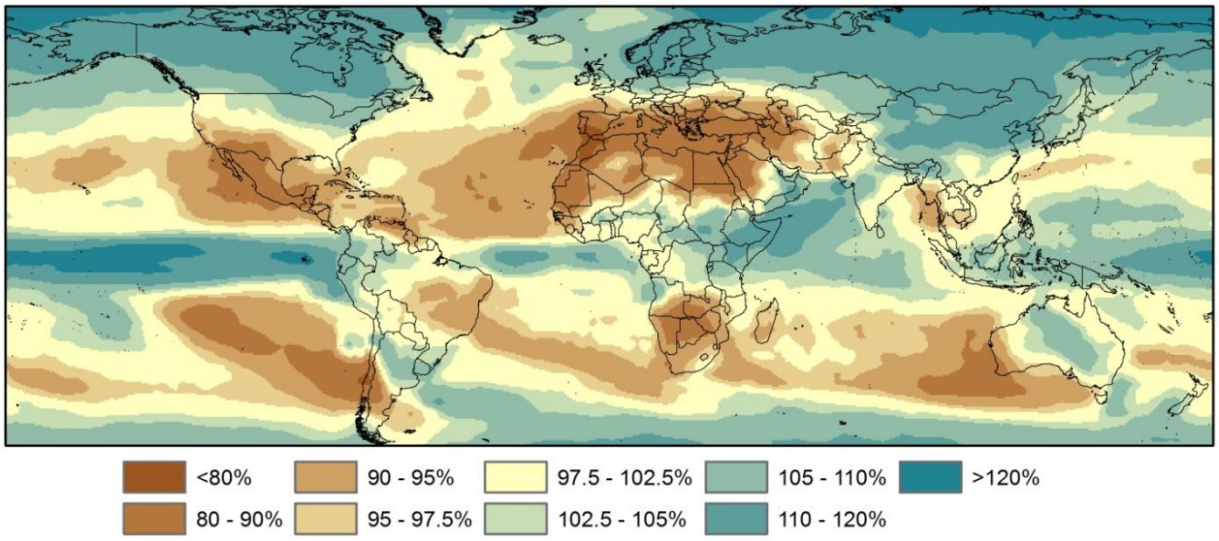

Figure 3-26: Projected change by the 13GCMs used in the current study for annual average precipitation amounts under 2°C average global warming compared with late 20th century conditions.

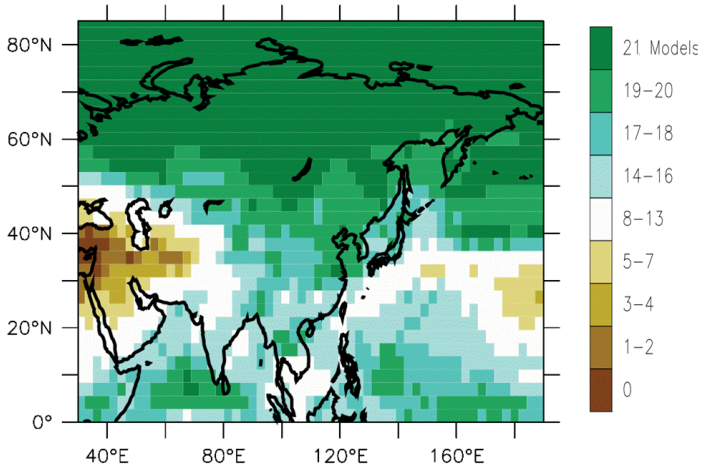

Figure 3-27: Number out of 21 climate models projecting an increase in precipitation under SRES scenario A1B (from: IPCC, 2007a).

3.3.4 Combined sub-models - outputs and discussion

As already outlined, two approaches to combining sub-model outputs are demonstrated here: an ordered weighted average of temperature and land suitability results, and use of specified limits for temperature and water availability to define an area within which land suitability can be considered.

In each case Nile tilapia (*Oreochromis niloticus*) were considered as a model species with a wide distribution in aquaculture terms.

Figure 3-28 shows outputs from the Combination of land suitability and temperature using an OWA under late 20th century conditions and under an average 2°C global temperature increase . For display purposes every second month is shown. Figure 3-29 highlights the difference between the images shown in Figure 3-28 under the two climate scenarios. In this example there are regions that stand to both gain and lose in terms of suitability depending on the time of year. The Bangladesh area provides a good example of this with improved suitability score being seen for the colder months (December and February) while looking at the outputs for August there is a slight decrease in suitability in association with temperature above those specified as optimum. A similar situation is seen in Thailand and some other areas of south East Asia. Southern China is also notable as somewhere where there could be potentially positive impact in terms of an improved growing season.

The results provided in the current example are obviously highly dependent on the reclassification of the temperature data. In the case of Nile tilapia it would potentially have been reasonable to extend the temperature ranges used to represent conditions that would more represent possible rather than optimal ranges while at the same time excepting a greater degree or risk in relation to unusually hot or cold periods. Such an approach, especially in the case of colder temperatures, could be used to indicate areas that would currently be considered marginal in terms of fish survival during colder months that may become more usable under warming conditions.

Figures 3-30 and 3-31 show examples of outputs obtained by using specified limits for mean, minimum, and maximum temperature along with water availability to specify areas which can then be considered in relation to land suitability. Table 3-13 shows areas (km^2) for Figures 3-30 and 3-31 as well as for where ponds are expected to contain water for 9 and 12 consecutive months per year. Results are shown based on both the GlobCover based land suitability sub-model output and that produced using MODIS land cover data. The areas defined by temperature and water availability are notably larger under the warming scenario which can be accounted for by the increased temperatures moving new areas into the defined acceptable range and again highlights the potential for increased production in many areas in relation to warmer conditions.

This method contrasts to the previous one in that there is no 'fuzziness' in relation to temperature suitability; areas are either considered useable or excluded. The advantage of such an approach is that by asking a number of specific questions of the database a potentially more focused answer is provided. In this case it allows for the land suitability sub model results to be considered without being 'diluted' through combination with other data. In theory this exercise could be repeated using a number of different temperature specifications to allow for a more detailed picture of suitability to be built up over different regions. Another potential advantage to using a decision tree approach to ask questions of the data is that it can avoid the need to standardise data to a common scoring system (Drobne and Lisec, 2009) which if not done with care may lead to potentially questionable results when factors are then traded against each other using weighted averaging methods. Finally, there is the potential to eliminate the risk of an area being indicated as suitable after combination of a range factors using a weighted average when according to one of the factors it is not.

A key disadvantage of a decision tree approach is that it forces those developing it to make choices that can have a very definitive effect on the final outcome in a way that can be conceptually much more complex. It also potentially forces strict decision-making in situations where that may be very difficult due to levels of uncertainties about how a given variable relates to suitability, especially in the case of variables that may influence suitability but which are not considered critical. Another consideration is that the reality of working with spatial data sets often involves some degree of uncertainty about data quality and again in situations where such data relates to non-critical attributes the ability to allow the data to have some degree of influence on the final outcome without it having to result in a definitive answer can be potentially very useful.

In summary, spatial data can be combined in a range of diverse ways to assist decision-making. A substantial advantage of a GIS approach is that once a spatial database is established changes can be made to decision support models relatively easily in relation to varying requirements and decision questions. It is suggested here that the use of multi-criteria evaluation approaches such as WLC and OWA would seem especially useful for the broad-scale assessment of aquaculture site suitability by allowing for the incorporation of variables with different levels of significance and degrees of uncertainty. The use of Boolean intersection, or constraints, is also valuable in allowing the exclusion of highly unsuitable areas as well as providing a means of investigating changes in potentially suitable area under changing conditions in relation to a specific set of requirements.

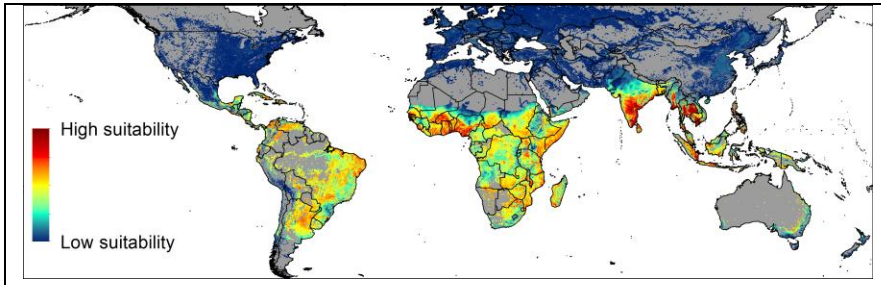

February (late 20th century conditions)

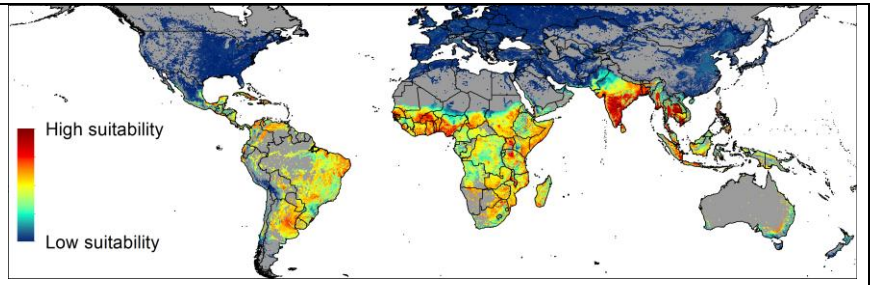

February (2°C average global warming)

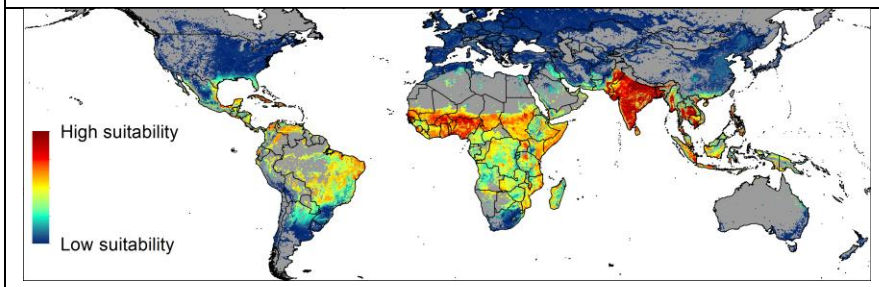

April (late 20th century conditions)

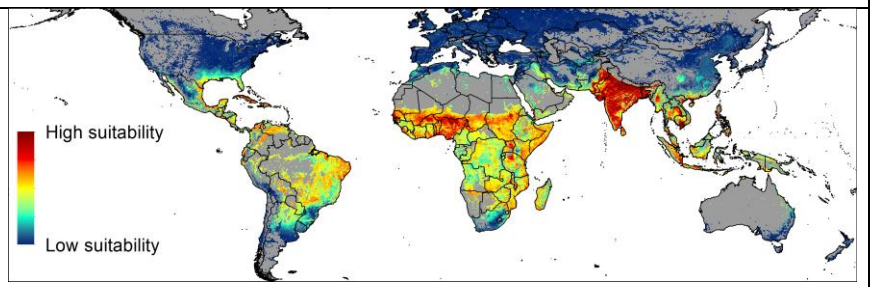

April (2°C average global warming)

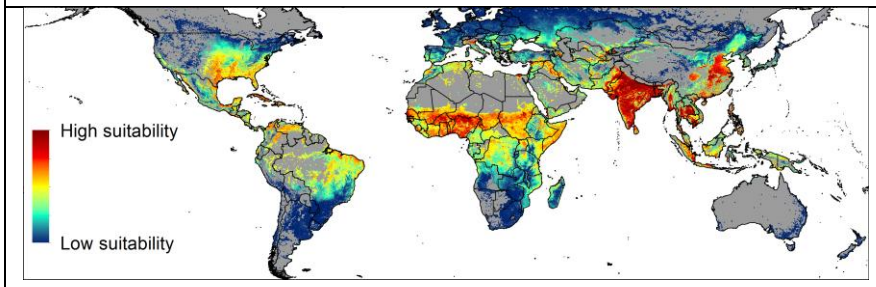

June (late 20th century conditions)

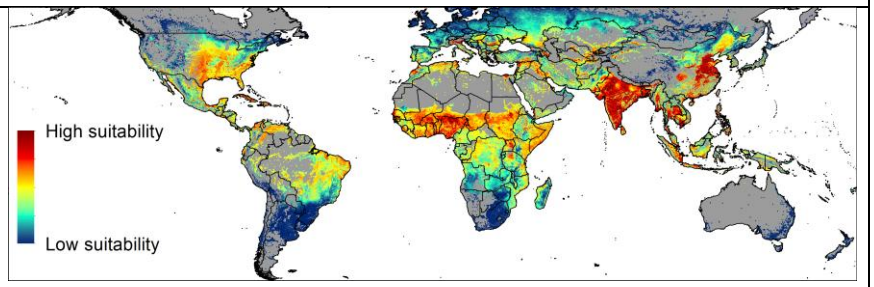

June (2°C average global warming)

Figure 3-28: Suitability for warm water fish culture (tilapia as model species) based on a combination of land suitability and temperature using an OWA.

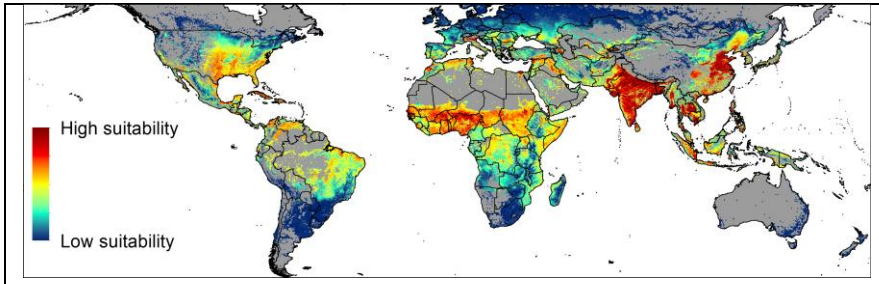

August (late 20th century conditions)

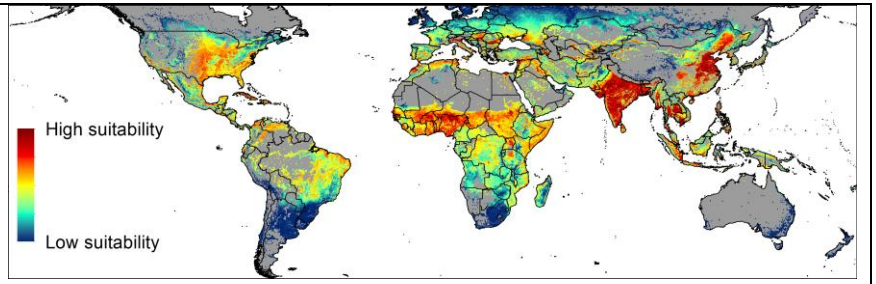

August (2°C average global warming)

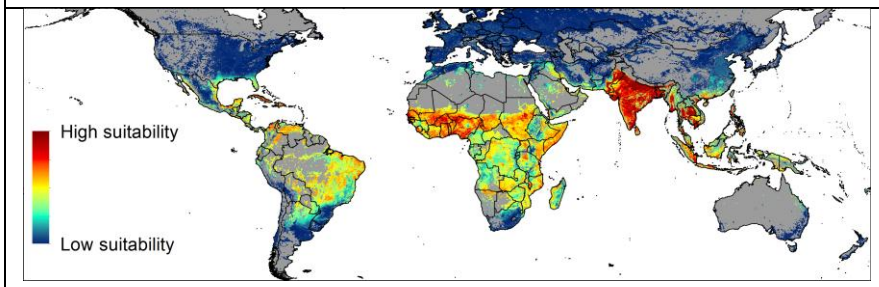

October (late 20th century conditions)

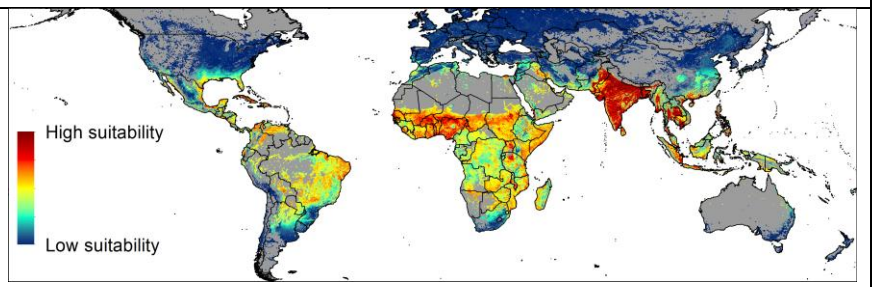

October (2°C average global warming)

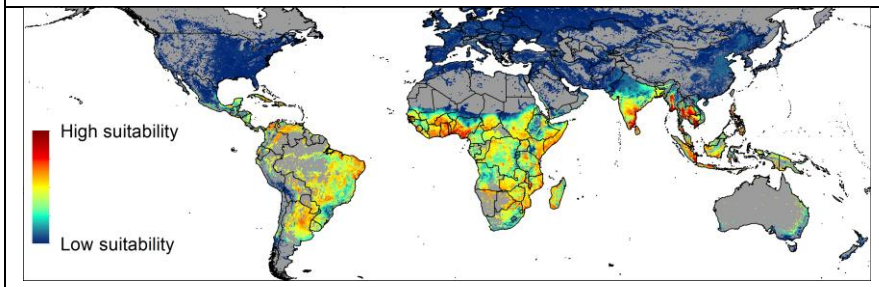

December (late 20th century conditions)

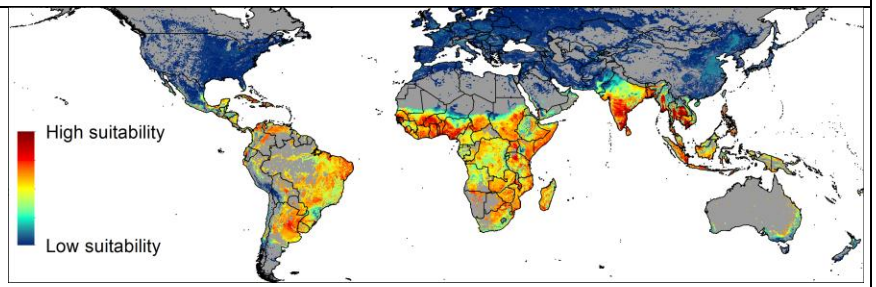

December (2°C average global warming)

Figure 3-28 continued. Suitability for warm water fish culture (tilapia as model species) based on a combination of land suitability and temperature using an OWA.

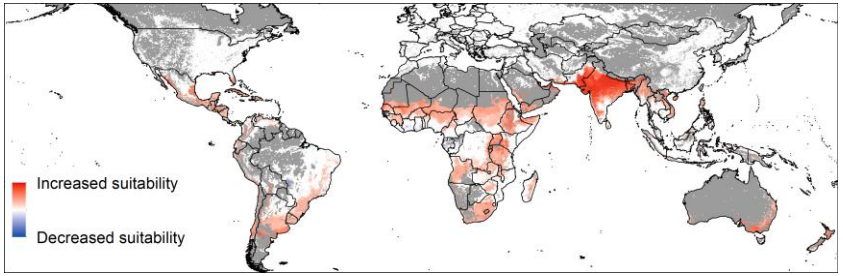

February

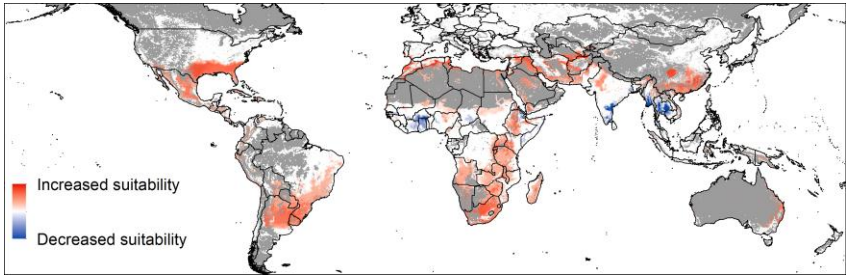

April

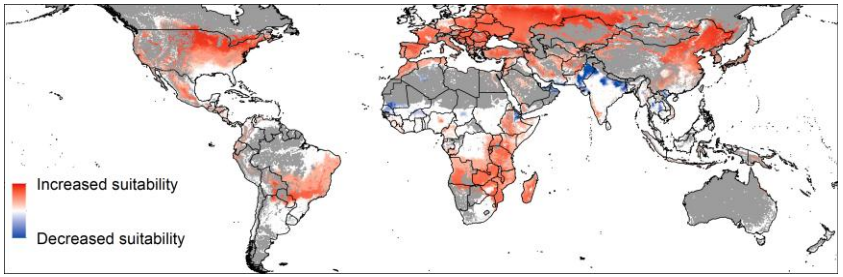

June

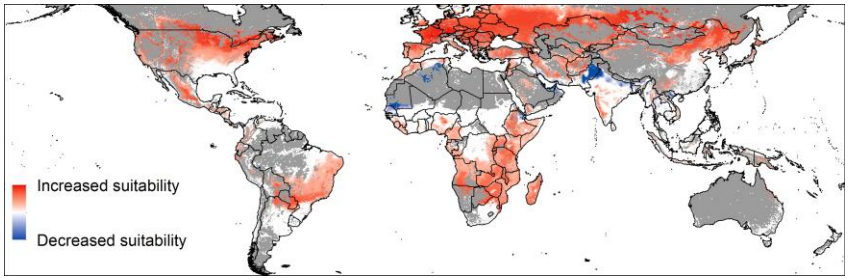

August

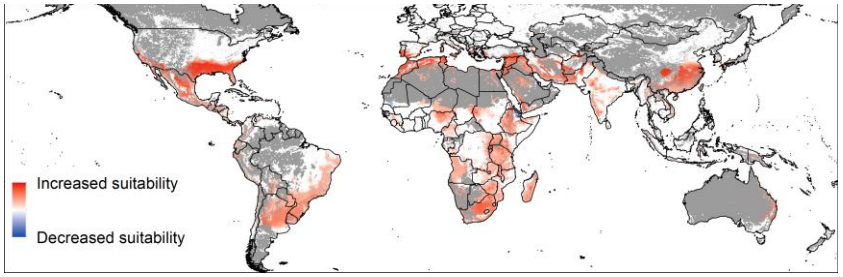

October

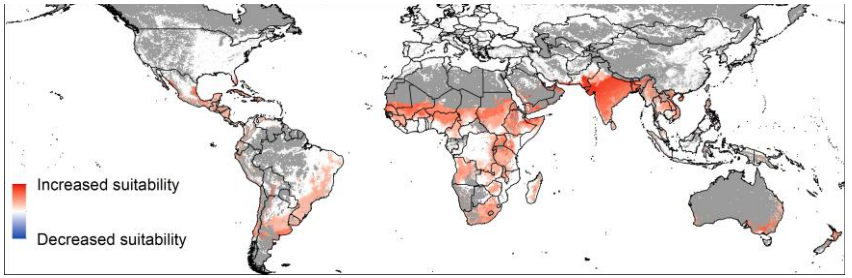

December

Figure 3-29: Change in suitability (increase or decrease) between the two climate scenarios presented in Figure 3-28.

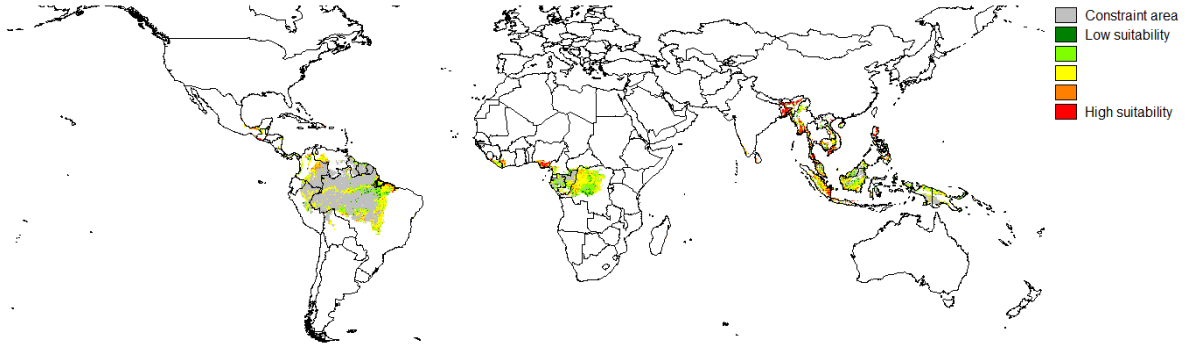

Figure 3-30: Areas meeting specified temperature requirements and with water predicted in rain fed ponds for at least 6 consecutive months based on the low seepage rates and precipitation over an area representing 150% pond surface area. All climate data based on late 20th century conditions. Defined areas are overlayed with outputs from the land suitability sub-model based on MODIS land cover data (See: Combination of sub-model outputs section for full details).

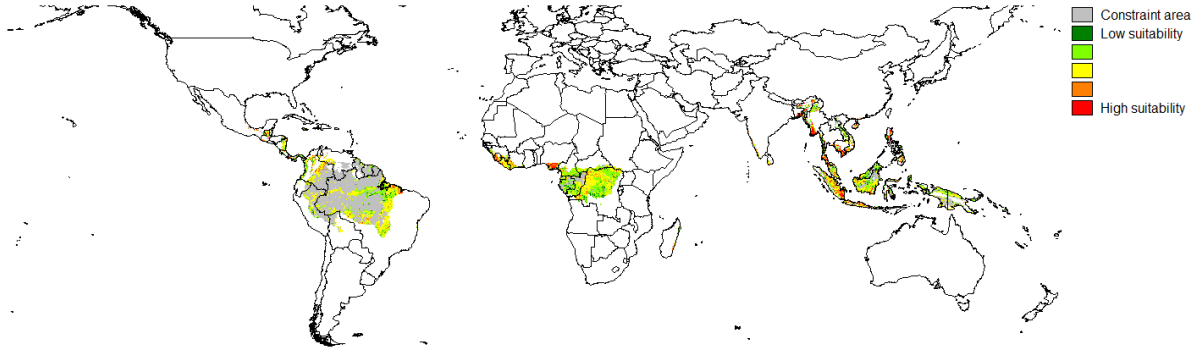

Figure 3-31: Shows the same output as Figure 3-30 but based on the 2°C average global warming scenario rather than late 20th century conditions.

3-13: Areas (km2) obtained by using specified limits for mean, minimum, and maximum temperature along with water availability using MODIS or GlobCover (see Figures 3-30 and 3-31).

							Percentage change between late 20th century and 2°C average global warming scenarios		
	Late 20th century conditions			2°C average global warming					
	Number of consecutive months where model ponds have at least a 90 percent change of being over half full.			Number of consecutive months where model ponds have at least a 90 percent change of being over half full.			Number of consecutive months where model ponds have at least a 90 percent change of being over half full.		
Suitability	6 months	9 months	12 months	6 months	9 months	12 months	6 months	9 months	12 months
MODIS									
Constraint	5,152,099	4,599,448	3,396,707	5,846,756	5,331,893	4,698,242	113.48	115.92	138.32
1	363,725	254,716	156,999	521,385	395,587	296,310	143.35	155.30	188.73
2	1,559,071	1,185,971	823,249	2,094,198	1,730,445	1,372,258	134.32	145.91	166.69
3	3,066,259	2,411,789	1,733,814	3,498,741	3,013,081	2,344,133	114.10	124.93	135.20
4	752,919	497,152	319,684	823,134	629,220	404,900	109.33	126.56	126.66
5	493,003	229,670	121,356	380,156	274,944	127,201	77.11	119.71	104.82
GlobCover									
Constraint	5,176,209	4,621,917	3,416,816	5,872,550	5,354,701	4,717,648	113.45	115.85	138.07
1	271,755	200,509	126,666	391,728	308,048	232,841	144.15	153.63	183.82
2	1,472,278	1,125,999	781,113	1,970,943	1,617,660	1,287,193	133.87	143.66	164.79
3	2,821,406	2,201,061	1,576,090	3,299,626	2,834,253	2,222,976	116.95	128.77	141.04
4	966,827	684,602	450,558	1,064,434	843,396	576,812	110.10	123.20	128.02
5	667,674	336,144	195,071	553,725	407,489	200,580	82.93	121.22	102.82

3.4 Concluding remarks

The current study represents a unique assessment of site suitability for aquaculture at the global scale with data represented at a high resolution of 10 arcseconds. To date the largest scale GIS based site suitability assessments for aquaculture have operated at the continental level focusing on Latin America (Kapetsky and Nath, 1997) and Africa (Aguilar-Manjarrez and Nath, 1998, Kapetsky, 1994) and have operated at resolutions ranging from 3 to 10 arcminutes. Another significant and valuable feature of the current study that differs from other GIS models of site suitability for aquaculture, is the use of projections from a group of climate models to allow for modelling of pond temperature under global warming conditions as well as those representing the recent past.

Two methods of combining data are demonstrated using Nile tilapia (*Oreochromis niloticus*) as a model warm water species that has temperature requirements that are broadly applicable to a range of commonly cultured tropical species. While outputs from the modelling process are best expressed as a series of images a number of general conclusions can be drawn:

- Pond temperatures are projected to increase less than air temperatures in most areas although for many regions a 2°C average global warming scenario results in a greater than 2°C projected increase in air temperatures over land.
- Depending on location and season both positive and negative impacts on suitability are projected in relation to the 2°C warming scenario. Some parts of Asia such as Bangladesh where aquaculture is highly significant show reduced suitability during the warmest part of the year. Overall viewed globally there would appear to be a positive trend for suitability in relation to increasing temperatures as a result of potential increases in growth performance in areas where colder temperatures are currently limiting. Such a trend may potentially allow for longer growing seasons or expansion into currently marginal areas.
- In terms of water availability for rain fed ponds there are areas of both projected increase and decrease. Globally there is a projected increase in potential area under most seepage and runoff scenarios examined. It is worth noting that while the projected increases appear large in percentage terms in some cases the overall area in relation to grid resolution is low meaning that change in a small number of cells has a significant impact. This is an area that could be considered for potential refinement if suitable data become available.

To date research relating to direct climate change effects on inland aquaculture has been extremely limited. In terms of the spatial implications of potential change the current assessment provides valuable insights into potential effects of changing climate on suitability for the growing pond-based aquaculture sector. While negative impacts are projected for a number of locations, it is suggested here that the indication of positive effects in many areas is extremely important in terms of the future development of the sector and further research is almost certainly warranted.

4 USE OF MODIS MULTISPECTRAL IMAGERY FOR IDENTIFICATION OF SURFACE WATERS AND FLOODING IN BANGLADESH

4.1 Introduction

Inland aquaculture, especially that based in ponds, typically has site selection requirements that favour certain soil types and relatively flat areas with access to surface water sources (e.g. Nath et al., 2000, Ross et al., 2009). Flood plain areas of river systems often meet these requirements and are thus popular locations for both aquaculture and terrestrial agriculture development. Regular seasonal flood patterns in many areas are anticipated and incorporated into production strategies of both aquatic and terrestrial farmers. However inter-annual variability in flooding is common in many areas resulting in potentially adverse consequences for areas generally assumed to be flood free (Mirza, 2002).

Bangladesh is a mostly low lying deltaic country with much of its area comprised of the floodplain for three large and converging rivers (the Ganges, Brahmaputra, and Meghna). 92.5% of the combined catchment area for these river systems lies outside the country over an area that includes the Himalayan region along with a significant area of India. The result of these extensive and diverse catchments is a large and varied volume of water draining through Bangladesh annually. (Mirza, 2002) suggests that Bangladesh experiences an annual average flood coverage of 20.5% of the country area and that peoples livelihoods are well adapted to these average patterns. However more severe flooding is relatively frequent with 70% of the country inundated in the case of the 1998 flood that resulted when peak discharges of the Brahmaputra and Ganges that normally take place at different times occurred within two days of each other (Mirza, 2002). Along with this significant river based flooding Bangladesh also experiences flash flooding as a result of direct rainfall over low lying inland areas, and storm surge based flooding in coastal regions in association with tropical storms (Handisyde et al., 2006).

While considerable uncertainty remains in relation to changing climate, and especially with regards to the water cycle and changing patterns of precipitation (IPCC, 2013), there are indications that monsoon and snow melt related runoff for the major drainage basins influencing Bangladesh is set to increase (Hasson et al., 2013, Lutz et al., 2014). Mirza et al. (2003) and Mirza (2011) found varied results when modelling flooding in Bangladesh under scenarios provided by 4 climate models. The

author also notes that in the case of models predicting increases in river discharge the greatest impact on flooding in terms of areas per °C increase in average global temperature occurred within the first 2°C of global warming. Mirza (2011) goes on to suggest that this result can be explained as a result of land elevation and that most potentially floodable areas would be inundated under modest increases in river discharge. Climate related changes may also influence flash flooding as a result of heavy rainfall directly over areas of Bangladesh with potential change in both spatial and temporal distribution as well as intensity (Nowreen et al., 2014).

Islam et al. (2010) suggests that compared to many regions of the world ground based mapping of flood inundation within Bangladesh is fairly limited, and that an understanding of spatial and temporal patterns of flooding play an important role in relation agriculture. While it may be theoretically possible to model flood risk through the use of hydrodynamic modelling (e.g. Masood and Takeuchi, 2012), such approaches are dependent on high quality data inputs, such as for elevation, which are often lacking.

Compared with traditional survey methods the use of remotely sensed data obtained from a range of instruments aboard earth observation satellites has opened up possibilities for relatively quick and cheap mapping of land cover types over large areas with the ability to incorporate a time dimension though the use of multiple images.

Synthetic aperture radar (SAR) data such as that provided by RADARSAT-1 and RADARSAT-2 is available at a range of resolutions and scene sizes and can provide extremely good land/*water* delineation. Another advantage of SAR based imagery is that it's performance is not impacted by atmospheric effects including cloud. This ability to record effective data in the presence of cloud cover makes it extremely useful for surface water detection during wet seasons when cloud cover is common. Hoque et al. (2011) used a series of RADARSAT images to monitor flood extent in Bangladesh during the period 2000 to 2004 with a considerably larger area than usual flooded in 2004. Dewan et al. (2006) and Dewan et al. (2007) used a series of six RADARSAT images spanning the time period of an extreme flood event (July to September 1998) in association with a GIS to assess flood risk for the greater Dhaka area. While SAR data is highly effective for detecting surface water it is generally not freely available thus its typical use, such as in the studies outlined above, involves a limited number of scenes with the aim of investigating specific events.

Data from a range of passive sensors has also been used to address the issue of surface water distribution and flooding. Islam and Sado (2000b) used three Advanced Very High Resolution Radiometer (AVHRR) images spanning a 21 day period to analyse the 1988 flood event that represented a 100 year record for Bangladesh. The authors went on to attempt to link dry season land cover type and elevation to the flooding described by the AVHRR images.

The AVHRR data used by Islam and Sado (2000b) has a spatial resolution of approximately 1.1km. The use of higher resolution data would seem to have significant advantages for regions such as Bangladesh where parcels of land are often small and therefore the likelihood that different surfaces will be contained within the area represented by a single pixel is high. The Thematic Mapper (TM) and subsequent Enhanced Thematic Mapper plus (ETM+) aboard Landsat satellites provide a number of bands in the visible and infrared spectrum at a ground resolution of 30m. With a scene size of approximately 170 by 183km Landsat data strikes a good compromise between resolution, coverage and usability for investigating land cover and associated change over large areas and as such has formed the basis of a large number of studies where land cover data is required (e.g. Kirui et al., 2013, Zeledon and Kelly, 2009) as well as more specific focus on surface water delineation (e.g. Ouma and Tateishi, 2006, Wang et al., 2002). While the data processing requirements for an extensive time series of Landsat images would be large, perhaps its key limitation in terms of time series work is the long return period meaning that at best images are only available for the same area every 16 days. Factoring in issues of cloud cover which can be significant for many areas during wet seasons then the number of useable images is often small with a tendency to focus on dryer times of year.

The Moderate-resolution Imaging Spectroradiometer (MODIS) is an instrument installed on the NASA Terra and Aqua satellites. MODIS collects data over 36 spectral bands, 7 of which are of interest in terms of land surface classification. Of these 7 bands 2 (red and near infrared) are available at approximately 250m resolution while the remaining bands (visible light and shortwave infrared) are provided at approximately 500m resolution. Due to the relatively quick return period of 1 or 2 days and large scene size MODIS provides a valuable tool where remotely sensed data is needed with a high temporal resolution. Another significant advantage of MODIS data is that it is made freely available as a set of pre-processed and highly useable products. Along with a large body of work relating to changes in land and vegetation cover, MODIS data have been used to investigate change in surface water coverage. For example Chipman and Lillesand (2007) used a MODIS-derived normalised

difference vegetation index (NDVI) to monitor change in lake area in southern Egypt. Murray-Hudson et al. (2014) used thresholds from a single MODIS band (band 1) to investigate flood distribution in an area of Botswana. The authors suggest that MODIS images showed a bimodal frequency distribution over the study areas with peaks representing wet and dry areas and that a threshold can be assigned in relation to the trough between the two peaks. It is worth noting that in the case of Bangladesh such a bimodal frequency distribution is not seen. This is likely a result of a much more complex land cover situation with a large number of pixels containing varied amounts of both vegetation and water. Huang et al. (2012) used thresholds from the Normalized Difference Vegetation Index (NDVI) and band 2 (near infrared) to analyse flood hazard in the Dongting lake area, China. Westra and De Wulf (2006) used Fourier analysis in association with short-wave infrared (band 7) data and the NDVI, the Normalized Difference Water Index (NDWI), and the Enhanced Vegetation Index (EVI) to monitor floodplain dynamics in northern Cameroon. Sakamoto et al. (2007) built on the work of Xiao et al. (2006) to develop an algorithm that used EVI, Land Surface Water Index (LSWI) and the difference value between EVI and LSWI to investigate annual flooding within the Mekong delta by classifying pixels as land, mixed, or water related.

The method developed by Sakamoto et al. (2007) has been applied with minor modification by Handisyde et al. (2014) to investigate flood risk for the Paraná river floodplain, Argentina in the context of aquaculture development. The same methodology has also been applied by Islam et al. (2010) to produce a flood inundation map of Bangladesh. The authors use the result to examine flood coverage during 2004 and 2007, both years with above average flood events. Islam et al. (2010) made use of a single RADARSAT image classified to show land and water to verify the MODIS result although the differentiation of mixed and water pixels does not seem to be included. The exact methodology used by Islam et al. (2010) for accuracy assessment, as well as the level of certainty over the RADARSAT image classification its self, are somewhat unclear.

The current study aims to investigate the validity of the method adapted from Sakamoto et al. (2007) and applied by Islam et al. (2010) in relation to flooding in Bangladesh through the introduction of surveyed ground truth data and higher resolution Landsat ETM+ data. Alternative methods for classifying pixels into the land, mixed and water classes are also investigated. The results are used to construct an up to date time series which is examined in relation to inundation frequency as a

proportion of the total time series and can contribute to broader site suitability modelling within the region.

4.2 Methods and data

The methodology and workflow for the current study can be briefly summarised as follows:

1. Collection of ground truth data.
2. Use of ground truth data to produce a set of ground control points (GCPs) half of which are used to classify data and the other half for verification.
3. Conversion of Landsat image digital numbers to surface reflectance values via comparison with corresponding MODIS images.
4. Removal of cloud and cloud shadows from Landsat images.
5. Production of normalised difference ratios along with EVI using Landsat data.
6. Use of training points to produce histograms from normalised difference ratios, EVI and DVEL for land, mixed, and water pixels.
7. Selection of best options from above and investigate thresholds for classification. Also consider multi stage classifications and multiband classification methods.
8. Conduct accuracy assessments for above Landsat based classifications using GCPs.
9. Production of normalised difference ratios along with EVI using MODIS data.
10. Classification of above MODIS-based combinations guided by results obtained from Landsat data
11. Accuracy assessment of MODIS combinations against best result from the Landsat data as well as GCPs.
12. Production of time series of flood, mixed and land pixels using MODIS data.
13. Analysis of time series to proportion of cloud free time series where water related pixels are present .

4.2.1 Collection of ground truth data

Ground truth data were collected for a range of locations within Bangladesh over a 4 day period (02/11/2008 to 05/11/2008) and consisted of a series of photographs with corresponding GPS information. Efforts were made to select areas from a diverse range of land cover types including areas of mixed land and water such as wetlands and flooded cropland.

4.2.2 Creation of ground control points

Ground control points (GCPs) were created based on recorded GPS points and corresponding photographs. Careful use was also made of high resolution satellite imagery, such as that provided by ESRI Basemaps, along with visual inspection of Landsat composites in order to produce GCPs for urban areas where field based records were limited. This method was considered appropriate in the case of well established urban areas where it is likely that temporal variation in land cover would be limited. While visual inspection of high resolution imagery may seem to provide a quick and easy

method for creating GCPs for other land cover classes such as those associated with crops and seasonal water coverage, it is suggested here that this would be inappropriate for a region such as Bangladesh where changes in land cover between the acquisition times of the high resolution imagery and the images to be classified could be significant.

GCPs were initially created for 9 land cover classes which were then further reduced down to three classes representing land, water, and mixed pixels. The 9 initial classes allowed the further division of the main land, mixed and water classes during the investigatory stage when attempting to develop and refine classification methods. Table 4-1 gives details of the classes used in the current study and the number of GCPs created. In each class GCPs were randomly split into two equally sized groups, one of which was used as training data for developing classification procedures and the other for verification of classified images.

Table 4-1: Land cover data used to create GCPs. Number of GCPs created shown in brackets (n = number of points).

Initial land cover classes before being assigned as either: land, mixed or water.	Land-mix-water classes	Land-mix-water classes excluding class 9
1. Water (n=431)	Water (n=698)	Water (n=698)
2. Mixed water and vegetation (land) (n=155)	Mixed (n=528)	Mixed (n=275)
3. Crops (n=253)	Land (n=1505)	Land (n=1505)
4. Crops with water (rice) (n=120)	Mixed (n=528)	Mixed (n=275)
5. Trees and shrubs (n=336)	Land (n=1505)	Land (n=1505)
6. Bare ground (n=297)	Land (n=1505)	Land (n=1505)
7. Urban (n=619)	Land (n=1505)	Land (n=1505)
8. Clear deep water (n=267)	Water (n=698)	Water (n=698)
9. Floating vegetation / dense vegetation in wetlands (n=253)	Mixed (n=528)	

One area of slight uncertainty and potential classification difficulty was class 9 which appeared to be areas of very dense vegetation based on having very high vegetation index values e.g. Normalized Difference Vegetation Index (NDVI) and Enhanced Vegetation Index (EVI). These areas were inaccessible when collecting ground truth data but consultation with local experts suggested that these were areas of floating vegetation associated with wetlands. In the current study wetlands were considered as mixed areas within the three class land, mixed, water scheme and it was decided to

include class 9 within the mixed pixel class. Due to its densely vegetated nature class 9 is potentially difficult to separate from land in terms of its spectral response. For example the classification scheme proposed by Sakamoto et al. (2007) that aims to classify areas as land, water or mixed uses an EVI value of greater than 0.3 to classify areas as land. Under this scheme the class 9 areas in the current study would be firmly classified as land. Due to these potential classification difficulties and given the relatively small overall area represented by this class it was decided to create two groups of GCPs representing mixed areas, one of which excluded class 9. This gave the option of assessing classification methods that may be accurate apart from these areas of dense wetland vegetation.

4.2.3 Selection of Landsat data and conversion of Landsat digital numbers to MODIS surface reflectance equivalent

Nine Landsat ETM+ scenes were used to form an area that, with the exception of the extreme north of the country, covers most of Bangladesh. Images were selected so that acquisition times corresponded as closely as possible to the dates on which ground truth data were collected. Details of the ETM+ images used are given in Table 4-2. Six of the Landsat scenes were supplied using the UTM-46n projection system while the remaining three used UTM-45n. Those using UTM-45n were re-projected to UTM-46n using nearest neighbour resampling to allow combination with the other images to form a single larger scene.

Table 4-2: Landsat ETM+ scenes used.

Path number	Row number	Acquisition date	Projection of data as supplied
136	43	09/11/2008	UTM-46n
136	44	09/11/2008	UTM-46n
136	45	09/11/2008	UTM-46n
137	43	31/10/2008	UTM-46n
137	44	31/10/2008	UTM-46n
137	45	31/10/2008	UTM-46n
138	43	07/11/2008	UTM-45n
138	44	07/11/2008	UTM-45n
138	45	07/11/2008	UTM-45n

Landsat ETM+ images are supplied with reflectance values for each band represented using an arbitrary 8-bit system of digital numbers ranging from 0 to 255. For the current study these digital numbers were converted to surface reflectance values (0-1) via comparison with equivalent MODIS images. This was achieved using MODIS product MOD09GA that supplies daily atmospherically corrected and standardised surface reflectance values. MOD09GA images were obtained for dates corresponding to the acquisition dates of the Landsat images being used. The images were then visually inspected to find areas of uniform reflectance that were large enough for Landsat and MODIS images to be compared without problems of varied Landsat values being represented in a single MODIS pixel. Efforts were made to find areas representing the lowest and highest reflectance values (excluding cloud) as well as those in-between. A linear relationship (see Figure 4-1) was then established between MODIS surface reflectance values and Landsat digital numbers for corresponding bands (Table 4-3). The advantages of this approach were that: a) it allowed for Landsat scenes collected on different days and under different atmospheric conditions to be standardised in terms of reflectance and thus combined into a single image that could then be classified, b) it would allow classification routines based on thresholds established using one set of data to be translated to the other.

Table 4-3: Comparison of Landsat ETM+ and equivalent MODIS bands.

Landsat		MODIS	
Band Number	Wavelength Interval	Band Number	Wavelength Interval
1	0.45-0.52 µm	3	0.459 - 0.479 µm
2	0.52-0.60 µm	4	0.545 - 0.565 µm
3	0.63-0.69 µm	1	0.620 - 0.670 µm
4	0.76-0.90 µm	2	0.841 - 0.876 µm
5	1.55-1.75 µm	6	1.628 - 1.652 µm
7	2.08-2.35 µm	7	2.105 - 2.155 µm

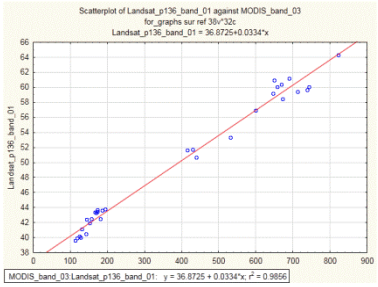
Scatterplot of Landsat_p136_band_01 against MODIS_band_03
for_graphs sur ref 38v*32c
Landsat_p136_band_01 = 36.8725+0.0334*x
Landsat_p136_band_01
MODIS_band_03,Landsat_p136_band_01: y = 36.8725 + 0.0334*x; r² = 0.9856

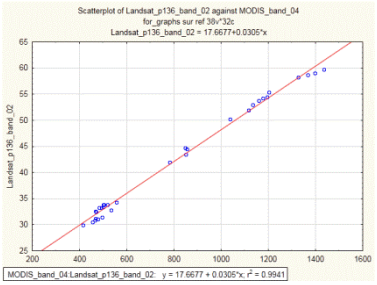
Scatterplot of Landsat_p136_band_02 against MODIS_band_04
for_graphs sur ref 38v*32c
Landsat_p136_band_02 = 17.6677+0.0305*x
Landsat_p136_band_02
MODIS_band_04,Landsat_p136_band_02: y = 17.6677 + 0.0305*x; r² = 0.9941

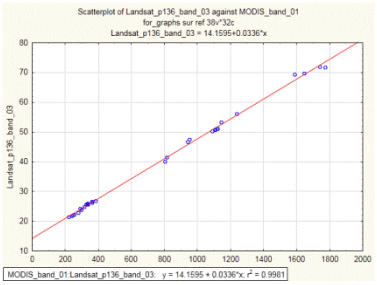
Scatterplot of Landsat_p136_band_03 against MODIS_band_01
for_graphs sur ref 38v*32c
Landsat_p136_band_03 = 14.1595+0.0336*x
Landsat_p136_band_03
MODIS_band_01,Landsat_p136_band_03: y = 14.1595 + 0.0336*x; r² = 0.9981

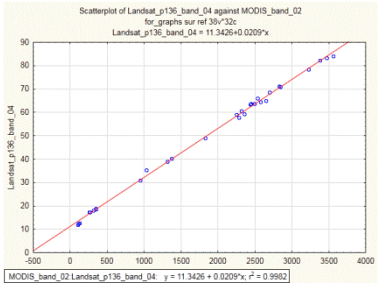
Scatterplot of Landsat_p136_band_04 against MODIS_band_02
for_graphs sur ref 38v*32c
Landsat_p136_band_04 = 11.3426+0.0209*x
Landsat_p136_band_04
MODIS_band_02,Landsat_p136_band_04: y = 11.3426 + 0.0209*x; r² = 0.9982

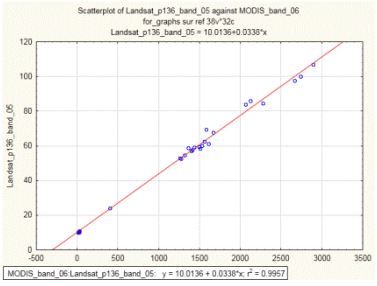
Scatterplot of Landsat_p136_band_05 against MODIS_band_06
for_graphs sur ref 38v*32c
Landsat_p136_band_05 = 10.0136+0.0338*x
Landsat_p136_band_05
MODIS_band_06,Landsat_p136_band_05: y = 10.0136 + 0.0338*x; r² = 0.9957

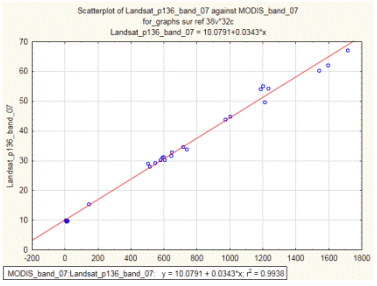
Scatterplot of Landsat_p136_band_07 against MODIS_band_07
for_graphs sur ref 38v*32c
Landsat_p136_band_07 = 10.0791+0.0343*x
Landsat_p136_band_07
MODIS_band_07,Landsat_p136_band_07: y = 10.0791 + 0.0343*x; r² = 0.9938

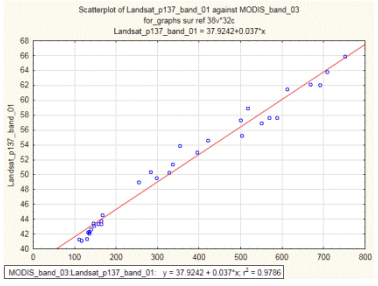
Scatterplot of Landsat_p137_band_01 against MODIS_band_03
for_graphs sur ref 38v*32c
Landsat_p137_band_01 = 37.9242+0.037*x
Landsat_p137_band_01
MODIS_band_03,Landsat_p137_band_01: y = 37.9242 + 0.037*x; r² = 0.9786

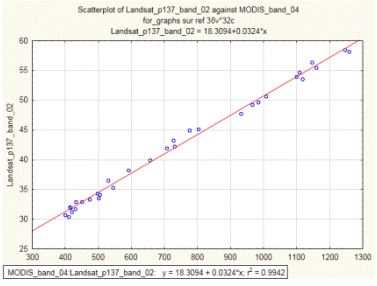
Scatterplot of Landsat_p137_band_02 against MODIS_band_04
for_graphs sur ref 38v*32c
Landsat_p137_band_02 = 18.3094+0.0324*x
Landsat_p137_band_02
MODIS_band_04,Landsat_p137_band_02: y = 18.3094 + 0.0324*x; r² = 0.9942

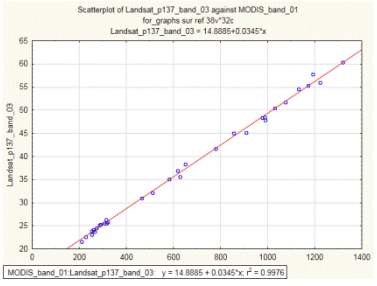
Scatterplot of Landsat_p137_band_03 against MODIS_band_01
for_graphs sur ref 38v*32c
Landsat_p137_band_03 = 14.8885+0.0345*x
Landsat_p137_band_03
MODIS_band_01,Landsat_p137_band_03: y = 14.8885 + 0.0345*x; r² = 0.9976

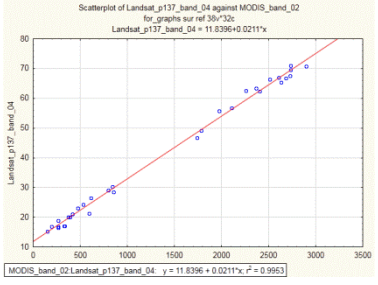
Scatterplot of Landsat_p137_band_04 against MODIS_band_02
for_graphs sur ref 38v*32c
Landsat_p137_band_04 = 11.8396+0.0211*x
Landsat_p137_band_04
MODIS_band_02,Landsat_p137_band_04: y = 11.8396 + 0.0211*x; r² = 0.9953

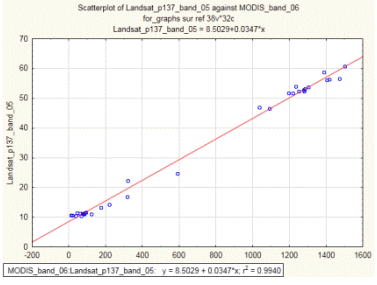
Scatterplot of Landsat_p137_band_05 against MODIS_band_06
for_graphs sur ref 38v*32c
Landsat_p137_band_05 = 8.5029+0.0347*x
Landsat_p137_band_05
MODIS_band_06,Landsat_p137_band_05: y = 8.5029 + 0.0347*x; r² = 0.9940

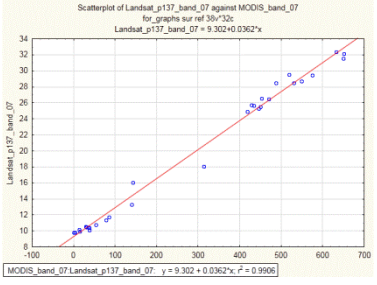
Scatterplot of Landsat_p137_band_07 against MODIS_band_07
for_graphs sur ref 38v*32c
Landsat_p137_band_07 = 9.302+0.0362*x
Landsat_p137_band_07
MODIS_band_07,Landsat_p137_band_07: y = 9.302 + 0.0362*x; r² = 0.9906

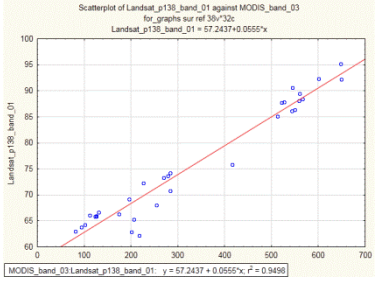
Scatterplot of Landsat_p138_band_01 against MODIS_band_03
for_graphs sur ref 38v*32c
Landsat_p138_band_01 = 57.2437+0.0555*x
Landsat_p138_band_01
MODIS_band_03,Landsat_p138_band_01: y = 57.2437 + 0.0555*x; r² = 0.9498

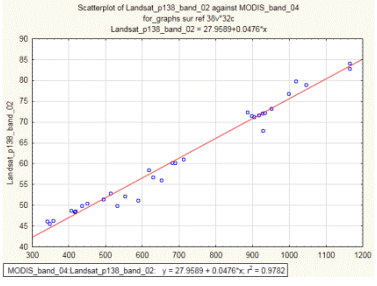
Scatterplot of Landsat_p138_band_02 against MODIS_band_04
for_graphs sur ref 38v*32c
Landsat_p138_band_02 = 27.9689+0.0476*x
Landsat_p138_band_02
MODIS_band_04,Landsat_p138_band_02: y = 27.9689 + 0.0476*x; r² = 0.9782

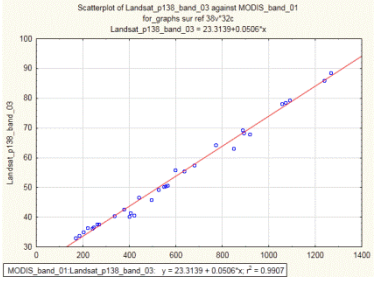
Scatterplot of Landsat_p138_band_03 against MODIS_band_01
for_graphs sur ref 38v*32c
Landsat_p138_band_03 = 23.3139+0.0506*x
Landsat_p138_band_03
MODIS_band_01,Landsat_p138_band_03: y = 23.3139 + 0.0506*x; r² = 0.9907

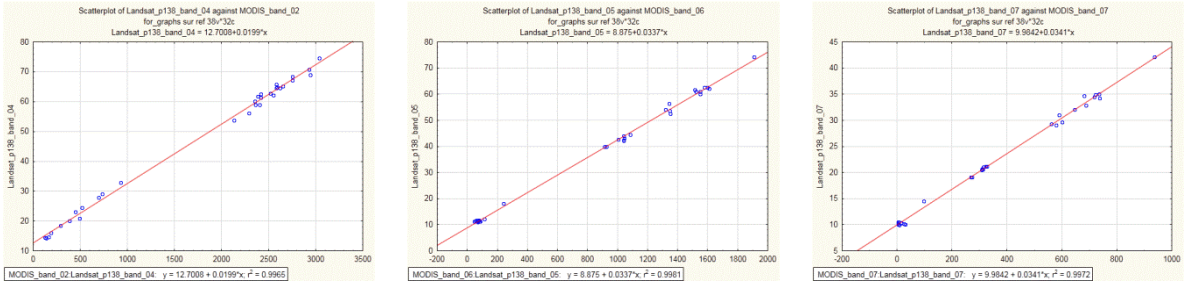

Figure 4-1: Relationship between MODIS surface reflectance values and Landsat digital numbers for images from Landsat paths 136, 137, and 138.

4.2.4 Removal of cloud and cloud shadow from Landsat ETM+ data

Cloud contamination of satellite images that use passive sensors such as Landsat ETM+ and MODIS is a major problem, especially during wet seasons. In the case of Landsat where the revisit time to a given area is relatively long (16 days) obtaining any number of wet season images can be extremely difficult. In the case of the current study the period for which ground truth data were collected and Landsat images obtained represented the end of the wet season and, fortunately, relatively little cloud contamination was present. The clouds that remained were mostly small in size and had the potential to impact on image analysis in two ways. The clouds themselves result in areas of high reflectance that could be potentially misinterpreted as areas of bare ground or manmade structures, this is especially true of less dense areas of cloud where reflectance values are not obviously higher than ground based objects. The other problem is with cloud shadows where areas of low reflectance, especially in the infrared bands, can be mistaken for water bodies.

A considerable amount of work has focussed on removing clouds and shadows from satellite images and then using a variety of methods to fill the gaps based around either using other images (e.g. Jin et al., 2013, Martinuzzi et al., 2007, Roy et al., 2008) or the original image (e.g. Zhang et al., 2007). In the case of the current study filling of gaps left by removal of cloud and shadow, as well as those resulting from the Landsat SLC-off issue, was considered unnecessary as the total cloud area was quite low and the overall aim was to use Landsat images to assess the performance of classification methods rather than produce uninterrupted Landsat images *per se*.

The areas of interest in terms of surface water and flooding in Bangladesh have the advantage of being extremely flat with the result that the distance between clouds and their shadows tended to be similar for a given scene. With this in mind an approach similar to that described by Martinuzzi et al.

(2007) was adopted where cloud is identified using a combination of Landsat ETM+ bands 2 and 6 (blue and thermal infrared). The detected cloud areas were enlarged using a buffer and then moved to cover shadow areas which were further defined using band 4 (near infrared). Full details of the cloud and cloud shadow removal procedure are given in box 4-1.

Text box 4-1: Details of cloud and cloud shadow removal procedure used for Landsat data.

1. Areas with band 1 (blue) surface reflectance values above 0.09 and band 6-2 (thermal infrared high gain) values below the mean for the scene are identified.
2. A 60 metre buffer was added to the areas identified in step 1 and the result was designated as cloud areas and removed from the image.
3. A 150m buffer was applied to the areas identified in step 1 and the resulting image was shifted so that the buffered cloud areas now covered the cloud shadows that could be seen in band 4 (near infrared).
4. Shadow areas were defined as those that were covered by the shifted buffered cloud mask described in step 3, and where band 4 surface reflectance was less than 0.15.

4.2.5 Classification of Landsat ETM+ images to show land, water and mixed pixels

Due to being densely populated and highly cultivated, land cover in Bangladesh is often highly intricate with different cover types present within a small areas. With this in mind it was decided that initial development of classification methods using higher resolution Landsat ETM+ images would potentially be more informative when assessing accuracy against GCPs as there would be less chance of multiple land cover types being present in a single pixel. The most promising classification procedures could then be investigated using MODIS data. It was also significant that practical limitations when collecting ground-truth data meant that some data points were fairly close together potentially limiting their use for verifying lower resolution MODIS based images. In view of this another goal when classifying ETM+ imagery was the development of an accurate map showing land, mixed, and water areas that could be used along with GCPs when accessing the accuracy of MODIS based classifications.

Four different classification methods were developed and investigated: A) a method adapted from Sakamoto et al. (2007) and common to Islam et al. (2010) and Handisyde et al. (2014), B) an unsupervised algorithm (ISOCLUST) used to assign pixels to a large number of classes that were then reclassified based on the use of GCPs, C) use of thresholds from a single Normalised Difference

Spectral Index (NDSI) (Landsat ETM+ bands 2 and 7), D) a two step process using thresholds from two NDSIs (Landsat ETM+ bands 2 and 7, and 3 and 4).

4.2.5.1 A. Use of EVI and Land Surface Water Index (LSWI) (Sakamoto method)

Sakamoto et al. (2007) demonstrated a method of classifying MODIS data to show land, water and mixed areas by using thresholds for EVI, LSWI and DVEL (EVI - LSWI). The method has been applied by Islam et al. (2010) to show flooding within Bangladesh and while RADARSAT images were used to verify results actual ground-truth data were not included. A key aim of the current study was to assess this methodology in the context of Bangladesh in relation to ground truth data both directly and via the use of higher resolution Landsat ETM+ images based on equivalent bands. The methodology applied in the current study differs from that described by Sakamoto et al. (2007) in that the wavelet transformation to smooth the data is omitted as it was considered important to highlight areas that are only flooded for short periods and that may be missed in an excessively smoothed data series. The method applied here is also consistent with that used by Islam et al. (2010). Details of the classification procedure and the indexes on which it is based are provided Figure 4-2.

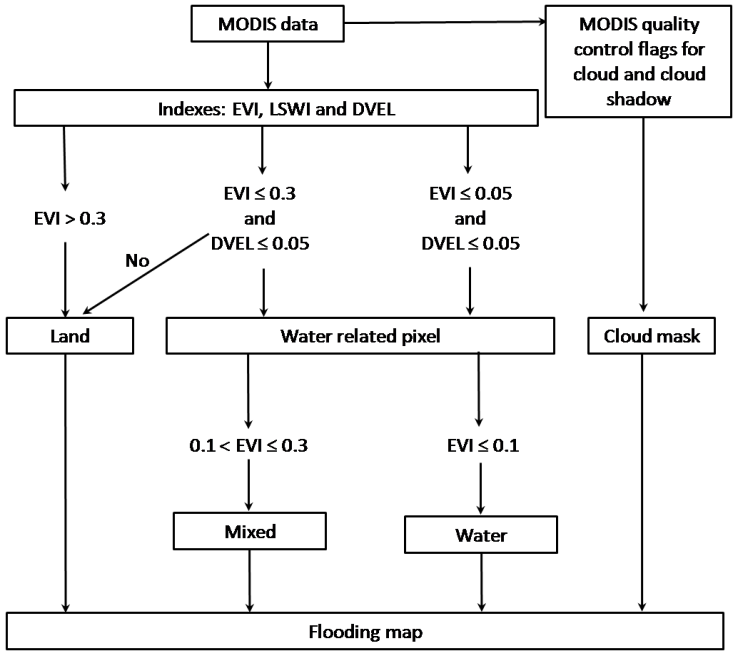

$$EVI = 2.5 \times \frac{NIR - RED}{NIR + 6 \times RED - 7.5 \times BLUE + 1}$$

$$LSWI = \frac{NIR - SWIR}{NIR + SWIR}$$

$$DVEL = EVI - LSWI$$

Figure 4-2: Classification method adapted from Sakamoto et al. (2007) used in the current study.

4.2.5.2 B. Unsupervised classification using ETM+ bands 1,2,3,4,5, and 7

Unsupervised classification methods typically share a common aim of identifying the major classes that exist in an image without the need for previous understanding of what these might be (Eastman, 2012). A technique often employed with such approaches is to generate a relatively large number of classes which are then re-categorised, and often grouped, into meaningful classes of land cover type via the use of ground truth data. In the context of the current study it was assumed that the broad water, land and mixed classes would each contain a number of sub-classes and it was considered valuable to test whether the identification, and subsequent reclassification, of these classes using all available spectral bands may offer superior performance when compared to simpler reclassification of NDSIs and vegetation indexes based on fixed thresholds.

The ISOCLUST model that forms part of the IDRISI package is a self-organizing unsupervised classifier that Eastman (2012) notes is similar in concept to the ISODATA routine described by Ball and Hall (1965). ISOCLUST was used with bands 1,2,3,4,5, and 7 to generate an image with 22 classes with the number of classes being chosen based on an obvious break in the frequency distribution (Eastman, 2012). The resulting 22 classes were then reclassified as either land, water or mixed based on highest frequency in a cross-tabulation with the set of training GCPs. This was done twice, once using training data including floating vegetation and once excluding it (Tables 4-4 and 4-5). Class one was not included in the cross tabulation as it effectively represented background data. It is worth noting that for some of the 22 classes the number of training points was very low and for two classes (15 and 20) there were no training points. Visual inspection of these classes suggested that they represented areas of sea surface and were therefore not relevant in terms of the current assessment.

Table 4-4: Cross tabulation of ISOCLUSTER results with training points (excluding floating vegetation areas).

	1	2	3	Total
2	447	1	1	449
3	85	2	0	87
4	37	12	0	49
5	114	0	0	114
6	12	0	0	12
7	0	0	23	23
8	0	3	107	110
9	2	0	0	2
10	0	0	2	2
11	0	0	57	57
12	1	56	0	57
13	32	0	0	32
14	1	0	0	1
16	6	4	0	10
17	2	15	33	50
18	1	49	30	80
19	0	0	3	3
21	0	0	13	13
22	0	0	56	56
Total	740	142	325	1207

Table 4-5: Cross tabulation of ISOCLUSTER results with training points (including floating vegetation areas).

	1	2	3	Total
2	447	1	1	449
3	85	6	0	91
4	37	12	0	49
5	114	0	0	114
6	12	52	0	64
7	0	0	23	23
8	0	3	107	110
9	2	4	0	6
10	0	0	2	2
11	0	0	57	57
12	1	130	0	131
13	32	3	0	35
14	1	0	0	1
16	6	4	0	10
17	2	15	33	50
18	1	49	30	80
19	0	0	3	3
21	0	0	13	13
22	0	0	56	56
Total	740	279	325	1344

4.2.5.3 C. Use of a single NDSI constructed from Landsat ETM+ bands

When addressing the specific problem of separating water and land a range of simpler band combinations have been suggested often based on the combination of two bands in the form of a NDSI that combines either two infra red bands, or one infrared band with one band from the visible spectrum, based on the assumption that water surfaces tend to reflect less infrared radiation than other surfaces (Ji et al., 2009).

For the current assessment the full range of potential combinations of visual with infrared, and infrared with infrared band combinations using ETM+ data were investigated along with the EVI and DVEL that were used by Sakamoto et al. (2007). For each index the set of GCPs designated as training data were used to generate frequency distributions of index values for land, mixed, mixed without floating vegetation, and water pixels using equal interval classes with a width of 0.05. The results are represented here in Fig 4-3 as a series of line graphs to allow for easy visual inspection of overlap between the different land cover types.

Inspection of the frequency distributions in Figure 4-3 suggests that for Bangladesh a combination of one of the visual bands (1 - 3) with one of the shortwave infrared bands (5 or 7) was more likely to allow for separation of land, water, and in some cases mixed pixels, than a combination of near infrared (band 4) with shortwave infrared (band 5) as in the case of the land surface water index (LSWI). In the case of the EVI there was considerable overlap between the land and mixed classes while for DVEL (LSWI minus EVI) there was substantial overlap between the water and mixed classes. Band combinations 2 and 5, and 3 and 7 showed a good degree of separation between land, water, and mixed areas (excluding floating vegetation) but appeared to be slightly surpassed by a combination of bands 2 and 7 which surprisingly seem to be able to separate the mixed class from water and land even when the floating vegetation was included. Using the second set of GCPs to verify the results of classifications using a range of thresholds for NDSIs using bands 2-5, 3-7, and 2-7 confirmed that in the case of Bangladesh the combination of bands 2 and 7 offered the best performance when attempting to classify ETM+ images using a single index. The most effective classification thresholds for the 2,7 band combination was: <0.1 = land, 0.1 to 0.6 = mixed, and >0.6 = water.

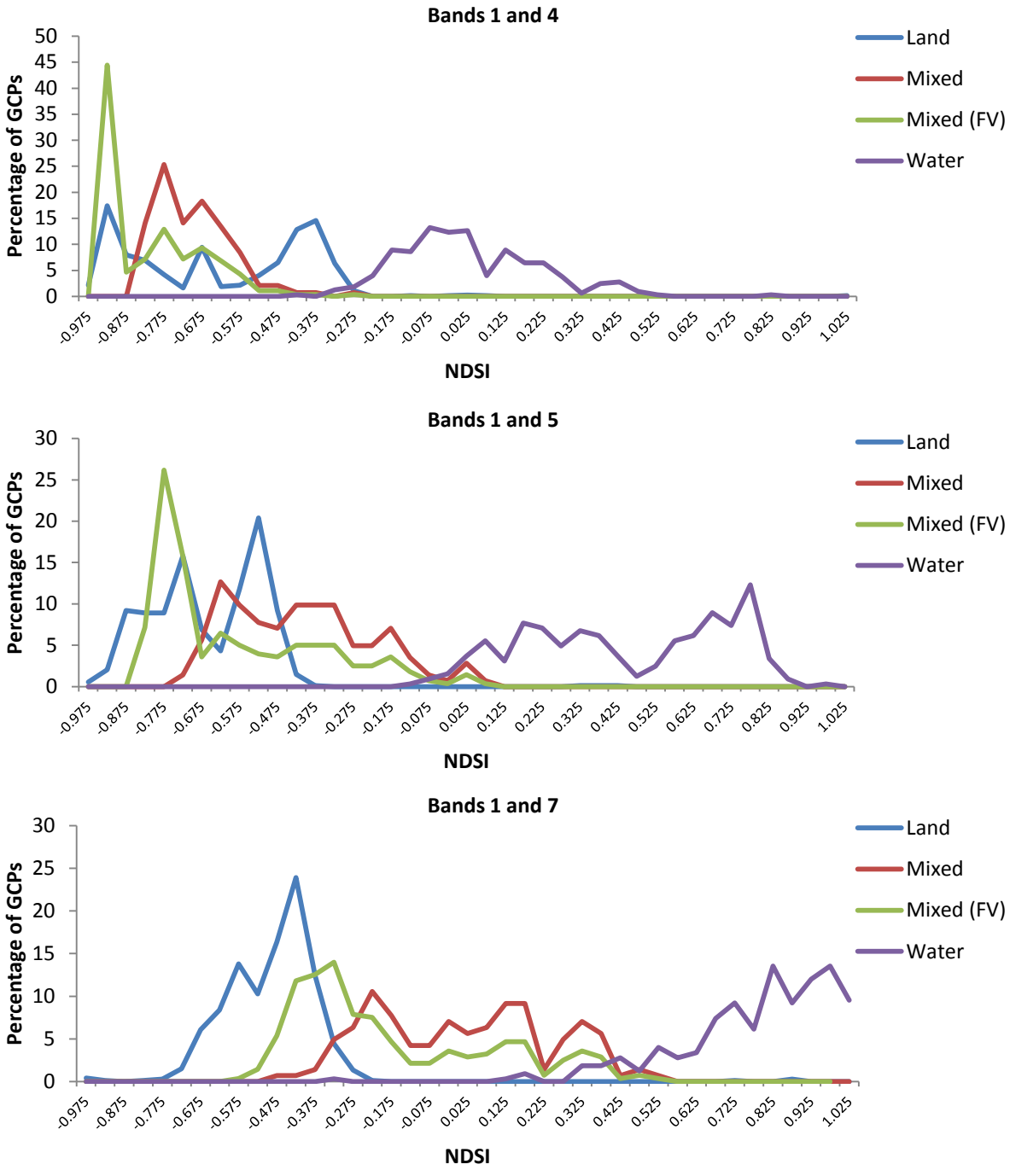

Figure 4-3: Frequency distribution of NDSIs as well as EVI and DVEL in relation to GCPs representing land, mixed, mixed including floating vegetation (FV), and water areas.

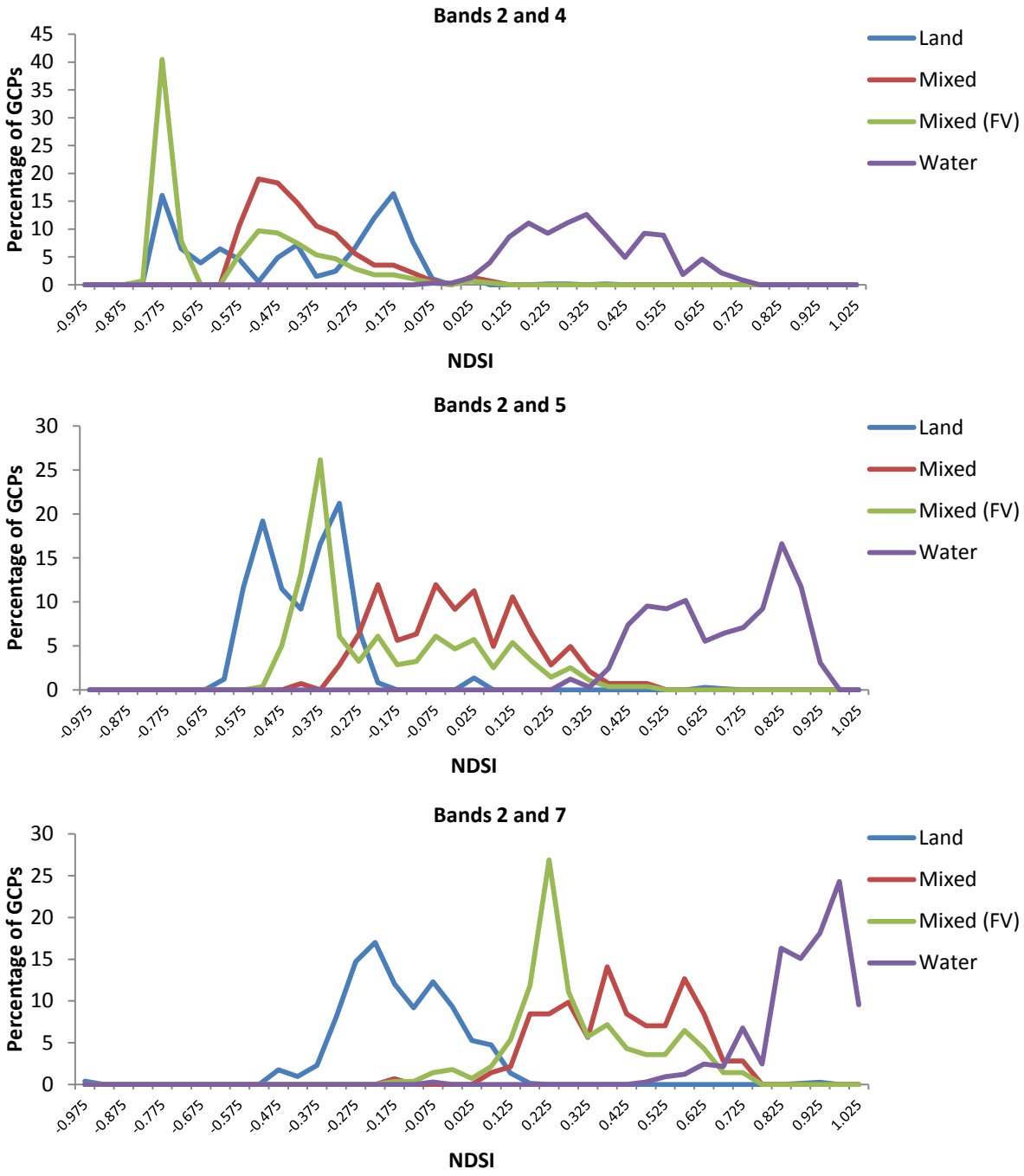

Figure 4-3 continued.

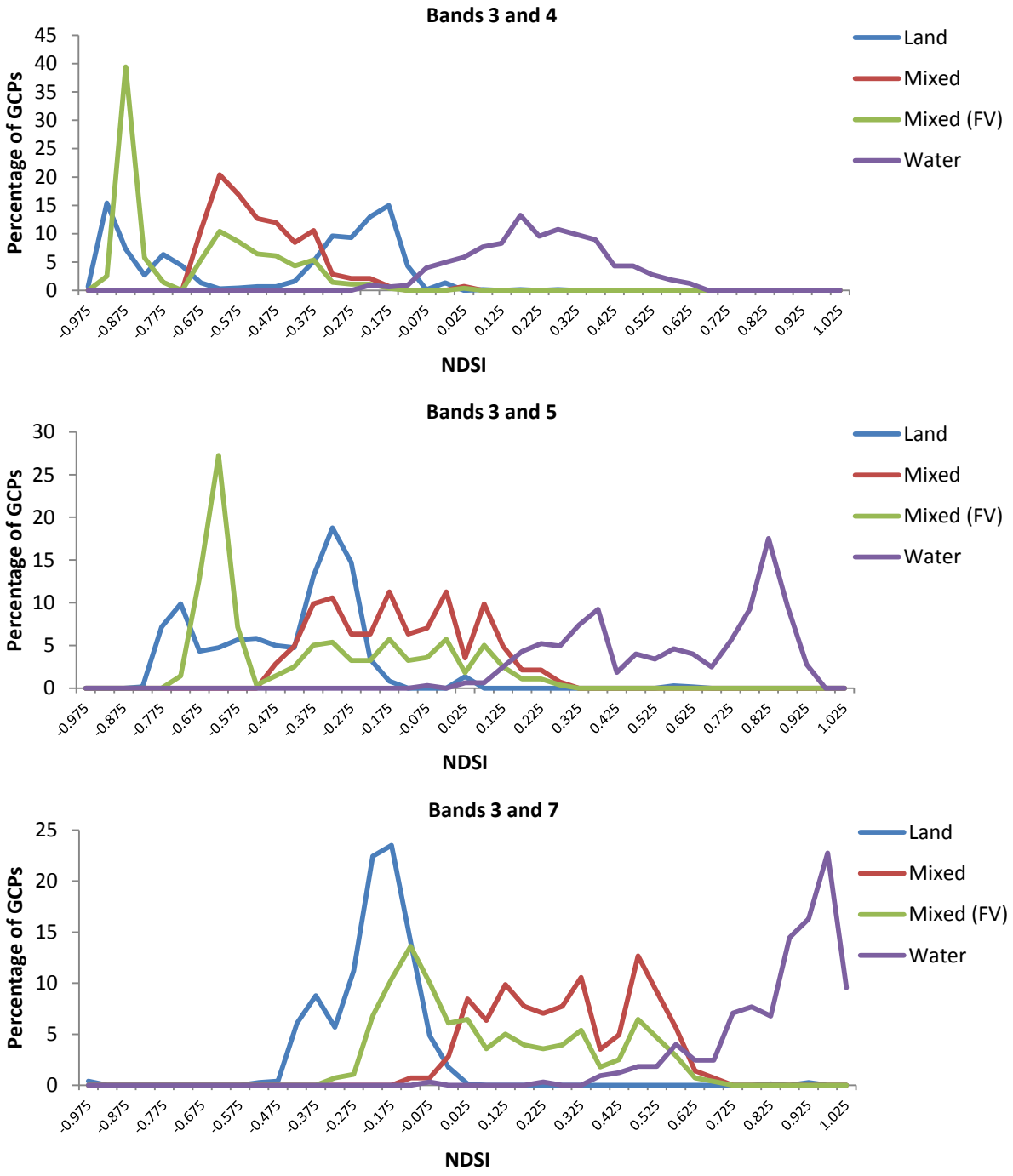

Figure 4-3 continued.

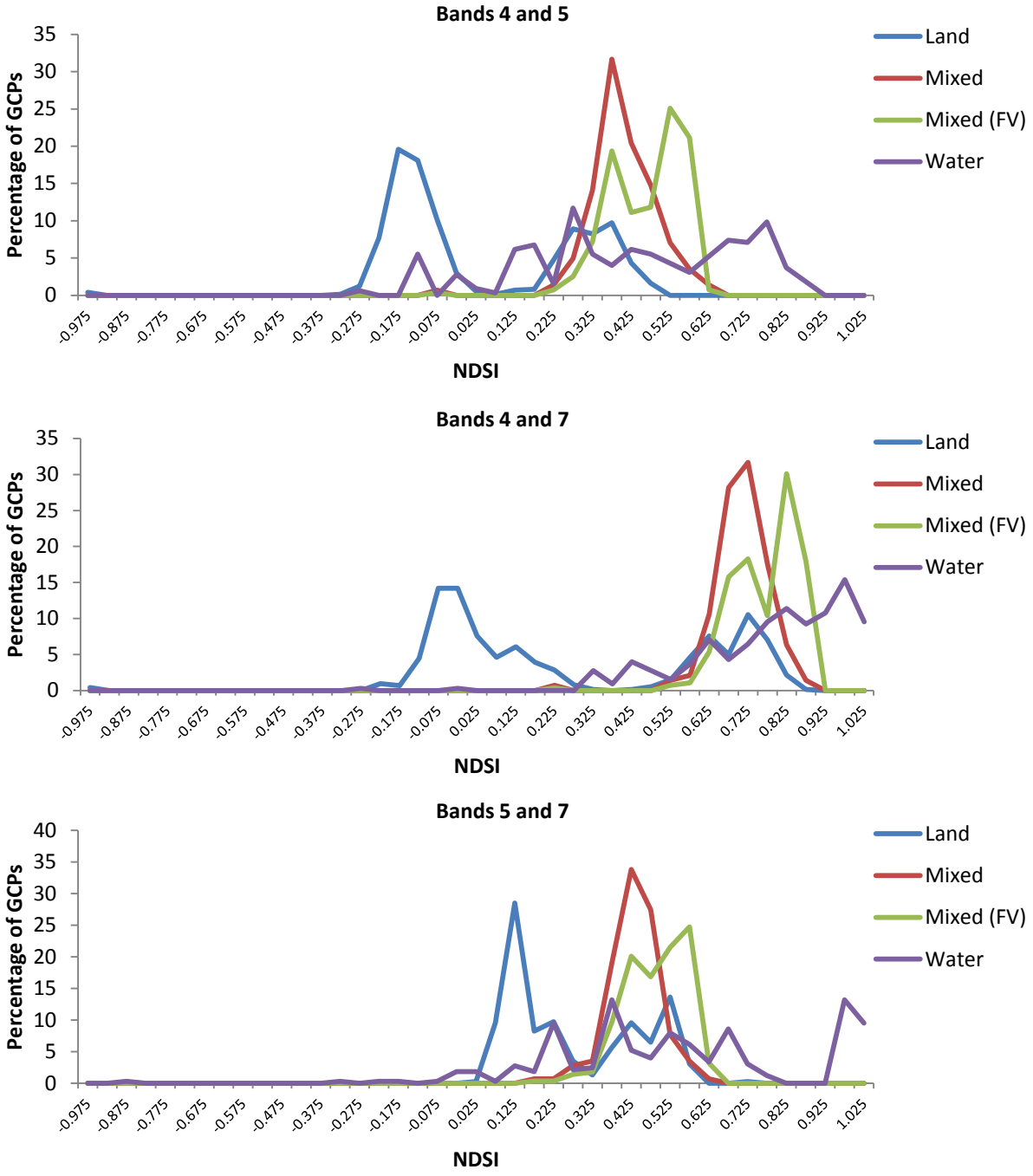

Figure 4-3 continued.

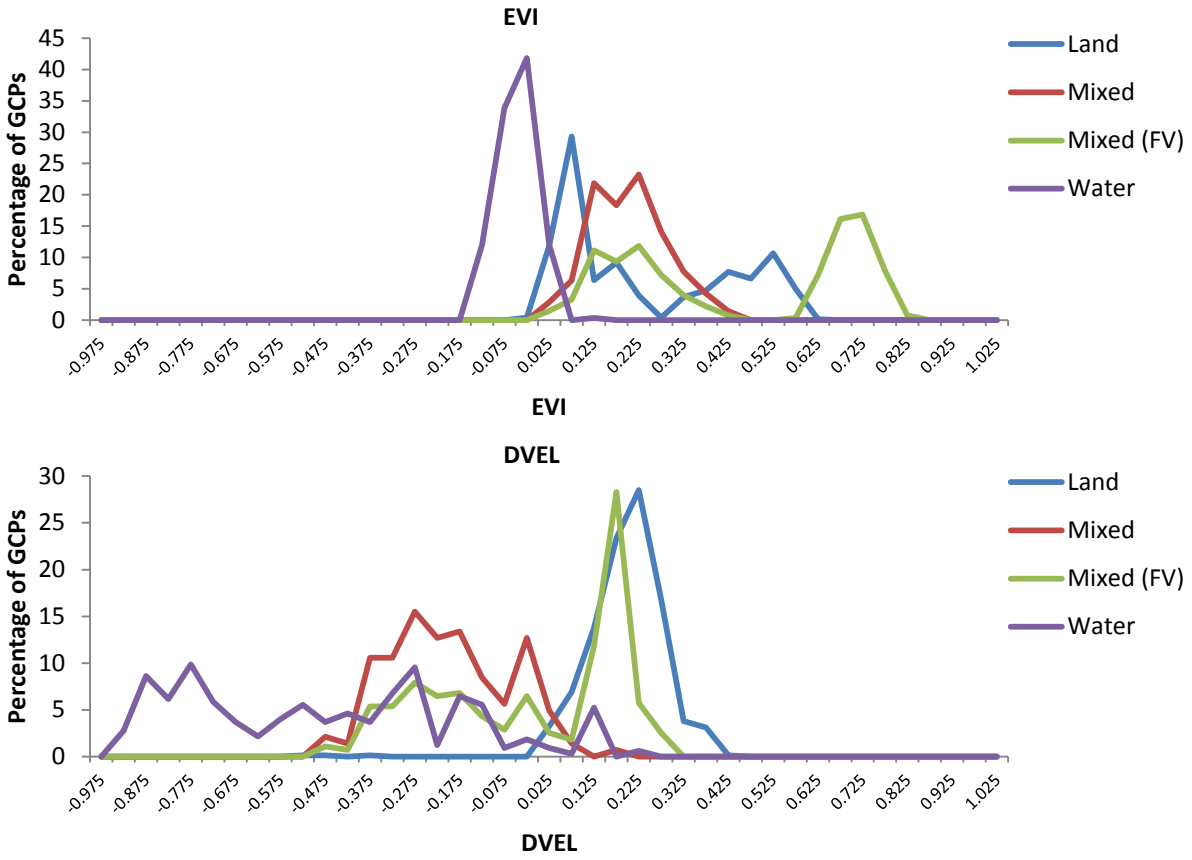

Figure 4-3 continued.

4.2.5.4 D. Two stage classification using NDSIs from bands 2 and 7, and 3 and 4.

The frequency distributions shown in Figure 4-3 suggest that while a combination of Landsat bands 3 and 4 (red and near infrared) are unable to effectively separate land and mixed pixels they appear to perform very well at separating mixed pixels from water. With this in mind, a two stage classification process was developed that uses the NDSI of Landsat bands 2 and 7 to define land areas and then bands 3 and 4 to classify the remaining pixels as either water or mixed. Details of the classification procedure are given in Figure 4-4. The use of bands 3 and 4 was also motivated by the fact that in the case of the equivalent MODIS data (bands 1 and 2) these are the two bands that are available at the higher resolution of approximately 250m in the form of the MODIS MOD09Q1 product. It was hoped that incorporating this higher resolution data would offer more detail and improved performance when attempting to separate mixed and water areas.

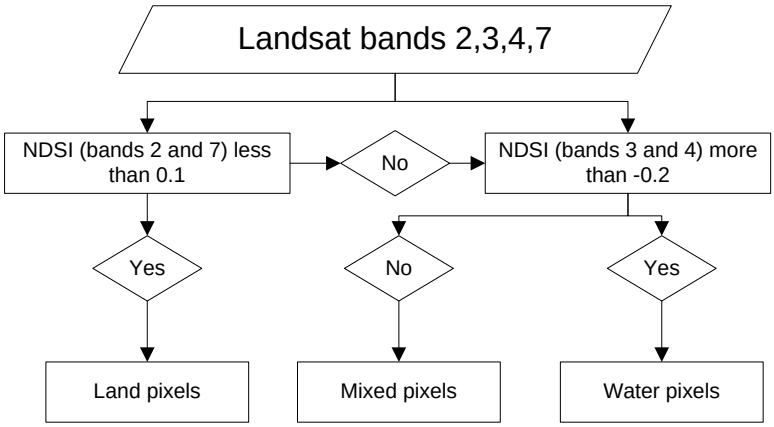

Figure 4-4: Two step process for defining land water and mixed pixels using Landsat bands 2,3,4,and 7.

4.3 Landsat ETM+ based classifications - outputs

Figure 4-5 shows land, water and mixed pixel layers derived from Landsat ETM+ scenes using the four previously described Methods. Total area (km^2) covered by each class within the borders of Bangladesh and excluding areas of cloud and missing data is given in Table 4-6. When viewed at the country scale all images show a superficially similar distribution of water and mixed areas with the possible exception of the image generated via the ISOCLUST routine which has areas indicated as mixed whereas in the other images they are displayed as water that forms part the annually flooded *Haor* basin in the north east of the country. Although no ground truth data were collected for that region, in view of what is known about that area it is likely that this constitutes an error on the part of the ISOCLUST output.

When compared to images C and D generated using the Landsat NDSIs, the image derived from the adapted Sakamoto method (A) has considerably less pixels classified as mixed while a greater proportion are classified as water and land. Images C and D appear to be quite similar. Image D which is derived from the two step classification process using Landsat bands 2, 3, 4, and 7 has a slightly larger area defined as water and a smaller area defined as mixed when compared to image C obtained using only Landsat bands 2 and 7.

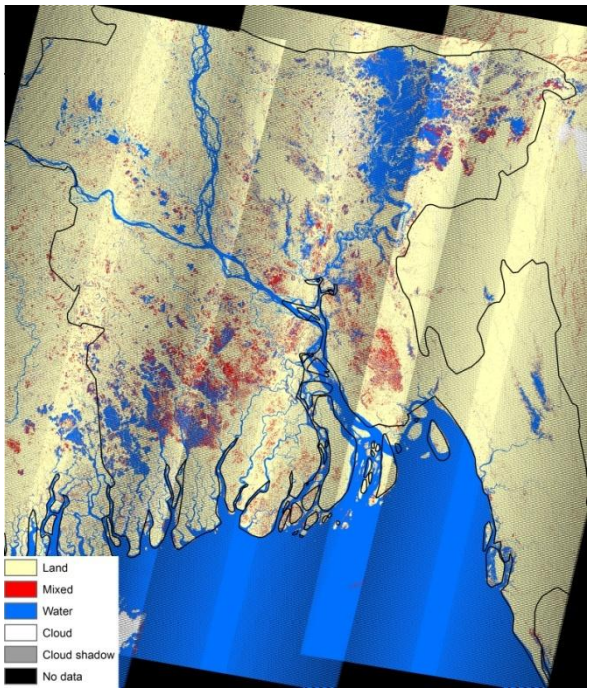

(A) Sakamoto method

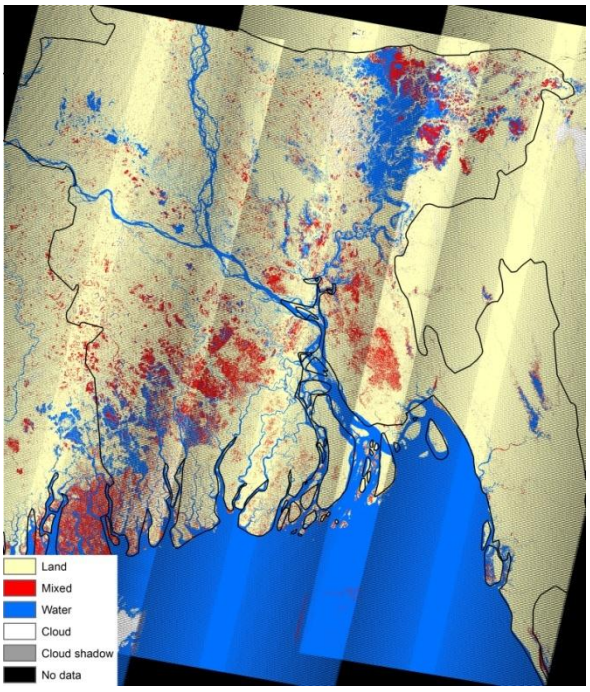

(B) ISOCLUST

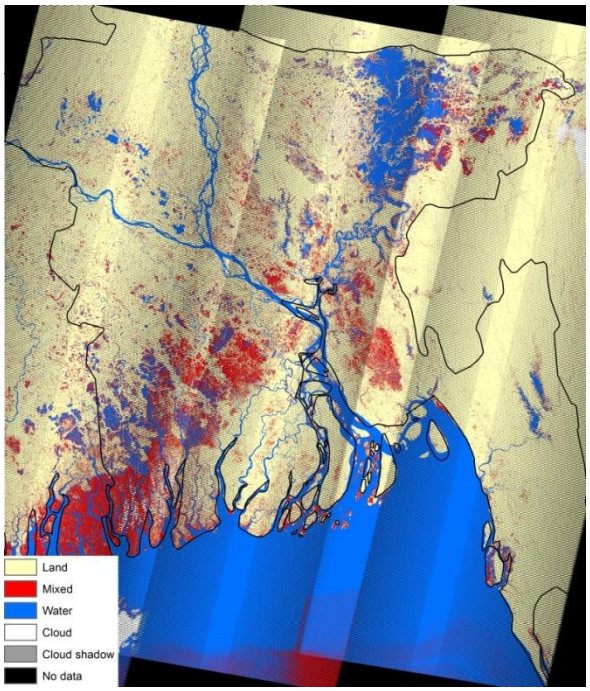

(C) Landsat bands 2 and 7

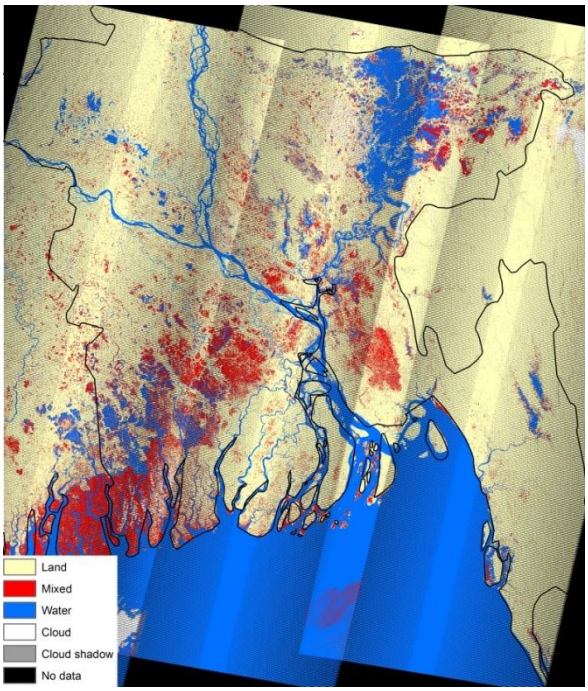

(D) Landsat bands 2, 3, 4, and 7

Figure 4-5: Results of Landsat ETM+ based image classifications.

Table 4-6: Total area (km^2) covered by each class within the borders of Bangladesh and excluding areas of cloud and missing data.

	Sakamoto (A)	Isoclust (B)	Landsat bands 2 and 7 (C)	Landsat bands 2, 3, 4, and 7 (D)
Land	78789.01	79896.89	75930.44	75930.43
Mixed	8458.64	9442.76	14397.28	13417.82
Water	14321.09	12226.05	11241.04	12220.49

4.3.1 Accuracy assessment of Landsat ETM+ based classifications

Accuracy assessment of classified satellite imagery typically compares the classified image to a source of reference data. The reference data can take a range of forms such as other maps obtained via traditional survey techniques, other classified satellite imagery, or a series of GCPs where land cover type has been recorded. An obvious but significant assumption is that the reference data itself is highly accurate (Campbell and Wynne, 2011). Where GCPs are being used then the number of samples becomes significant with smaller samples sizes increasing the degree of uncertainty in the accuracy assessment. Campbell and Wynne (2011) cite Congalton and Green (2009) and suggest a sample size of 50 samples per land cover class as a general guideline with the suggestion to increase this to 75-100 when more than 12 classes are present or the total area of the image exceeds a million acres (approximately 4047 km^2).

The current study makes use of GCPs that were not used when classifying images to produce error matrices for each of the classified images shown in Figure 4-5. For each classification method two accuracy assessments were conducted, one using ground truth data that excludes areas of floating vegetation and the other that includes it. Accuracy statistics are summarised in tables: 4-7 (classification scheme A), 4-8 (classification scheme B), and 4-9 (classification schemes C and D). Full error matrices are provided in Appendix 2 (Tables 9-1 to 9-9) where in each case ground truth data (columns) is compared against the classified image (rows). Errors of commission (ErrorC), and omission (ErrorO) are provided in each case. Errors of commission, sometimes referred to as user accuracy (where 1 - error of commission = user accuracy), represent reliability in terms of the likelihood that a pixel on the classified map represents that pixel on the ground. Errors of omission may be referred to as producer accuracy (where 1 - error of omission = producer accuracy) and represent how well a certain area can be classified i.e. what proportion of the ground truth data were

correctly classified. For each error matrix a total error (number of correctly classified control points / total number of control points) is also provided. Figures representing the kappa coefficient, or kappa index of agreement (KIA), are also provided for each row and column as well as an overall kappa figure for the accuracy assessment. The kappa coefficient is widely used for accuracy assessment of classified imagery and is a measure of proportional improvement by the classification method over completely random assignment to classes (Campbell and Wynne, 2011).

When collecting ground truth data for the purpose of accuracy assessment an ideal sampling scheme would be one that uses completely random locations in sufficient quantity that all potential classes have a sufficient number of samples. (Campbell and Wynne, 2011, Stehman and Czaplewski, 1998). The reality of the current project was that field access was only possible for a relatively short period while in Bangladesh. As a result sampling could only be conducted from roads and was significantly constrained by time, access, finances, and other logistical issues. The result for the current project was that within reason ground truth data were taken where ever possible, but cannot be considered to have the statistical power of a properly designed and implemented random sampling scheme. That said, as much effort as possible was made to record field data accurately from a wide range of land cover types. With this in mind and considering that the classification is concerned with only three broad classes it is considered that the data collected represents a significant improvement over scenarios where no ground truth data is present and where accuracy assessment may involve significant reliance on alternative data sources such as: other classified satellite imagery, paper maps, and the interpretation of high resolution true colour images such as those provided by Google earth. Such data sources may be subject to their own inaccuracies as well as those of interpretation. There may also be issues with data representing different points in time for a region with very dynamic land cover.

4.3.2 Accuracy assessment of Landsat ETM+ based classifications - results

Classification schemes C and D based on using thresholds for Landsat-derived NDSIs both appear to offer a high degree of accuracy even when areas of dense floating vegetation are included in the assessment. It is also interesting that they appear to outperform the ISOCLUST based classification (B). The classification (A) based on the method adapted from Sakamoto et al. (2007) appears to perform least well in terms of overall error and kappa scores. However bearing in mind the previous discussion regarding the collection of ground truth data, it should be considered that while separate

data points were used for guiding classification and for accuracy assessment, all the data were collected at the same time from a limited number of areas. This in theory has the potential to give classification methods B, C and D that were constructed as part of the current study an advantage. Another related consideration is that the three classes of land, mixed, and water represent a continuum. In the case of Bangladesh there will be a large number of mixed pixels that contain both land and water either in the case of a transition between large water areas being covered by a single pixel, or in cases such as wetlands and flooded crops where there is a more even coverage of water and vegetation. The consequence of this is that the definitions of where the land and water classes transition to the mixed class are somewhat open to interpretation. Again, the classification schemes constructed as part of the current study, and guided by the collected ground truth data, would perhaps be expected to show an advantage over the independently established method of Sakamoto et al. (2007). That said while it seems likely that the method adapted from Sakamoto et al. (2007) would show errors between the land and mixed, or water and mixed classes due to differences in interpretation, it's most significant error was in misinterpreting land areas as water. Comparison with the original ground truth data showed that this error was mostly accounted for by urban areas being mistaken for water as they tend to have low EVI and LSWI scores. If urban areas are excluded from the ground truth data then the method adapted from Sakamoto et al. (2007) becomes notably more effective with most of the remaining error being accounted for by confusion between land and mixed, or water and mixed areas while errors between land and water are very low (see Table 4-7).

Table 4-7: Summary statistics for classifications of Landsat ETM+ data using the method adapted from Sakamoto et al. (2007).

	Sakamoto method. Accuracy assessed against GCPs including areas of floating vegetation.		Sakamoto method. Accuracy assessed against GCPs excluding areas of floating vegetation.		Sakamoto method. Accuracy assessed against GCPs excluding areas of floating vegetation and urban areas.	
	producer accuracy %	user accuracy %	producer accuracy %	user accuracy %	producer accuracy %	user accuracy %
Land	89.22	84.50	89.22	97.90	99.34	96.98
Mixed	46.03	98.21	82.71	98.21	82.71	98.21
Water	100	79.08	100	79.08	100	97.01
Overall accuracy %	83.96		91.44		97.15	
Overall kappa	0.717		0.844		0.952	

Table 4-8: Summary statistics for classifications of Landsat ETM+ data using the ISOCLUST routine.

	ISOCLUST routine. Accuracy assessed against GCPs including areas of floating vegetation.		ISOCLUST routine. Accuracy assessed against GCPs excluding areas of floating vegetation.	
	producer accuracy %	user accuracy %	producer accuracy %	user accuracy %
Land	97.41	97.41	99.89	98.26
Mixed	88.28	84.74	83.46	84.73
Water	94.15	97.14	94.15	97.14
Overall accuracy %	94.91		96.47	
Overall kappa	0.913		0.934	

Table 4-9: Summary statistics for classifications of Landsat ETM+ data using a threshold value for a single NDSI (bands 2 and7), or two NDSIs (bands 2 and 7, and 3 and 4).

	NDSI from bands 2 and 7. Accuracy assessed against GCPs including areas of floating vegetation.		NDSI from bands 2 and 7. Accuracy assessed against GCPs excluding areas of floating vegetation.		NDSIs from from bands 2 and 7, and 3 and 4. Accuracy assessed against GCPs including areas of floating vegetation.		NDSIs from from bands 2 and 7, and 3 and 4. Accuracy assessed against GCPs excluding areas of floating vegetation.	
	producer accuracy %	user accuracy %	producer accuracy %	user accuracy %	producer accuracy %	user accuracy %	producer accuracy %	user accuracy %
Land	99.59	98.12	99.59	99.59	99.59	98.12	99.59	99.59
Mixed	91.21	96.04	92.48	93.18	93.31	98.67	96.24	97.71
Water	98.15	97.85	98.15	97.85	100	99.39	100	99.39
Overall accuracy %	97.69		98.40		98.54		99.33	
Overall kappa	0.960		0.970		0.975		0.987	

4.4 MODIS data used in the current study

A single MODIS scene covered the study area as defined by the Landsat coverage and Bangladesh boarder (h26v6). For initial classification and comparison with Landsat data MODIS products MOD09A1 and MOD09Q1 were obtained from the Terra satellite collection for 31st October 2008.

Both data sets are available at 8 day intervals and represent a composite image of best available data. Details of the contents of the two MODIS products used are given in Table 4-10.

Table 4-10: Contents of MODIS products used in the current study.

MOD09A1 (approx. 500m resolution)	MOD09Q1 (approx. 250m resolution)
500m Surface Reflectance Band 1 (620–670 nm)	250m Surface Reflectance Band 1 (620–670 nm)
500m Surface Reflectance Band 2 (841–876 nm)	250m Surface Reflectance Band 2 (841–876 nm)
500m Surface Reflectance Band 3 (459–479 nm)	250m Reflectance Band Quality
500m Surface Reflectance Band 4 (545–565 nm)	
500m Surface Reflectance Band 5 (1230–1250 nm)	
500m Surface Reflectance Band 6 (1628–1652 nm)	
500m Surface Reflectance Band 7 (2105–2155 nm)	
500m Reflectance Band Quality	
Solar Zenith Angle	
View Zenith Angle	
Relative Azimuth Angle	
500m State Flags	
Day of Year	

4.5 MODIS cloud and cloud shadow mask

The MODIS MOD09A1 product includes two sets of bit field quality control data (500m Reflectance Band Quality, and 500m State Flags). Both data sets contain information relating to cloud cover however the MODIS surface reflectance user guide (Vermote et al., 2011) states that the data labelled as reflectance band quality should not be considered as reliable as the state flags. For the current study masks for cloud areas and cloud shadow areas were extracted via the use of the *'create_mask*' tool that forms part of the Land Data Operational Products Evaluation (LDOPE) tools package (Roy et al., 2002). Inspection of the MODIS data, especially bands relating to the visible spectrum, and in particular band 3 (459–479 nm), suggested that the cloud state flags were generally quite conservative with areas designated as cloud even where it was not visually obvious in the data. That said, there were a small number of instances where high reflectance values were seen in the visible

spectrum for areas not marked as clouds. It was also noted that in some cases these areas had straight edges and had the appearance of errors in the data other than that caused by cloud. Inspection of the other parameters available from the bit field quality control data did not reveal any masks that seemed to relate specifically to these errors. In view of this the decision was taken to also use band 3 with a threshold value of 0.2 to mask out cloud and other errors not covered by the state flags for cloud and cloud shadow. The band 3 value of 0.2 is slightly above the maximum reflectance seen in relation to ground objects and as an approach has been adopted in a number of previous studies in relation to MODIS data (Handisyde et al., 2014, Islam et al., 2010, Sakamoto et al., 2007, Xiao et al., 2006).

4.6 Classification of MODIS data

With the exception of the ISOCLUST classification which would not be easily implemented across a time series, the four classification methods applied to the Landsat ETM+ images were applied to the MODIS data. For the two methods based on the use of thresholds of NDSIs slight changes were made to the thresholds used as it was found that this gave superior results with the lower resolution MODIS data.

4.6.1 Sakamoto method

The method adapted from Sakamoto et al. (2007) was applied to MODIS data using the same classification scheme as was applied to the Landsat data (see Figure 4-2) but was applied twice: once using all the data from the MOD09A1 product at a resolution of approximately 500m, and once using higher resolution (approximately 250m) data available for bands 1 and 2 from the MOD09Q1 product. In this case the band 3 and 6 data were resampled to the higher resolution using nearest neighbours.

4.6.2 Classification using a single NDSI from bands 4 and 7 (equivalent of Landsat ETM+ bands 2 and 7)

In terms of spectral response MODIS bands 4 and 7 are comparable to Landsat ETM+ bands 2 and 7 and are used here to generate a land, mixed, and water map in a similar fashion to the Landsat data through the use of thresholds of a normalised difference index. Examination of NDSI values in relation to the frequency distribution of ground control points representing land, water and mixed areas did not result in obvious threshold points as was the case for the higher resolution Landsat data. Given the lower resolution of the data this may be the result of an increased proportion of mixed pixels that contain more than one land cover type. Instead, the use of different classification thresholds was investigated through the direct effect on classification accuracy when compared to GCPs as well as the most accurate Landsat based classification. When compared to Landsat it was found that while the best threshold for defining land remained the same, a reduction in the mixed to water threshold gave better overall classification accuracy. The MODIS data were classified as follows <0.1 = land, 0.1 to 0.4 = mixed, and >0.4 = water.

4.6.3 Two stage classification of MODIS using NDSIs from bands 4 and 7 and 1 and 2 at 250m

The two stage classification process using the green and shortwave infrared bands to define land areas followed by the red and near infrared bands to separate the remaining areas in to mixed or water classes was implemented using MODIS data from the MOD09A1 and MOD09Q1 data sets. The MOD09Ql provides the red and near infrared bands at a resolution twice that of MOD09A1 (approximately 250m). To allow combination of the two data sets bands 4 and 7 from MOD09A1 were resampled to the higher resolution based on nearest neighbours. While the threshold of the NDSI from bands 2 and 7 used for defining land areas remained the same as used for the equivalent Landsat based classification, it was found that a change in threshold used for the NDSI of bands 1 and 2 gave better results. Details are provided in Figure 4-6.

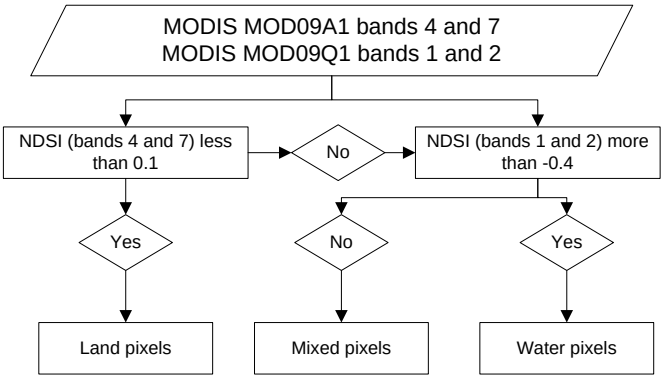

Figure 4-6: Two step process for defining land water and mixed pixels using MODIS bands 1,2,4,and 7.

4.7 MODIS based classifications - outputs

Figures 4-7 and 4-8 show classification results using MODIS data for a single time point (31-10-08) corresponding as closely as possible to the previously conducted Landsat ETM+ based classification. Images A and B were produced using the method adapted from Sakamoto et al. (2007). Image A was produced with a resolution of approximately 500m with all data coming from MOD09A1 data set. Image B was created with a resolution of approximately 250m using data sets MOD09A1 and MOD09Q1. Image C was produced at approximately 500m resolution using the single NDSI of MODIS bands 4 and 7, while image D was produced at approximately 250m resolution using the 2 stage classification process with NDSIs of bands 4 and 7 from MOD09A1, and 1 and 2 from MOD09Q1. Table 4-11 shows areas covered by the different classes in image A to D. Image B has noticeably less mixed pixels compared with image A. The analysis in Table 4-11 support this and show that the difference is made up by increases in both water and land area. Image D has a considerably larger area classified as water and less as mixed compared with image C, while the land area classification method, data and therefore area is the same in both images. Comparing the images C and D with those produced using the Sakamoto method there is a noticeable difference in the distribution of mixed pixels with much of the Sundarban region classed as mixed in images C and D. Given that the region is comprised of a mangrove ecosystem the mixed classification may well be reasonable. Another difference between the two pairs of images is that when compared to images C and D images A and B have noticeably more defined (i.e. wider) major river systems.

Figure 4-8 shows a magnified area of south western Bangladesh for each of the images from Figure 4-7. Comparing the two images (A and B) produced using Sakamoto method; image B produced using

higher resolution data for two of the four input bands appears to show more detail, especially in relation to small areas of water such as smaller river channels that tend to be shown as mixed pixels and / or become fragmented with the lower resolution output (image A). Comparing images C and D shows a similar situation although less pronounced as, while mixed and water pixels are separated at the higher resolution, the separation of land from mixed or water areas is the same for both images.

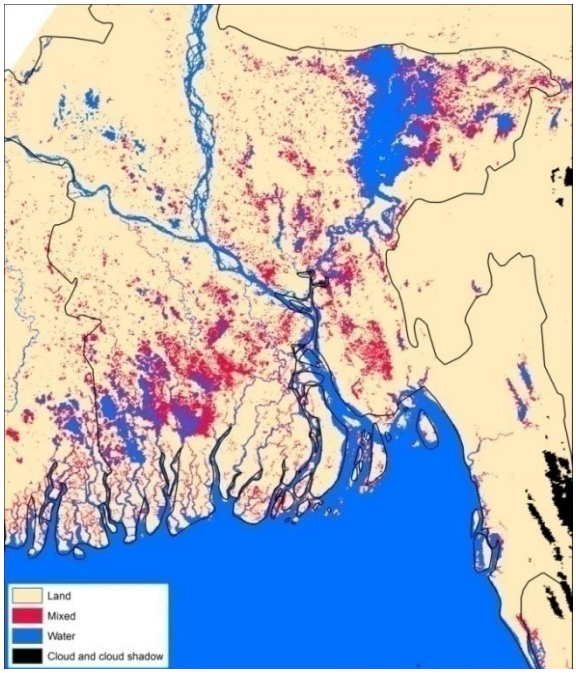

(A) Sakamoto method at approximately 500m resolution with all data from MOD09A1

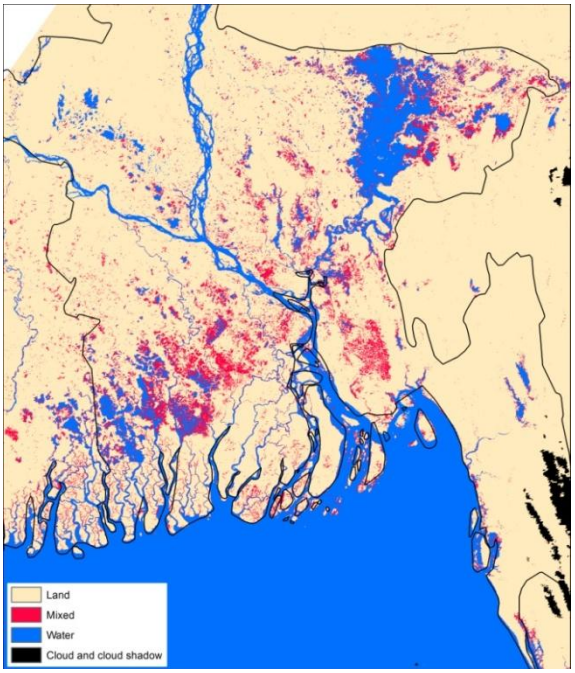

(B) Sakamoto method at approximately 250m resolution with bands 1 and 2 from MOD09Q1

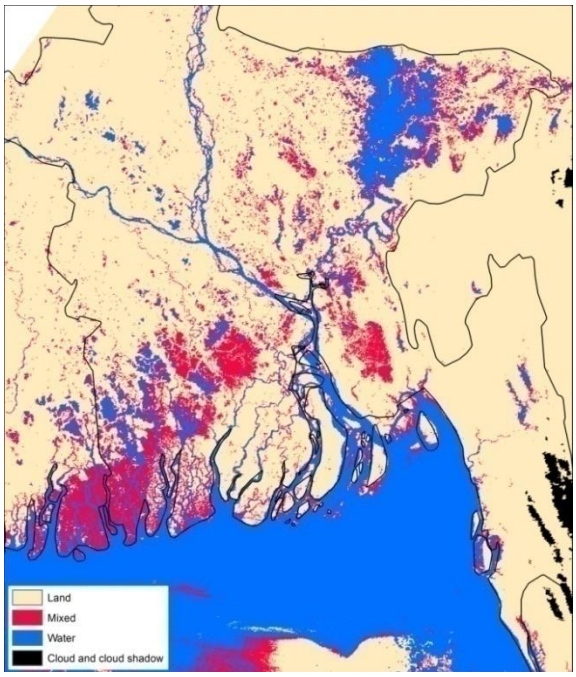

(C) Classification of a single NDSI from bands 4 and 7 at approximately 500m resolution with all data from MOD09A1

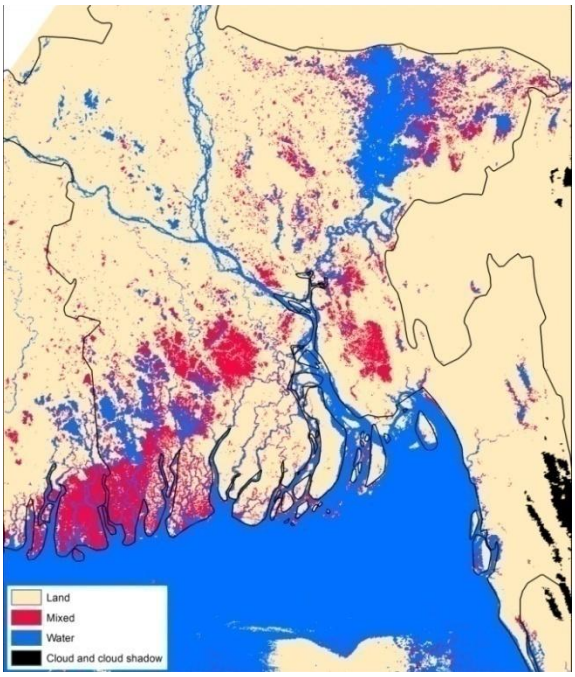

(D) Two stage classification using NDSIs - bands 4 and 7 from MOD09A1, bands 1 and 2 from MOD09Q1. Output at approximately 250m resolution.

Figure 4-7: Comparison of MODIS-derived classifications for Bangladesh.

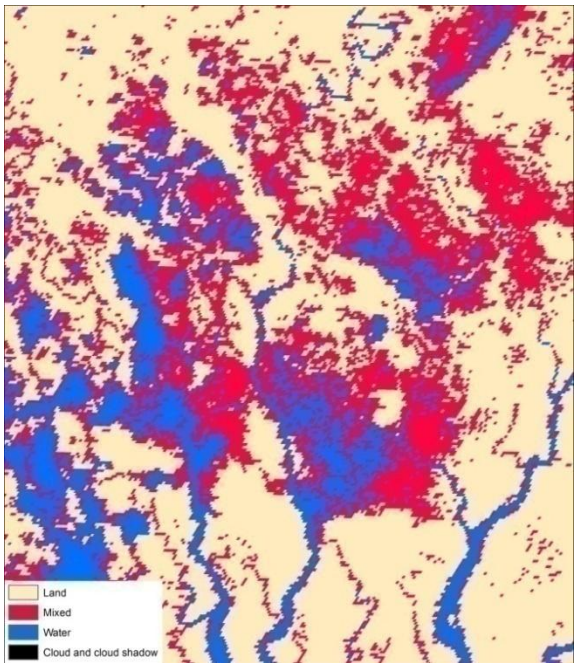

(A) Sakamoto method at approximately 500m resolution with all data from MOD09A1

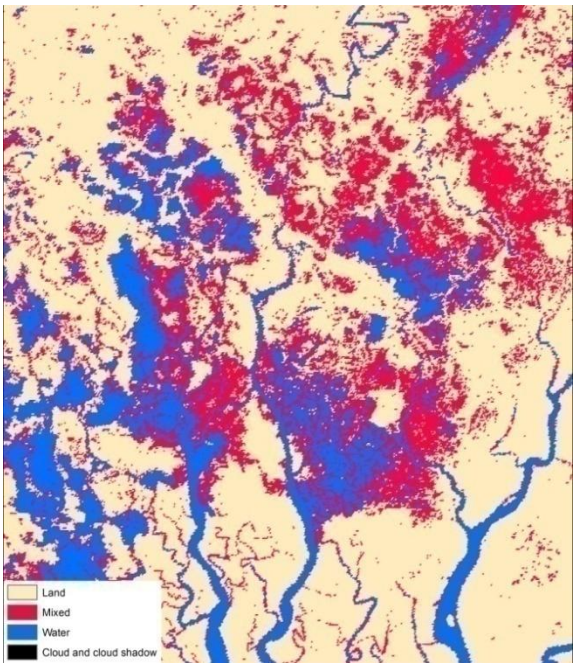

(B) Sakamoto method at approximately 250m resolution with bands 1 and 2 from MOD09Q1

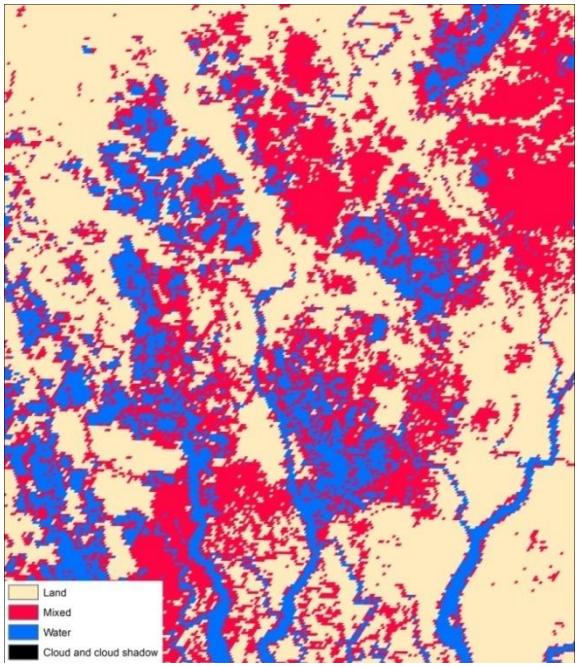

(C) Classification of a single NDSI from bands 4 and 7 at approximately 500m resolution with all data from MOD09A1

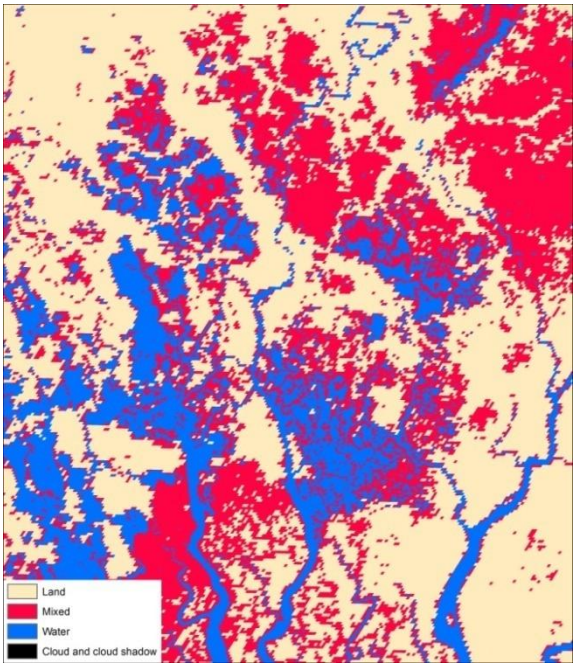

(D) Two stage classification using NDSIs - bands 4 and 7 from MOD09A1, bands 1 and 2 from MOD09Q1. Output at approximately 250m resolution.

Figure 4-8: Comparison of MODIS-derived classifications in an area of South-western Bangladesh.

Table 4-11: Total area (km2) covered by each class within the borders of Bangladesh and excluding areas of cloud and missing data for the MODIS based images shown in figure 7.

	(A) Sakamoto all bands from MOD09A1 (approx. 500m resolution)	(B) Sakamoto using MOD09Q1 for bands 1 and 2 (approx. 250m resolution)	(C) MODIS bands 4 and 7 from MOD09A1 (approx. 500m resolution)	(D) MODIS bands 4 and 7 from MOD09A1, bands 1 and 2 from MOD09Q1 (approx. 250m resolution
Land	79125.33	80568.04	78178.02	78178.02
Mixed	11065.97	8927.75	12704.41	10913.95
Water	10800.26	11495.78	10109.13	11899.60

4.7.1 Accuracy assessment of MODIS classification - procedure and results

Accuracy assessments were conducted for the four MODIS based classifications used to produce the layers displayed in Figures 4-7 and 4-8. For each classification method two accuracy assessments where conducted: one against the same GCPs that were used previously when assessing the accuracy of the Landsat ETM+ based classifications, and the other against the results of the most accurate of the Landsat based classification. Tables 4-12 and 4-13 provide summaries of the accuracy assessments against GCPs and the previously classified Landsat imagery respectively, while full error matrices for each accuracy assessment are provided in Appendix 2 (Tables 9-10 to 9-17).

The accuracy assessment against the previously classified Landsat imagery was included as it was felt that due to the high degree of accuracy it had shown it potentially provided a useful source of data, assumed to be reasonably accurate, and with a far larger sample size that covered the whole country. It was also felt that, compared to the limited sample size of the GCPs, it would potentially be more useful in highlighting the effects of the reduced resolution seen in the MODIS data. This can be illustrated in particular by looking at the accuracy assessment for image D that used the same two stage classification process as the Landsat based image which it was classified against. Given that the images where produced using the same methodology it would be expected that accuracy would be high. However the result is an overall Kappa value of 0.5919 with fairly poor accuracy scores seen in relation to mixed pixels. As the same methodology was used for creating both images the level of accuracy shown probably gives a reasonable indication of the limit of accuracy that may be expected when comparing MODIS imagery against Landsat under the current land, mixed, water classification scheme.

The fairly good overall accuracy scores that are seen under all four classification schemes can be largely attributed to the land class which covers a large portion of each image and is relatively well classified in each case. Out of the two classifications based on using the Sakamoto method the one making use of the higher resolution data for the red and near infrared bands seems to offer marginally better performance when compared against the previously classified Landsat image. The classification based on the use of a single NDSI from bands 4 and 7 performed poorly when assessed against GCPs and no better than the adapted Sakamoto method when assessed against the classified Landsat image. In summary, both of the classification schemes (B and D) making use of higher resolution data for bands 1 and 2 seem to offer marginally better performance than the lower resolution classifications. While the two stage classification of NDSIs (D) appears to offer slightly better performance than the adapted Sakamoto method (B), due to reasons already discussed here, and previously in relation to the collection of ground truth data, this difference may well not be significant.

Table 4-12: Summary of accuracy assessments for the four different MODIS based classifications with accuracy assessed against GCPs.

	(A) Sakamoto 500m		(B) Sakamoto 250m		(C) NDSI bands 4 and 7 (500m)		(D) NDSIs from bands 4 and 7, and 1 and 2 (250m)	
	producer accuracy %	user accuracy %	producer accuracy %	user accuracy %	producer accuracy %	user accuracy %	producer accuracy %	user accuracy %
Land	95.50	87.17	94.00	81.35	98.64	80.96	98.64	80.96
Mixed	56.39	36.06	39.10	40.31	37.59	30.67	45.11	52.63
Water	46.77	84.44	60.00	90.70	37.85	91.11	55.38	97.83
Overall accuracy %	77.83		78.59		75.23		80.86	
Overall kappa	0.5772		0.5726		0.4969		0.6059	

Table 4-13: Summary of accuracy assessments for the four different MODIS based classifications with accuracy assessed against the most accurate map obtained from classification of Landsat ETM+ data (two step process with NDSIs of bands 2 and 7, and 3 and 4).

	(A) Sakamoto 500m		(B) Sakamoto 250m		(C) NDSI bands 4 and 7 (500m)		(D) NDSIs from bands 4 and 7, and 1 and 2 (250m)	
	producer accuracy %	user accuracy %	producer accuracy %	user accuracy %	producer accuracy %	user accuracy %	producer accuracy %	user accuracy %
Land	92.36	81.35	93.54	87.54	92.59	89.27	92.59	89.27
Mixed	33.90	40.31	29.44	44.19	40.55	42.81	41.85	51.42
Water	69.93	90.70	76.73	81.57	64.88	78.43	76.94	79.01
Overall accuracy %	81.94		83.05		82.38		84.00	
Overall kappa	0.5324		0.5512		0.5503		0.5919	

4.8 Construction of a classified MODIS data time series

MODIS data from MOD09A1 and MOD09Q1 were downloaded from the earliest available date (18-02-2000 until 09-05-2014). Images were available at 8 day intervals and the time series was complete with the exception of 18-06-2001 giving 654 images in total. Given the discussion above in relation to accuracy assessment and the comparable performance of the different methods considered, three time series of classified images were initially created using: the Sakamoto method with all data coming from MOD09A1 to produce images at approximately 500m resolution, the Sakamoto method with data from MOD09A1 and MOD09Q1 with an output at approximately 250m, and the two stage classification using NDSIs and data from MOD09A1 and MOD09Q1, again with an output at approximately 250m.

While ground truth data were only available for the one time point, the resulting time series were inspected for obvious errors and in relation to prior knowledge regarding surface water patterns within Bangladesh. The two classifications based on the adapted Sakamoto method appeared to show consistent performance throughout the time series with the version using higher resolution data seemingly showing more detail in a similar fashion to the images shown in Figure 4-8. The results of the time series based on the reclassification of NDSIs from bands 4 and 7, and 1 and 2 were less

encouraging due to the fact that some images seemed to suffer atmospheric effects, such as would normally be associated with cloud contamination, beyond the areas covered by the cloud mask. There was also the tendency, as discussed in relation to the images in Figure 4-7, to reduce the width of rivers compared to the Sakamoto method. This was especially noticeable during the dry season but without adequate ground truth data for these periods it is not possible to say if this is valid or not.

4.9 MODIS time series outputs

Figure 4-9 shows, on a pixel by pixel basis, the total number of cloud free images that were available from the time series. Figure 4-10 shows the percentage of cloud free images that were classified as water, while Figure 4-11 shows the percentage of cloud free images that are water related (classified as either water or mixed). The dark blue areas in Figure 4-10 highlight areas of permanent water including major river channels and a significant area in the south west of the country that is associated with pond aquaculture. Areas with regular seasonal inundation such as the large *Haor* basin in the North West of the country are also clearly visible when the data is viewed at the national scale. Areas in orange i.e. those that are only inundated occasionally may be vulnerable in terms of flood risk (Handisyde et al., 2014). Such areas may represent situations where significant flooding does not normally take place and thus may be treated as largely flood free, but where flooding can occur during more extreme scenarios. It is tentatively suggested that such areas could be of interest under changing climate conditions involving increased precipitation and / or runoff as locations potentially prone to more severe inundation.

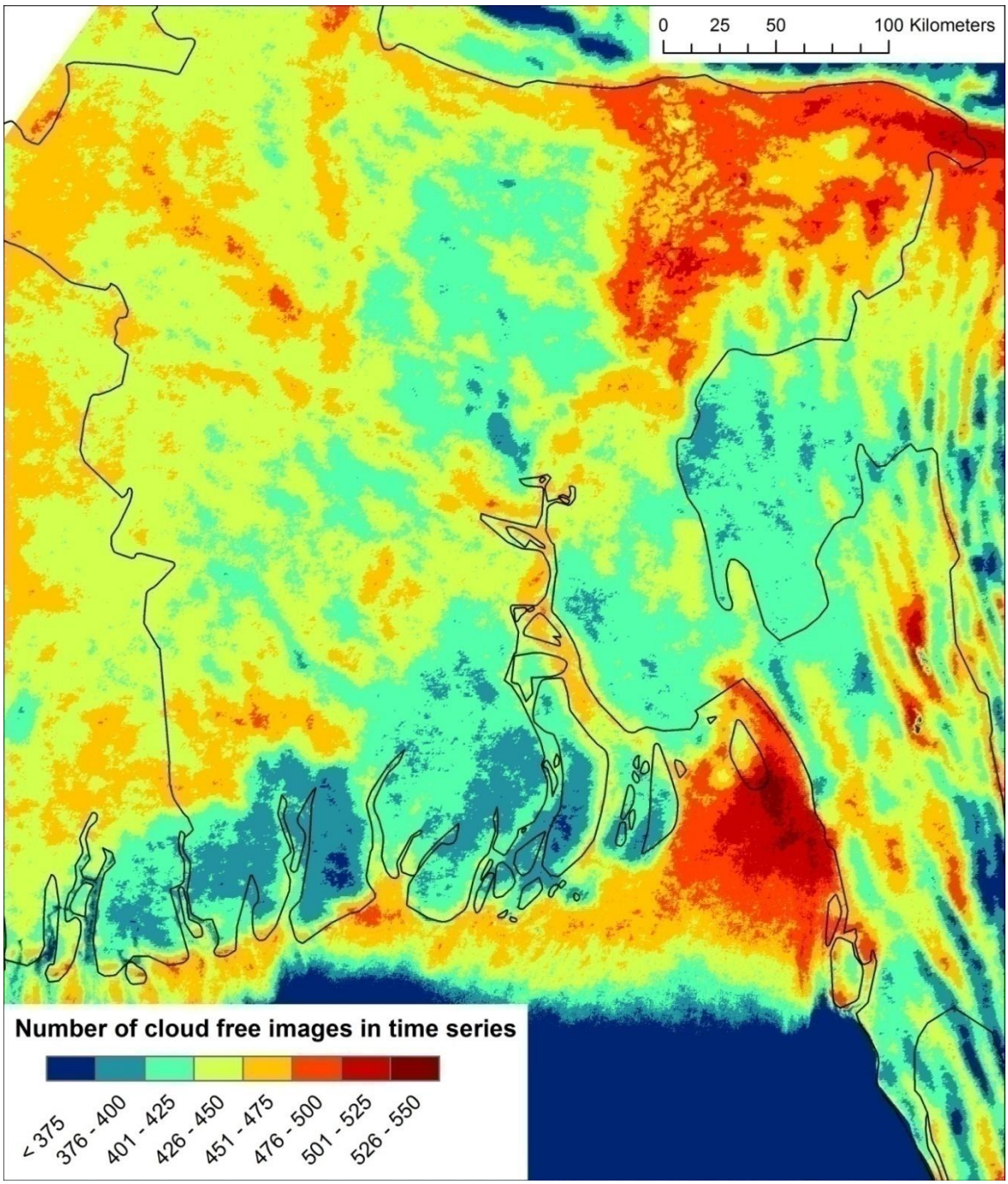

Figure 4-9: Number of available MODIS images for Bangladesh (2000-2014), after removal of cloud and cloud shadow.

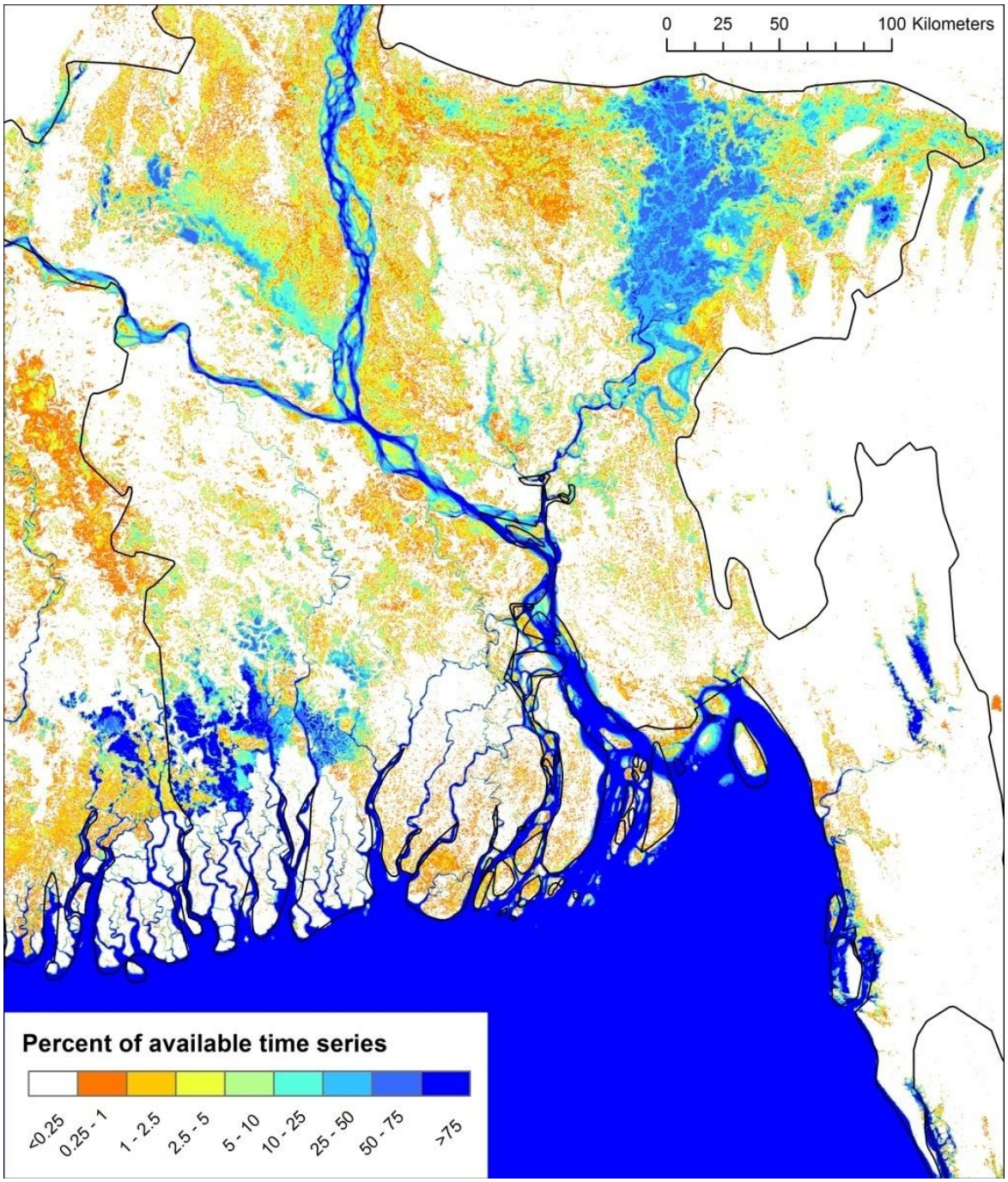

Figure 4-10: Percentage of the available time series for Bangladesh (2000-2014), where pixels classified as water are present.

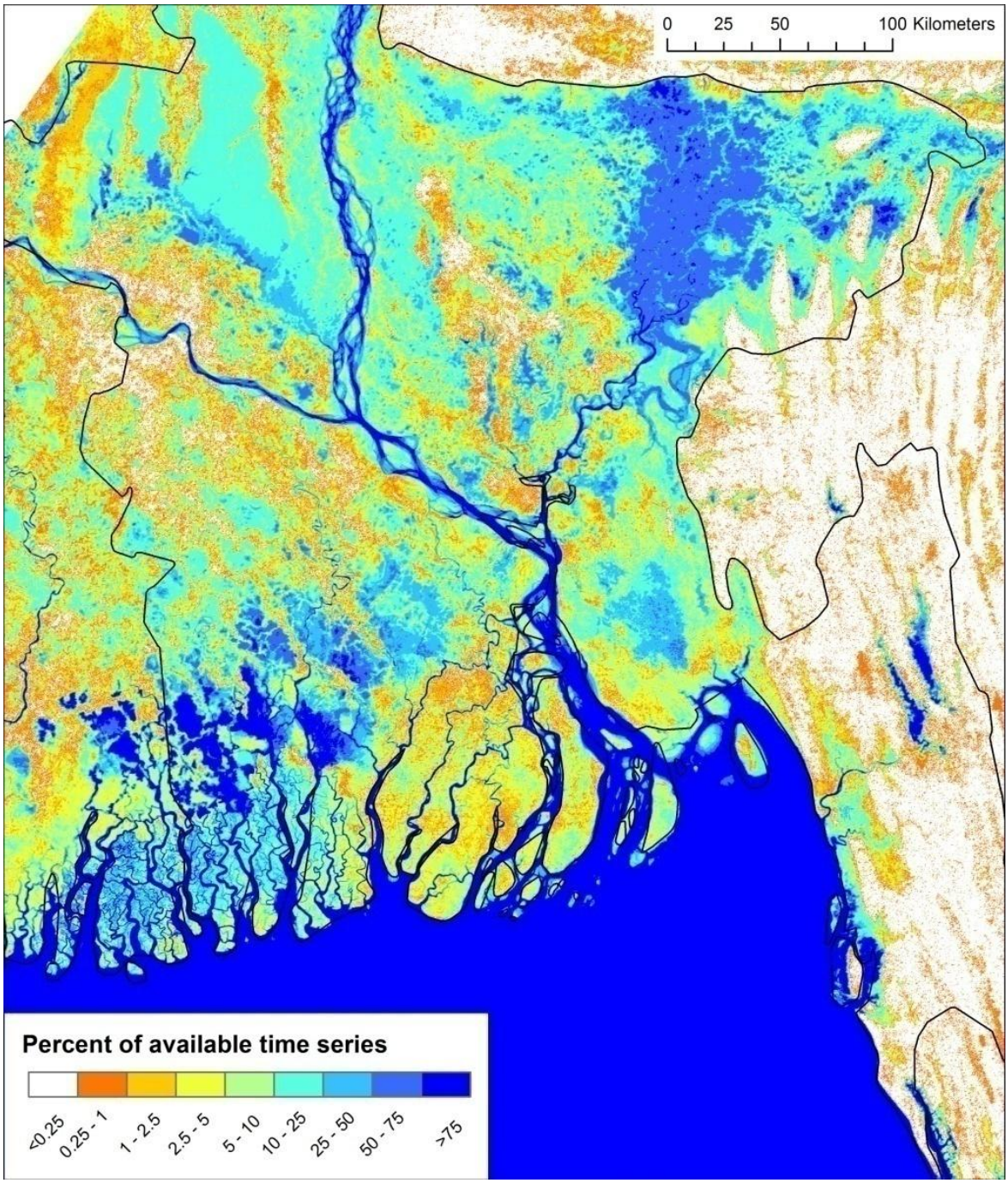

Figure 4-11: Percentage of available time series for Bangladesh (2000-2014),where water related pixels classified as belonging to the mixed or water class are present.

4.10 Concluding remarks

Based on the previous discussion in relation to the construction of classified MODIS time series, the results of the accuracy assessments, and its track record within the literature it is suggested here that the approach described by Sakamoto et al. (2007) and adapted for use in the current study offers a valid means of attempting to define land, mixed and water related pixels using MODIS data within Bangladesh.

The time series presented here in terms of inundation frequency as a percentage of total time series provides valuable insight into areas that contain largely permanent water, are frequently flooded, or infrequently flooded and therefore perhaps areas that are considered largely flood free but may be at risk under future climate regimes. Such information, while valuable in itself, can also make important contributions to broader site suitability models designed to inform development activities such as aquaculture and it is in this context that the current study was originally conceived.

The classification methods investigated based on the use of NDSI thresholds while not outperforming the Sakamoto method when classifying MODIS data performed very well with Landsat ETM+ images for the Bangladesh region and may prove useful in that sense in their own right.

Often classification of water areas using MODIS has aimed to detect relatively large and distinct water bodies or areas of flooding and have made use of a two class system with pixels designated as land or water (e.g. Feng et al., 2012, Li et al., 2011, Khan et al., 2011, Huang et al., 2012). While Bangladesh does contain large uninterrupted areas of water, especially during flood season, much of its area presents a genuinely mixed scenario when attempting classify land cover using moderate resolution data. As such the inclusion of a mixed class as in the case of the current study would seem useful.

In the case of the current study regardless of classification method the mixed class achieved low accuracy scores when using both ground control points and higher resolution ETM+ classifications and ground truth data. Visual inspection of MODIS based classifications using the method adapted from Sakamoto et al., (2007) in comparison and similarly classified ETM+ data, as well as true and false colour composites of ETM+ bands, suggests that overall patterns of land cover appear accurate. This and the fact that low accuracy scores are seen for mixed areas when MODIS based classified data is assessed against ETM+ data classified using exactly the same methods suggests that much of the problem lies in the lower resolution of the MODIS data. Due to the complex and intricate nature of

land and water coverage in Bangladesh many areas could be seen where ETM+ based classifications would show patterns of land and water pixels within an area that would be covered by a single MODIS pixel. In such a situation the classification of MODIS data as mixed could be viewed as technically correct although it would be viewed as incorrect when accuracy is assessed against the higher resolution data and corresponding ground control points.

With the above in mind it would seem there is potential for further research with regard to mixed pixels over Bangladesh when using MODIS data. Two broad approaches can probably be considered: 1) algorithms that attempt to quantify the level of land and water within a pixel, and 2) data blending methods where data with a high spatial but low temporal resolution (e.g. ETM+) is blended with low spatial resolution, high temporal resolution data (e.g. MODIS).

Guerschman et al. (2011) developed the Open Water Likelihood (OWL) algorithm that has been applied in a number of further studies (Chen et al., 2013, Huang et al., 2014, Karim et al., 2011). The OWL algorithm aims to predict the probability that a MODIS pixel contains water, however it's development and evaluation was based around the proportion of a MODIS pixel occupied by water based on higher resolution Landsat data. It's development and subsequent use has focused on areas within Australia, an environment that is very different to Bangladesh where truly mixed surfaces are likely to be common even at the higher resolutions found in Landsat imagery. Even so the methodology and principles behind it may be worthy of further investigation in the context of Bangladesh.

Methods for blending of MODIS and Landsat data with the spatial resolution of Landsat and temporal resolution of MODIS have been reviewed by Emelyanova et al. (2012). The authors note that the complex algorithms: Spatial and Temporal Adaptive Reflectance Fusion Model (STARFM, Gao et al., 2006), and the Enhanced version of STARFM (ESTARFM, Zhu et al., 2010) were computationally expensive and didn't always outperform simpler methods: the Linear Interpolation Model (LIM) and the Global Empirical Image Fusion Model (GEIFM). In the context of Bangladesh while the implementation of data blending approaches may be worth further consideration, the highly dynamic nature of land cover combined with often very infrequent availability of cloud free Landsat imagery may well limit the feasibility of such methods.

A key consideration with regards to the implementation of any of the mixed pixel approaches outlined above would be obtaining ground truth data of sufficient quality and quantity to make such exercises worthwhile.

5 LANDSAT ETM+ DERIVED 30 METRE RESOLUTION LAND COVER FOR BANGLADESH

5.1 Introduction

Maps that detail land cover type (e.g. crops, forest, bare ground, urban, water etc.), either used directly or as part of a more complex modelling process, are potentially highly useful sources of information for a wide range of decision making processes (Herold et al., 2008) including those relating to aquaculture site suitability (e.g. Giap et al., 2004, Giap et al., 2005, Karthik et al., 2005, Nath et al., 2000, Rajitha et al., 2007, Salam et al., 2003).

While it is technically possible to produce high quality and detailed land cover maps through traditional survey techniques, for all but the smallest survey areas such an approach will be extremely resource intensive and as a result detailed mapping is often dated, or not available at all for many regions. This situation is likely to be especially true for developing regions where due to the potentially high costs, the development of detailed mapping may not be a priority.

An alternative and common approach to the development of land cover maps is the use of remotely sensed data that in the majority of cases is obtained from satellite mounted sensors. While active sensors using synthetic aperture radar (SAR) such as RADARSAT-1 and RADARSAT-2 are highly useful in that they are unaffected by atmospheric conditions such as cloud, most land cover classification work makes use of imagery obtained by passive sensors that provide a number of distinct bands within the electromagnetic spectrum. A wide range of techniques exist for classifying remotely sensed data that at a basic level are built around the principle that different land cover types will have different reflectance values at given points within the electromagnetic spectrum. In theory this allows ground based objects to have a unique spectral pattern that can be compared with known spectral responses obtained from either existing spectral signature libraries, or often from carefully selected sample areas on the ground that specifically relate to the required land cover classes (Campbell and Wynne, 2011, Eastman, 2012, Jensen, 2006).

Resolution of multi band remotely sensed data varies considerably. At one extreme instruments such as GeoEye-1 and QuickBird achieve resolutions of less than a metre for the panchromatic band, while

other sensors such as the Advanced Very High Resolution Radiometer (AVHRR) have resolutions of over 1km. As would be expected the swath width and thus area covered by individual scenes varies with sensor resolution and thus there is a trade off between resolution and coverage. While it is common practice to combine more than one scene in order to cover a study area resolution still becomes relevant in as much as while it would be theoretically possible to cover a large area with a large number of very high resolution images, the data acquisition, processing and storage implications of such an exercise are likely to be restrictive.

Low resolution instruments with frequent return periods and a large swathe width such as AVHRR and the Moderate-resolution Imaging Spectroradiometer (MODIS) instruments aboard the Aqua and Terra satellites are extremely useful in terms of estimating land cover and monitoring change over large areas or even globally, and have formed the basis of a number of global land cover products (Friedl et al., 2010, Hansen et al., 2000, Loveland et al., 2000). However low resolution sensors such as these are unable to pick out smaller land cover features and are more likely to suffer from mixed pixel situations where an individual pixel includes more than one land cover type making accurate classification considerably more challenging (Kaptué Tchuenté et al., 2011). The Landsat program launched its first satellite in 1972 carrying the MultiSpectral Scanner (*MSS*) instrument that recorded data across multiple bands at a resolution of 80m. In 1982 the launch of Landsat 4 carrying the Thematic Mapper (TM) instrument saw the resolution increased to 30m, while Landsat 7 launched in 1999 with its Enhanced Thematic Mapper (ETM+) saw the inclusion of a panchromatic band with a resolution of 15m. Landsat TM and ETM+ with their swathe widths of approximately 185km strike a good compromise between detail and coverage. This, combined with the fact that there is a large archive of freely available data spanning a number of decades, means that along with Terra ASTER, Landsat TM imagery is the most commonly used source for regional land cover assessment (Lu and Weng, 2007, Purkis and Klemas, 2011).

The current study details the production of a classified land cover layer for Bangladesh at 30m resolution via the use of Landsat ETM+ imagery. This land cover layer will contribute to geographic information system (GIS) based model of site suitability for aquaculture. Bangladesh is one of the world's most densely populated countries with a 2013 estimate of 1203 people per square kilometre (World_Bank, 2014b). As a consequence land use in the country is intensive and intricate with many small parcels of land resulting in interesting but challenging land cover classification scenarios.

5.2 Methods and data

5.2.1 Data choice and acquisition

Images obtained by the Enhanced Thematic Mapper Plus (*ETM+*) instrument aboard the Landsat 7 satellite were used for the current study. A major advantage of ETM+ data is that it is freely available for download as a level 1T product meaning that images are georeferenced and terrain corrected based on the use of a digital elevation model (DEM) and a number of ground control points. Images had an individual scene size of approximately 185 x 185km allowing for virtually the whole of Bangladesh to be covered by combining 9 scenes into a single image with an overall resolution that still allows for relatively easy processing. Another advantage of Landsat is that data is collected continuously with a return period of approximately 16 days. This contrasts with the on-demand nature of data collection with instruments such as ASTER and SPOT meaning that the potential of obtaining images that cover the whole country over a relatively small time period is higher and that it is more likely that this time period can be close to that when ground truth data were collected.

While Landsat ETM+ data have a lot to recommend it one disadvantage results from the failure of the scan line corrector (SLC) on 31st May 2003 (Markham et al., 2004). The result is that ETM+ images obtained since that time are complete in the centre but show increasingly large gaps in data towards the edge of the swath with approximately 22 percent of each scene missing. For the current study ETM+ images created before the SLC error were used to fill gaps in data. Details of all Landsat data used are provided in Table 5-1. The dates for the primary images were chosen to correspond as closely as possible to the dates on which ground truth data used to guide image classification was collected. It was fortunate that images for this period were largely cloud free resulting in all primary images used being obtained from dates within a week each side of ground truth data collection. Images used for gap filling the primary images were obtained for dates as close as possible to the primary images in terms of time of year while at the same time providing cloud free data.

Table 5-1: Landsat scenes used in the current study

Path and row	Acquisition data of main scene	Acquisition data of fill scene
P136 R43	09/11/2008	08/10/2002
P136 R44	09/11/2008	08/10/2002
P136 R45	09/11/2008	19/12/1999
P137 R43	31/10/2008	31/10/2002
P137 R44	31/10/2008	31/10/2002
P137 R45	31/10/2008	31/10/2002
P138 R43	07/11/2008	17/11/2000
P138 R44	07/11/2008	17/11/2000
P138 R45	07/11/2008	17/11/2000

5.2.2 Cloud and cloud shadow removal

The primary ETM+ scenes contained a small amount of cloud. These clouds were mostly small but had the potential to cause errors in two ways: the clouds themselves result in high reflectance values that can be mistaken for areas of bare ground or urban structures, while cloud shadows result in low reflectance values, especially in the infrared bands, which gives the potential for wrongly identifying them as areas associated with water. Clouds and cloud shadow areas were removed using an approach similar to that described by (Martinuzzi et al., 2007). For a full discussion and details of the cloud removal procedure see section 4.2.4.

5.2.3 Filling gaps in primary ETM+ images

A number of methods have been proposed to address the issue of gaps in ETM+ images as a result of the SLC problem. Gap filling methods can generally be categorised as those that attempt to fill gaps using the original image (i.e. interpolation, segmentation and kriging methods), and those that make use of additional images from a different time point and attempt to adjust the relative reflectance of the fill pixels to match the main scene. Table 5-2 (adapted from: Jabar et al., 2014) provides an outline of potential methods for dealing with SLC-off related gaps.

Table 5-2: Potential methods for dealing with SLC-off related gaps

Gap filling method	Single or multi source	Advantages	Limitations	Relevant publications
Simple interpolation	Single source	Simple and easy implementation	Inaccurate results because the gap value calculated from surrounding pixels	
Multi-scale segmentation	Single source	Most of gap pixels with high accuracy were interpolated	At pixel level the accuracy of the reflectance prediction is low	(Maxwell et al., 2007)
Global histogram matching (GHM)	Multi source	Suitable results with invariant terrain scene	Visible error in heterogeneous scene where there were transient areas	(Scaramuzza et al., 2004)
Local linear histogram matching (LLHM)	Multi source	Suitable results with predefined condition of minimal cloud, snow and time acquired separation	Inaccurate results when there were differences in target radiances	(Scaramuzza et al., 2004)
Adaptive window local histogram matching (AWLHM)	Multi source	Good results in homogeneous landscape	Still, gaps visible when the significant change has occurred in areas smaller than the local window size	(NASA., 2004)
Geo statistical methods	Kriging (single source) Co kriging (multi source)	Provide uncertainty of prediction	1 - Could not predict the reflectance well at a pixel level 2 - computationally complex	(Zhang et al., 2007) (Pringle et al., 2009)
Multispectral projection transformation based on principal component transformation.	Multi source	Preserving the radiometric characteristic of multispectral data	Visible gap lines with sharp radiometric differences areas.	(Boloorani et al., 2008)

Neighbourhood similar pixel interpolator (NSPI)	Single source	1 - Recovering heterogeneous landscape 2-The spatial continuity of the filled images can be retained even using the auxiliary image with a long time interval	Cannot produce statistical uncertainty of prediction	(Chen et al., 2011) (Zhu et al., 2012)

The current study makes use of the adaptive window local histogram matching (AWLHM) approach (NASA., 2004) via the use of the freeware program Frame and Fill produced by Richard Irish (SSAI/NASA). Potential options for gap filling included using multiple SLC-off images where the gaps are at slightly different locations, or to use a single SLC-on image obtained prior to the SLC malfunction. Choice of fill scenes was significantly limited by cloud contamination and after preliminary investigation it was decided to use a single SLC-on fill image. These images where then used to fill gaps resulting from both the SLC-off issues as well as those where cloud and cloud shadow had been removed.

5.2.4 Standardisation and concatenation of images

ETM+ images are supplied with surface reflectance values expressed using an arbitrary 8bit scale (0-255) of digital numbers. These numbers indicate relative variation of reflectance over an individual image but are not directly comparable between images with values being influenced by atmospheric effects. The MODIS MOD09GA product has bands with a similar spectral response to ETM+, albeit at a much lower resolution, and provides daily images that are atmospherically corrected and have standardised surface reflectance values. By carefully selecting areas of homogeneous pixels within the ETM+ images a linear relationship was established between MOD09GA and ETM+ on a band by band basis for each of the images enabling all ETM+ images to be converted to standardised surface reflectance values. It was then possible to combine the 9 ETM+ scenes to form one large one using a simple concatenation process within a GIS. This process is described in full section 4.2.3.

5.2.5 Ground truth data collection

Ground truth data were collected for a range of locations within Bangladesh and covered a variety of land cover types including areas of mixed land and water such as wetlands and flooded cropland. Data collection took place over a 4 day period (02/11/2008 to 05/11/2008) and consisted of a series of photographs with corresponding GPS information.

5.2.6 Creation of ground control points and selection of land cover classes

Land use in Bangladesh is very diverse both in space and time with very little land in low lying areas remaining unused. An ideal land cover data set would contain a large number of classes that would cover variables such as types of crops and cropping / land use patterns throughout the year. In reality data availability, both in terms of cloud free images and corresponding ground truth data, does not allow for such detailed analysis and there is a trade-off between number and specificity of classes and classification accuracy.

The ground control points GCPs produced and described in relation to Chapter four where they were reclassified to represent water, mixed, and land classes were used here under a more complex classification scheme. Data were initially assigned to nine classes: clear water, turbid water, mixed vegetation and water, crops, crops with water, trees and shrubs, bare ground, floating vegetation/dense vegetation in wetland areas, and urban. Preliminary investigation suggested that separating areas of crops and water from other mixed water and vegetation areas using a single Landsat image was not feasible so these two classes were combined into a single mixed vegetation and water class. The two water classes were subsequently combined as the point of transition between the two was arbitrary and the distinction was considered unimportant in terms of application of the resulting land cover map. Vegetation indexes such as the enhanced vegetation index (EVI) indicate the floating vegetation/dense vegetation in wetland areas class as being densely vegetated which in a sense it is, although the areas would be more accurately classed as water, or mixed land and water areas. Examination of the spectral response for individual ETM+ bands, as well as combinations of bands, suggested that these areas would easily be confused with other densely vegetated areas such as trees. Given the small overall area occupied by this class and the potential for

it to introduce errors when classifying important areas such as trees and croplands, it was decided to exclude it from the classification process. The result of these refinements was a six class scheme:

1. Water
2. Bare ground including crop areas post harvest / pre-planting
3. Trees and shrubs
4. Crops
5. Mixed water and vegetation
6. Urban

GCPs derived from collected ground truth data were randomly split into two equally sized groups: one used to guide classification, often referred to as training data, and the other set reserved for accuracy assessment. Ideally GCPs for the purposes accuracy assessment would be derived from a totally random sampling scheme with a sufficient number of points that all classes are adequately represented (Campbell and Wynne, 2011, Foody, 2002, Stehman and Czaplewski, 1998). As discussed in Chapter four in relation to accuracy assessment of ETM+ classifications, sampling was conducted from roads and was constrained by time, access, finances, and other logistical issues. The result is that sampling points tended to be grouped in a number of areas and cannot be considered randomly distributed. While GCPs were randomly allocated for either training or verification of image classification in reality they are likely to be from similar areas in many cases which in turn has the potential to indicate a greater degree of accuracy than would be seen under a truly random sampling scheme.

With the above in mind a second set of GCPs were produced. Given the small overall area occupied by urban areas, in particular when compared to other classes, an unrealistically large number of sample points would be required under a completely random sampling scheme in order to achieve a reasonable quantity for accuracy assessment. To compensate for this, images were loosely classified under the 6 class scheme described above using a basic decision tree approach and the resulting layer was used to create a stratified random sampling scheme where 125 points were randomly selected across the areas occupied by each class. Each point was then assigned to one of the six classes on a best effort basis through careful inspection of high resolution true colour satellite images (Google Earth and Bing maps), false colour ETM+ composites, and ETM+ based vegetation indices whilst

making use of knowledge gained from field visits and working with the original ground truth data. Any points that bordered equally between more than one land cover type or where class membership was considered uncertain were discarded. The resulting distribution of sample sites is shown in Figure 5-1.

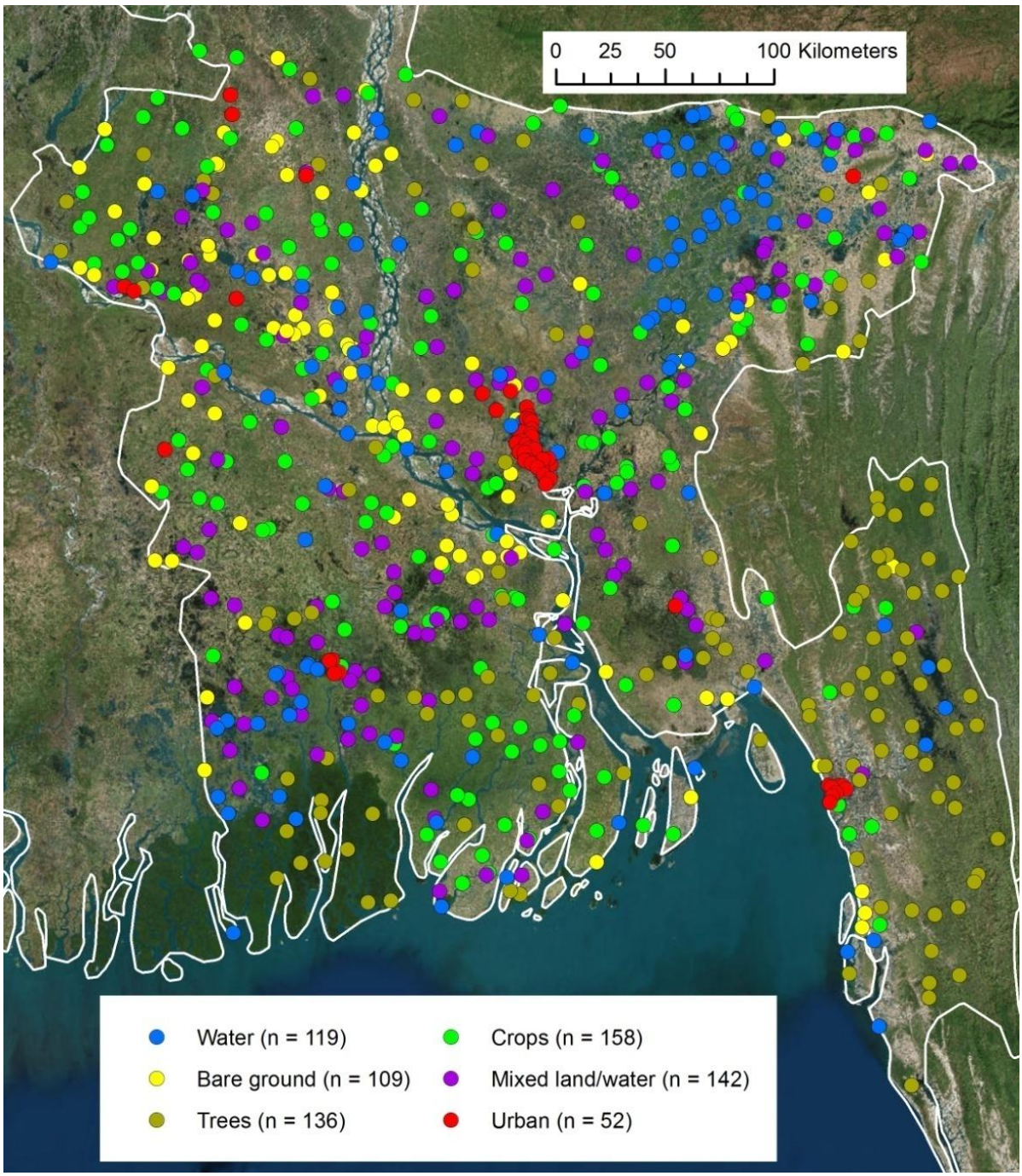

Figure 5-1: Ground control points created using a stratified random sampling scheme.

5.2.7 Image classification

Classification routines can be broadly classed as supervised or unsupervised with outputs taking the form of hard or soft classifications. Supervised classification makes use of training data (i.e. the previously described GCPs) that represent the desired classes. The job of the classification algorithm is then to compare the spectral patterns of these areas with that of the pixels to be classified and estimate the degree of membership a pixel has to each class. In the case of a hard classification output the pixel is then assigned completely to the class which it matches most closely regardless of the proportional membership. Alternatively soft classification outputs use a number of approaches that indicate the relative membership of a pixel to the different available classes. Unsupervised classification methods work quite differently and can essentially be viewed as a method looking for common and distinctive spectral patterns and consequently grouping pixels into a number of classes without any knowledge of what those classes may represent (Eastman, 2012). It is then the job of the analyst to assign meaningful labels to these classes i.e. through cross referencing with ground truth data.

In the case of the current study preliminary investigation into the use of unsupervised classification highlighted a number of issues. If a small number of classes were specified then they did not match well with the desired classification system resulting in a low overall classification accuracy. Specifying a large number of classes, in order to narrow the range of pixel in a single class, and then reclassifying and grouping these classes into the desired classes would in theory be expected to improve classification performance. However, in practical terms this process was significantly limited by the quantity and detail of ground truth data. This was especially true in the case of classes that represented a small portion of the overall image.

In view of the issues discussed above the decision was made to focus on supervised classification methods. The current study made use of the IDRISI software package which addresses both image processing and classification as well as GIS operations. A variety of classification routines available within the software package were evaluated (see Table 5-3 for details). In addition to the established routines a unique decision tree approach constructed in relation to the current study was also evaluated. For each classification method results were tested against the GCPs derived from the

collected ground truth data as well as the second set of GCPs based on a stratified random sampling strategy.

Table 5-3: Established classification routines tested in the current assessment. Brief descriptions are provided based on Eastman (2012).

Classifier	Description
Maximum Likelihood classification (MAXLIKE)	Uses a probability density function related to training site signatures. Pixels are assigned to classes based on comparison of the posterior probability that it belongs to the signatures being considered. There is also the option to incorporate prior knowledge by providing a probability that each class exists. Probabilities can be applied equally to all pixels or on a pixel by pixel basis using a probability image. In the case of the current assessment all classes and pixels where given equal prior probability.
Minimum Distance to Means classification (MINDIST)	In common with MAXLIKE MINDIST uses a set of signature files created from specified training sites. Mean reflectance values for each class and spectral band are established from the signature files and pixels are assigned to the class where they most closely correspond to these means.
Parallelepiped classification (PIPED)	Again uses a set of signature files derived from training sites. Upper and lower reflectance thresholds are established for each signature in relation to each band. Pixels are then assigned to a class based on reflectance values falling between these thresholds. Parallelepiped is a computationally light classifier and runs quickly but is potentially inaccurate.
Self-Organizing Map (SOM)	Can be used to undertake supervised and unsupervised classification based on Kohonen's Self-Organizing Map (SOM) neural network. Tends to be computationally intensive.
Multi-Layer Perceptron neural network classifier (MLP)	Uses information from training sites to classify remotely sensed data via a Multi-Layer Perceptron neural network using a back propagation algorithm.
Adaptive Resonance Theory (ARTMAP) classifier	Can perform supervised and unsupervised classification using Adaptive Resonance Theory (ART) based neural network analysis.
K-Nearest Neighbour classifier (KNN)	Uses k-nearest neighbours from a specified size subset of potential training samples in determining a pixel's class.
FISHER Linear Discriminant Analysis (LDA) classifier	The FISHER (LDA) classifier uses a linear discriminant analysis of the specified training areas to produce a set of linear functions that express the degree of support for each class. Pixels are then assigned to classes based on which one receives the highest level of support when all functions are considered.
Classification Tree Analysis (CTA)	Splits data into homogenous subsets and produces a hierarchical set of decision rules that are used to classify data.

5.2.7.1 Decision tree approach

A decision tree approach was devised that uses a series of Boolean intersections in relation to threshold values for a number of ETM+ derived normalised difference spectral indices (NDSIs) and the enhanced vegetation index (EVI). The use of population density data from the Landscan 2008 data set is reviewed thoroughly in section 3.2.1.7. Here, Landscan data were used in order to separate urban areas from bare ground. Threshold values for ETM+ data were selected by using the set of GCPs designated as training data to generate frequency distributions of values from all individual ETM+ bands as well as NDSIs and EVI for each of the land cover classes. The classification process is described in Figure 5-2 while the frequency distributions for the each of the band combinations used are shown in Figures 5-3 to 5-6.

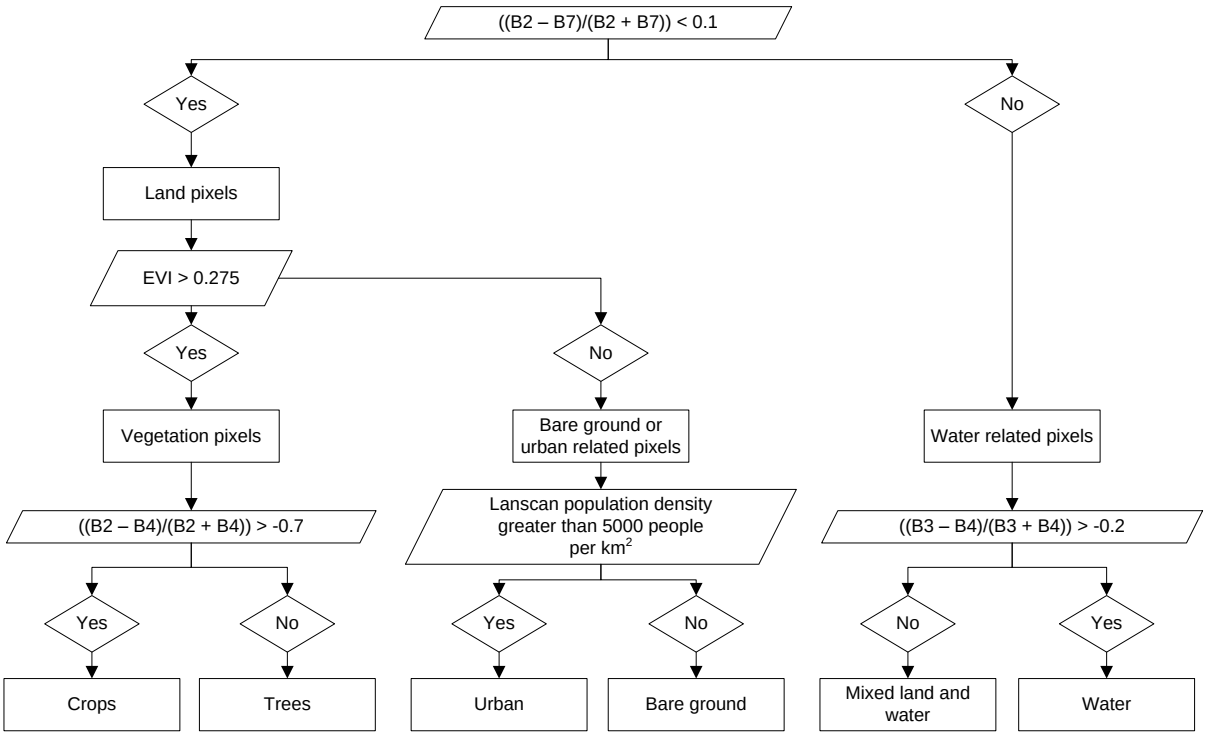

Figure 5-2: Decision tree created for current study to classify data into 6 land cover classes. B2, B3, B4, and B7 = Landsat ETM+ bands 2, 3, 4, and 7 respectively. EVI = enhanced vegetation index calculated from Landsat ETM+ bands 1, 3, and 4. Population density

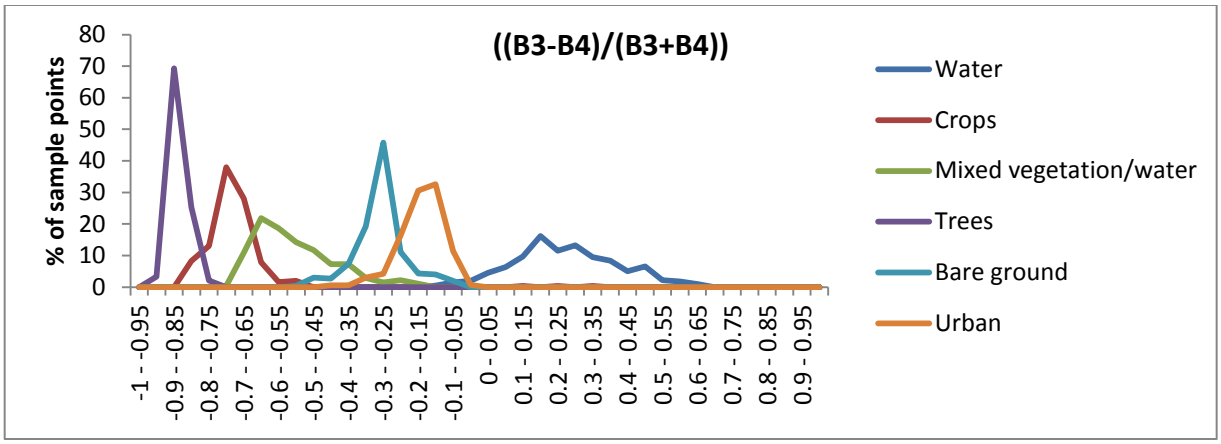

Figure 5-3: Frequency distribution of ETM+ band combination ((B3-B4)/(B3+B4)) in relation to GCPs representing land cover classes.

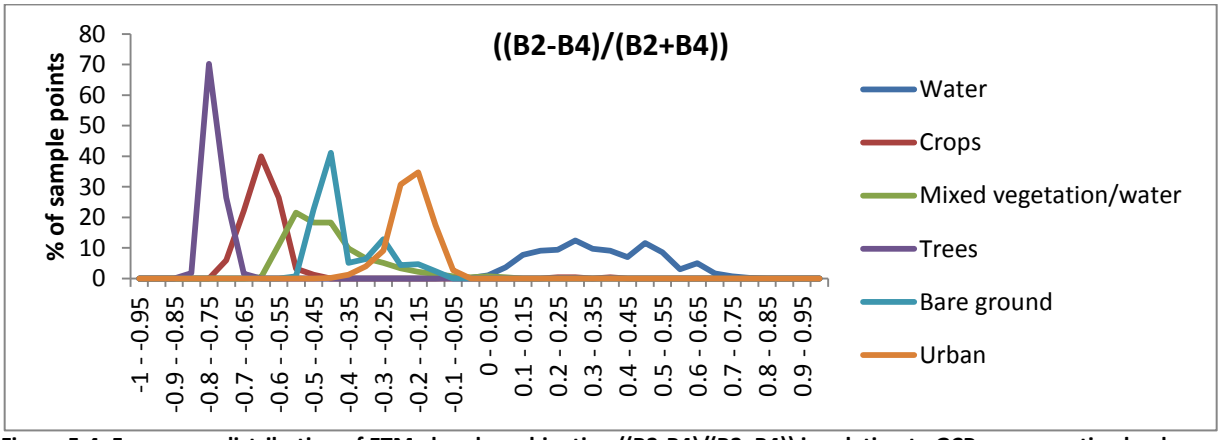

Figure 5-4: Frequency distribution of ETM+ band combination ((B2-B4)/(B2+B4)) in relation to GCPs representing land cover classes.

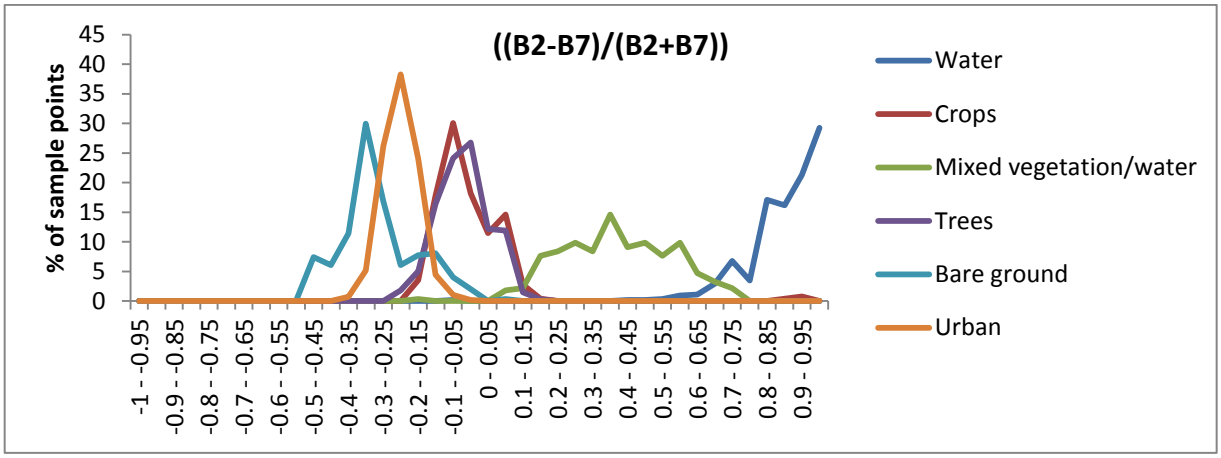

Figure 5-5: Frequency distribution of ETM+ band combination ((B2-B7)/(B2+B7)) in relation to GCPs representing land cover classes.

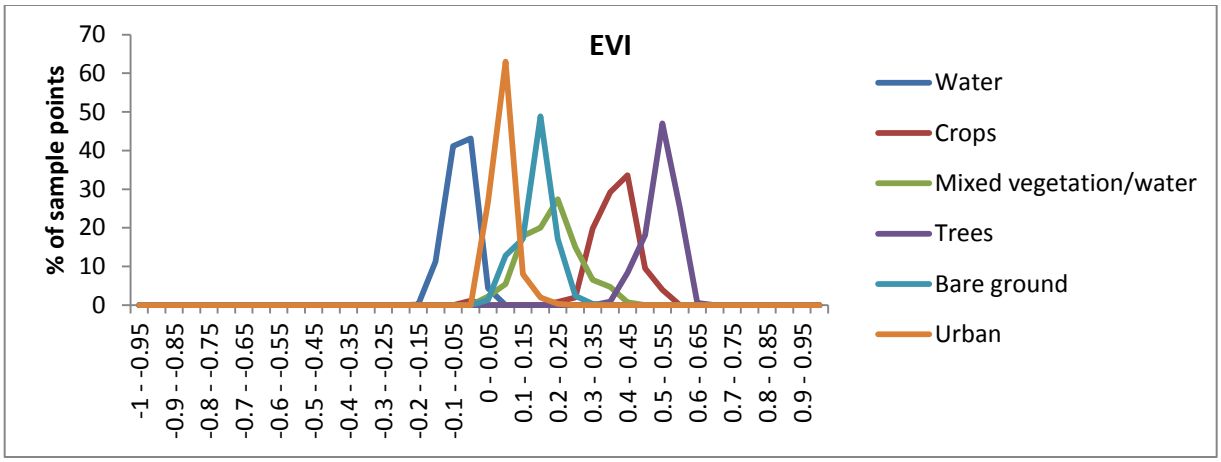

Figure 5-6: Frequency distribution of ETM+ Enhanced Vegetation Index (EVI) in relation to GCPs representing land cover classes.

5.2.8 Accuracy assessment

Accuracy was assessed through the use of error matrices providing results in terms of proportional error for both errors of commission and errors omission. Kappa Index of Agreement (KIA) values are also provided. The KIA is similar to a proportional accuracy figure with the difference being that it adjusts for chance agreement (Eastman, 2012). For each classification two accuracy assessments were made: one using the set of GCPs designated for verification that were produced from ground truth data collected in the field, and one from the second set of GCPs produced using the stratified random sampling scheme.

5.3 Results

Table 5-4 shows a summary of error matrix results for each of the 10 classification methods tested where accuracy is being tested against the set of GCPs designated for verification that were derived from ground truth data collected in the field. An overall error figure is given i.e. proportion of pixels out of the total available that are wrongly classified, along with an overall KIA figure. Results are ranked from highest to lowest (right to left) based on overall KIA score. With the exception of PIPED all the classifiers performed well with the MLP and decision tree approach achieving the highest levels of accuracy. As already discussed in relation to GCP creation, while the GCPs used in this instance for verification were different from those used for classification purposes they were both derived from a

common set of ground truth data and It would seem reasonable to assume that this would increase accuracy above what would be achieved with a truly random set of verification points. With this in mind the relatively poor performance of the PIPED classifier should perhaps be considered even more significant.

Table 5-5 shows a similar summary of error matrix results assessed for accuracy against the set of GCPs produced using the random stratified sampling scheme. Compared to values in Table 5-4 there is a noticeable reduction in accuracy scores. While every effort was made to produce GCPs as accurately as possible it should be remembered that in this case they were produced without direct ground truth data and therefore it is possible that some level of error may be present in the classification of GCPs themselves, which in turn could theoretically lead to an underestimation of accuracy. Results are again ranked from highest to lowest Kappa value from right to left. The decision tree classifier is notable in having the highest accuracy scores followed by the MLP classifier that also scores noticeably higher than the other methods. The PIPED classifier again comes last achieving an extremely low level of accuracy.

With the exception of the poorly performing PIPED classifier Appendix 3 (Tables 10-1 to 10-9) provides full error matrices for each classification method tested with accuracy assessed against the GCPs created using the stratified randomly sampling scheme. In the case of the decision tree classifier (Table 10-1) the largest cause of error was between bare ground and urban areas with a considerable number of bare ground areas wrongly classified as urban. As would be expected with two classes that are similar in their spectral response there was some degree of error between tree and crop areas with trees wrongly classed as crops and crops wrongly classed as trees in roughly equal proportions. The MLP classifier (Table 10-2) also had problems classifying bare ground as urban areas as well as tree areas as crops, and overall had slightly lower accuracy scores in these areas compared with the decision tree approach. The remaining classifiers (Tables 10-3 to 10-9) had similar issues but with increasing severity.

Table 5-4: Summary of error matrix results for each of the 10 classification methods. Accuracy assessed against GCPs derived from ground truth data collected in the field.

	MLP	Decision tree (current study)	MAXLIKE	CTA	SOM	ARTMAP	KNN	LDA	MINDIST	PIPED
Overall error (95% confidence interval)	0.0176 (0.0075)	0.0243 (0.0088)	0.0260 (0.0090)	0.0327 (0.0101)	0.0327 (0.0101)	0.0361 (0.0106)	0.0487 (0.0122)	0.0605 (0.0135)	0.0630 (0.0138)	0.2049 (0.0229)
Overall Kappa	0.9782	0.9699	0.9679	0.9596	0.9595	0.9555	0.942	0.9396	0.9219	0.7490

Table 5-5: Summary of error matrix results for each of the 10 classification methods. Accuracy assessed against GCPs produced using a stratified random sampling approach in association with careful inspection of ETM+ composites and high resolution true colour imagery.

	Decision tree (current study)	MLP	ARTMAP	KNN	MAXLIKE	LDA	SOM	MINDIST	CTA	PIPED
Overall error (95% confidence interval)	0.1955 (0.0291)	0.2193 (0.0303)	0.2556 (0.0320)	0.2737 (0.0327)	0.2779 (0.0328)	0.2863 (0.0331)	0.2933 (0.0333)	0.2989 (0.0335)	0.3017 (0.0336)	0.5642 (0.0363)
Overall Kappa	0.762	0.7326	0.6894	0.6677	0.6604	0.6532	0.6448	0.6372	0.6306	0.3436

Figure 5-7 shows the resulting land cover layers from the decision tree and MLP classifications. The relative areas occupied by each class within Bangladesh are compared in Figure 5-8. The decision tree classification results in a greater proportion of the total area allocated to the bare ground, trees, and mixed land and water classes, while the MLP classifier assigns a greater area to the crops and urban classes with the difference in the case of the urban class being particularly striking. The areas classified as water is similar for both methods. Comparing the two images in Figure 5-7 and focusing specifically on the northwest quarter of the country there is a significant amount of land classed as urban by the MLP classifier, and as bare ground by the decision tree method. In reality most of this area is not urbanised to the extent suggested by the MLP classifier and highlights the difficulties that the classifiers encountered in separating the two classes. Another notable difference can be seen in the Sundarban area in the south west of the country where when compared to the MLP classifier the decision tree approach classes much more of the mangrove area as mixed vegetation and water rather than trees. In this case, since much of the area is a tidal ecosystem, both classifications could be argued to be correct.

Figures 5-9 to 5-12 focus on some specific areas within Bangladesh in more detail to allow for a visual comparison to be made between the classification methods. Along with the two classified images a true colour high resolution image is also shown. The date of the true colour imagery is unknown although it most likely represents the dry season due to the higher probability of cloud free images being obtained. Regardless of when the true colour image was obtained the important point to consider is that the classified images are not meant to represent exactly what is seen in the true colour image. Observation of the true colour image can provide some useful insight into features less likely to change over time such as trees, urban areas and river channels, and open areas that may represent bare ground, crops, water, or mixed land and water depending on conditions at the time. Figure 5-9 shows Barisal and its surrounding area. In these images the decision tree classifier can be seen to produce a larger urban area as a result of designating a greater area as belonging to either the bare ground or urban classes and then using the lower resolution population density dataset to split the two. The decision tree classifier also shows a greater area of tree cover although the overall pattern of distribution is similar between the two methods and when compared to the true colour image both appear to represent the overall pattern of tree cover quite accurately. Figure 5-10 shows Khulna and its surrounding area. Again, the decision tree classifier shows denser tree cover as well as the effect of the lower resolution population density data. Some degree of striping is also evident in

this area as a result of the gap filling process that was required for the SLC-off ETM+ data. It is worth remembering that the gaps were filled using data recorded from a period between 6 and 8 years before that of the primary image and it is possible that land cover may have changed in that time. This is especially true in the case of the mixed land and water areas that will change over a relatively short time in response to weather, as well as in relation to seasonal patterns and inter-annual variability. Figure 5-11 shows an area in southwest Bangladesh that contains a significant area of ponds and which borders on the Sundarbarns. As is the case with all the images discussed thus far the distribution of water appears very similar between the two classification methods. The distribution of the mixed land/water class also appears fairly consistent between the two methods in the areas examined with exception been here in Figure 5-11 where some of the mangrove area is classified as mixed land/water by the decision tree classifier and as tree cover by the MLP method. Figure 5-12 shows the area around Dhaka where the image produced by the decision tree approach can again be seen to show a trend for more tree and bare land coverage compared to the MLP classifier. Water and land/water areas are very similar in both images while the effect of the lower resolution population density used by the decision tree classifier is manifested by the blocky appearance of the urban class.

****

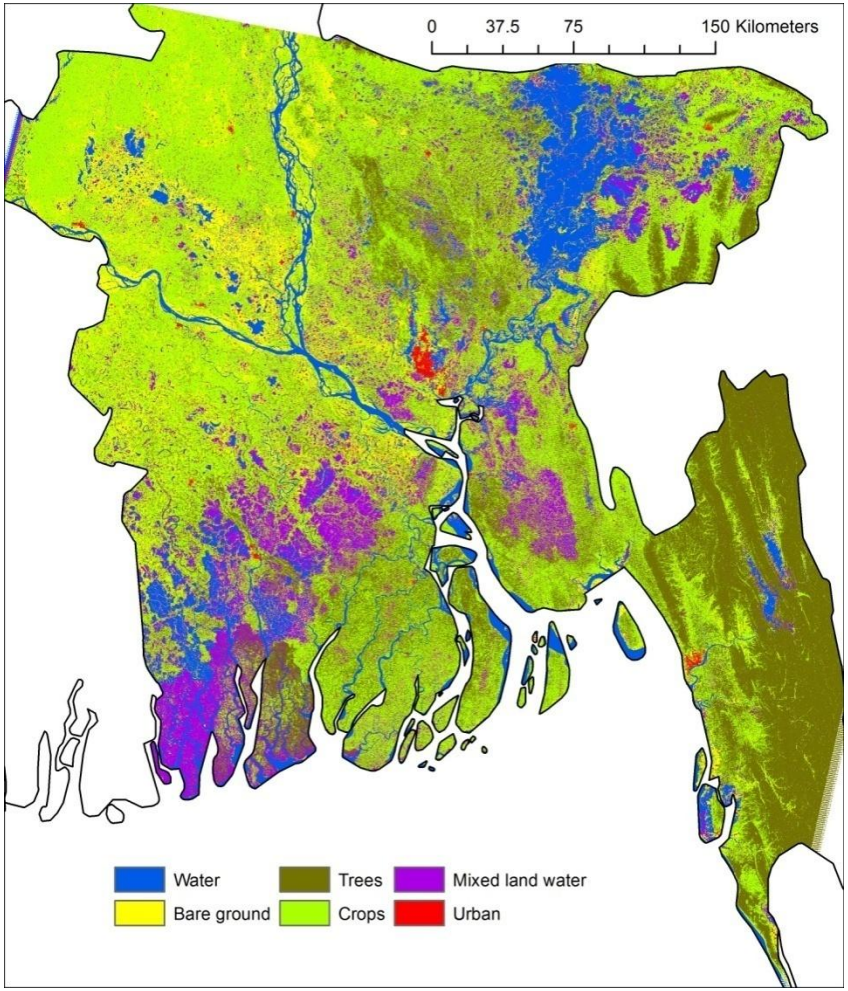

Decision tree classifier.

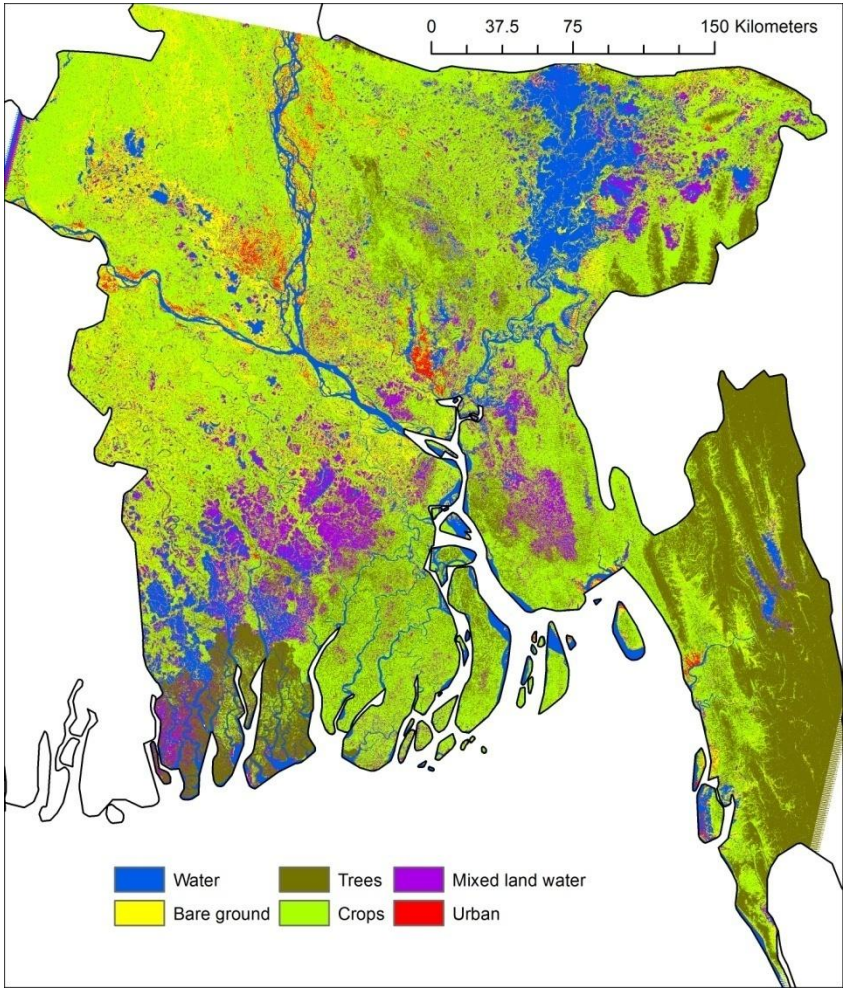

MLP classifier.

Figure 5-7: Comparison of decision tree and MLP classifier outputs.

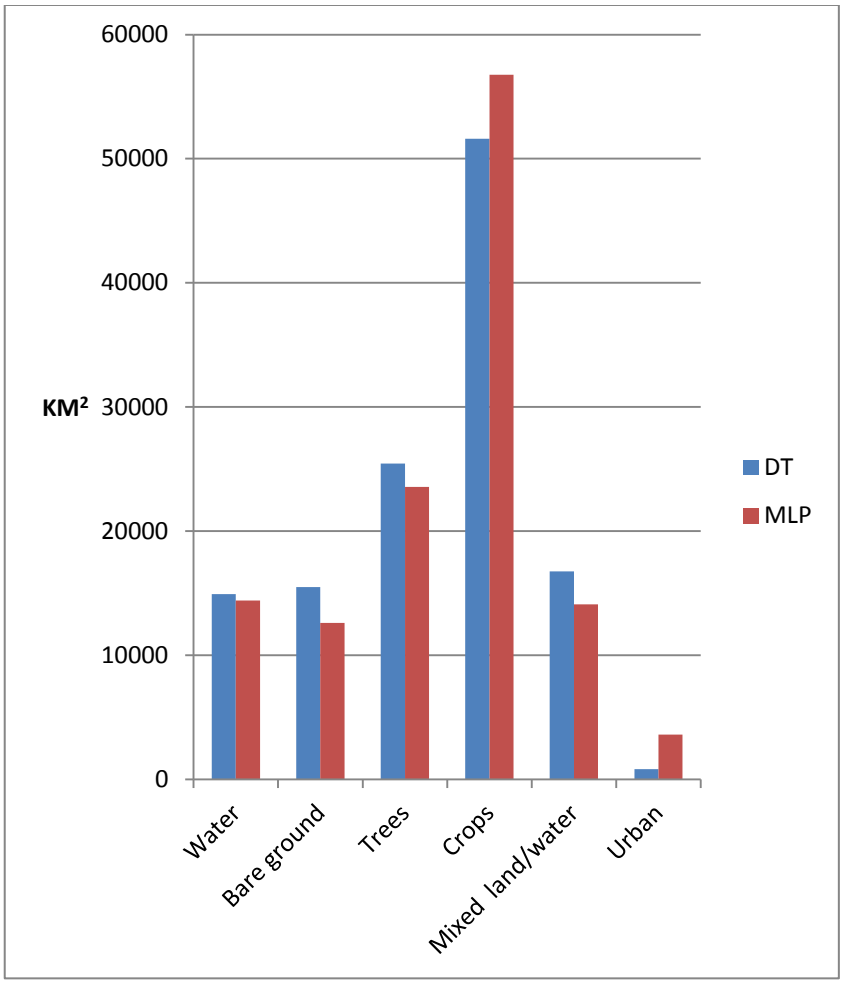

Figure 5-8: Differences in area (km2) covered by the six land cover classes produced by the decision tree and MLP classifiers.

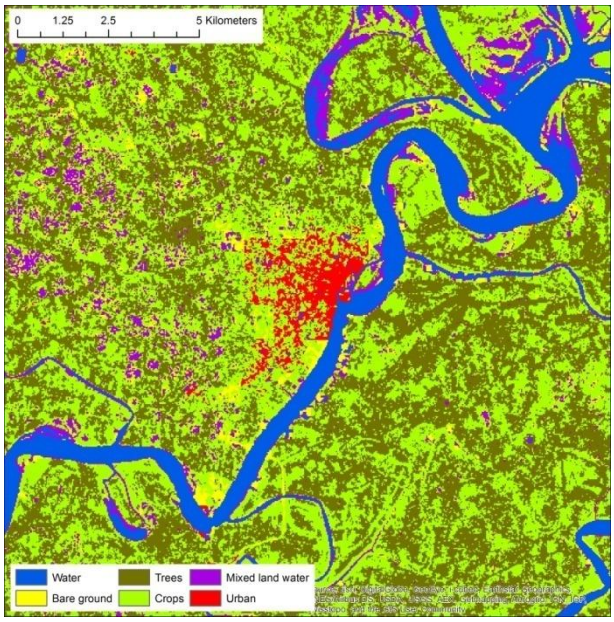

Decision tree classifier

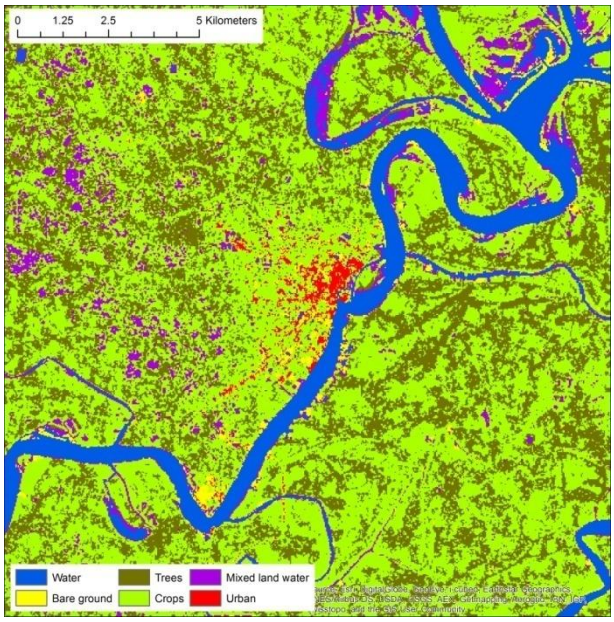

MLP classifier

True colour image (ESRI base map). Date unknown.

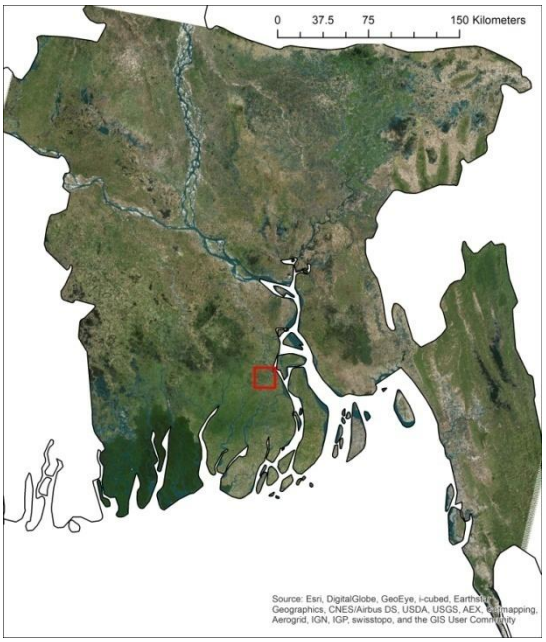

Location of area shown

Figure 5-9: Comparison of decision tree and MLP classification results for Barisal and surrounding area.

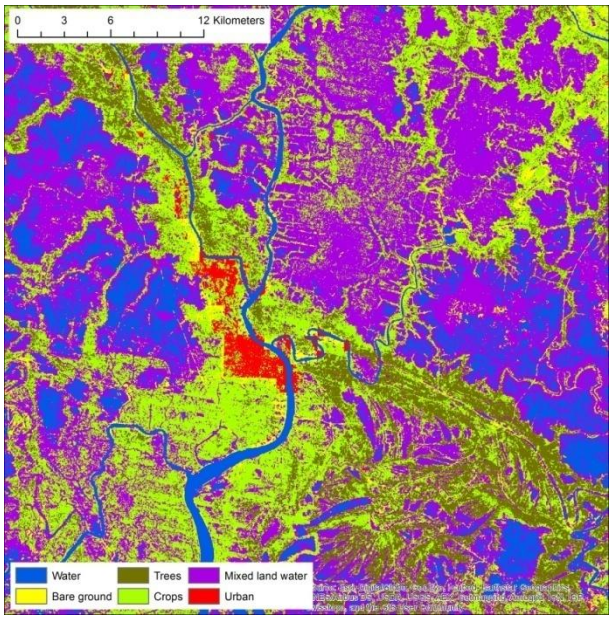

Decision tree classifier

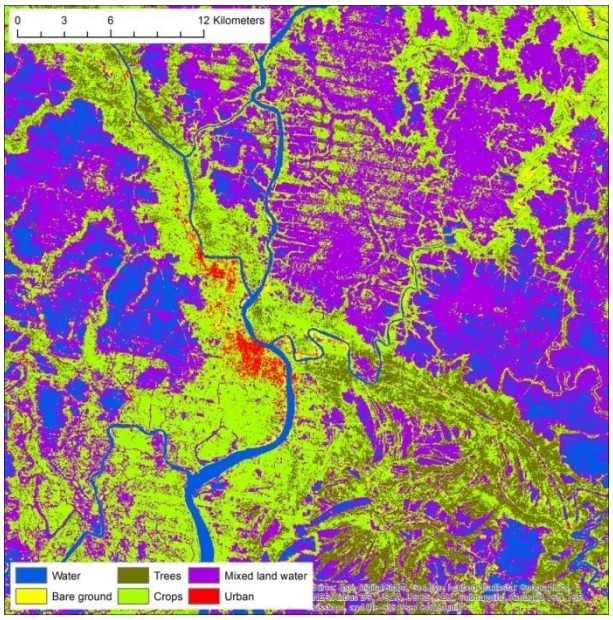

MLP classifier

True colour image (ESRI base map). Date unknown.

Location of area shown

Figure 5-10: Comparison of decision tree and MLP classification results for Khulna and surrounding area.

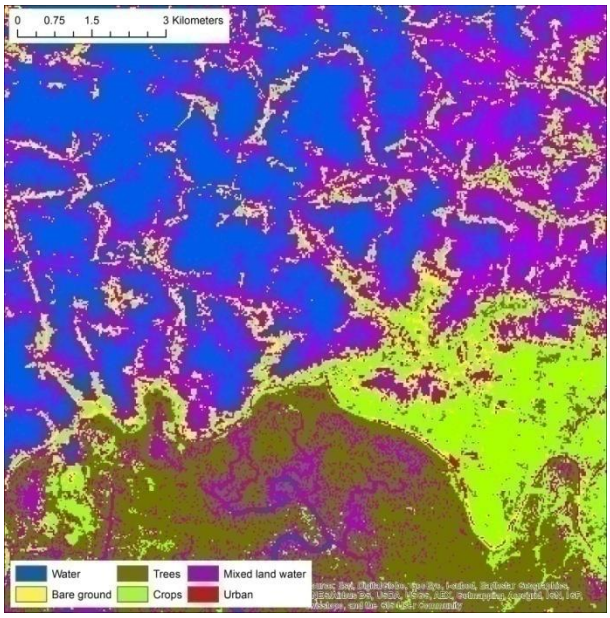

Decision tree classifier

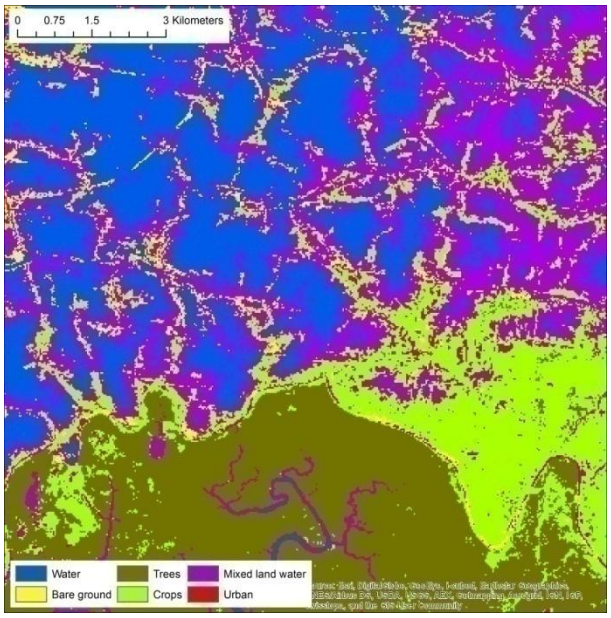

MLP classifier

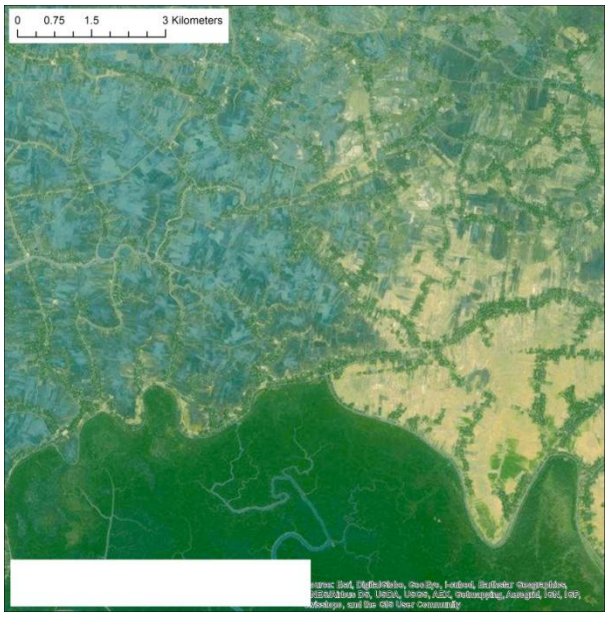

True colour image (ESRI base map). Date unknown.

Location of area shown

Figure 5-11: Comparison of decision tree and MLP classification results for an area in southwest Bangladesh showing ponds and the edge of the Sundarbans.

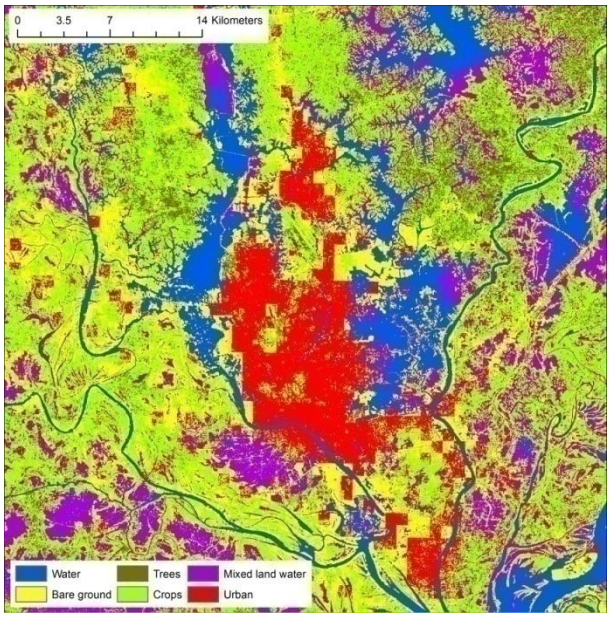

Decision tree classifier

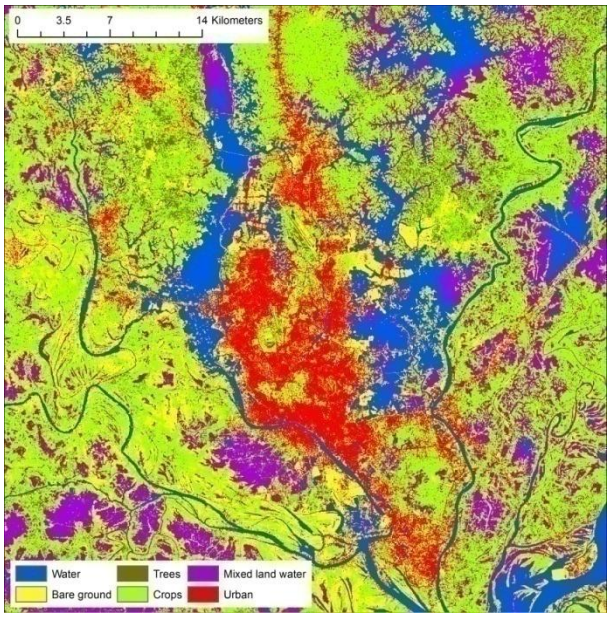

MLP classifier

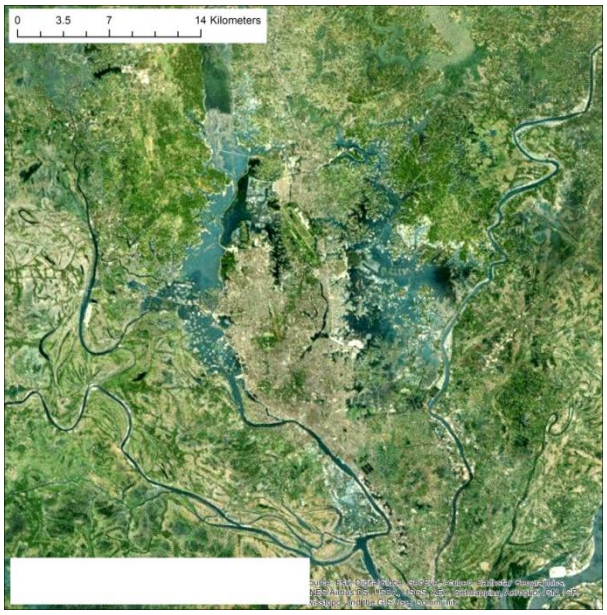

True colour image (ESRI base map). Date unknown.

Location of area shown

Figure 5-12: Comparison of decision tree and MLP classification results for the Dhaka area.

5.4 Discussion

Remotely sensed data have seen a moderate amount of use within the Bangladesh region for classifying land cover, with its application often focusing on using images from different dates as a means of detecting change. Giri et al. (2007) used a series of images spanning a number of Landsat missions to investigate potential change to the Sundarbans between 1975 and 2000 with the conclusion that on the Bangladesh side at least there had been very little change. Redowan et al. (2014) used Landsat Thematic Mapper (TM) data from 1988 and 2010 to investigate change in forest cover in the Khadimnagar national park, Sylhet, Bangladesh. The authors used a simple 3 class system (dense forest, medium dense forest, and bare) in association with a supervised classification method (maximum likelihood). In terms of classification accuracy Redowan et al. (2014) report Kappa values of 0.75 and 0.8 for the 1988 and 2010 images respectively although it should be noted that the sample size for ground control points was extremely small with a total of 13 and 16 points used for the two classifications. Dewan and Yamaguchi (2009a) used a maximum likelihood classifier along with post classification refinement to classify Landsat data (MSS, TM and ETM+) in order to investigate land use and land cover change for the Dhaka area. A six category system that is relatively similar to the one used in the current study (bare soil/land, built-up, cultivated land, vegetation, water bodies, and wetlands/lowlland areas) was used to classify land cover for the years: 1975 1992 and 2003. Kappa values of 82.7, 87.5 and 87.9 are given for the three classifications although full confusion matrices are not provided. The authors state that a stratified random sampling method was used although the total number of sample points used for accuracy assessments were somewhat moderate at 125 for the 1975 and 1992 images and 100 for the 2003 image.

Remotely sensed data have been incorporated into a range of GIS models with the aim of guiding site selection for aquaculture. For example Karthik et al. (2005) used a land cover product derived from data obtained by the LISS III instrument aboard the Indian IRS 1D satellite when modelling site suitability for brackish water aquaculture in Palghar Taluk, Thane district of Maharashtra, India. Giap et al. (2005) incorporated SPOT data when modelling shrimp farming potential in Haiphong, Vietnam. Within Bangladesh Hossain et al. (2007) used ASTER data as part of a GIS-based land-suitability model for tilapia farming in Sitakunda Upazila, Chittagong, Bangladesh. Hossain et al. (2009) and Hossain and Das (2010) conducted similar exercises using ASTER data and focusing on carp species and giant prawn (*Macrobrachium rosenbergii*) respectively. Unfortunately the methodology described by

Hossain et al. (2007), Hossain et al. (2009), and Hossain and Das (2010) is somewhat lacking in detail. Salam et al. (2003) used Landsat TM data when assessing land use as part of GIS model designed to evaluate site suitability for the development of crab and shrimp aquaculture in south western Bangladesh.

A notable feature of the studies outlined thus far in relation to remotely sensed data use within Bangladesh, as well as its broader use in relation to aquaculture site suitability assessments, is that the focus has been on localised study areas. Use of remotely sensed data at the national scale for Bangladesh has been fairly limited. Islam and Sado (2000a) used three Advanced Very High Resolution Radiometer (AVHRR) images that covered a period of 21 days to analyse the extent of Bangladesh's extreme flood event of 1988. Islam et al. (2010) used a MODIS time series along with a methodology originally described by Sakamoto et al. (2007) to examine flooding patterns within Bangladesh. In terms of country wide mapping of multiple land cover classes Giri and Shrestha (1996) used AVHRR data with its relatively low resolution at nadir of approximately 1.1km to produce land cover layers and examine changes in cover between the periods 1985–86 and 1992–93. For higher resolution land cover mapping over the entire Bangladesh region the only work in the peer-reviewed literature relates to the recent efforts to produce a Landsat-derived global 30m resolution land cover product. Gong et al. (2013) described the development of a global land cover map at 30m resolution based on Landsat TM and ETM+ data. The authors tested four classification methods: maximum likelihood, the J4.8 decision tree classifier, the random forests ensemble classifier, and the support vector machine (SVM) with the SVM found to be most effective with an overall classification accuracy of 64.89%. Yu et al. (2013) refined the dataset through the use of a segmentation approach to allow the integration of data sets at varied resolutions including: MODIS EVI time series data, Bioclimatic variables (1km) (Hijmans et al., 2005), global DEM (1km) (Hijmans et al., 2005), Soil-water variables (1km) (Trabucco and Zomer, 2010, Zomer, 2007, Zomer et al., 2008). The result when assessed using the same verification points as Gong et al. (2013) had an improved overall accuracy of 67.08%. Yu et al. (2014) have attempted further improvement by aggregating the two land cover products of Gong et al. (2013) and Yu et al. (2013) with two low resolution maps indicating impervious surfaces: Night time Light Impervious Surface Area (Elvidge et al., 2007) and MODIS urban extent (Schneider et al., 2009, Schneider et al., 2010). Figures 5-13 to 5-15 show results for the whole country and the Dhaka area from the three classifications described above. Results from the decision tree used in the current study are shown for the same Dhaka area for comparison purposes (Figure 5-16). The images in

Figure 5-14 (Yu et al., 2013) appear to show an increase in cropland, bare land, and water areas (much of which represents seasonal water within Bangladesh) with reduced forest area when compared with Figure 5-13 (Gong et al., 2013). The classification output from the aggregation approach shown in Figure 5-15 (Yu et al., 2014) has some of the Dhaka area classified as impervious/urban while this is missed by the previous two classifications. When viewing the country as a whole a noticeable feature of all three classifications shown in Figures 5-13 to 5-15 is the sudden transition between adjacent Landsat images with quite different classification seen from one scene to the next. This may well be a consequence of applying a common classification method to images obtained at different times over what is a temporally dynamic landscape. Alternatively it may highlight a need for improved atmospheric correction methods and standardisation between images. The different classification schemes, and lack of knowledge in terms of acquisition dates for the images used, preclude formal accuracy assessment of the images shown in Figures 5-13 to 5-15 against the GCPs constructed for the current study. However, careful visual inspection suggests some degree of inaccuracy beyond that created by differing Landsat scenes, part of which seems to be a result of clouds and associated shadow. The production of an accurate global 30m land cover product would be highly useful and such efforts should be strongly supported however in view of the outlined issues the land cover data sets described by Gong et al. (2013), Yu et al. (2013), and Yu et al. (2014) clearly require further refinement when applied to Bangladesh.

The maximum likelihood classification (MAXLIKE) is a very commonly used routine for classification of remotely sensed data and has been suggested as superior to other methods where classes have normally distributed data(Bolstad and Lillesand, 1991, Dewan and Yamaguchi, 2009a, Dewan and Yamaguchi, 2009b) However in the case of the current study it was outperformed by a number of classifiers when tested against the randomly distributed sample points. From the pre-existing classification routines investigated the MLP classifier stood out as producing the best results. One feature that was noted for the MLP routine was that running the process more than once with identical inputs would produce slightly different results due to the random initialization of weights used in the 'learning' process.

The decision tree approach developed for the current assessment outperformed all the pre-existing classification routines when tested against the randomly distributed GCPs. While part of this success is likely as result of the careful inspection of the spectral response of individual, and combinations of,

ETM+ bands in relation to GCPs, there was also the inclusion of additional geographic information in the form of the Landscan (2008) gridded population data set.

Inspection of the error matrices for the various classification routines used showed that the largest cause of error was confusion between the bare land and urban classes, and the crop and tree classes. In both cases this can be considered a result of the variable nature of each class in terms of spectral response with considerable overlap between the two. The issue of overlapping spectral patterns from differing land cover is a common one and it is in these instances that the rule based inclusion of additional data, such as the population density data set in the current study, within a GIS can be especially useful. Such processes are often described in terms of post classification refinement and are fairly common in the literature (e.g. Dewan and Yamaguchi, 2009a, Manandhar et al., 2009, Rozenstein and Karnieli, 2011, Shalaby and Tateishi, 2007). Unfortunately in the case of the current study potentially useful geographic data at the national scale was lacking. Elevation data and values derived from it such as those relating to slope and runoff are potentially useful sources of data for classification refinement in many areas (e.g. Sesnie et al., 2008). Gridded elevation values can be obtained as a globally consistent data set with 90m resolution in the form of the Shuttle Radar Topography Mission (SRTM) product (Jarvis et al., 2008). The use of these data as part of a land classification process was investigated. However much of Bangladesh is extremely flat to the point that much of the variation in elevation values seen can be accounted for by ground based objects such as tree canopies. The result was that obtaining meaningful indicators relating to land cover was not found to be feasible.

The use of multi-temporal data have received attention as a means to potentially improve land cover classification based on the assumption that many land use practices such as crop production have seasonal cycles with associated variation in reflectance. For example (Zhang et al., 2008) used a one year MODIS-based time series along with land surface temperature and slope values to classify land cover over the North China plain. The methodology involved noise reduction of the MODIS time series via harmonic analysis and subsequent classification into 100 classes using a self organising ISODATA routine. A rule-based decision tree based on time series EVI values along with information provided by the ancillary data were then used to group the ISODATA output into a smaller number of classes representing land cover. Mingwei et al. (2008) used unsupervised ISODATA as well supervised maximum likelihood classification routines on a Fourier transformed one year time series of MODIS

NDVI data at an 8 day temporal resolution to identify crop areas and crop type in northern China. Wardlow et al. (2007) demonstrated the ability of a 12 month time series of MODIS EVI and NDVI data with a 16 day temporal resolution to differentiate between crop types in Kansas, USA. Wardlow and Egbert (2008) used MODIS based 250m resolution NDVI time series in conjunction with a a hierarchical classification approach that made use of an unsupervised ISODATA routine as well as a commercially available decision tree based classifier (See5) to map crops in Kansas, USA. Brown et al. (2013) used the same classifier (See5) in association with MODIS vegetation index data to map cropping patterns over a five year period in Mato Grosso, Brazil. The authors compared classifications using both EVI and NDVI data with no significant difference in accuracy found between the two data sets. Carrão et al. (2010) used a stack of 6 bimonthly MERIS scenes in combination with a supervised classification routine (Linear Discriminant Classifier) to map land cover over Portugal. Van Niel and McVicar (2004) compared methods for using multi date ETM+ images to classify crop type (4 potential classes) in an area of New South Wales, Australia. The authors used maximum likelihood classification to classify scenes from 17 dates throughout a one year period. The authors compared classification results from a single scene with those obtained from two routines using data from multiple time points: a) an iterative approach where the best performing classification of the 17 scenes was identified. That crop area was then masked out and the 17 scenes were analysed again based on the remaining three potential crops where again the best performing classification was used. The process was repeated for a third time for the two remaining crop species. b) All 7 spectral bands from the three scenes identified during the iterative process were combined into a single image stack which was then analysed with the same maximum likelihood classifier. The two methods were also tested with a reduced number of bands for each scene (bands 3,4, and 5). Overall the iterative process was found to outperform the image stack. The authors note that applying the iterative method to situations where individual crops are not identified with a high degree of accuracy the care consideration would be needed in relation of propagating errors from one iteration to the next. A similar iterative approach was applied by Turker and Arikan (2004) when using ETM+ to identify and map crops in Karacabey, Turkey.

The use of multi-temporal data for classifying land cover in Bangladesh and similar regions is a potentially interesting area for future research with the aim of improving accuracy and the amount of information provided by land cover assessments with the ultimate goal of gaining significant understanding of land use as well as land cover. The success of such approaches will be highly

dependent on the availability of cloud free images at multiple dates with accompanying quality ground truth data, requirements that in the Bangladesh context are likely to be challenging due to the often intricate nature of land use and the potential for considerable year on year variability in response to flood patterns. The methodologies in the examples above can be broadly grouped into three categories: 1) applying a classifier to a stack of scenes from multiple time points either directly or using transformed data, 2) iterative approaches, and 3) rule based decision trees constructed based on knowledge of the region and land use practices. While these three approaches are certainly not mutually exclusive and all may be useful in a Bangladeshi context, it is suggested here that the incorporation of a rule based approach may be a good place to start in situations where land cover data have been produced as part of wider assessments and where particular land cover and use scenarios are considered significant.

Another area that has received considerable attention in recent years is object based classification of remotely sensed data (e.g. Blaschke et al., 2014, Myint et al., 2011, Whiteside et al., 2011). Whereas traditional classification methods treat pixels individually, object based classifiers typically group common pixels into segments before using rule based decision processes to classify segments based on features such as shape, texture, reflectance and spatial relationship to other objects. A general requirement of object based classification is imagery with a spatial resolution considerably smaller than the objects being classified (Myint et al., 2011) with much work making use of the current generation of very high resolution sensors. Given the intricate nature of land cover in Bangladesh it would seem likely that data with a resolution considerably higher than that used in the current study would be required for object based classification to be implemented successfully. With this in mind while object based land classification for Bangladesh should be considered as a potential option it may be better suited for more localised endeavours where the use of higher resolution data sets would be more practical.

****

In summary the land cover maps produced for the current study were created with the intention of supporting climate focused GIS modelling of site suitability for inland aquaculture within Bangladesh. However in view of the above discussion in relation to the relative lack of existing land cover data for Bangladesh the land cover layers produced here can be considered unique in terms of covering the majority of the country while at the same time having a reasonable degree of total accuracy (80.45%

in the case of the decision tree approach) resulting from thorough ground truthing. As such they can be considered as a highly useful source of spatial data that can be integrated into spatial databases with the potential to play a valuable role in addressing a range of spatial questions and contributing to modelling exercises that require a land cover component.

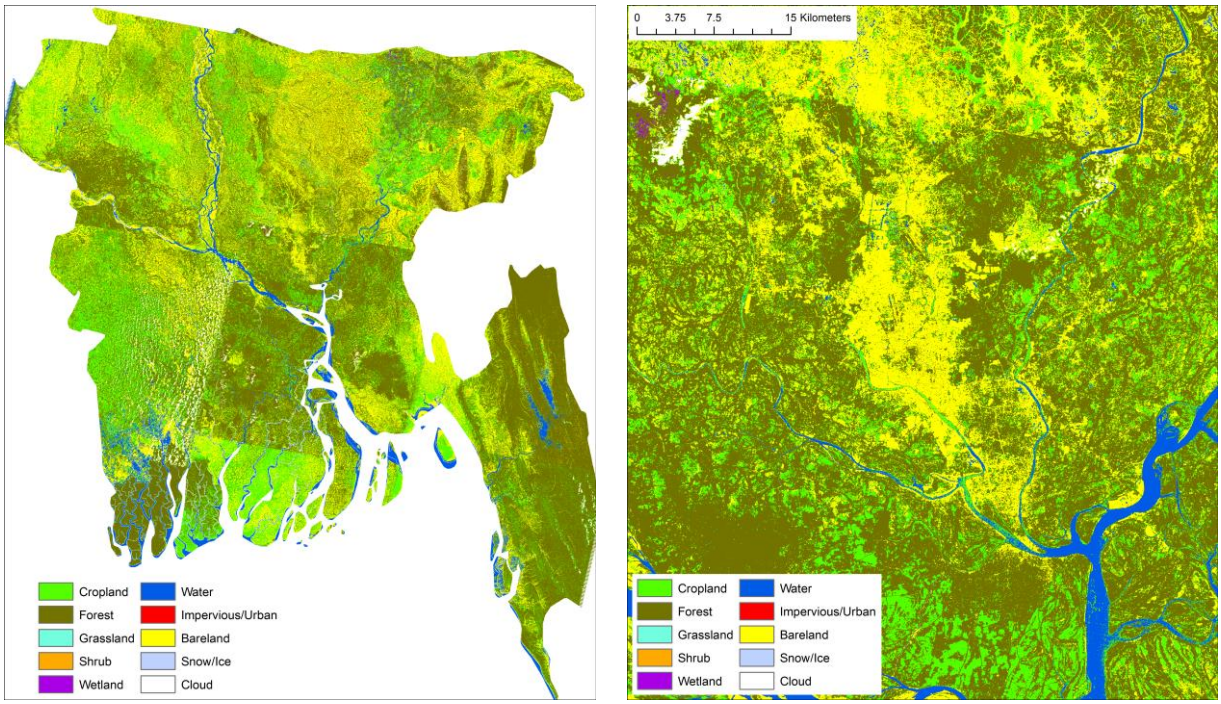

Figure 5-13: Land cover for Bangladesh and focused on the Dhaka area. Data source: Global 30m land cover data set as described by Gong et al. (2013).

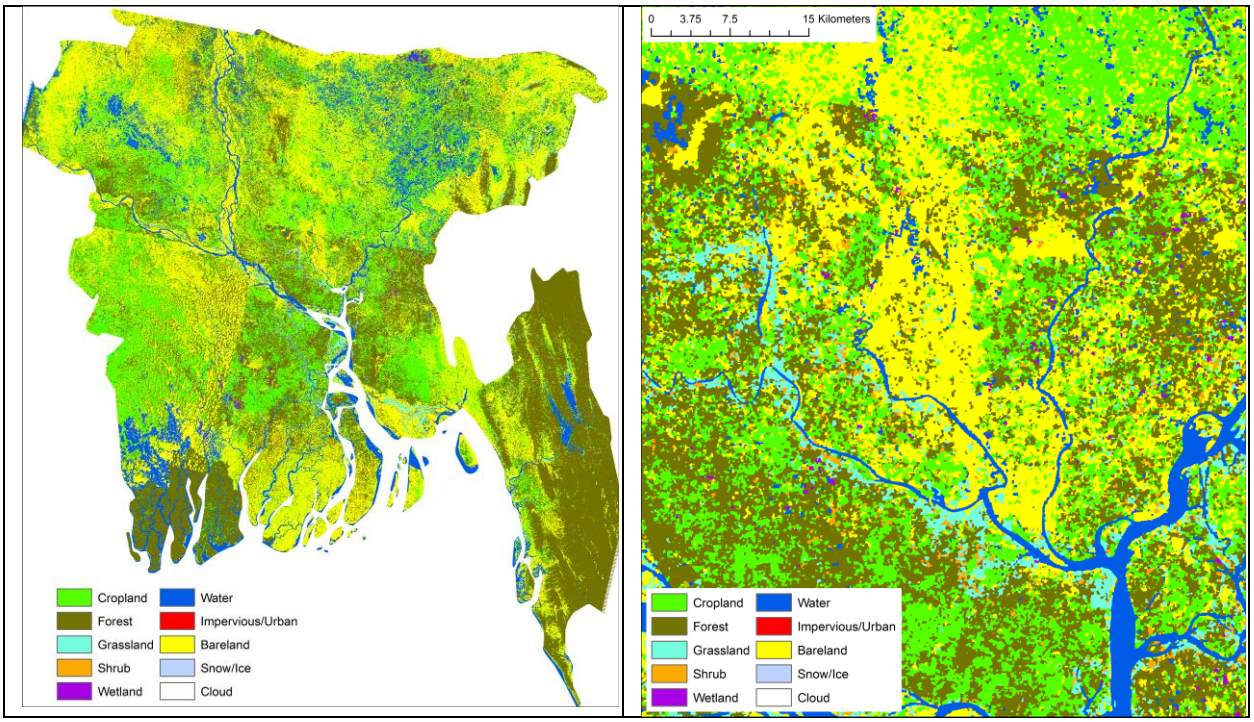

Figure 5-14: Land cover for Bangladesh and focused on the Dhaka area. Data source: Global 30m land cover data set as described by Yu et al. (2013).

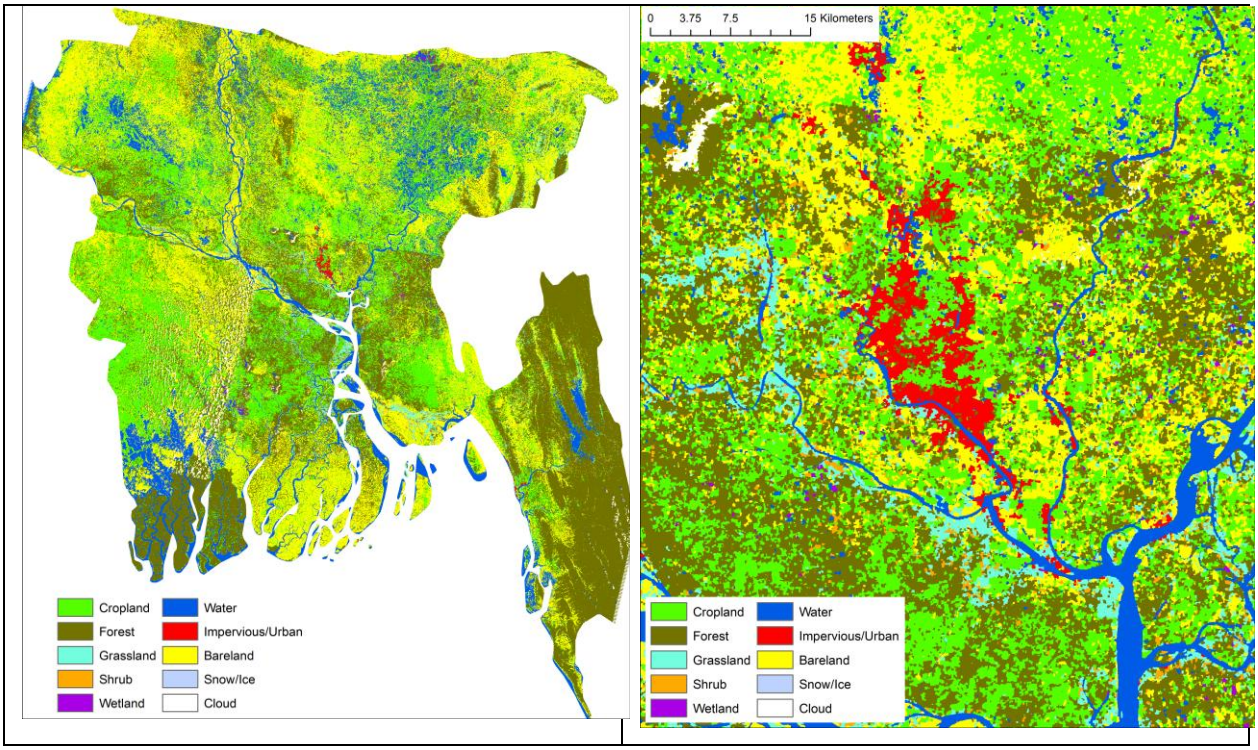

Figure 5-15: Land cover for Bangladesh and focused on the Dhaka area. Data source: Global 30m land cover data set as described by Yu et al. (2014)

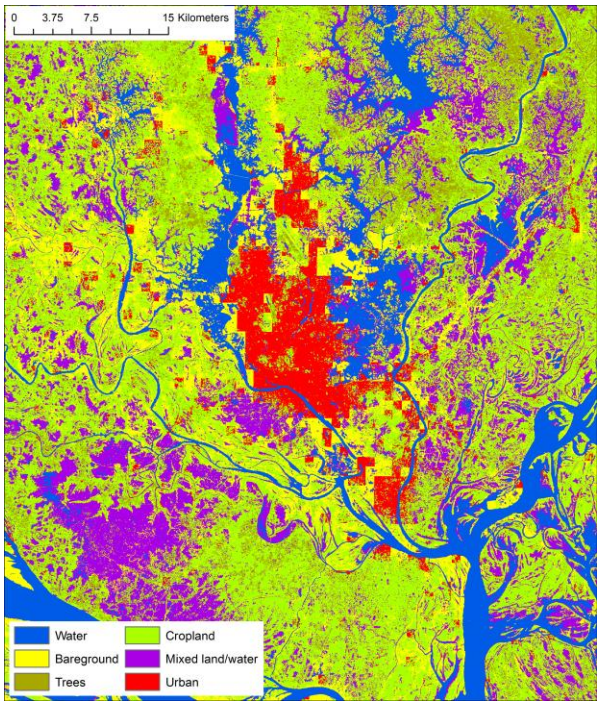

Figure 5-16: Land cover for the Dhaka area using the decision tree classifier described in the current study. For comparison with figures 13 to 15.

6 CLIMATE RELATED SITE SUITABILITY FOR AQUACULTURE – A CASE STUDY FOR BANGLADESH

6.1 Introduction

Bangladesh is the developing world's most densely populated country with approximately 1203 people per square kilometre in 2013 (World_Bank, 2014b). The total population of Bangladesh has increased steadily with an annual growth rate of over one percent during the last decade (World_Bank, 2014b). While projecting future population growth is challenging a range of projections produced by the United Nations Population Division (United_Nations, 2014) give a median projection of total population peaking at just over 200 million around the year 2060. Higher estimates suggest a more substantial increase while even under the lowest estimate population is projected to increase considerably beyond where it is today (Figure 6-1).

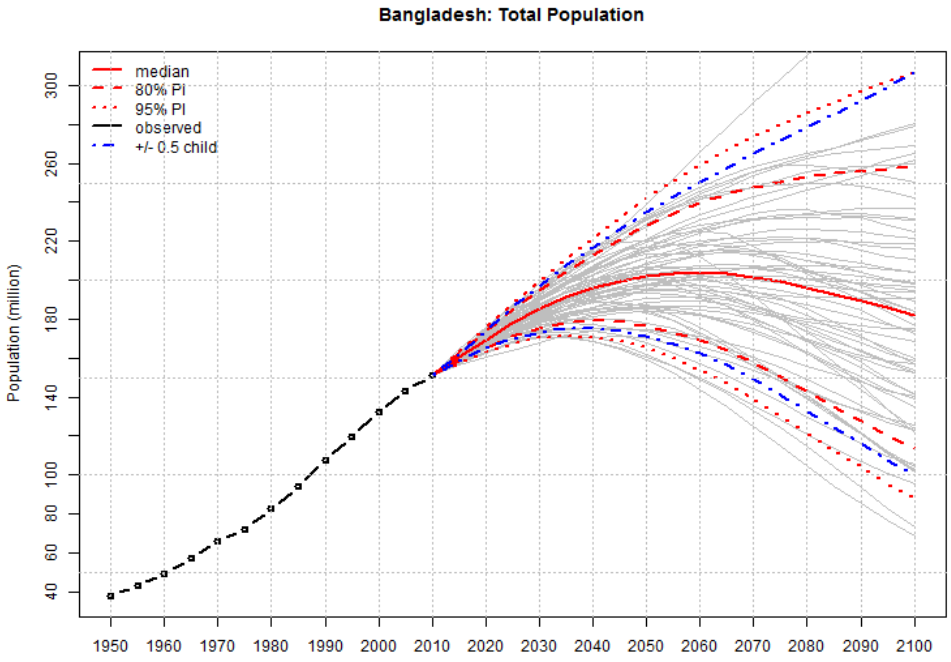

Figure 6-1: Projected population growth for Bangladesh.

Bangladesh can also be considered financially poor with an estimated 43.3% of the population living on less than 1.25USD per day as of 2010 (World_Bank, 2014c). As may be expected given a dense and poor population issues of food security are not uncommon. The Food and Agriculture Organisation (FAO) estimates that 16.7% of the population can be considered undernourished, a figure that has remained relatively static over the last decade (FAOSTAT, 2014).

Average fish consumption in Bangladesh is approximately 20kg per capita per year and accounts for more than half of total animal protein intake (FAO, 2012). Capture fishery production in Bangladesh is strongly linked to annual flooding with many small indigenous fish species being a popular food source. Fish also represents an important source of micronutrients in diets often lacking in diversity and as such can be viewed as highly important in terms of food security (Belton et al., 2014). Statistics compiled by the FAO and made available via FishStatJ software suggest capture fishery output has declined since 2009 (see Figure 6-2). While it is almost certain that reporting of fish production from both caught and cultured sources will be subject to errors, the view that capture fishery growth is limited or in decline has been supported by a number of authors (Belton et al., 2011, Belton et al., 2014, Halls et al., 2008) with factors such as water management, intensification of agriculture, urban expansion, pollution, and increased fishing effort being cited as contributory.

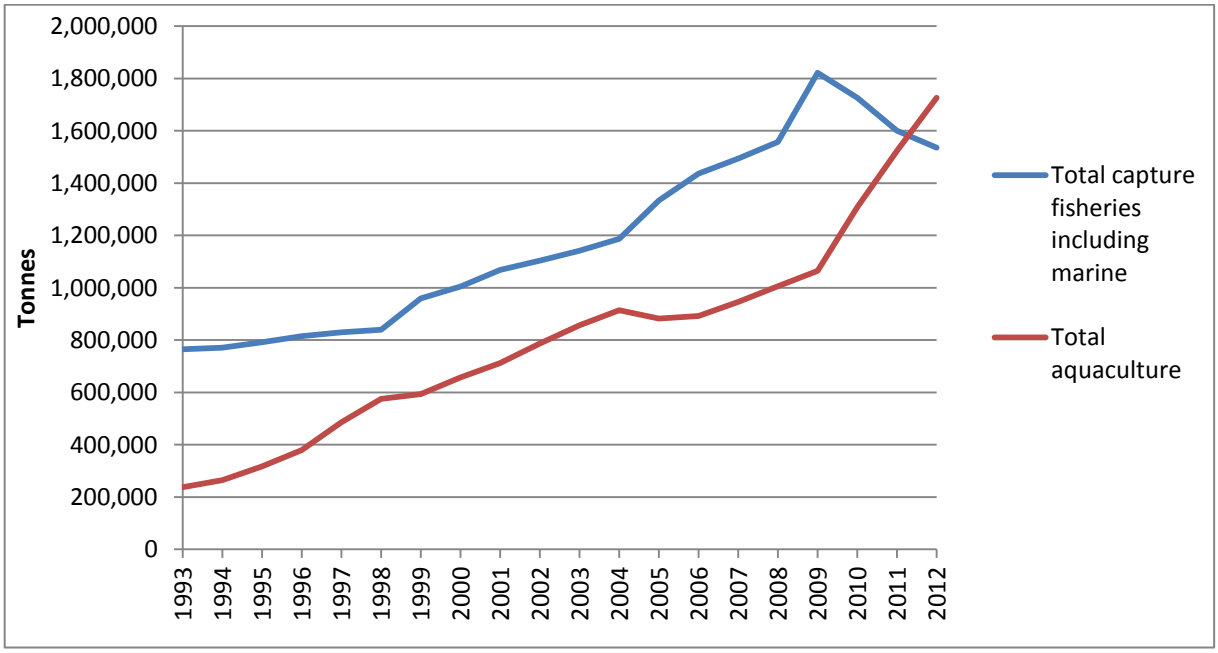

Figure 6-2: Aquaculture and capture fisheries production quantities for Bangladesh.

In terms of percentage growth rate aquaculture production has increased considerably faster than that from capture fisheries over the last several decades, and based on FAO data have exceeded capture fisheries production since 2012 (see Figure 6-2) (FishStatJ, 2014). Belton et al. (2014) analysed changes in fish consumption using data collected by the International Food Policy Research Institute (IFPRI) during the periods 1996/7 and 2006/7. The authors noted that while there had been a shift towards eating more cultured fish among all household income levels the greatest shift had been seen within the poorest quartile of households with farmed fish as a percentage of total fish consumed increasing from 23 to 52 percent. It is also worth noting that total fish consumption had increased slightly among all household groups but the disparity between the poorest and richest households in terms of total fish consumption remained large with annual per capita figures of 10.5 and 33.2kg respectively. Overall, aquaculture would appear to have had a strong positive effect in compensating for reduced capture fisheries production and as such can be viewed as extremely important in food security terms (Belton et al., 2014, Dey et al., 2008, Jahan et al., 2010). There has been suggestion that consideration needs to be given to nutritional quality of aquaculture products when compared to wild alternatives (Allison, 2011, Belton et al., 2014), especially in the case of poorer households where total fish consumption and food diversity is low, and that there may be benefits in promoting the culture of smaller indigenous fish species that are often eaten whole. However, regardless of the species cultured aquaculture would appear to have an increasingly important role to play if fish consumption levels are to be maintained, or increased, for Bangladesh's growing population.

At the national level aquaculture makes a significant contribution to the Bangladesh economy representing approximately 3.37 percent of GDP for 2012 (FishStatJ, 2014, World_Bank, 2014a). Cultured shrimp (*Penaeus monodon*) and giant freshwater prawn (*Macrobrachium rosenbergii*) represent a significant export commodity, only exceeded by the garment industry, with a value of 412 million US$ in 2009/2010 (Belton et al., 2011). At a more localised level aquaculture represents a source of income in rural areas either through self-employment or as hired labour (Dey et al., 2008, Karim et al., 2006). Small scale aquaculture promotion has been demonstrated as a means of enhancing livelihoods within poor communities (Barman and Little, 2011, Barman and Little, 2006) and recent work by Pant et al. (2014) demonstrated livelihood improvement within extremely poor, landless and marginalised communities through the introduction of aquaculture and associated technologies. It has also been suggested that commercial aquaculture may have an important role to

play within Bangladesh by potentially providing more stable employment, either through direct involvement in production or in connection with associated goods and services (Belton et al., 2012).

6.1.1 Aquaculture production systems in Bangladesh

In recent years Bangladesh has seen a move towards more intensified and larger scale aquaculture operations (Belton and Azad, 2012). Figure 6-3 shows production quantities for the years 2008 to 2012 for the 12 highest volume species in terms of weight, while Figure 6-4 shows production for the same species in terms of product value. Data for both graphs was extracted from the FAO FishStatJ database and while the data should probably be interpreted with care it does suggest a number of significant trends: 1) there has been a increase in recorded production for most species, 2) in terms of quantity the Indian and Chinese carp species (*Labeo rohita, Catla catla, Hypophthalmichthys molitrix, and Cirrhinus mrigala*) have dominated production in recent years, 3) As in other areas of Asia *Pangasianodon hypophthalmus*has seen a rapid increase in production in recent times and now represents an important aquaculture species within Bangladesh, 4) the production of crustaceans (*Penaeus monodon* and and *Macrobrachium rosenbergii*) are high value species that represent a major contribution in monetary terms, 5) Tilapia (*Oreochromis niloticus*) have seen a notable increase in production during recent years that along with the increase in *Pangasianodon hypophthalmus* production is likely related to increasing interest in more intensified and commercially orientated aquaculture practices.

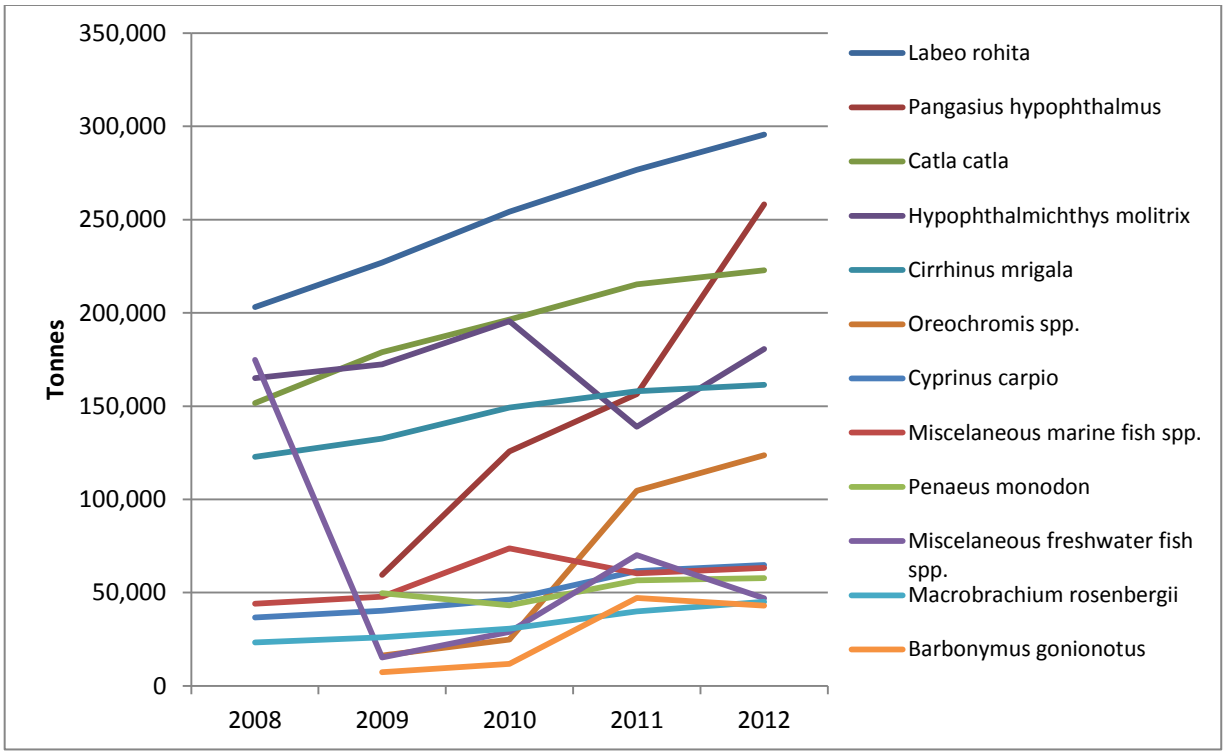

Figure 6-3: Aquaculture production quantities for most commonly cultured species in Bangladesh.

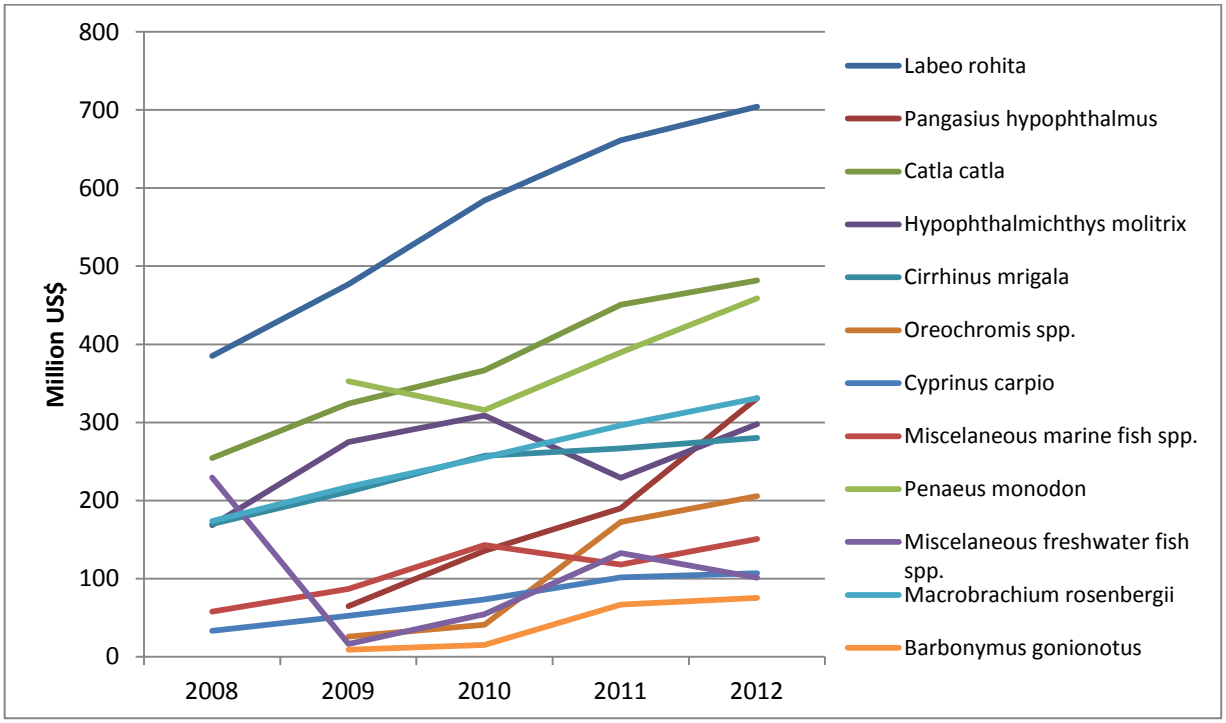

Figure 6-4: Aquaculture production value for most commonly cultured species in Bangladesh.

At it's most basic level aquaculture in Bangladesh takes the form of homestead ponds that are often formed when soil is removed in order to create a raised area on which houses can be built with some resistance to flooding. Such ponds are typically small with average areas of between 0.08 and 0.1 hectares (Belton and Azad, 2012) and often serve multiple purposes such as washing and watering livestock. Traditionally such ponds were often allowed to fill with fry of native species during the flood season that were then left to grow with little if any input. However a number of development projects have encouraged improved management of such ponds through practices such as deliberate stocking of selected species at appropriate densities and application of feeds and fertilizer. The result has been a considerable improvement in yields (Belton and Azad, 2012, Belton et al., 2011) with some evidence suggesting that carp species are most common (Bloomer, 2012).

Larger commercial aquaculture operations generally take place in purposely constructed ponds that most often comprise of converted rice fields although the enclosure of other natural water bodies is also practiced. Such operations typically make use of pelleted feeds with the main culture species being pangasius and tilapia (Belton et al., 2011) although other species including carps, prawn, and shrimp (in areas nearer the coast) are also produced in such systems. Pangasius grow-out from fingerlings generally takes between 7 and 10 months (Belton et al., 2011, Griffiths et al., 2010) with the main growing season running from March to September. Farms with better financial capital are likely to grow fish for longer in order to obtain a better market price and in such cases harvesting may be as late as December (Belton et al., 2011). Tilapia produced by commercial pond-based operations are often harvested at a relatively small size (200-300g) which can be achieved after a 3-4 month grow-out period potentially making 2 cycles a year possible (Anwar, 2011, in Belton et al., 2011).

Aquaculture is also conducted by making use of Bangladesh's extensive seasonal floodplains. Embankments are constructed to retain flood waters creating large culture areas in the region of 50-100 hectares which are then stocked with a range of indigenous and exotic species that are then cultured with the aid of added fertilisers and feed. During the dry season a crop of irrigated rice can also be grown (Gregory et al., 2007). Some questions have been raised with regard to the loss of access by subsistence fishers and potential impacts of stocking non native species. However there would seem to be significant benefits of such systems to local economies as a result of improved fish

yields in the region of 1-3 t/ha/year, a figure approximately 10 times that of unstocked floodplains (Belton et al., 2011, Gregory et al., 2007).

Combined rice and fish culture has the potential to provide an extra cash crop in the form of harvested fish while the fish themselves may provide additional benefits including: supply of nutrients, release of nutrients from sediments, and control of pests and weeds (Ahmed and Garnett, 2011). Methods involve the improvement of embankments surrounding rice fields and the creation of deeper refuge areas where fish can congregate during times of limited water. Rice and fish may be cultured at the same time and depending on water availability fish may be stocked either for the aman (rain fed summer rice) season only, or both the summer and winter (boro) rice crops. An alternative method is to alternate between mono crops of boro rice and then fish during the summer wet season (Belton et al., 2011). The most common species stocked are Indian and Chinese carps along with tilapia and silver barb (*Barbonymus gonionotus*) (Belton et al., 2011), while the use of freshwater prawn (*Macrobrachium rosenbergii*) with small native species has also been successfully trialled (Kunda et al., 2008).

The majority of shrimp (*Penaeus monodon*) farming takes place in the southwest of Bangladesh in ghers (converted rice fields) found on very low lying land often protected from the sea by a system of polders. The area consists of a complex network of tidal channels that are often connected to shrimp ghers through a series of canals and sluice gates. Due to the saline nature of the ground water in many of these areas the opportunity for traditional agriculture, especially during the dryer parts of the year when salinity is higher, can be limited making culture of brackish water species an attractive option. Giant freshwater prawn (*Macrobrachium rosenbergii*) are also cultured in ghers and in practice there is considerable cross over between the on growing stages of the two species in terms of salinity tolerances and the species may be cultured together along with salt tolerant fish species (Belton et al., 2011, Wahab et al., 2012). While shrimp and prawn may coexist simultaneously they may also be cultured in seasonal rotation. Such systems are for a large part determined by salinity which is in turn influenced by the wet and dry seasons as well as land elevation and distance from the sea. During the low salinity period (August to December) the inclusion of prawn and freshwater fish species is likely to be more common as well as the culture of aman rice in some instances (Belton et al., 2011). Freshwater prawn are typically stocked in May/June and harvested from November to January (Ahmed et al., 2008, Hasanuzzaman et al., 2011). Shrimp grow out periods are generally

quicker depending on harvest size, intensity of culture, and feed input with grow out ranging from 3.5 to 6 months (Kongkeo, 2005).

Land cover in Bangladesh varies considerably both spatially and seasonally, and is strongly influenced by annual flooding that on average covers 20.5% of the country while in the extreme case of the 1998 flood around 70% of the country was inundated (Mirza, 2002). As already highlighted Bangladesh has an extremely dense, and growing, population that places considerable strain on available land in terms of its agricultural and fisheries resources. Another potentially significant factor is that of changing climate and its influence on temperature and precipitation regimes as well as sea level. Given the increasing significance of aquaculture, both as a source of food and income, an understanding of which areas may be most suitable for further aquaculture promotion and development should be seen as highly useful. The potential of geographic information systems (GIS) as a means of assessing and modelling site suitability for aquaculture has been discussed earlier. Chapter three also contain an overview of climate change and its potential impact on aquaculture along with the description of the use observed values, weather reanalysis data, and modelled future projections to model pond temperature and water balance under late 20th century conditions, as well for a 2°C mean global warming scenario. These components along with the MODIS-derived surface water time series (chapter four), and the Landsat ETM+ derived land cover data (chapter five) are used here to investigate site suitability for pond-based aquaculture in Bangladesh including consideration of changing climate conditions. Issues surrounding sea level rise and tropical storms are also discussed and MODIS time series data is used to show storm surge inundation resulting from cyclone Aila which hit Bangladesh on the 25th May 2009.

6.2 Methods and data

6.2.1 Land cover and associated aquaculture systems

As described earlier, remotely sensed data from the Landsat Enhanced Thematic Mapper Plus (ETM+) instrument was used to produce a land cover data layer for Bangladesh with a six class classification scheme. The land cover data were derived from 9 ETM+ scenes obtained between dates 31-10-08 and 09-11-08 which represents the transition from the wet to dry seasons (see Figure 6-5 for average monthly precipitation over the whole of Bangladesh). The use of a single time period, and the specific

dates, for which Landsat was obtained was dictated by the need to coincide with the collection of field based ground truth data. That said, the time period in question can be considered favourable in that it represents a transition from wet to dry. For example, areas classified as mixed water and vegetation are quite likely to be wetland areas that would have experienced deeper flooding during the peak of the wet season but are now drying out and will probably become totally dry during the dry season.

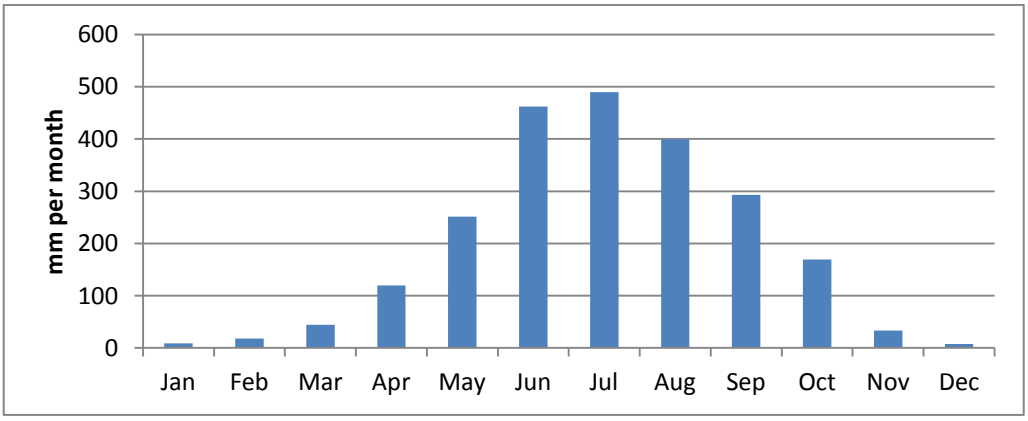

Figure 6-5: Average monthly rainfall over the whole of Bangladesh. Derived from the CRU CL2.1 data set(New et al., 2002).

Chapter four describes the development of a Moderate Resolution Imaging Spectroradiometer (MODIS) based time series that classifies pixels as being either: land, water, or mixed. The time series, which spans a 14 year period and consists of 654 images, was analysed to produce two summary layers: one showing the percentage of the total time series where water is indicated, and the other showing the percentage of the time series where water or mixed land cover is indicated. These time series results are used here in combination with the ETM+ based land cover data to obtain greater insight into the seasonal nature of land cover than would be possible using the single time point ETM+ derived data alone. Table 6-1 summarises the process of combining the two data sets in order to produce a new classification that indicates where different aquaculture methods may be considered in relation to other variables e.g. population density and temperature.

Table 6-1: The combination of ETM+ based land classification and MODIS time series surface water data to create a new 6 class system based on potential aquaculture scenarios.

Landsat ETM+ derived land cover classes	Assumptions based on land cover type being present at the beginning of November, and potential land cover scenarios throughout a typical year	Incorporation of MODIS-derived time series data showing the percentage of the available time series where land is classified as being covered by water, or both mixed and water. In the case of areas indicated as having tree cover Shuttle Radar Topography Mission (SRTM) data is used to calculate slope values in order to differentiate forested hill areas .	Potential aquaculture scenarios. Numbers indicate membership of one of six classes.
Cropland	The majority of crops at this time of year are likely to be aman rice which is planted from the end of May to September and harvested in November and December. It is likely that such areas don't normally experience prolonged periods of deep flooding and are probably fields that are used year round for a number of crops. Such fields can be considered for conversion to fish ponds, or fish/rice type systems.	Water < 2.5 % Likely to represent areas of fields with potential year round use with a relatively low risk of flooding.	Areas where conversion of fields to pond aquaculture or combined fish/rice culture could be considered. (1)
		Water>2.5% Likely to represent areas of fields with potential year round use with an increased risk of flooding.	Areas where conversion of fields to pond aquaculture or combined fish/rice culture could be considered but in an area with a greater risk of flooding. (2)
Bare land	There is little in the way of permanent bare land in Bangladesh. At the time period over which the Landsat data were collected areas indicated as bare land are most likely to represent areas of recently harvested or planted crops, or areas that have recently	Mixed and water > 25% Assumed to represent areas that have recently dried out after wet season inundation and may be used for winter crops or pond culture.	Could be considered for seasonal floodplain aquaculture. May also be some potential for more traditional pond culture outside of the wet season. (3)

	dried out after being covered in water during the wet season.	Mixed and water <25% water <2.5% Assumed to represent recently harvested or planted areas. Given the time of data collection recently harvested aman rice would be most likely with fields then prepared for winter vegetable crops or boro rice.	Potential for conversion of fields to pond aquaculture or combined fish/rice culture. (1)
		Mixed and water <25% water >2.5%	Potential for conversion of fields to pond aquaculture or combined fish/rice culture but in an area with a greater risk of flooding. (2)
Trees	With the exception of hilly areas in the west of the country and a few forests, areas indicated as having tree cover tend to small and represent areas of homes and associated homestead ponds. *Shuttle Radar Topography Mission (SRTM) elevation data at 90m resolution was used to calculated slope values. The resulting slope values were filtered using a 5x5 cell mean to reduce noise associated with vegetation of differing heights in otherwise flat areas.*	Slope < 5%	Areas of homes and where the potential for increase in the number and/or efficiency of homestead ponds can be considered. (5)
		Slope > 5% These areas were assumed to represent areas of forest in the hilly areas in the west of the country where population density is low and aquaculture would not be practical.	Areas considered unsuitable for aquaculture. (6)
Water	Areas indicated as water could be: 1. Aquaculture ponds. 2. Flooded fields - ready for boro rice planting or from recently harvested aman - unless vegetation is really	Water <40% Assumed to be temporary water areas associated with wet season flooding .	Areas could be considered in relation to floodplain aquaculture methods in association with receding water levels. (4)

	sparse and there is lots of water these may well show up as mixed. 3. Permanent water e.g. rivers, natural ponds and lakes, and canals. 4. Semi permanent water still standing from wet season that will dry up at some point as the dry season progresses. In this situation given that water is still present at the start of the dry season it is likely that water is present for at least two or three months in these areas.	Water>40% Assumed to be permanent or semi permanent areas of water where water is present for a large part or the year and is likely to be deed during the wet season.	Considered unsuitable for aquaculture. (6)
Mixed water and vegetation	Based on careful inspection of MODIS time series outputs it seems that mixed areas largely represents areas that are drying after wet season flooding. There may be some flooded cropland but not much. There may also some small areas of genuine mixed pixels that represent a fairly permanent situation e.g. vegetation at the edge of a river or canal.	Mixed and water<30%	Areas could be considered in relation to floodplain aquaculture methods in association with receding water levels.. In this cases the areas indicated maybe those where flooding is less deep and prolonged. (3)
		Mixed and water >30% < 60%	Areas could be considered in relation to floodplain aquaculture methods in association with receding water levels. (4)
		Mixed and water> 60%	May represent areas of permanent mixed water and vegetation, or areas where flooding is present for much of the year. Assumed to be unsuitable for aquaculture.(6)
Urban			13. Considered unsuitable for aquaculture. (6)

6.2.2 Pond temperature

Pond water temperature is determined by pond design and a range of climatic variables including: solar radiation, air temperature, humidity, and wind speed. From an aquaculture perspective water temperature regimes are highly significant in terms of: a) growth performance, both in terms of specific growth rate, and food conversion efficiency, and b) survival rates of culture organisms which may be impacted acutely if temperature exceeds a species thermal limits, or chronically as a result of stress related increases in disease susceptibility.

6.2.2.1 Suitable temperature ranges for pond aquaculture in Bangladesh

The investigation of critical thermal maxima and minima (CT_{max} and CT_{min}) under laboratory conditions has been completed for a range of aquaculture species. Animals are typically acclimated at a constant temperature (e.g. for 30 days) and then subjected to a steady increase or decrease in temperature (e.g. 0.3°C per minute) until loss of equilibrium is observed. High acclimation temperatures generally result in higher CT_{max} and CT_{min} values while lower acclimation temperatures tend to lower CT_{max} and CT_{min}. CT_{max} and CT_{min} values from a number of studies for relevant species are summarised in Table 6-2. Rakocy (2005) suggests minimum and maximum temperature tolerance of 11-12°C and 42°C for Nile tilapia (*Oreochromis niloticus*) while Hassan et al. (2013) cites Ernst et al. (1991) and suggests that Nile tilapia will not survive below 10-12°C for more than a few days. While critical thermal maxima and minima are relatively easy to establish in the laboratory they are not generally directly applicable to pond aquaculture situations where temperatures are liable to change at slower rates and persist for longer periods. Although laboratory based investigation of chronic lethal temperature values for fish species are less common, Beitinger et al. (2000) cites Fields et al. (1987) and notes that for the North American largemouth bass (*Micropterus salmoides*) heating at 1°C per day compared with 0.2°C per minute resulted in upper lethal temperatures between 1.8 and 3.6°C lower for the slow heating regime. In the case of ponds within Bangladesh extremes of high and low temperatures will almost certainly take place during the respective warm and cold seasons and thus from a critical thermal tolerance perspective animals are likely to be relatively well acclimatised.

From a site suitability and pond temperature modelling perspective the use of critical thermal tolerance data as outlined above is perhaps most applicable in relation to temperature extremes that may be experienced during brief periods of unusually hot or cold weather. Perhaps more applicable in

the case of average temperature regimes are studies that consider survival rates for animals cultured at different temperatures along with measures of growth performance such as specific growth rate (SGR) and food conversion ratio (FCR). Key outcomes from a number of such studies for relevant culture species are outlined in Table 6-3.

In summary, it would appear that the optimum culture temperature for common aquaculture species in terms of growth performance can be considered be from the upper twenties to low thirties. At higher and lower temperatures FCR, and in some cases SGR, is reduced indicating increased physiological stress. For the popularly cultured crustaceans laboratory based studies suggest potential impacts on survival when maintained at constant high temperatures.

Table 6-2: Critical thermal maxima and minima for a number of significant aquaculture species.

Species	**Acclimation temperature(°C)**	**CT_{max}(°C)**	**CT_{min}(°C)**	**Reference**
Macrobrachium rosenbergii Values are for juveniles	20	36.5 ± 1.1	10.5 ± 0.3	(Díaz Herrera et al., 1998)
	23	38.4 ± 0.1	11.3 ± 0.1	
	26	39.2 ± 0.8	13.3 ± 0.9	
	29	41.5 ± 1.0	14.6 ± 0.1	
	32	42.0 ± 0.8	16.4 ± 0.7	
Macrobrachium rosenbergii	25	40.73 ± 0.16	14.9 ± 0.13	(Manush et al., 2004)
	30	41.06 ± 0.17	15.4 ± 0.14	
	35	41.96 ± 0.17	16.98 ± 0.21	
Labeo rohita Values are for fry (aprox. 10 - 19g)	26	42.33 ± 0.07	12.00 ± 0.08	(Das et al., 2005)
	31	44.81 ± 0.07	13.46 ± 0.04	
	33	45.35 ± 0.06	13.80 ± 0.10	
	36	45.60 ±0.03	14.43 ± 0.06	
Labeo rohita	25	40.2 ± 0.04	12.9 ± 0.04	(Chatterjee et al., 2004)
	30	41.6 ± 0.08	14.2 ± 0.04	
	35	42.2 ± 0.11	15.0 ± 0.05	
Labeo rohita	26	40.63 7 0.17	13.73 7 0.07	(Das et al., 2004)
	31	41.91 ± 0.22	14.20 ± 0.25	
	33	42.65 ± 0.01	15.00 ± 0.18	
	36	42.86 ± 0.05	15.58 ± 0.06	
Catla catla	26	40.45 ± 0.38	13.92 ± 0.01	
	31	41.39 ± 0.38	14.40 ± 0.03	
	33	42.63 ± 0.02	15.20 ± 0.09	
	36	42.73 ± 0.02	15.63 ± 0.13	
Cirrhinus mrigala	26	42.25 ± 0.14	12.12 ± 0.22	
	31	42.55 ± 0.01	13.70 ± 0.31	
	33	42.76 ± 0.05	13.81 ± 0.22	
	36	43.07 ± 0.08	13.95 ± 0.10	

Table 6-3: Summary of key findings from a number of studies investigating growth performance and or survival of significant aquaculture species in relation to temperature regimes.

Species	Key findings	Reference
Oreochromis niloticus	Investigation of growth performance at 25, 28, 31, 34, and 37°C. Growth performance was found to be best in the 28, 31, and 34°C groups while optimum growth temperature was estimated at 30.1°C with maximum protein retention at 28°C. At 37°C growth performance and protein retention was worse than all other treatments	(Xie et al., 2011)
Oreochromis niloticus	Investigation of SGR and FCR at 24, 26, 28, 30, 32, and 34°C. The best SGR and FCR was at 32°C followed by 30°C, then 28°C, then 34°C, 26°C, and 24°C.	(Workagegn, 2012)
Labeo rohita	Fry reared at 26, 31, 33, and 36°C. The 31°C treatment resulted in the highest SGR and FCR (0.89 ± 0.05 and 1.01 ± 0.01). The 33°C treatment gave results with no statistical difference ($p<0.05$) (0.81 ± 0.02 and 1.02 ± 0.04). The next best in terms of growth performance was the 26°C (0.64 ± 0.02 and 1.32 ± 0.02) with 36°C been the worst overall (0.52 ± 0.02 and 1.59 ± 0.02).	(Das et al., 2005)
Macrobrachium rosenbergii	Investigation of the effects of temperature and salinity on growth and reproduction with salinity set at 0, 8, or 16 ppt and temperature at 24, 29, and 34°C. The lowest salinity treatment performed best at each temperature in terms of final weight of both animals and eggs. In terms of temperature the 29°C treatment performed best with a final weight of prawns in the 0ptt salinity treatment being 40.53±3.707g. This was followed by the 24°C treatment (33.1±2.346g), and then a substantial decrease in the case of the 34°C treatment (16.93±1.76). A similar pattern but with lower final weights was seen at the higher salinity levels.	(Habashy and Hassan, 2011)
Macrobrachium rosenbergii	Similar experiment to that described above with temperatures of 26, 30, and 34°C and salinity values of 0, 6, 8, 12, and 16ppt. In this case growth and egg production was higher at moderate salinities (6 and 8ppt). Overall the 30°C temperature treatment gave resulted in the best growth of animals as well as greatest egg production followed by the 26°C then 34°C treatments.	(Ch et al., 2012)
Macrobrachium rosenbergii	In a guide to freshwater prawn farming New (2002) states the following "Temperature is a key factor. Seasonal production is possible in semi-tropical zones where the monthly average air temperature remains above 20°C for at least seven months of the year. This occurs, for example, in China and some southern States of continental USA. For successful year-round farming, sites with large diurnal and seasonal fluctuations should be avoided. The optimum temperature	(New, 2002)

	range for year-round production is between 25 and 31°C, with the best results achievable if the water temperature is between 28 and 31°C."	
Penaeus monodon	Investigation of survival over a 96 hour period for post larvae at different stages (pl1 and pl15) at temperatures of 29, 33, and 35°C, and salinities of 25, 33, and 35ppt. While salinity didn't appear to have any obvious effect on survival rate temperature did with lower temperature being preferable. The effect was most pronounce in the case of the PL15 larvae and especially at 35°C. Average survival rates for all salinities were as follows: PL1: 29°C = 95.8%, 33°C = 87.1%, 35°C = 69.8%. PL15: 29°C = 70.6%, 33°C = 67.2%, 35°C = 43.1%.	(Chaitanawisuti et al., 2013)
Litopenaeus vannamei	Survival and SGR of postlarvae under a range of temperature and salinity treatments were investigated over a 40 day period with twice daily unlimited feeding. Salinities of 20, 25, 30, 35, 40, and 50ppt were used and for each salinity there where treatments with temperatures of: 20, 25, 30, and 35°C. The authors note that growth was considerably lower at 20°C than at other temperatures. At the higher temperatures (20 and 35°C) growth rate was best but in the case of the 35°C treatment survival rates were considerably reduced at all salinities.	(Ponce-Palafox et al., 1997)

6.2.2.2 Reclassification of modelled pond temperature data

The use of spatially represented climate and weather data based on observed values, weather reanalysis data, and an ensemble of future climate projections to model of pond temperature under late 20th century conditions, as well for a 2°C mean global warming scenario, are described in detail in chapter three. The modelled data takes the form of a time series of daily mean pond temperatures spanning two ten year periods (late 20th century conditions and 2°C average global warming).

For the current assessment the monthly average temperature was reclassified on a continuous scale from least suitable (0) to most suitable (255). Temperatures between 29°C and 32°C were considered most suitable while those below 22°C and above 37°C were considered least suitable. The minimum and maximum temperatures reached during the time series for each month were also reclassified as a means of considering the effects of unusually hot and cold weather events. Figure 6-6 illustrates the suitability classification applied to the mean, maximum, and minimum monthly temperatures. Finally Boolean layers where generated for any areas with temperatures above 37°C or below 16°C as a means of highlighting situations where temperatures may be approaching the critical thermal limits of culture species.

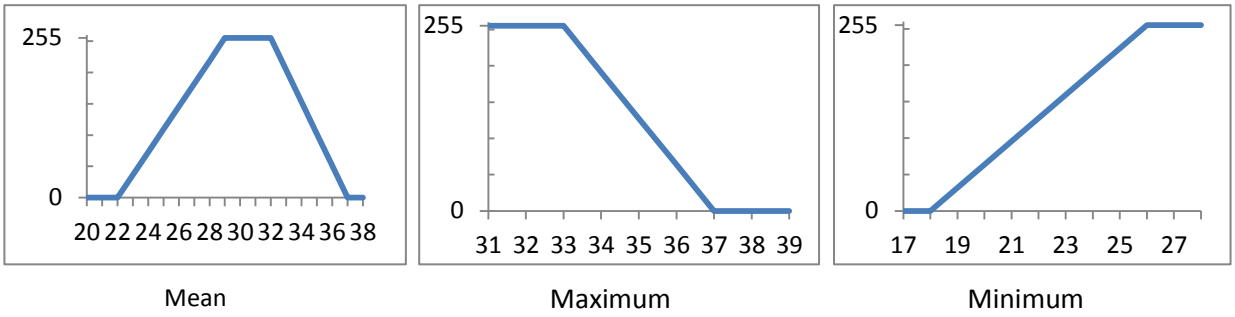

Figure 6-6: Temperature suitability for average monthly temperatures as well as maximum and minimum values reached for each month during the 10 year time series. The horizontal axis shows temperature (°C) while the vertical axis represents corresponding suitability on a scale of 0 to 255.

6.2.3 Precipitation, evaporation and water balance and water balance

As well as estimates of pond temperature chapter three also described the use of historic climate data sets along with climate model output to estimate rates of precipitation and evaporation (from a water surface) under the late 20th century and 2°C warming climate scenarios. Subtracting evaporation from precipitation to obtain a water balance figure provides a useful indicator of water availability for rain fed ponds. Chapter three made use of a number of seepage scenarios in combination with water balance to estimate the likelihood of ponds containing water at a given time of year. Given the nature of extensive surface water coverage in Bangladesh potentially allowing for immediate filling of ponds it seems probable that such a method would often underestimate pond water availability. With this in mind water balance is considered in the current assessment as a means of comparing the relative wet or dryness both spatially and between climate scenarios. This is achieved by normalising the water balance range (lowest to highest values within Bangladesh, including both climate scenarios) over a range of 0-255 to allow combination with other variables using a common scale.

6.2.4 Low elevation coastal zones and associated storm surge flooding

Much of Bangladesh is extremely low lying and essentially consists of the delta areas for a number of major rivers. Many coastal regions employ polder systems; areas of land surrounded by dikes that prevent salt water inundation and thus allow for agricultural activity. Bangladesh experiences relatively frequent tropical storms and cyclones with an average of one severe cyclone every three years (Dasgupta et al., 2010). Such storms often result in storm surges where a combination of extreme low pressure and wind action can cause a temporary dramatic increase in coastal sea level. In the case of Bangladesh surge heights of between 3 and 6 meters are experienced, with theoretical predictions of up to 7.5m (Salam and Ross, 2000), resulting in flooding of low lying coastal areas.

A number of studies have attempted to model potential storm surge impacts on coastal regions in the bay of Bengal under a range of sea level rise and surge height scenarios (e.g. Karim and Mimura, 2008, Lewis et al., 2013). While such efforts should be encouraged they are typically constrained by availability of high quality data, notably that relating to elevation. At a more local scale factors such as the height and quality of dikes surrounding polder areas will be extremely relevant in terms of flood risk, and it is in this respect that a generally unpredictable and constantly changing human element can play a significant role.

While detailed hydrodynamic modelling is beyond the scope of this case study use was made of Shuttle Radar Topography Mission (*SRTM*) data to highlight low elevation coastal zones (LECZ) and thus gain some insight into potential flood risk. SRTM data is available globally with a horizontal resolution of 3 arcseconds (approximately 90m), and a vertical resolution of 1m. An unfortunate characteristic of SRTM data, when compared to high resolution data provided by technologies such as airborne light detection and ranging (LiDAR), is that it is affected by the height of vegetation and other ground based objects (Sanders, 2007). In order to reduce the impact of scattered tree cover on elevation values a mean value 7x7 grid square filter was applied to effectively smooth the data. A cost distance algorithm within a GIS was then adapted to highlight all contiguous pixels with an elevation of 5 metres or less, and 3 metres or less, that have contact with the sea.

6.2.4.1 Visualising the impact of cyclone Aila using MODIS surface water time series

Cyclone Aila made landfall in Bangladesh on the 25th of May 2009 with an associated storm surge height in the region of 2 to 3 metres and resulted in an estimated 3500 casualties (IFN, 2009). A polder area in south western Bangladesh was visited in early October 2009 that was still inundated with saline water resulting in the displacement of a significant number of people.

The MODIS based surface water time series described in chapter 4 is used to demonstrate the extent of flooding throughout coastal Bangladesh in the immediate aftermath of cyclone Aila. The extent of flooding in the polder area is shown in more detail at the time of visit, over 5 months after initial inundation, and compared to its pre-flood state.

6.2.5 Combining factors to assess site suitability

A number of studies have used the combination of varied spatial data sets within a GIS in conjunction with multi criteria evaluation (MCE) approaches to model site suitability for aquaculture within Bangladesh (Hossain et al., 2007, Hossain et al., 2009, Hossain and Das, 2010, Salam et al., 2005, Salam et al., 2003). Such work has focussed on relatively small areas within the country and made use of locally sourced data sets, often involving data collection in the field, that include variables such as: water sources, water quality, local markets, road networks, and location of hatcheries. While in theory such an approach could be expanded to encompass the whole country, in practice there are significant limitations. As discussed in chapter three in relation to global site selection modelling there is a strong need for data used to be consistent across the entire extent of the study area. In the case of Bangladesh the availability of high quality nationwide data is extremely limited. During the current study considerable time was invested in trying to acquire suitably detailed data for highly significant indicators such as road networks and population centres. Ultimately, little was obtained and while some available datasets looked promising initially, checking against high resolution true colour satellite imagery such as that seen in Google earth showed that they were inaccurate and spatially inconsistent.

In common with other GIS site suitability assessments for aquaculture such as those listed above the current study made use of an MCE approach using weighted linear combination. Given the data limitations it is stressed that the aim is not to try to produce a detailed site suitability outcome as

would be expected from localised assessments with a greater body of data to draw on. Instead, the aim is to provide a broad suitability assessment at the country scale with the focus on climate variables that can be overlaid with the ETM+ and MODIS-derived land classification data.

Normalised maximum, minimum and mean temperature suitability values were used along with normalised water balance data was also included. Population density and soil property data that form part of global gridded data sets were included with full details of data sources and reclassification to the 0-255 suitability ranking system described in chapter three. A number of areas were considered as completely unsuitable for aquaculture production and excluded from the final output. These consisted of: Areas with a slope above 3% or an elevation above 30 metres (the vast majority of Bangladesh is extremely low lying and flat and this effectively excluded the hilly forested areas to the east and north where aquaculture potential would be extremely limited), Urban areas as designated by the reclassified ETM+ data, and areas with very high or low population densities (see figure 3-9).

Three different MCE combinations were made using slightly different weightings (Table 6-4) with outcomes geared towards the aquaculture scenario related land classifications produced from the ETM+ land cover and MODIS surface water data.

Table 6-4: Weightings used for MCE.

Site suitability factors	**Weightings**		
	Conversion of fields to pond aquaculture	**Floodplain aquaculture**	**Homestead ponds**
Temperature - mean - normalised	0.3	0.4	0.3
Temperature - maximum - normalised	0.1	0.1	0.1
Temperature - minimum - normalised	0.1	0.1	0.1
Water balance (normalised)	0.2	0.2	0.2
Population density	0.2	0.1	0.15
Soil suitability	0.1	0.1	0.15
Constraints:			
Slope >3%, Elevation >30m, Population density (see chapter 3), Urban areas.			

6.3 Results and discussion

6.3.1 Land cover reclassification

Figure 6-7 shows the result of the reclassification of the Landsat based land cover data using additional input from the MODIS-derived surface water time series and SRTM elevation data to indicate how land cover may relate to different potential aquaculture systems assuming other suitability factors are favourable.

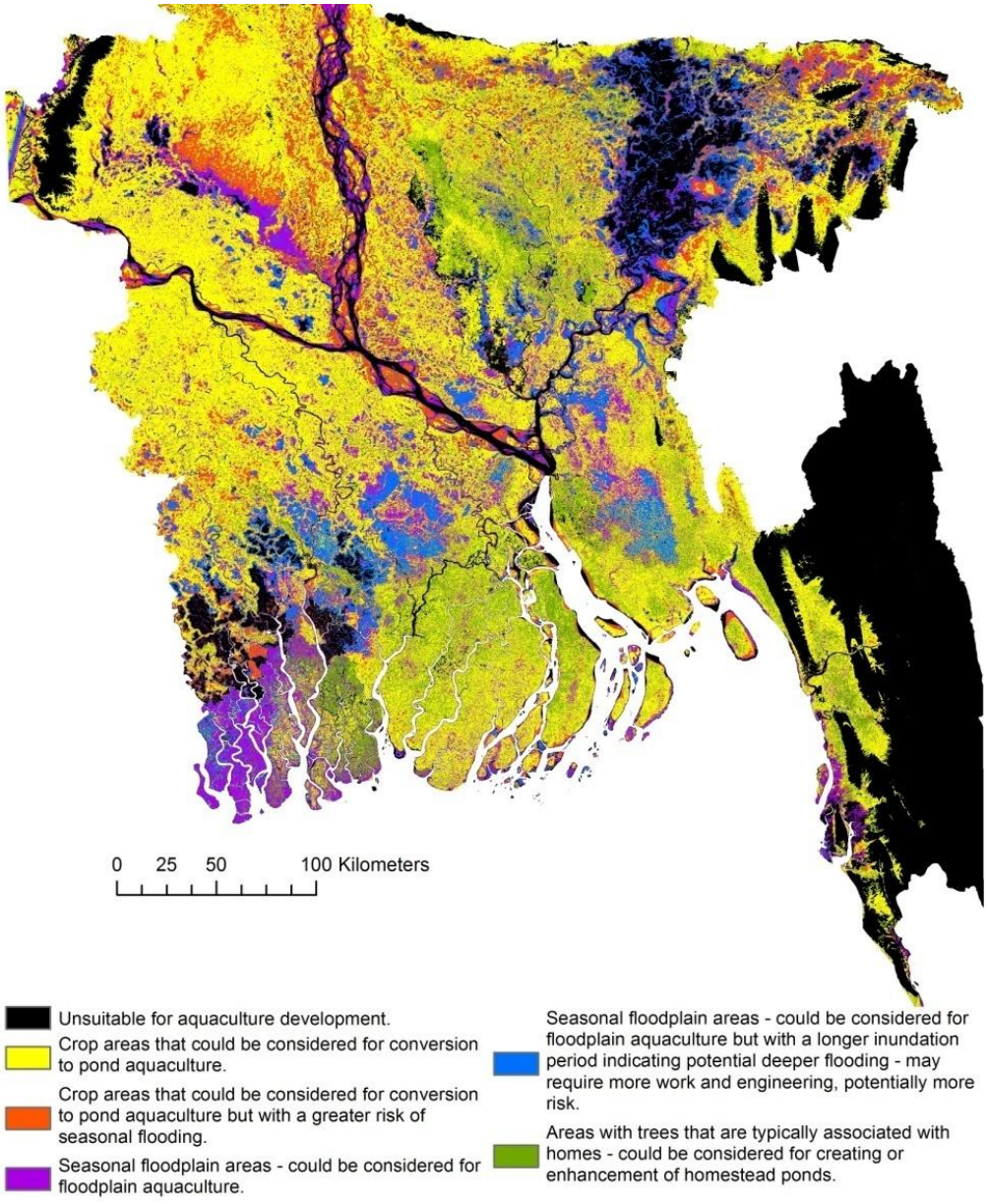

Figure 6-7: Land cover in Bangladesh and how it may relate to potential aquaculture systems.

6.3.2 Temperature suitability

Figure 6-8 shows annual modelled pond temperature profiles for different regions within Bangladesh. It should be noted that temperatures represent daily mean values i.e. mean pond temperature represents the average of all daily mean pond temperatures for a given month during the 10 year time series while the maximum and minimum temperatures represent the single highest or lowest average daily value achieved for each month. From an aquaculture perspective there is also likely to be some degree of diurnal temperature fluctuation taking temperatures beyond the mean daily maximum and minimums presented here and thus potentially placing greater stress on culture organisms. However, as discussed earlier under normal conditions unless a pond is artificially mixed, very shallow, or wind speeds are very high, then there is likely to be a degree of stratification during daytime warming. Studies aiming to model pond water temperature in aquaculture ponds while taking account of stratification have noted temperature variations of around 1 - 3°C in ponds of around one meter deep while surface fluctuation have been much greater (Culberson and Piedrahita, 1996, Losordo and Piedrahita, 1991). The issue of pond depth was highlighted during discussions with aquaculturists in Bangladesh who very much viewed lack of water and high temperatures as a common problem in that temperature related stock losses occurred when water depths were significantly reduced.

In terms of spatial variation areas in the south of the country nearer the coast (Khulna and Cox's Bazar) show the least seasonal temperature variability while Bogra in the north west of the country showed the highest, with both maximum and minimum temperatures exceeding those in other areas. In terms of fish culture potential the southern sites and especially Cox's Bazar in the extreme south east would seem to be most favourable with a considerable part of the year experiencing temperatures in the ideal 28-30°C range whilst maintaining higher temperatures during the coldest part of the year, potentially allowing for better growth performance, and having less in the way of extreme maximum temperatures.

The impact of the 2°C global warming scenario is potentially both positive and negative depending on location and season. In all regions of the country higher temperatures during the colder months

(November to March) would almost certainly have a positive effect in terms of growth performance of commonly cultured species. During the warmest part of the year (June to September) mean temperatures are projected to be in the low thirties in most areas and thus still reasonably favourable, while in Cox's Bazar they are mostly one or two degrees lower. In terms of extremes of temperature directly impacting on production through loss of stock it seems unlikely that minimum low temperatures will be significant for most culture species with the risk continuing to reduce in line with increasing global temperatures. In terms of the short-term impact of maximum temperatures the months of May and June probably represent the greatest risk in situations where ponds are low in water and waiting to be filled during the monsoon period. Under the 2°C warming scenario modelled maximum temperatures range from around 34°C in Cox's Bazar to approximately 37°C in Bogra in the north west of the country. These temperatures in the warmer parts of the country are likely to represent a significant source of stress for many aquaculture species. If factors such as ponds with a limited water depth and thus a greater degree of diurnal temperature fluctuation and other possible water quality issues are considered then it would seem that the potential for damage to stocks during these extreme hot periods could be considerable.

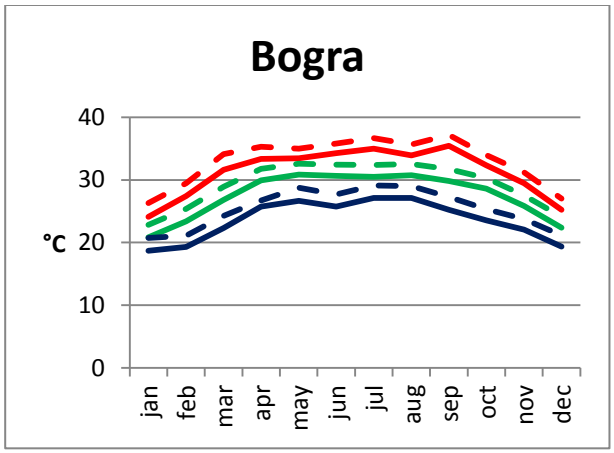

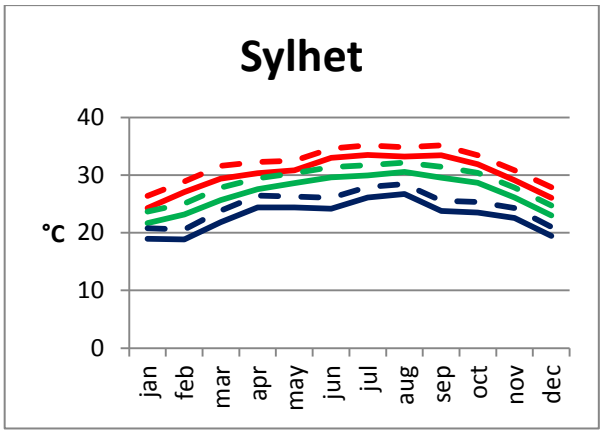

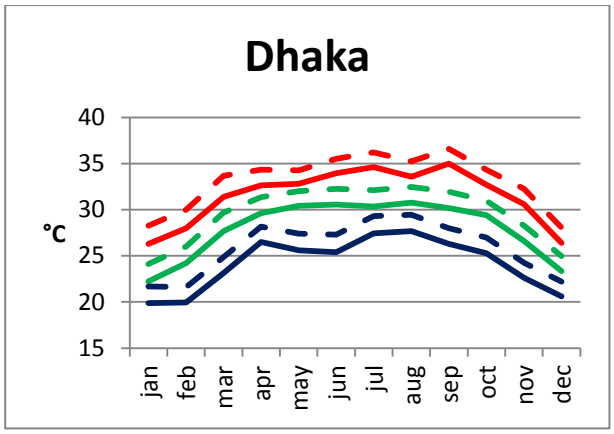

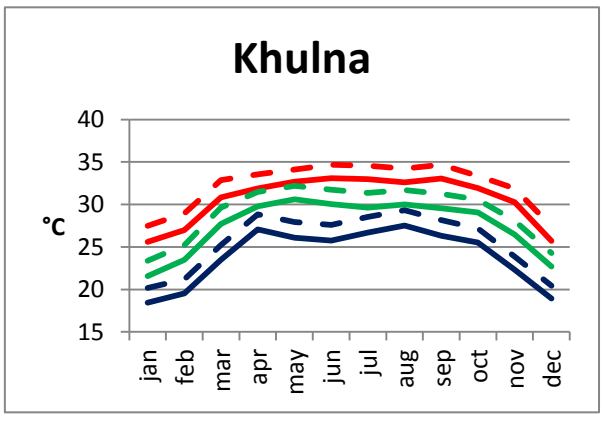

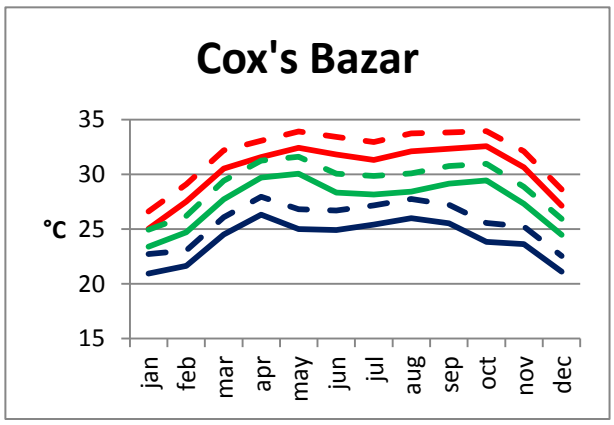

Figure 6-8: Modelled pond temperature data for different regions of Bangladesh. Solid lines represent late 20th century conditions while dashed lines represent 2°C average global warming. Green = average monthly temperature, blue = monthly minimum, and red = monthly maximum.

Figure 6-9 shows average annual (mean of monthly suitability scores) suitability scores for pond aquaculture using the classification schemes outlined in Figure 6-6 for both climate scenarios as well as the difference between the two. In terms of mean pond temperature there is an overall increase in suitability in most areas as a result of more favourable temperatures during colder parts of the year. This effect is further emphasised when looking at the reclassified minimum temperature data. The impacts of the 2°C warming scenario on maximum temperature suitability is quite striking with the biggest reduction in suitabiilty seen in the north west of the country. A small area is highlighted as having temperatures exceeding 37°C although this was only the case in June and July, and only by about 0.5°C. Overall, in terms of temperature regime the south and east areas of the country would appear to be more suitable for aquaculture production.

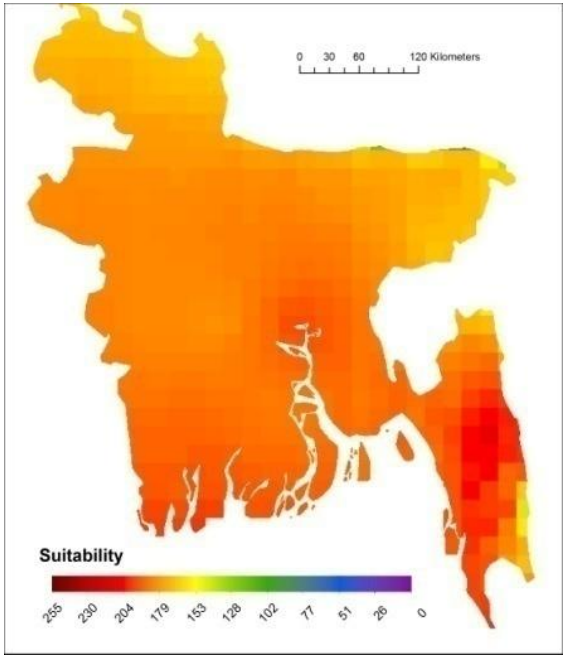

Suitability based on modelled mean pond temperature under late 20th century conditions.

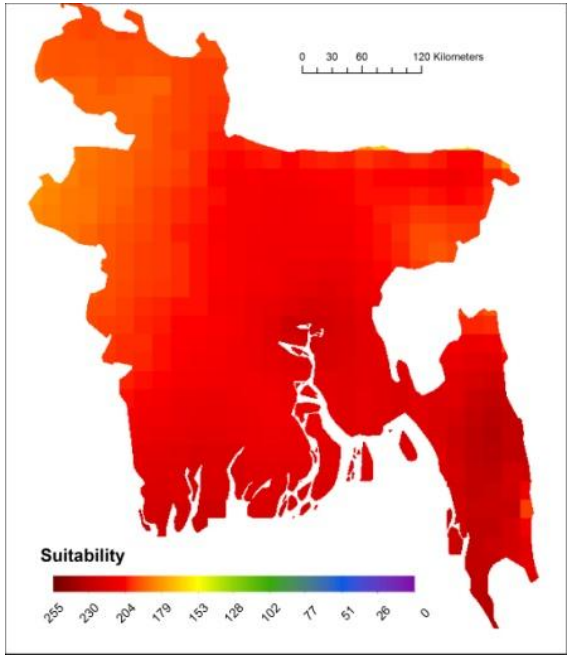

Suitability based on modelled mean pond temperature under 2°C average global warming scenario.

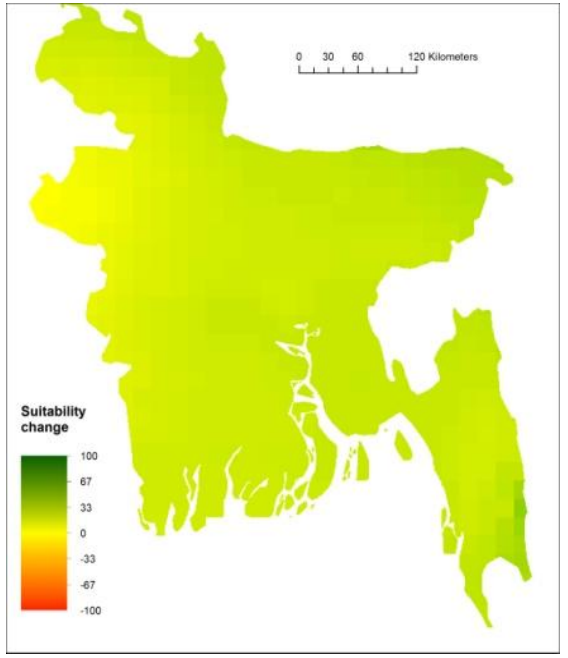

Change in suitability between 2 scenarios - based on modelled mean pond temperature.

Figure 6-9: Annual average suitability of monthly mean, minimum and maximum temperatures.

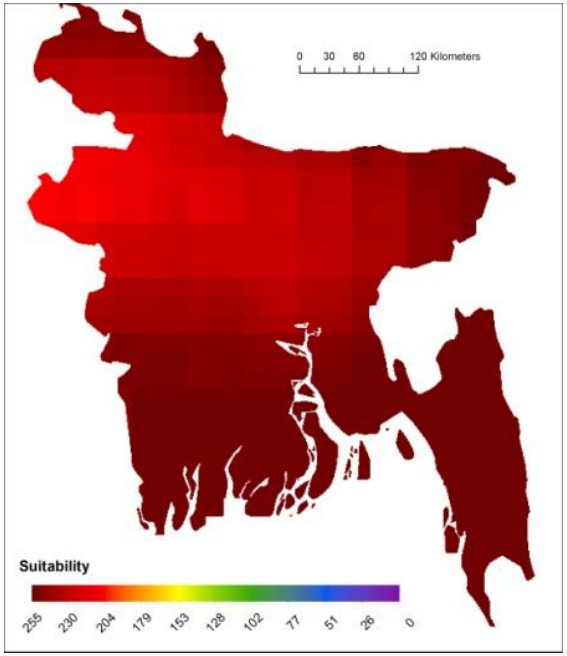

Suitability based on modelled maximum pond temperature under late 20th century conditions.

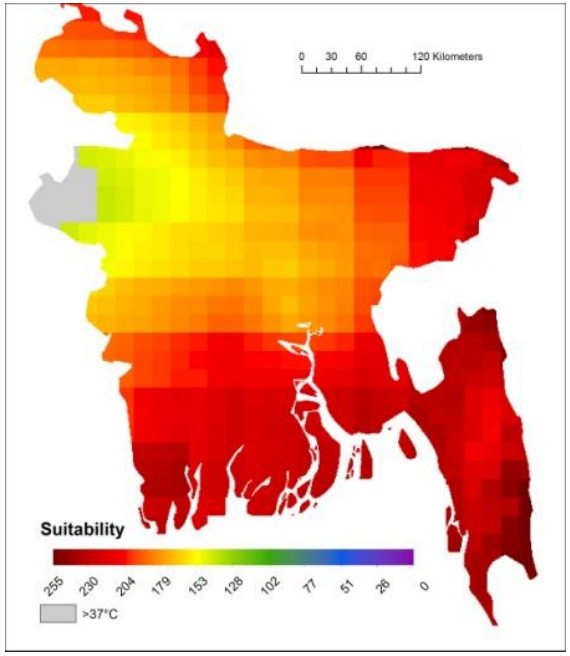

Suitability based on modelled maximum pond temperature under 2°C average global warming scenario.

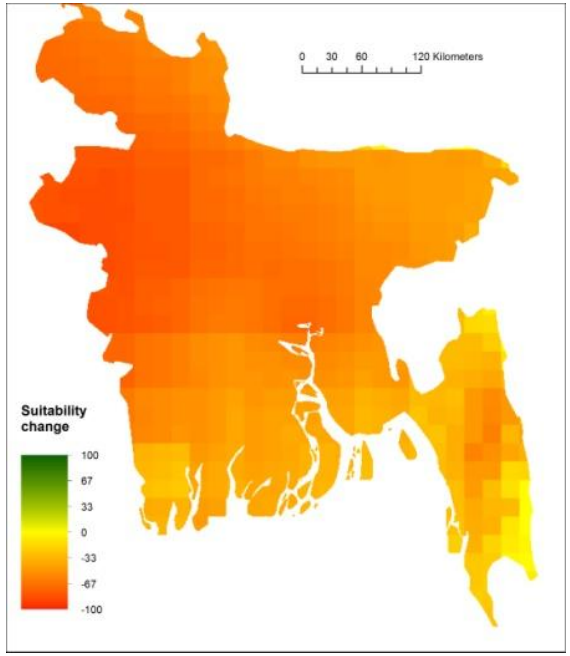

Change in suitability between 2 scenarios - based on modelled maximum pond temperature.

Figure 6-9 continued.

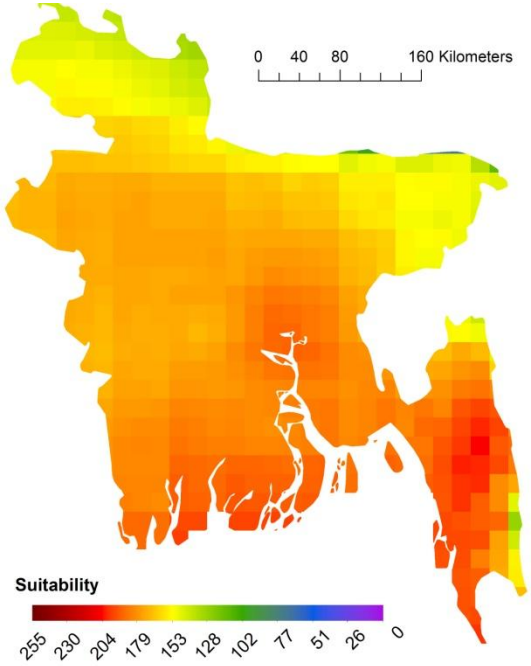

Suitability based on modelled minimum pond temperature under late 20th century conditions.

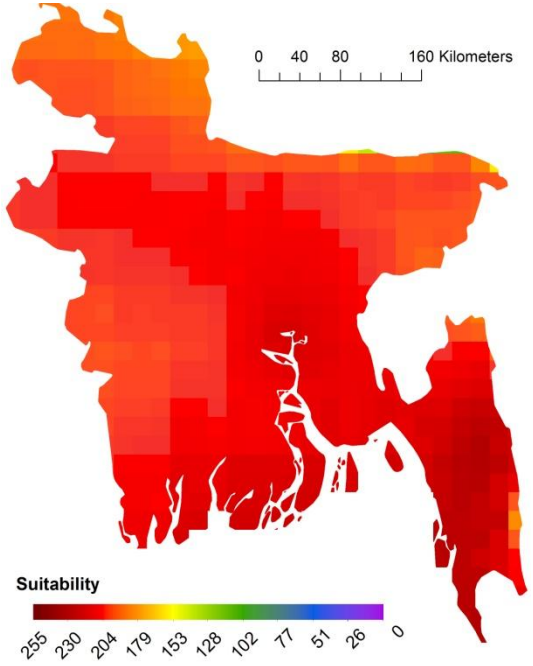

Suitability based on modelled minimum pond temperature under 2°C average global warming scenario.

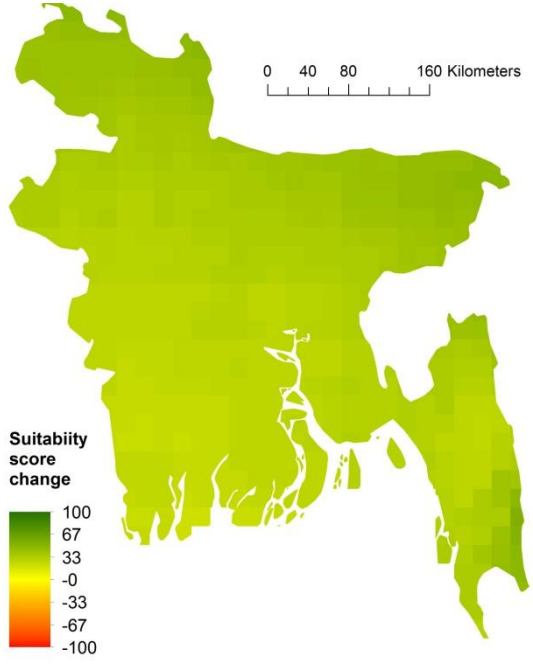

Change in suitability between 2 scenarios - based on modelled minimum pond temperature.

Figure 6-9 continued.

6.3.3 Water balance

Figure 6-10 shows water balance as mm per year under late 20th century conditions and for the 2°C average global warming scenario along with the difference between the two, while Figure 6-11 shows water balance values for the two scenarios normalised (lowest to highest values encounter across both scenarios) over the same scale (0-255) as used to describe suitability in the case of pond temperature. Results suggest that the west of the country is driest with the northwest and southwest corners being wettest. Under the 2°C warming scenario there is a slight increase in water balance throughout the country with the largest increase being in the already wetter northeast of the country.

From an aquaculture perspective the drier conditions in the west of the country can be considered less favourable for ponds that have limited access to water sources other than rain. As highlighted in relation to pond temperature regimes the west of the country is also where higher maximum temperatures are to be expected potentially compounding issues arising from inadequate water supply.

The 2°C climate change scenario used in the current assessment was created using a consensus of 13 Atmosphere-Ocean Global Circulation Models (*AOGCM*s). While the use of multi-model ensembles is generally considered superior to individual models in terms of accuracy (Fordham et al., 2011, Pierce et al., 2009, Reichler and Kim, 2008) it is still worth considering that uncertainties remain and while agreement between models over patterns of temperature change is quite strong, for patterns of precipitation change model agreement is generally weaker. In terms of precipitation patterns over Bangladesh and the surrounding areas the ensemble of 39 climate models (CMIP5 (Taylor et al., 2012)) used to inform Intergovernmental Panel on *Climate Change* (*IPCC*) fifth assessment report (AR5) (IPCC, 2013) broadly agree with the (CMIP3) climate model ensemble used to guide the previous assessment report, as well as provide the climate model data used in the current study, in suggesting an increase in wet season rainfall while the dry season will remain relatively unchanged or very slightly wetter. In AR5 (IPCC, 2013) the IPCC states that there is medium confidence that monsoon inter annual rainfall variability will increase, that an increase monsoon related precipitation extremes are very likely, and that there is medium confidence that the Indian monsoon will weaken

but increased atmospheric moisture will compensate for this leading to more rainfall. Monsoon statistics based on the CMIP5 ensemble are summarised in Figure 6-12 extracted from IPCC AR5 (IPCC, 2013). While it is difficult to draw definite conclusions for aquaculturists in Bangladesh it seems that there will be more water for rain fed aquaculture but much of this will be during the monsoon period where water is already in plentiful supply and in some cases increased flood risk may be more of a concern.

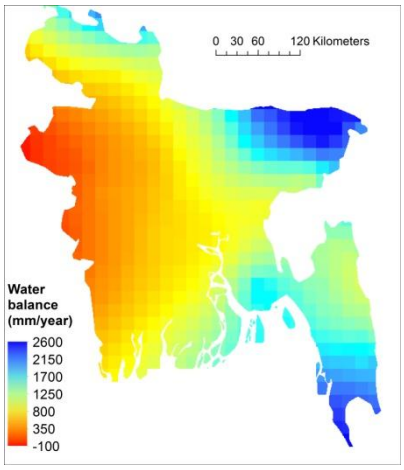

Average annual total water balance (precipitation - potential evaporation from a water surface) under late 20th century condistions (mm).

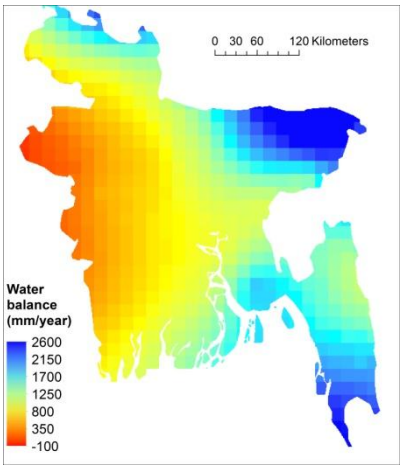

Average annual total water balance (precipitation - potential evaporation from a water surface) under 2°C average global warming scenario (mm).

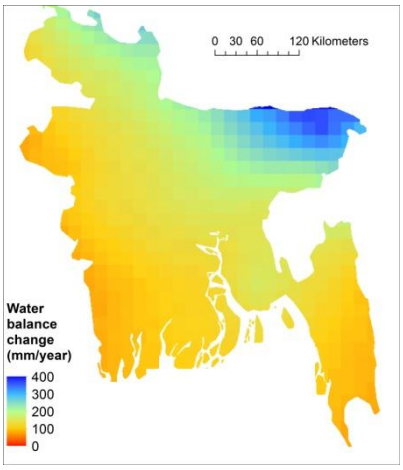

Change in average annual total water balance between late 20th century and 2°C average global warming scenarios (mm).

Figure 6-10: Water balance.

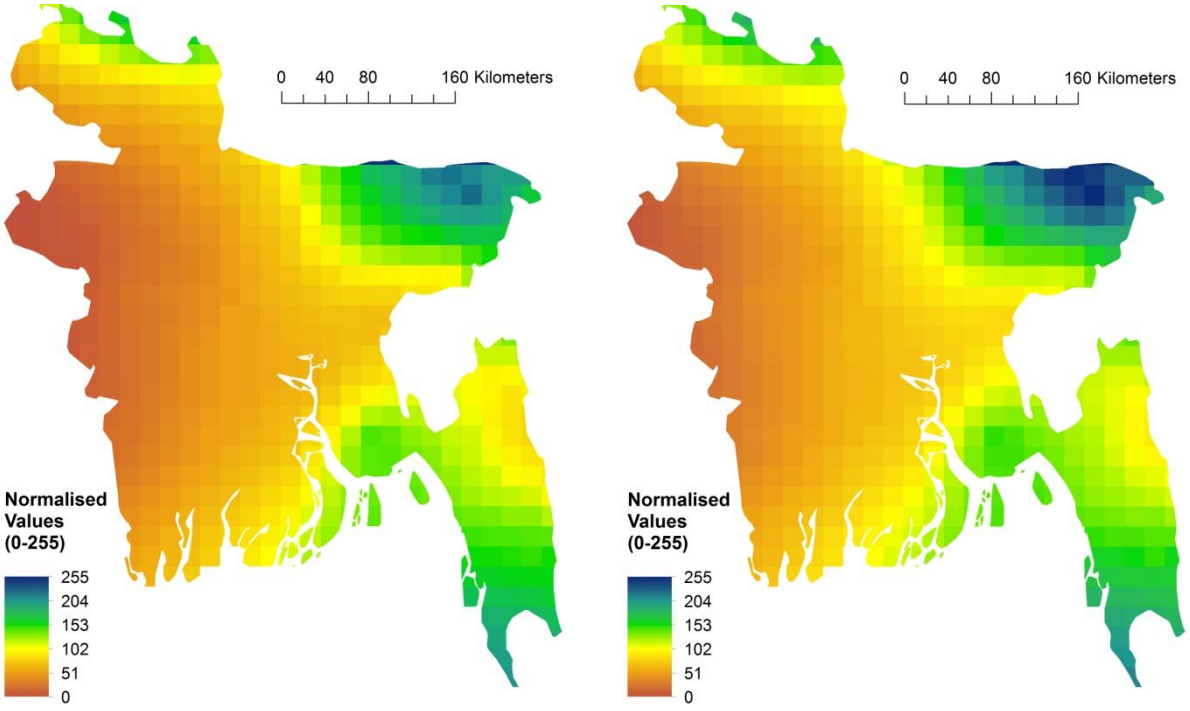

Normalised water balance values for late 20th century conditions

Normalised water balance values under the 2°C average global warming scenario

Figure 6-11: Normalised water balance values.

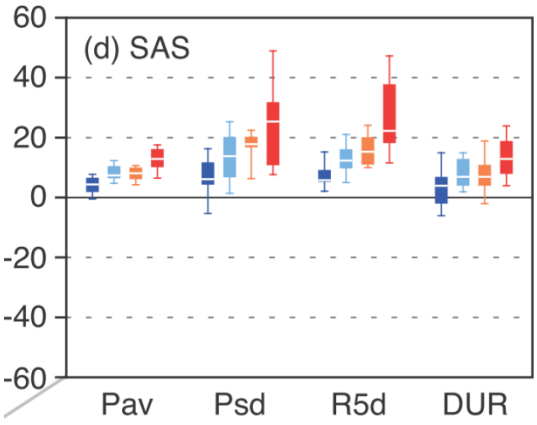

Figure 6-12: Projected percentage change in monsoon statistics for 4 emissions scenarios using the CMIP5 climate model ensemble. Comparison between time periods (1986–2005) and the future (2080–2099). Emissions scenarios: RCP2.6 (dark blue: 18 models), RCP4.5 (blue: 24), RCP6.0 (yellow: 14), and RCP8.5 (red: 26). Statistics: seasonal average precipitation (Pav), standard deviation of inter-annual variability in seasonal precipitation (Psd), seasonal maximum 5-day precipitation total (R5d) and monsoon season duration (DUR). Source: (IPCC, 2013).

6.3.4 Low elevation coastal zone and potential risk of storm surge flooding

Figure 6-13 shows low elevation coastal zones (LECZ) using SRTM data and highlighting contiguous pixels with contact to the sea with thresholds of 3 metres or less, and 5 metres or less. In terms of storm surge related flooding distance from the sea will also have a significant impact with storm surges typically loosing intensity in relation to distance, elevation and roughness of the land surface. The 3 metre elevation threshold highlights substantial areas in the southwest of the country that is particularly low lying and much of which contains large areas of aquaculture ponds with an emphasis on brackish water production of shrimp and prawn. Using the 5 metre threshold a much larger area is highlighted. While some of the highlighted area is a considerable distance inland and may be at lesser risk, areas highlighted nearer the coast and on the many islands of the delta should probably be considered vulnerable in relation to large storm surge events.

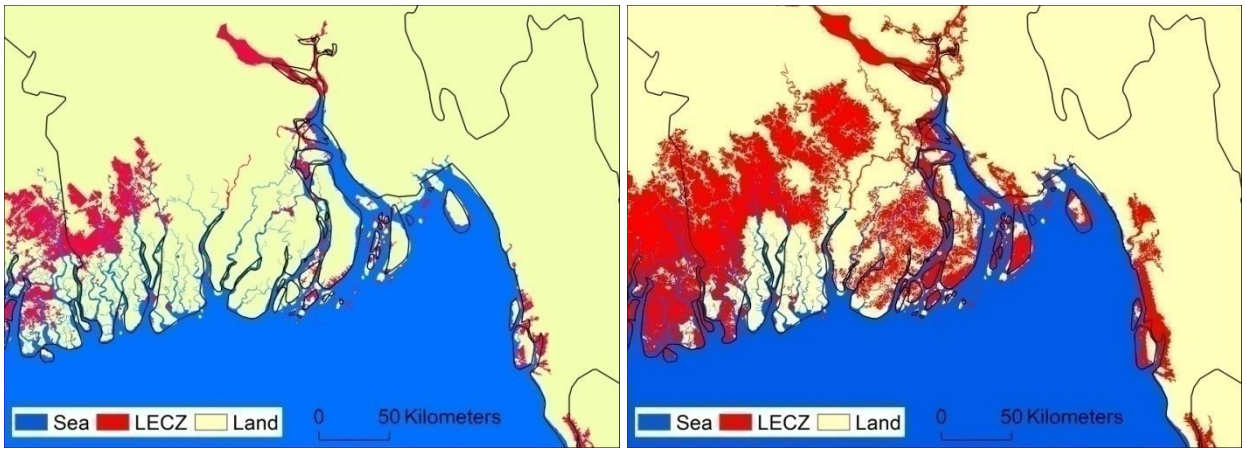

Contiguous pixels with contact with the sea and an elevation of 3m or less.

Contiguous pixels with contact with the sea and an elevation of 5m or less.

Figure 6-13: Low elevation coastal zones.

Figure 6-14 shows a time sequence of images extracted from the MODIS surface water time series that focuses on flooding associated with cyclone Aila. The immediate effect of the cyclone can be seen in the third image in the series with an increase in surface water area in the south west of the country that corresponds to some extent with the 3 metre LECZ highlighted in Figure 6-13 and is probably a result of storm surge flooding. The large increase in areas classified as mixed in many regions may well be a result of the extreme rainfall that typically accompanies tropical storms.

While the extent of flooding shown in Figure 6-14 can be seen to reduce gradually during the time periods after the cyclone event there are likely to be areas where water remains for a considerable period. This is likely to be especially true for very low lying polder areas which, once inundated, may be difficult to drain. An example of such an event is provided here via a series of images in Figure 6-15. Image A shows the area of interest which is a polder in the southwest of Bangladesh, image B shows elevation and while the highlighted area has predominantly low elevation values of around 2-3m it is no lower than areas to the north that remain unaffected. It is also worth noting that the area to the east indicated as being higher in elevation is part of the Sundarban and actually represents very low lying land with dense mangrove cover giving a false impression of elevation height , Image C shows ETM+ derived land cover and indicates that the area in question mostly consists of cropland, image D show the percentage of the MODIS surface water time series where water is present and highlights that the area is not normally flooded, image E shows MODIS surface water data for a single time point in early October 2008, while image F shows MODIS surface water data for early October 2009 when the area, still flooded after cyclone Aila, was visited. The first two photographs in Figure 6-16 show part of the flooded area including homes and trees which appeared in some cases to be dying as a consequence of the saline water, the third image highlights the immediate human impact and shows people forced to abandon their homes and take refuge on the road which represents the only area of land in the immediate vicinity that is significantly above flood height. The final image shows pens funded by an NGO and being used to culture tilapia in the flood water.

Taken together the information outlined above highlights a number of points: 1. The human impact of storm surge events can be severe and can persist long after the event with saline water being particularly damaging for agriculture, 2. Vulnerability to such flooding depends on local factors and cannot be reliably predicted with relatively low resolution elevation data, although it can help in indicating areas that may be at risk and should be considered for further evaluation. While no direct evidence was observed it is interesting to note that during discussion with affected people there was a suggestion that protective dikes had been damaged by people attempting to fill shrimp ponds with saline water, a situation that would be hard to account for within a risk modelling exercise no matter how sophisticated, 3. That the use of remotely sensed data can be useful in monitoring such events, and 4. That aquaculture represents a flexible technology that may have potential benefits in helping adaptation to climate driven events (Karim et al., 2014).

Bangladesh is often highlighted as one of the world's most vulnerable countries in terms of sea level rise (Houghton, 2009) with the suggestion that land subsidence (Ericson et al., 2006) is leading to an effective sea level rise beyond the global average (Pethick and Orford, 2013, Singh et al., 2000). Brammer (2014) suggests that some sea level rise scenarios described for Bangladesh are perhaps overly pessimistic and points out that both the coastal geomorphology and people of Bangladesh are dynamic, and it is not a simple case of them being overwhelmed one contour at a time. That said it does seem likely that for the very low lying and polder areas increases of sea level will increase the risk of flooding in the face of storm surge events.

Coastal regions of Bangladesh, especially the southwest, show a salinity gradient of surface and ground waters that extends a considerable distance inland. A long term gradual effect of sea level rise combined with impacts on freshwater inputs such as upriver damming is to increase salinity levels, effectively moving salinity contours further inland with potential negative consequences for agriculture (Rahman et al., 2011, Haider and Hossain, 2013). In areas where salinity has negatively affected rice production (Haider and Hossain, 2013) showed that farmers had taken up shrimp culture as an alternative livelihood strategy. However there is also evidence that shrimp farming itself leads to increased salination of surrounding land (Pouliotte et al., 2009, Rahman et al., 2011). Clearly this is an area where ongoing research is needed in line with careful policy making to promote sustainable production across all sectors. Nevertheless, in situations where salinity levels arising from increasing sea levels and reduced freshwater inputs preclude the majority of agricultural practices, the culture of salt tolerant aquaculture species would seem to provide a means of income and food generation from land that may have little in the way of alternative value.

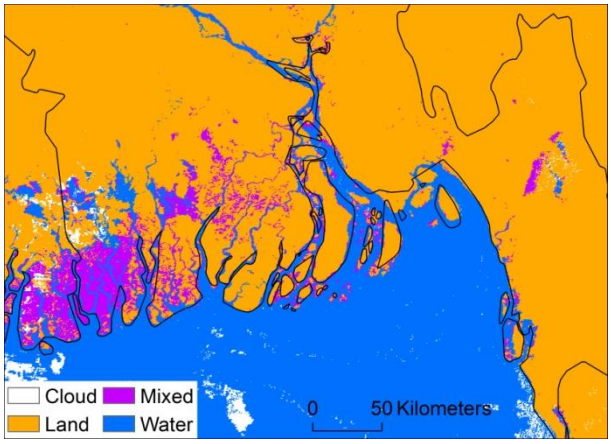

09-05-2009

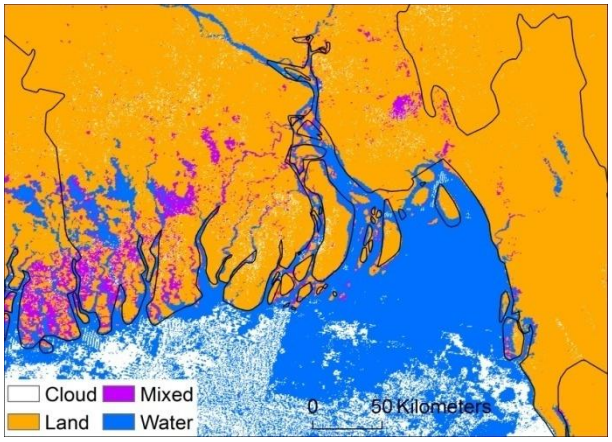

17-05-2009

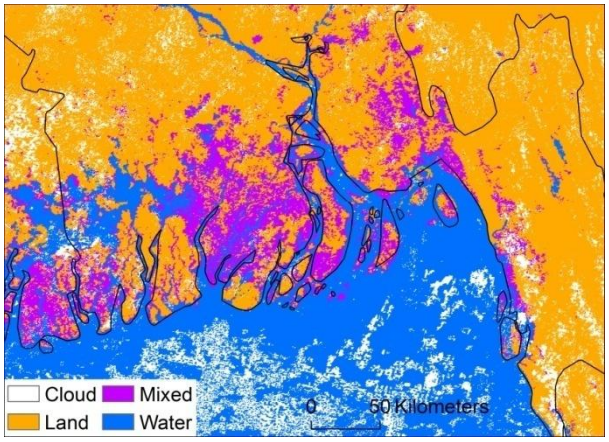

25-05-2009 (cyclone Aila)

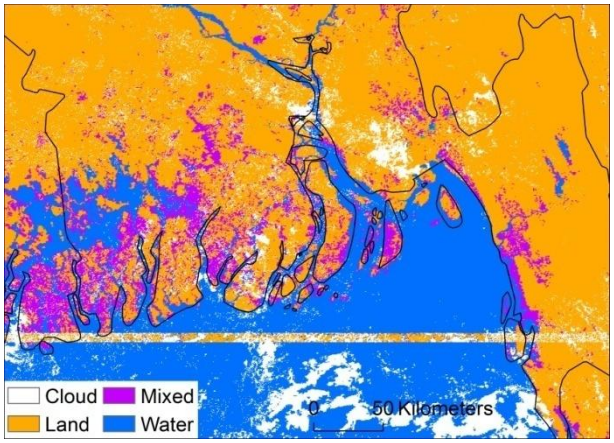

02-06-2009

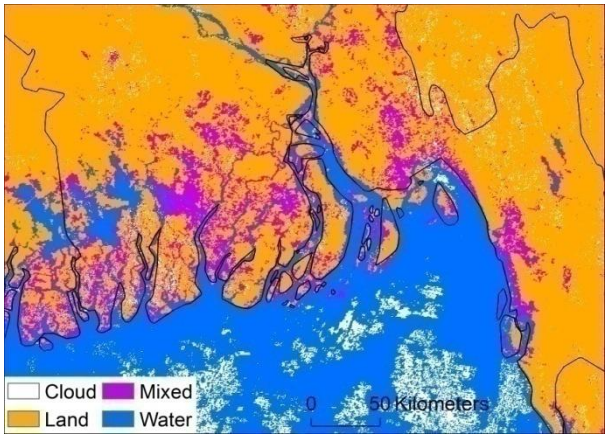

10-06-2009

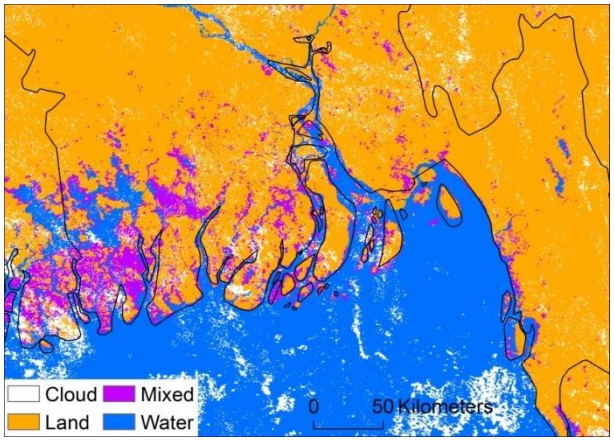

18-06-2009

Figure 6-14: Time series of images showing flooding caused by cyclone Aila on 25th May 2009.

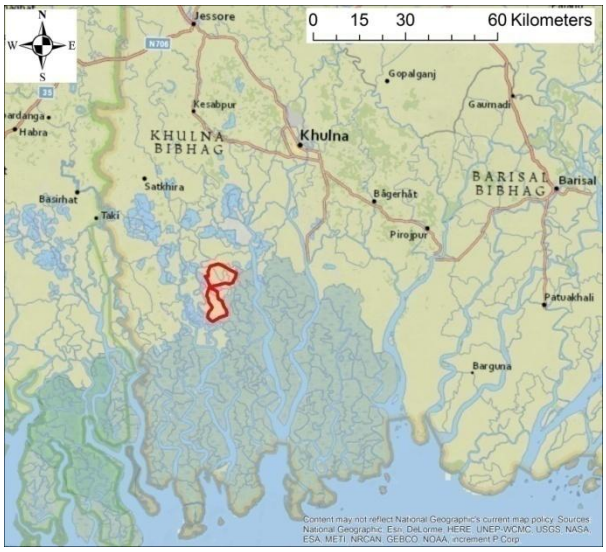

A. Area of interest.

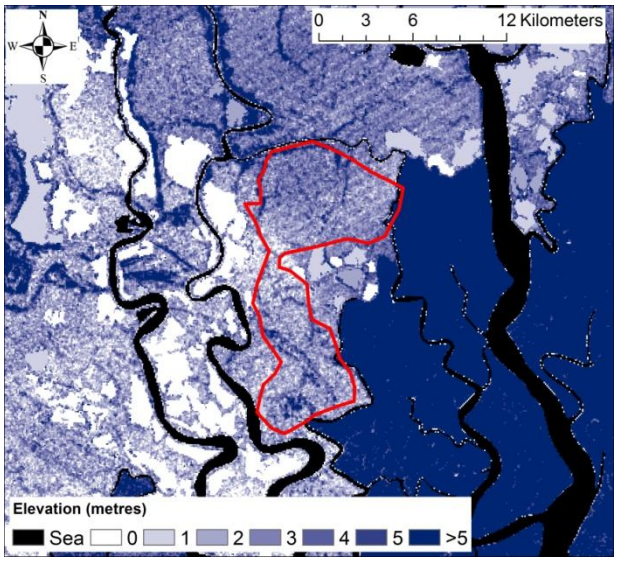

B. Elevation based on unfiltered SRTM data.

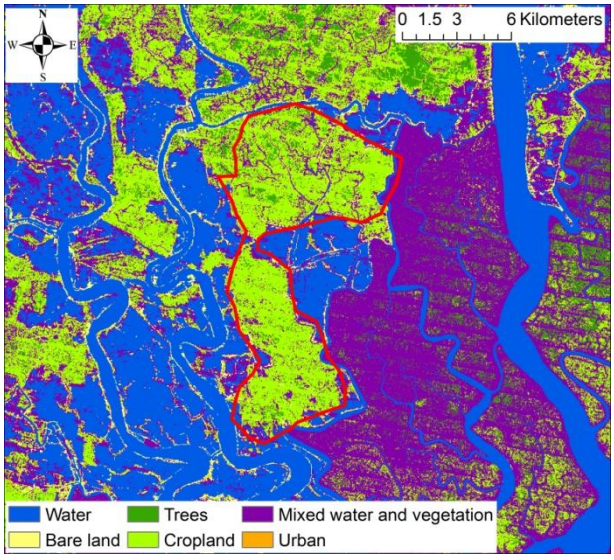

C. Landsat ETM+ land cover classification.

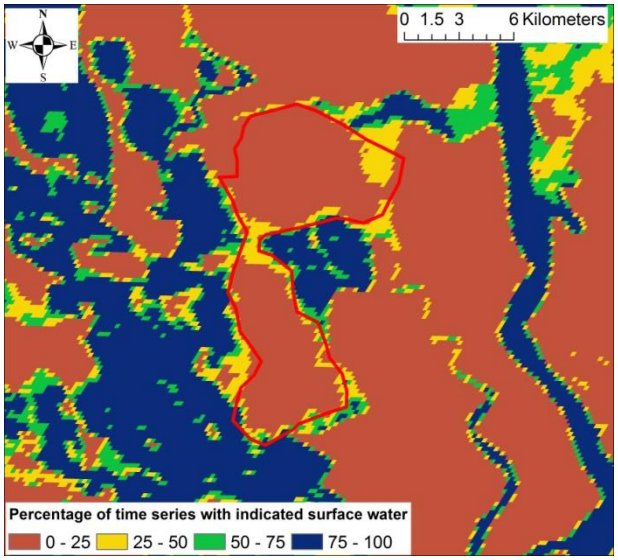

D. MODIS surface water time series - inundation frequency.

Figure 6-15: Inundation of a polder area with sea water during cyclone Aila.

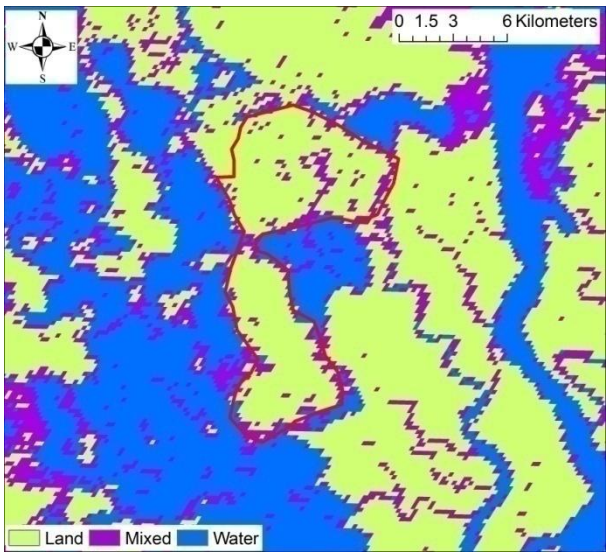

E. Early October 2008.

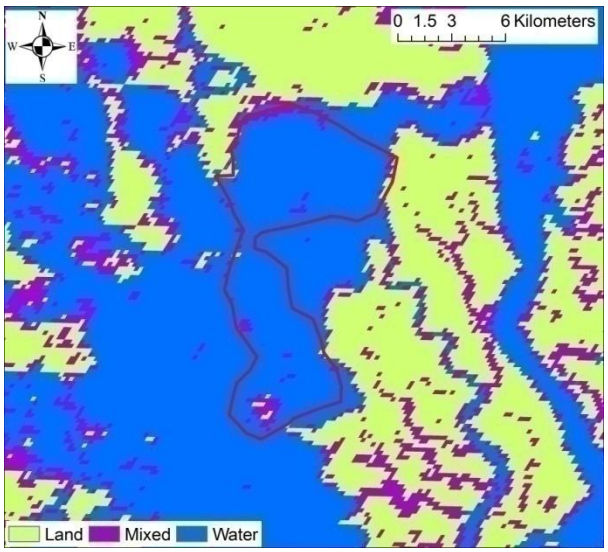

F. Early October 2009 - time of field visit.

Figure 6-15 continued.

Figure 6-16: The impact of cyclone Aila on a polder area in southwest Bangladesh. Top images give an impression of flooding, the bottom left image shows people forced to live in temporary accommodation on the road, bottom right shows NGO sponsored pen culture of tilapia in flood waters.

6.3.5 MCE results combined with land cover classifications

The results of the land cover reclassification described in Figure 6-7 overlaid with the results from the site suitability MCE are shown in Figures 6-17 to 6-21 with each land cover class represented separately. In each case results for late 20th century conditions are shown along with changes in suitability in response to the 2°C global warming scenario. The MCE weightings used were chosen so as to place quite a strong emphasis on the climate-related variables of water balance along with mean, minimum, and maximum temperature. In each of the classifications there is a general trend towards lower levels of suitability in the north west of the country as a result of higher maximum temperatures and lower water balance figures, while the east of the country, and particularly the extreme south east, are considered most favourable. Comparing the two climate scenarios shows an increase in suitability in the east of the country driven by: more favourable mean temperatures throughout the year, increased water balance figures in the northeast, and limited impact in terms of maximum temperatures. This contrasts with the northwest regions where suitability is decreased due to the effects of higher maximum temperatures. It is worth noting that while changing the weightings used when combining the temperature and water balance data have some bearing on outcome in terms of the extent of suitability differences seen between both regions and climate scenarios, the general pattern remains largely the same suggesting a fairly robust result.

The results displayed in Figures 6-17 to 6-21 have a strong focus on climate and surface water patterns and in doing so provide unique and valuable insights not seen in the much more localised site suitability conducted within Bangladesh to date. This focus combined with the already discussed scarcity of quality data at the national level means that many areas highlighted as suitable here maybe less than ideal when viewed at a more local level with an increased variety and resolution of data. Given that a key strength of site suitability modelling within a GIS environment is the iterative process and ability to build on and improve existing models and databases, the current assessment can be viewed as a strong foundation which can be used to inform future work within the region.

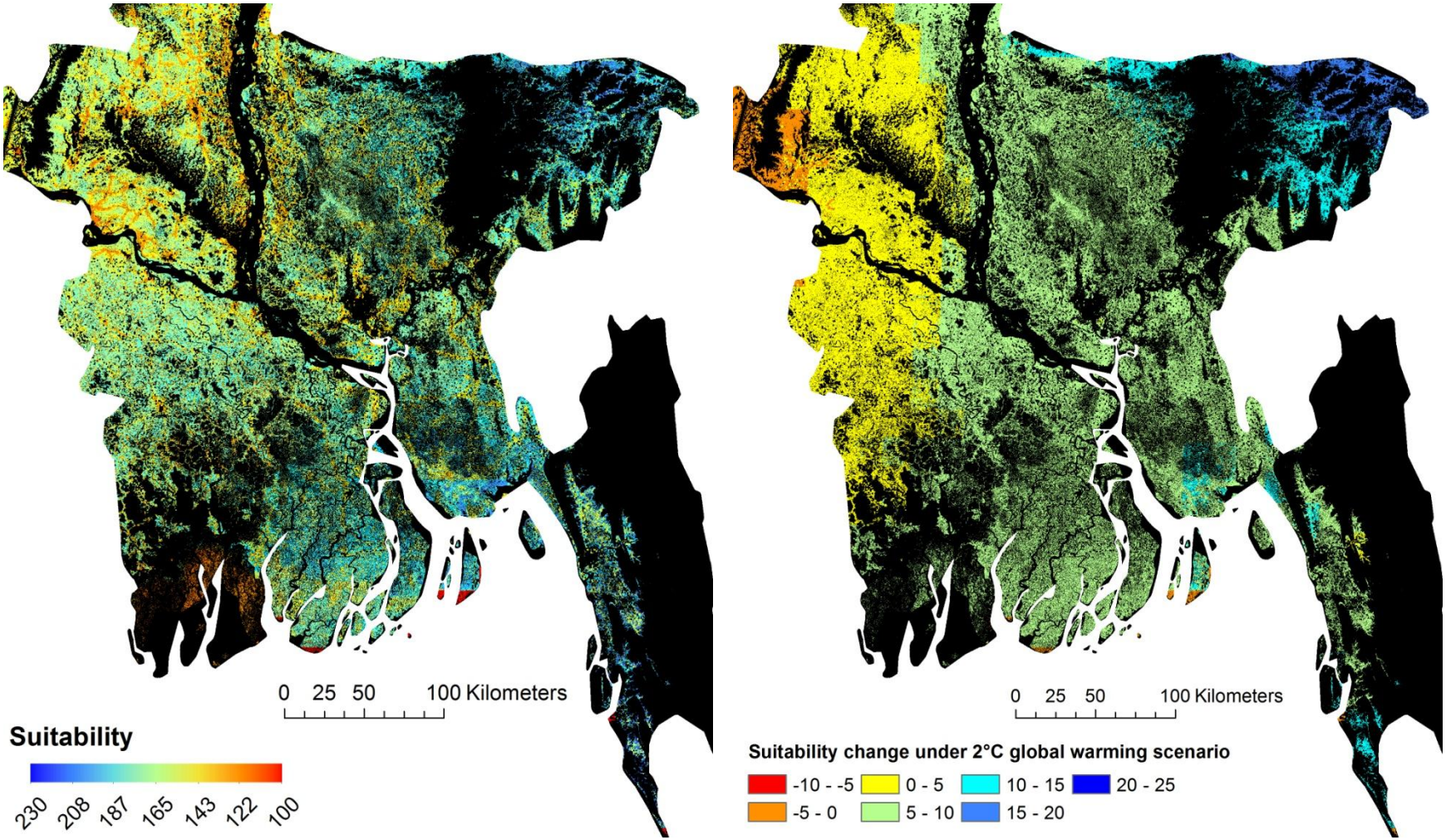

Figure 6-17: Suitability MCE results overlaid with areas classified as crop areas that could be considered for conversion to pond aquaculture. Image on left shows suitability under late 20th century climate conditions while the image on the right shows suitability change in response to the 2°C average global warming scenario.

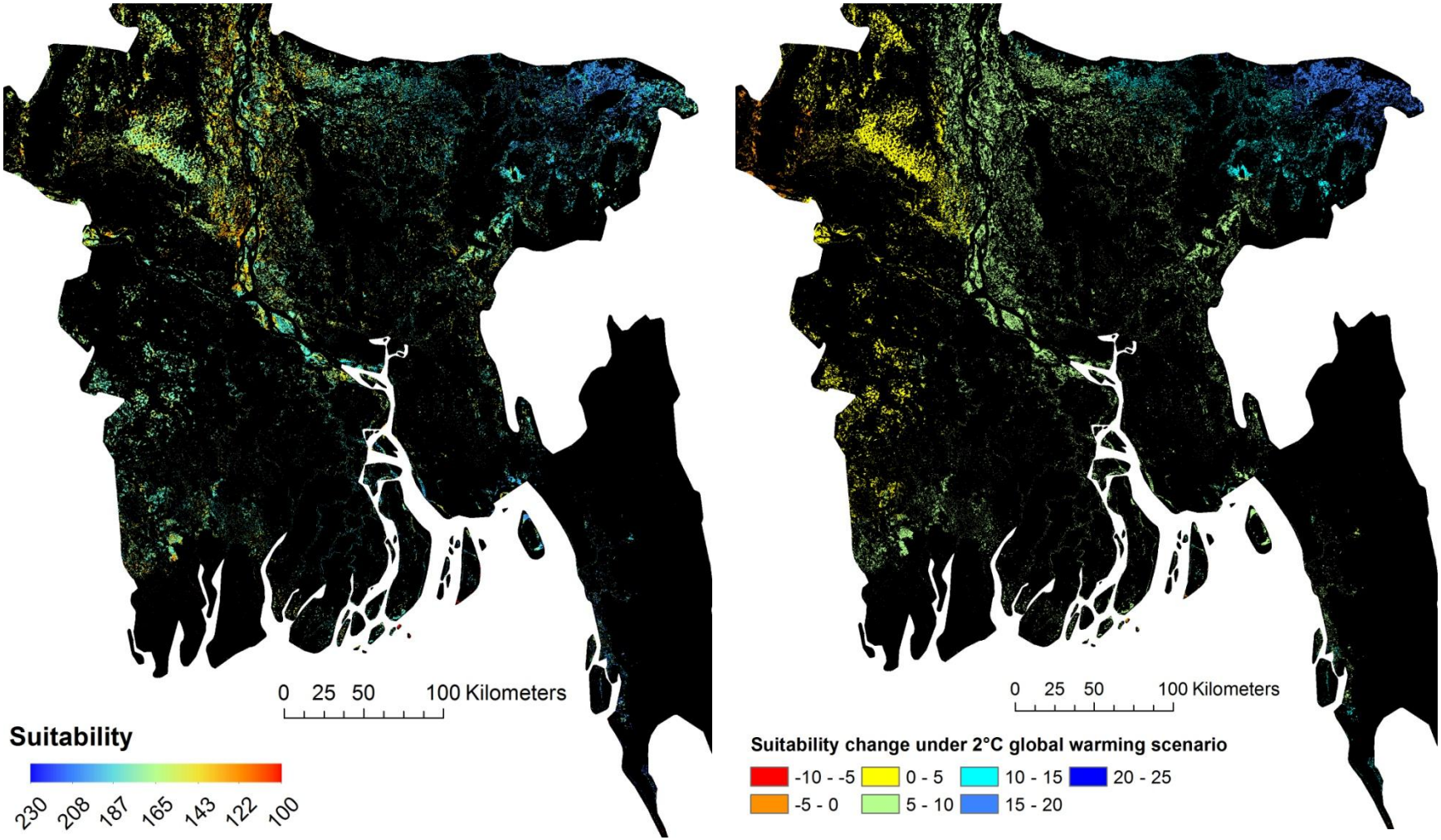

Figure 6-18: Suitability MCE results overlaid with areas classified as crop areas that could be considered for conversion to pond aquaculture but with potentially greater flood risk. Image on left shows suitability under late 20th century climate conditions while the image on the right shows suitability change in response to the 2°C average global warming scenario.

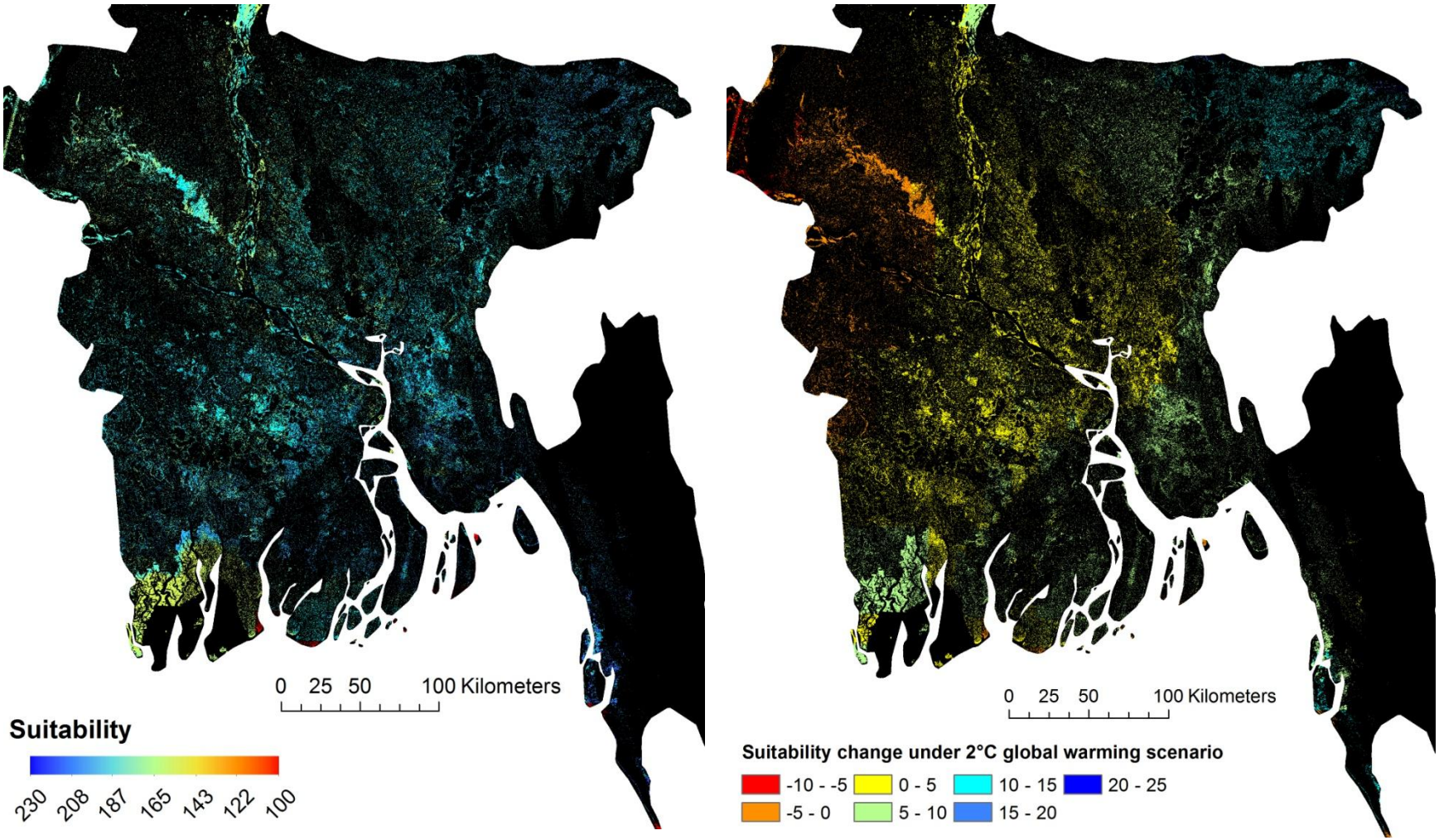

Figure 6-19: Suitability MCE results overlaid with areas that receive a moderate amount of seasonal inundation and that could be considered in relation to floodplain aquaculture or well protected ponds. Image on left shows suitability under late 20th century climate conditions while the image on the right shows suitability change in response to the 2°C average global warming scenario.

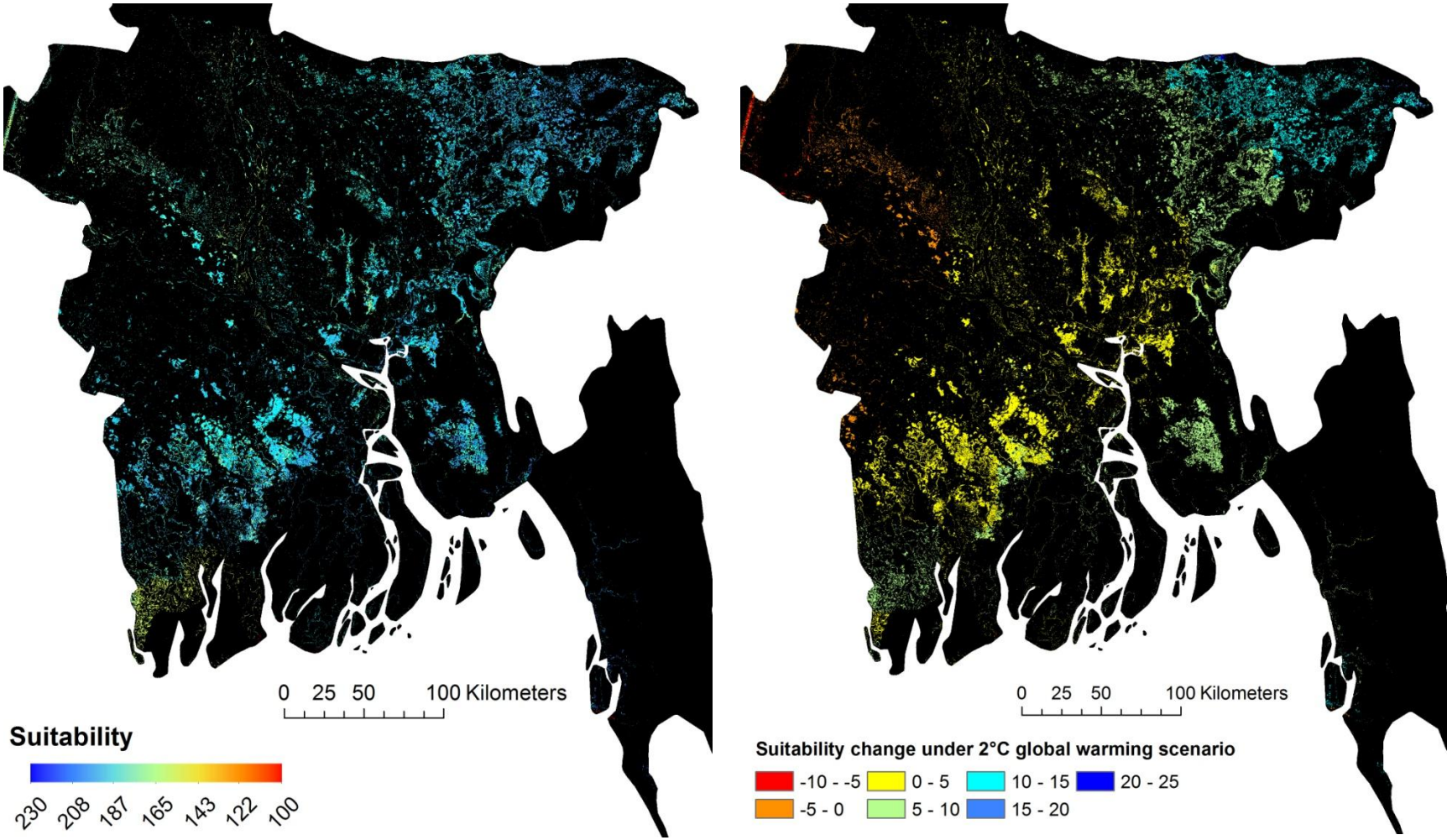

Figure 6-20: Suitability MCE results overlaid with areas that receive larger amounts of seasonal inundation and that could be considered in relation to floodplain aquaculture. Image on left shows suitability under late 20th century climate conditions while the image on the right shows suitability change in response to the 2°C average global warming scenario.

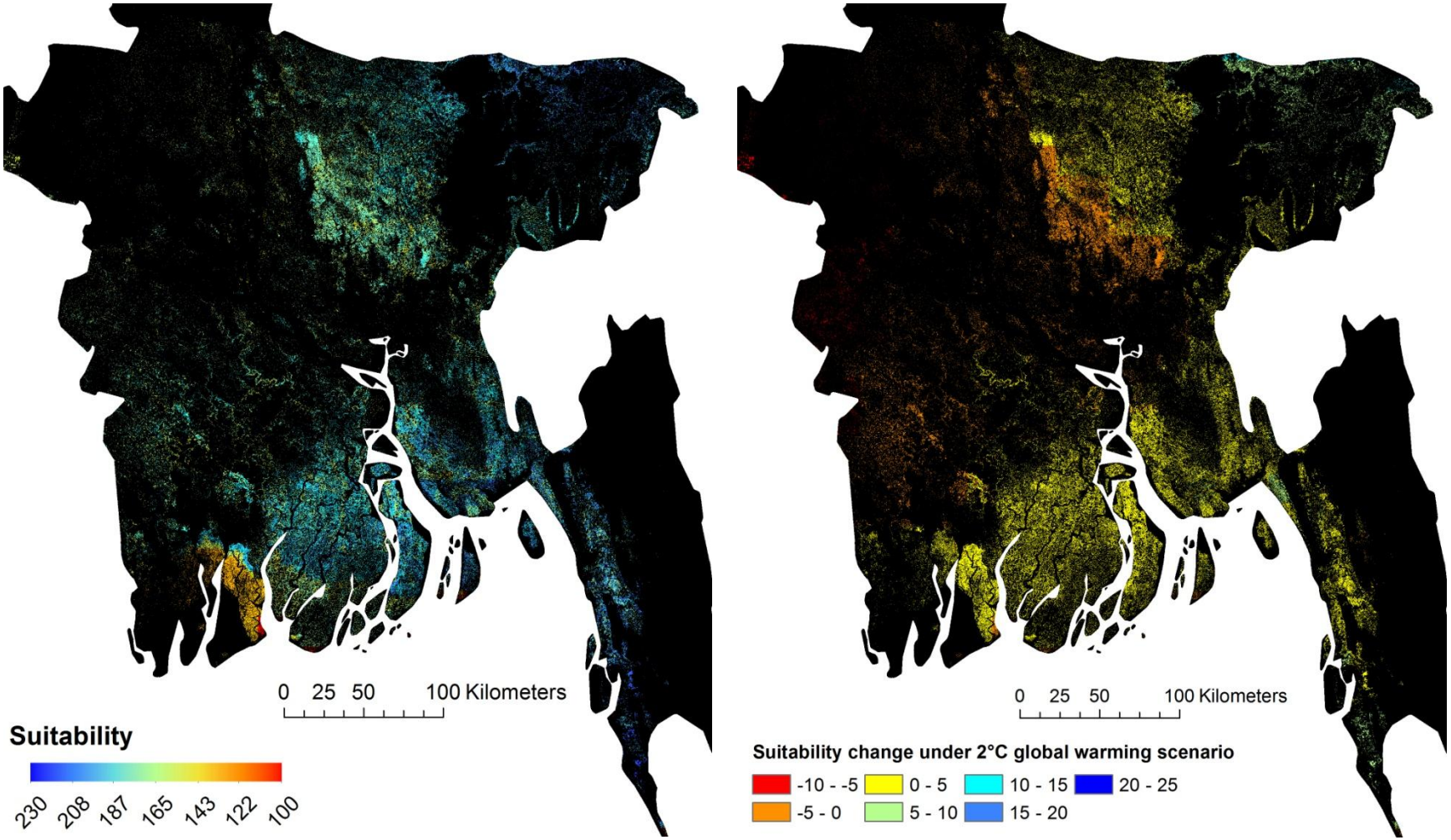

Figure 6-21: Suitability MCE results overlaid with area that have tree cover that in many instances will represent areas with homes and could be considered in relation to creating, or enhancement of, homestead ponds. Image on left shows suitability under late 20th century climate conditions while the image on the right shows suitability change in response to the 2°C average global warming scenario.

6.4 Concluding remarks

Bangladesh is often highlighted as especially vulnerable to climate change due to a combination of factors including: being an extremely low lying deltaic country that experiences inland river based flooding as well as that in coastal areas as a result of storm surge activity, an extremely dense human population, and significant issues of poverty. The aquaculture sector is growing rapidly in Bangladesh and production is now believed to have overtaken that of capture fisheries (FishStatJ, 2014). Aquaculture is extremely important for the country both in terms of food security and as a source of income generation (Dey et al., 2008, Karim et al., 2006).

The current case study incorporates the land cover data set described in chapter 4 with the surface water time series described in chapter 5 to evaluate land cover in terms of potential aquaculture environments. The pond temperature model described in chapter 3 is also incorporated along with water balance data, population density data, and elevation derived slope values to assess site suitability for pond-based aquaculture under late 20th century conditions and for a 2°C global warming scenario. Outputs are presented as a series of raster images with a ground resolution of 30m.

To date site suitability assessments for inland aquaculture within Bangladesh and elsewhere have been localized in nature (Giap et al., 2005, Hossain et al., 2007, Hossain et al., 2009, Hossain and Das, 2010, Salam et al., 2005, Salam et al., 2003) and have focused on individual species. Such studies have typically made use of localised data sources many of which are not available at the national scale. As such the current study does not attempt to emulate these previous assessments but instead makes a number of valuable, and to date unique, contributions to the understanding of site suitability for aquaculture in Bangladesh: a) by covering the majority of the country it provides insights into suitability at the national level, b) the incorporation of remotely sensed data describing land cover and surface water distribution allows for the indication of areas in terms of potential aquaculture environments (conversion of fields to fish ponds, floodplain aquaculture, and smaller homestead ponds), c) the inclusion of climate data, and especially modelled pond temperature data, representing both recent and potential future conditions provides an extremely useful indication of how changing climate conditions may impact on aquaculture at the national scale.

Overall The south and east of the country was indicated as most suitable for aquaculture as a result of more favourable cold season temperatures and higher water balance values. The north west of the country was considered least suitable due to higher maximum modelled pond temperatures and lower water balance values. The effect of the 2°C warming scenario was to enhance these trends throughout the country in terms of temperature while the already wetter north east corner is projected to have a noticeable increase in precipitation.

The idea that climate change may have both positive and negative impacts for Bangladesh depending on location is an important one in that it underlines the potential for further aquaculture development while emphasising the value of spatial modelling exercises such as the current one in relation to guiding development.

7 SUMMARY

7.1 Global assessment of vulnerability of aquaculture related livelihoods to climate change

The modelling process and results described in chapter two provide a global assessment of where changing climate may have the greatest impacts on aquaculture related livelihoods. While the model was similar in concept to previous assessments of climate related vulnerability (Allison et al., 2005, Allison et al., 2009, Metzger et al., 2005, o'Brien et al., 2004, Schröter et al., 2005) in that it viewed vulnerability as a function of exposure (extent of climate change), sensitivity (significance of potentially impacted resource - in this case aquaculture, and adaptive capacity, it differed in that it deliberately used a moderate number of focussed indicators to specifically target aquaculture.

To date there has been one previous global scale assessment of climate change-driven vulnerability of aquaculture related to livelihoods (Handisyde et al., 2006) that also made use of spatial data and was based around the concept of vulnerability as a function of sensitivity, exposure and adaptive capacity. Notable improvements in the current assessment included the use of a more sophisticated set of climate change projections in the form of a multi-model ensemble of data obtained using the MAGICC/SCENGEN package, and improved methods of data combination including the use of geometric rather than arithmetic means to reduce the likelihood of countries with very small aquaculture sectors (low sensitivity) being considered as highly vulnerable in situations where metrics for exposure and adaptive capacity scored highly. To complement this approach the impacts of exposure and adaptive capacity were also considered in isolation to provide insight into where vulnerability may exist irrespective of national aquaculture industry size. Such a view may be especially useful when considering areas with emerging aquaculture industries that may be expected to develop significantly in the future.

Unsurprisingly, due to their substantial aquaculture industries a number of Asian countries, notably Vietnam, Laos, Bangladesh, and to a lesser extent China, were considered most vulnerable to impacts on freshwater aquaculture production. Vietnam along with Ecuador was also considered highly vulnerable in terms of brackish water production meaning that when inland aquaculture production (brackish and freshwater) is considered as a whole Vietnam stands out significantly in terms of vulnerability.

In terms of mariculture Norway was indicated as most vulnerable despite being one of the world's most highly developed countries. Chile, another nation with relatively high levels of development also scored highly. The results in the case of Norway and Chile were influenced by the extremely high per capita levels of production compared with other nations. Other notable areas with indicated mariculture vulnerability include: China, Vietnam, the Philippines, Thailand, Greece, and Madagascar.

The current assessment has a number of limitations. Much of the data used is only available at the national scale. Data availability, quality and resolution are typically the limiters for spatial modelling exercises and the current study was no exception. While higher resolution data for indicators such as aquaculture production may exist in some regions it is extremely unlikely that such data will become available with a consistent global coverage and resolution. With this in mind it would seem that for global scale impact assessments the best strategy at the current time is to focus on making best use of available data that provides consistent coverage across the entire study area. Another potential limitation is the widely held assumption that exposure to a greater degree of climate change, i.e. temperature increase, results in a greater negative impact. Such an approach is common in terms of global vulnerability assessments (Allison et al., 2005, Allison et al., 2009, Handisyde et al., 2006), and again given the data limitations with a global scale model there would seem to be little practical alternative. However real impact will depend on a complex combination of factors including the base climate before change and its relationship to specific culture species and practices where in reality impacts may range from strongly negative to strongly positive. With this in mind an important consideration is the context in which the model and its outputs are viewed. As with most modelling exercises results should not be followed blindly but should be considered as a valuable contribution to an informed decision making process.

In summary, the model of vulnerability provides a highly useful tool to be used by informed decision makers when assessing where aquaculture-related vulnerability to climate change may occur. While further refinement of the model may be possible if improved data sets become available, future research may be best focused on more detailed regional analysis guided by the current findings.

7.2 Modelling site suitability in relation to climate changes at a global scale

To date, the largest scale GIS-based site suitability assessments for aquaculture have been at the continental scale with good examples for Africa (Aguilar-Manjarrez and Nath, 1998, Kapetsky, 1994) and Latin America (Kapetsky and Nath, 1997). These studies were based on raster grids with resolutions of 10 arcminutes, 3 arcminutes, and 5 arcminutes respectively. Along with a global extent, the current assessment makes considerable advances in resolution by making use of land cover and elevation data at 10 arcseconds (approximately 300 metres at the equator) along with population density and soil property data to indicate site suitability. Another way in which the current assessment improves on previous on previous work that that has made use of climate data when investigating site suitability for aquaculture (e.g. Aguilar-Manjarrez and Nath, 1998, Kapetsky, 1994, Kapetsky and Nath, 1997) is through the use of data from an ensemble of GCMs when modelling pond temperature. The approach of using combined output from multiple climate models has potential benefits in projection accuracy when compared to results from a single model (IPCC, 2007b, Pierce et al., 2009) and was used in the current study to represent conditions under a 2°C average global warming compared with late 20th century conditions. These climate change scenarios were then applied to a 10 year daily time series of reanalysed gridded weather data as a means of gaining valuable insight into potential variability and temperature extremes that would not be visible if only monthly averages had been used. Along with temperature effects, water availability for rain fed ponds was also considered for the two climate scenarios and in relation to low, medium and high rates of water loss via seepage.

The three main model components (land suitability (based on topography, soil and population), pond temperature, and water availability) each provide valuable insights in their own right. However a key advantage of a GIS modelling approach is that once a spatial database is established it is relatively easy to combine data in a range of ways to ask specific questions of the data. For the current assessment, two methods of data combination were demonstrated with Nile tilapia (*Oreochromis niloticus*) used as a model species representing warm water culture conditions. Firstly pond temperature data were reclassified over a continuous range of values (0-255) representing the least to most suitable conditions. This reclassified data were then combined with a land suitability (topography, soil properties and population density) component that was classified using the same 0-255 scheme by means of an ordered weighted average. The second method made use of thresholds for temperature and pond water availability to create a Boolean layer indicating areas of potential

aquaculture that were then overlaid with the land suitability layer. In both cases layer combinations were made for both late 20th century conditions and for the 2°C global warming scenario.

While outputs from the modelling processes described above are best viewed as a series of spatial images it is possible to draw a number of general conclusions:

- Pond temperatures are projected to increase less than air temperatures in most areas. It should, however, be noted that in the case of the 2°C average global warming increase in air temperatures over land will be greater than the 2°C average in many areas.
- Projected changes in suitability in relation to reclassified temperature data vary depending on location and time of year, however overall there would appear to be a positive trend for culture of warm water species in most tropical regions. This positive trend is especially pronounced in relation to colder seasons. There are some significant areas from an aquaculture perspective that are indicated as having lower levels of suitability during warmer parts of the year, notably parts of Asia including Bangladesh, Thailand, Myanmar, and parts of India. There were also some negative impacts projected for the warmest part of the year in western Africa, notably in Ghana.
- Location is again significant when interpreting water availability for rain fed ponds results. Overall, under most seepage and runoff scenarios used there is a projected increase in potential pond area. However, while the projected increases appear quite large in percentage terms for many of the scenarios it is worth noting that the overall areas involved are quite small in relation to the pixel size of the data used meaning that the inclusion of a small number of extra pixels would have a substantial impact on results.

As it stands the current model provides a useful and unique evaluation of site suitability for pond-based aquaculture at the global scale while at the same time providing insight into the potential implications of a warming climate. There are a number of areas where future work could complement the existing database and model. One area of particular value would be that of water availability for ponds that make use of permanent or semi permanent surface water sources. One potential approach would be the use of remotely sensed data as a means of detecting existing water bodies, ideally at a number of time points throughout the year to give an indication of how permanent a water source may be. MODIS data have been demonstrated as a means of monitoring surface water both as part of the current work and elsewhere (e.g. Guerschman et al., 2011, Handisyde et al., 2014,

Sakamoto et al., 2007). While the manageable resolution and frequent return period would make detecting surface water at a global scale for multiple time points a feasible exercise, the resolution of MODIS is not sufficient to resolve smaller water bodies, especially those taking the form of smaller rivers and canals. There have been recent attempts to produce a global land cover data set at 30m resolution based on Landsat data (Gong et al., 2013, Yu et al., 2014, Yu et al., 2010). Such work could be beneficial in terms of identifying surface water but in its current state only represents a single time point that varies depending on location and as such cannot really be considered suitable at this stage. For some regions detailed vector based mapping may be available with one potential source of freely available data being the OpenStreetMap project. Unfortunately such data is not available consistently at a global scale and is significantly lacking in detail for some areas such as Bangladesh in the case of the current work. Modelled runoff data based on digital elevation data have been used as an indicator of water availability at the global scale in relation to climate changes (e.g. Islam et al., 2007, Murray et al., 2012, Oki et al., 2003, Sperna Weiland et al., 2012) although it is important to note that such studies have used very low resolutions e.g. 0.5 degrees. While the idea is attractive the application at resolutions appropriate for aquaculture site selection over large areas, let alone globally, is probably not realistic. There is also the added issue that aquaculture often takes place in very flat areas where the relative noise in data such as SRTM originating from surface features such as vegetation and buildings may make results unreliable.

7.3 MODIS as a tool for monitoring surface water for Bangladesh

Sakamoto et al. (2007) proposed a method for using MODIS data to classify areas as either land, water, or mixed based on the use of the Enhanced Vegetation Index (EVI) and a Land Surface Water Index (LSWI). This method was applied to Bangladesh as a means of indicating areas of flooding by Islam et al. (2010). While the authors make some effort to assess the accuracy of the data classification through the use of a single RADARSAT image no use was made of ground based data and the exact methodology used was somewhat unclear.

The current study made use of data collected on the ground to evaluate the accuracy of the method described by Sakamoto et al. (2007) for use within Bangladesh. A broad range of alternative classification options were considered using both single and multiple NDSIs and all classification methods were initially examined using higher resolution Landsat ETM+ data which has a similar range

of spectral bands to MODIS. Another key area of investigation was whether it was possible to make use of the two MODIS bands (red and near infrared) that are available at approximately 250 metre resolution compared with approximately 500 metres for the remaining bands in the visual and infrared parts of the spectrum, and whether this would improve overall results.

While best results from Landsat ETM+ data were obtained using a combination of two NDSIs it was found that the classification scheme originally described by Sakamoto et al. (2007) gave the most consistent results when using MODIS data. Careful visual inspection of the data classified using the method described by Sakamoto et al. (2007) but using the higher resolution data from the red and near infrared bands appeared better able to show smaller water surface water features such as rivers. However when tested against ground control points overall accuracy was very similar to that of the lower resolution data although the ability to separate water areas was improved.

A time series was created based on the Sakamoto method and using all available MODIS images covered the time period 18-02-2000 until 09-05-2014 resulting in 654 images. Areas of cloud were masked out and then the entire time series was analysed to show the percentage of the time series where water, or mixed and water pixels where present.

The surface water time series produced during the current study provides a highly useful insight in to surface water distribution and flood pattern in Bangladesh. It is also worth noting that the method described by Sakamoto et al. (2007) has been applied in an aquaculture development context within the Parana river basin (Handisyde et al., 2014). It's evaluation here against other classification methods using ground truth data can also be seen as highly valuable in terms of making best use of the data within the Bangladesh region.

In terms of future research and development in relation to remote sensing and surface water for Bangladesh, and similar low-lying areas appropriate for aquaculture, it is worth considering that land cover and flood patterns within the region are often complex and intricate with parcels of land frequently being small. Efforts to quantify water coverage within mixed pixels or produce higher resolution representations of water patterns using data such as that supplied by Landsat and ASTER at a range of time points may be useful in creating a greater understanding of flood distribution at a more local level. Ideally such work should involve further collection of ground truth data that coincides with the time of data acquisition. In reality such work is likely to be challenging due to the

presence of cloud cover which is especially common during the wetter parts of the year when flooding is most prevalent.

7.4 Land cover data set for Bangladesh

A 30m resolution land cover data set was produced using 9 Landsat ETM+ scenes that focused on late October early November 2008 and classified data as either: crops, trees, bare land, water, mixed vegetation and water, or urban areas . Overall 10 classification routines were tested, 9 of these formed part of the IDRISI software package and included commonly used classifiers such as 'maximum likelihood' and 'minimum distance' along with more complex classification routines. In addition, a unique decision tree type classifier was constructed for the current study.

Accuracy of classifications was assessed against two sets of ground control points (GCPs). The first set was produced using data collected in the field at a time that coincided with the acquisition dates of the ETM+ data used. An ideal sampling scheme would involve the collection of ground truth data at pre-selected random sample points that cover the study area and have sufficient density to provided an acceptable number of samples for each land cover class (Congalton and Green, 2009, Foody, 2002). The current work was focused on a large (national scale) study area and available resources and practical access issues meant that data collection was limited to a range of locations accessible by road. With this in mind a second set of ground truth data were produced using a stratified random sampling scheme in conjunction with careful inspection of high resolution true colour imagery as well as false colour ETM+ composites.

Classification accuracy results were considerably higher for the non-randomly distributed sample points. This would be expected to some extent as while different points were used for classifying data and accuracy assessment they were all derived from a common set of ground truth data collected over a limited number of sample sites. Under both accuracy assessments the two best performing classifiers were the decision tree classifier constructed for the current study and the Multi-Layer Perceptron (MLP) neural network based classifier. In the case of the stratified random GCPs the decision tree method achieved the best results with an overall accuracy of 80.5% and a Kappa value of 0.762.

To date, land cover data for Bangladesh beyond what is available from global products is very limited. The recent efforts to produce a global land cover data set based on 30m Landsat-derived data (Gong et al., 2013, Yu et al., 2013, Yu et al., 2014), while commendable, appear to have significant issues in accurately representing Bangladesh. With this in mind, while the land cover data set was produced in the current study was created with the intention of contributing to a site suitability assessment for inland aquaculture, it can be seen as a potentially valuable resource for other analyses where land cover information is required.

There is strong potential for further development and refinement of land cover data for Bangladesh. As well as improving accuracy efforts to gain an increased understanding of land use as well as land cover could be extremely useful. In this respect and as discussed in detail previously (section 5.4) use of multi-temporal data is suggested as a potential area for further research.

7.5 Bangladesh case study

Bangladesh is a financially poor country with an extremely high, and increasing, population density. Much of the country is extremely low lying and consists of the deltas and floodplains for a number of major river systems (Ganges, Brahmaputra, Meghan). Approximately 92.5% of the combined catchment area for these rives is outside of Bangladesh with much of this areas being subject to monsoon rainfall resulting Bangladesh experiencing significant cross border drainage (Mirza et al., 2001) resulting in widespread seasonal flooding. Despite these annual flood events lack of water during the dry season can also a potential issue (Yu et al., 2010). Many coastal regions are extremely low lying with polder systems being common. As a result many regions are potentially vulnerable to increases in sea level increases either through gradual increases in salinity potentially affecting crop production, or as a result of sudden flooding from storm surges that are associated with the relatively frequent cyclone activity within the region. With these points in mind it is unsurprising that Bangladesh is often highlighted as one of the most vulnerable nations in terms of climate change impact (Yu et al., 2010).

Fish from inland sources is an extremely important commodity within Bangladesh both in terms of food security as well as income generation (Belton et al., 2014, Dey et al., 2008, Karim et al., 2006). Aquaculture within Bangladesh has seen substantial development over recent decades while at the

same time capture fishery production would appear to have peaked with production figures suggesting that aquaculture production has now surpassed that of capture fisheries (FishStatJ, 2014).

The Landsat ETM+ based land cover layer described in chapter five was combined with the MODIS based surface water frequency distribution layer (chapter four) as well as elevation and population density data to produce site suitability layers for three potential aquaculture environments: conversion of fields to ponds, floodplain aquaculture, and homestead ponds. Modelled pond temperature (chapter four) was also incorporated along with water balance data with both these variables being considered for late 20th century conditions as well as under 2°C average global warming.

Overall the south and east of the country, and in particular the south east corner, were shown to be most suitable for aquaculture production of commonly cultured species. The effect of the 2°C warming scenario was to increase suitability in eastern regions and reduce it in the north west. The south west of the country remained relatively unchanged. While the north east of the country was projected to have increased water availability, most of the increase in suitability seen in most eastern regions was a result of projected higher average pond temperatures during the colder months of the year potentially allowing for improved growth performance of aquaculture species. The low suitability indicated for western regions was a result of projected high maximum pond temperatures during the warmest months of the year in combination with lower water balance values. The decrease in suitability seen in the north west of the country in response to the 2°C warming scenario was a result of increased maximum pond temperatures which especially when combined with limited water availability at the end of the dry season could potentially put cultured animals under stress resulting in reduced growth performance and/or loss of stock.

Use was made of SRTM data to highlight low elevation coastal zones and the MODIS surface water time series data were also used to show the impact of storm surge flooding resulting from cyclone Aila which struck Bangladesh on 25th May 2009. Particular attention was given to a polder area in the south west of the country that had been visited in October 2009 when it was still severely flooded after the cyclone Aila storm surge event. It was interesting to note that aquaculture was taking place in pens in the flood water illustrating its potential use as an adaptive strategy (Karim et al., 2014).

In summary the current study provides a valuable insight into site suitability for aquaculture in a number of environments at the national scale under both late 20th century conditions and a 2°C global warming scenario. Aquaculture is extremely important to Bangladesh. The sector has seen significant growth in recent years and there appears to be considerable scope for further expansion, a process in which site suitability modelling can be extremely useful. The effects of the 2°C warming scenario in the current assessment were mixed with the east of the country projected to see increased suitability for aquaculture while the while in the north west it is reduced due to high maximum modelled pond temperatures.

The idea that climate change may have both positive and negative implications is an important one, especially when it come to adaptation, a process in which aquaculture may be able to play an valuable role. In this respect there would appear to be scope for considerable further research within Bangladesh in which spatial modelling may play a role. It is suggested that the following topics be considered:

- Pond temperature data from a range of locations where temperature is taken at specified depths and for a number of time points throughout the day would be useful in validating and potentially calibrating models such as the one applied in the current study to local conditions. The investigation of more complex stratified pond temperature models (e.g. Cathcart and Wheaton, 1987, Culberson and Piedrahita, 1996, Losordo and Piedrahita, 1991) would be potentially useful in terms of providing insight into the effects of depth and diurnal temperature fluctuations. However in reality the data requirements for such exercises may be a limiting factor. With this in mind the investigation of simpler methods for estimating pond temperatures such as those based on air temperature relationships (e.g. Wax and Pote, 1990) may also be useful.
- There may be options for further development of site suitability models if more data is available. Studies that focus on specific regions within the country may also play a role in making use of more localised data sources.
- The incorporation of salinity data into spatial models could be valuable. Consideration should be given to the possibility of aquaculture of brackish water species offering an adaptation strategy in areas where saline intrusion has affected traditional agriculture. The aim should

be to promote and develop aquaculture in a sustainable way that doesn't exacerbate existing problems (Ahmed, 2013).

7.6 Concluding remarks

Globally aquaculture represents a highly important, and rapidly growing, industry both in terms of food security and income generation. While the potential effects of changing climate and atmospheric carbon dioxide concentrations have seen a moderate amount of research in relation to marine aquaculture in recent years, research focusing on impacts for inland aquaculture has been very limited. The literature that does exist, while valuable, largely takes the form of either general reviews of possible interactions and implications for aquaculture (e.g. Bell et al., 2013, Cochrane et al., 2009, Rosa et al., 2012), or focuses on specific issues, species, and locations (e.g. Hanson and Peterson, 2014, Villanueva et al., 2013).

For aquaculture operations to be successful they are dependent on a broad range of factors of which those relating to climate such as temperature and water availability play an extremely important role. Given that these factors vary depending on location, site suitability for aquaculture can be viewed as a spatial problem. Potential changes in climate are also predicted to show considerable variability depending on location and as such add considerable uncertainty to potential future aquaculture site suitability.

The current study provides an important global investigation of potential vulnerability of aquaculture related livelihoods to changing climate. In addition highly valuable and unique site suitability assessments are made for inland pond-based aquaculture both at the global scale and for the potentially vulnerable nation of Bangladesh. Site suitability is assessed in relation to both recent climate conditions as well as those under 2°C global warming with results suggesting areas of both reduced and increased suitability for warm water aquaculture.

It is suggested here that a focus on the positive, as well as negative, effects of climate change is important in terms of aiding adaptation. In this context assessments such as the current one can be highly useful in providing insight into where negative impacts may affect existing aquaculture methods and where alternative strategies may need to be sought. Conversely by understanding

where positive impacts are likely it may be possible to capitalise on changing conditions and locations that may previously been unfavourable.

While the current assessment provides a strong starting point for understanding climate related site suitability issues for aquaculture, there is considerable scope for further work and development in this so far under researched field. It is hoped that the work presented here can contribute to future efforts.

REFERENCES

ADGER, N. W. & KELLY, M. P. 1999. Social vulnerability to climate change and the architecture of entitlements. *Mitigation and adaptation strategies for global change,* 4**,** 253-266.

ADGER, W. N., BROOKS, N., BENTHAM, G., AGNEW, M. & ERIKSEN, S. 2004. *New indicators of vulnerability and adaptive capacity*, Tyndall Centre for Climate Change Research Norwich.

AGUILAR-MANJARREZ, J. & NATH, S. S. 1998. *A strategic reassessment of fish farming potential in Africa*, Food & Agriculture Org.

AHMED, N. 2013. Linking prawn and shrimp farming towards a green economy in Bangladesh: Confronting climate change. *Ocean & Coastal Management,* 75**,** 33-42.

AHMED, N., BROWN, J. H. & MUIR, J. F. 2008. Freshwater prawn farming in gher systems in southwest Bangladesh. *Aquaculture Economics & Management,* 12**,** 207-223.

AHMED, N. & GARNETT, S. T. 2011. Integrated rice-fish farming in Bangladesh: Meeting the challenges of food security. *Food Security,* 3**,** 81-92.

ALLEN, R., G, PEREIRA, S., RAES, D. & SMITH, M. 1998. Crop evapotranspiration—Guidelines for computing crop water requirements. *FAO Irrigation and drainage paper,* 56.

ALLISON, E., ADGER, W., BADJECK, M.-C., BROWN, K., CONWAY, D., DULVY, N., HALLS, A. & PERRY, A. 2005. Effects of climate change on the sustainability of capture and enhancement fisheries important to the poor: analysis of the vulnerability and adaptability of fisherfolk living in poverty. Final Technical Report.

ALLISON, E. H. 2011. *Aquaculture, fisheries, poverty and food security* [Online]. Available: http://www.worldfishcenter.org/resource_centre/WF_2971.pdf.

ALLISON, E. H., PERRY, A. L., BADJECK, M. C., NEIL ADGER, W., BROWN, K., CONWAY, D., HALLS, A. S., PILLING, G. M., REYNOLDS, J. D. & ANDREW, N. L. 2009. Vulnerability of national economies to the impacts of climate change on fisheries. *Fish and fisheries,* 10**,** 173-196.

ALLRED, E. R., MANSON, P. W., SCHWARTZ, C. M., GOLANY, P. & REINKE, J. W. 1971. Continuation of Studies on the Hydrology of Ponds and Small Lakes. Univ. Minn. Agric. Exp. St. Tech. Bull. 274. .

ANWAR, J. 2011. Market study on some freshwater farmed fish: Tilapia and pangas. Consultancy report prepared for the PRICE Project.

AUSTRALIAN_BUREAU_OF_METEOROLOGY. 2013. Available: http://www.bom.gov.au/cyclone/faq/ [Accessed 03-08-14.

BAI, L. 2010. *Comparison and Validation of Five Land Cover Products over the African Continent.* Lund University, Sweden.

BALL, G. H. & HALL, D. J. 1965. ISODATA, a novel method of data analysis and pattern classification. DTIC Document.

BARMAN, B. K. & LITTLE, D. C. 2006. Nile tilapia (*Oreochromis niloticus*) seed production in irrigated rice-fields in Northwest Bangladesh-an approach appropriate for poorer farmers? *Aquaculture,* 261**,** 72-79.

BARMAN, B. K. & LITTLE, D. C. 2011. Use of hapas to produce Nile tilapia (*Oreochromis niloticus* L.) seed in household foodfish ponds: A participatory trial with small-scale farming households in Northwest Bangladesh. *Aquaculture,* 317**,** 214-222.

BATJES, N. 2009. Harmonized soil profile data for applications at global and continental scales: updates to the WISE database. *Soil Use and Management,* 25**,** 124-127.

BÉCHET, Q., SHILTON, A., PARK, J. B., CRAGGS, R. J. & GUIEYSSE, B. 2011. Universal temperature model for shallow algal ponds provides improved accuracy. *Environmental science & technology,* 45**,** 3702-3709.

BEITINGER, T. L., BENNETT, W. A. & MCCAULEY, R. W. 2000. Temperature tolerances of North American freshwater fishes exposed to dynamic changes in temperature. *Environmental biology of fishes,* 58**,** 237-275.

BELL, J. D., GANACHAUD, A., GEHRKE, P. C., GRIFFITHS, S. P., HOBDAY, A. J., HOEGH-GULDBERG, O., JOHNSON, J. E., LE BORGNE, R., LEHODEY, P. & LOUGH, J. M. 2013. Mixed responses of tropical Pacific fisheries and aquaculture to climate change. *Nature Climate Change,* 3**,** 591-599.

BELTON, B. & AZAD, A. 2012. The characteristics and status of pond aquaculture in Bangladesh. *Aquaculture,* 358-359**,** 196-204.

BELTON, B., HAQUE, M. M. & LITTLE, D. C. 2012. Does Size Matter? Reassessing the Relationship between Aquaculture and Poverty in Bangladesh. *Journal of Development Studies,* 48**,** 904-922.

BELTON, B., KARIM, M., THILSTED, S. H., MURSHED-E-JAHAN, K., COLLIS, W. & PHILLIPS, M. 2011. *Review of Aquaculture and Fish Consumption in Bangladesh*, WorldFish.

BELTON, B., VAN ASSELDONK, I. J. M. & THILSTED, S. H. 2014. Faltering fisheries and ascendant aquaculture: Implications for food and nutrition security in Bangladesh. *Food Policy,* 44**,** 77-87.

BERRY, P., ROUNSEVELL, M., HARRISON, P. & AUDSLEY, E. 2006. Assessing the vulnerability of agricultural land use and species to climate change and the role of policy in facilitating adaptation. *Environmental Science & Policy,* 9**,** 189-204.

BEVERIDGE, M., THILSTED, S., PHILLIPS, M., METIAN, M., TROELL, M. & HALL, S. 2013. Meeting the food and nutrition needs of the poor: the role of fish and the opportunities and challenges emerging from the rise of aquaculturea. *Journal of fish biology,* 83**,** 1067-1084.

BICHERON, P., DEFOURNY, P., BROCKMANN, C., SCHOUTEN, L., VANCUTSEM, C., HUC, M., BONTEMPS, S., LEROY, M., ACHARD, F. & HEROLD, M. 2008. Globcover: products description and validation report. *MEDIAS France, Toulouse*.

BLANCHARD, J. L., JENNINGS, S., HOLMES, R., HARLE, J., MERINO, G., ALLEN, J. I., HOLT, J., DULVY, N. K. & BARANGE, M. 2012. Potential consequences of climate change for primary production and fish production in large marine ecosystems. *Philosophical Transactions of the Royal Society B: Biological Sciences,* 367**,** 2979-2989.

BLANCHET, S., HELMUS, M. R., BROSSE, S. & GRENOUILLET, G. 2014. Regional vs local drivers of phylogenetic and species diversity in stream fish communities. *Freshwater Biology,* 59**,** 450-462.

BLASCHKE, T., HAY, G. J., KELLY, M., LANG, S., HOFMANN, P., ADDINK, E., QUEIROZ FEITOSA, R., VAN DER MEER, F., VAN DER WERFF, H. & VAN COILLIE, F. 2014. Geographic Object-Based Image Analysis–Towards a new paradigm. *ISPRS Journal of Photogrammetry and Remote Sensing,* 87**,** 180-191.

BLOOMER, J. 2012. *Homestead Aquaculture in Bangladesh: Current Status and Future Directions.* MSc, KING'S COLLEGE LONDON, UNIVERSITY OF LONDON.

BOLOORANI, A. D., ERASMI, S. & KAPPAS, M. Multi-source image reconstruction: exploitation of EO-1/ALI in Landsat-7/ETM+ SLC-off gap filling. Electronic Imaging 2008, 2008. International Society for Optics and Photonics, 681219-681219-12.

BOLSTAD, P. V. & LILLESAND, T. 1991. Rapid maximum likelihood classification. *Photogrammetric engineering and remote sensing,* 57**,** 67-74.

BOSTOCK, J., MCANDREW, B., RICHARDS, R., JAUNCEY, K., TELFER, T., LORENZEN, K., LITTLE, D., ROSS, L., HANDISYDE, N. & GATWARD, I. 2010. Aquaculture: global status and trends. *Philosophical Transactions of the Royal Society B: Biological Sciences,* 365**,** 2897-2912.

BOYD, C., WOOD, C. & THUNJAI, T. 2002. Aquaculture pond bottom soil quality management. Pond Dynamics, Aquaculture Collaborative Research Support Program. *Oregon State University, Corvallis***,** 41.

BOYD, C. E. 1982. Hydrology of small experimental fish ponds at Auburn, Alabama. *Transactions of the American Fisheries Society,* 111**,** 638-644.

BOYD, C. E. Water conservation measures in fish farming. Fifth Conference on Applied Climatology. American Meteorological Society, Boston, Massachusetts, USA, 1987. 88-91.

BOYD, C. E. 1990. Water Quality in Ponds for Aquaculture. Alabama Agricultural Experiment Station, Auburn University. Birmingham Publishing.

BOYD, C. E. 1995. *Bottom Soils, sediment, and pond aquaculture*, Chapman & Hall, NY.

BOYD, C. E. & J.R., B. 1997. Pond bottom soils. *In:* BOYD, C. E. & EGNA, H. S. (eds.) *Dynamics of Pond Aquaculture.* CRC Press, Boca Raton/New York.

BOYD, C. E. & SHELTON, J. L. 1984. Observations on the hydrology and morphometry of ponds on the Auburn University fisheries Research Unit. Bulletin 558, Alabama Agricultural Experiment Station, Auburn University, Alabama. .

BOYD, C. E. & TUCKER, C. S. 1998. *Pond aquaculture water quality management*, Kluwer Academic Publishers, Boston.

BRAMMER, H. 2014. Bangladesh's dynamic coastal regions and sea-level rise. *Climate Risk Management,* 1**,** 51-62.

BROWN, C., FULTON, E., HOBDAY, A., MATEAR, R., POSSINGHAM, H., BULMAN, C., CHRISTENSEN, V., FORREST, R., GEHRKE, P. & GRIBBLE, N. 2010. Effects of climate-driven primary production change on marine food webs: implications for fisheries and conservation. *Global Change Biology,* 16**,** 1194-1212.

BROWN, J. C., KASTENS, J. H., COUTINHO, A. C., VICTORIA, D. D. C. & BISHOP, C. R. 2013. Classifying multiyear agricultural land use data from Mato Grosso using time-series MODIS vegetation index data. *Remote Sensing of Environment,* 130**,** 39-50.

BUISSON, L., GRENOUILLET, G., VILLÉGER, S., CANAL, J. & LAFFAILLE, P. 2013. Toward a loss of functional diversity in stream fish assemblages under climate change. *Global change biology,* 19**,** 387-400.

CALLAWAY, R., SHINN, A. P., GRENFELL, S. E., BRON, J. E., BURNELL, G., COOK, E. J., CRUMLISH, M., CULLOTY, S., DAVIDSON, K. & ELLIS, R. P. 2012. Review of climate change impacts on marine aquaculture in the UK and Ireland. *Aquatic Conservation: Marine and Freshwater Ecosystems,* 22**,** 389-421.

CAMPBELL, J. B. & WYNNE, R. H. 2011. *Introduction to Remote Sensing: Fifth Edition,* New York, Guilford Press.

CARRÃO, H., ARAUJO, A., GONÇALVES, P. & CAETANO, M. 2010. Multitemporal MERIS images for land-cover mapping at a national scale: a case study of Portugal. *International Journal of Remote Sensing,* 31**,** 2063-2082.

CATHCART, T. P. & WHEATON, F. W. 1987. Modeling temperature distribution in freshwater ponds. *Aquacultural Engineering,* 6**,** 237-257.

CH, S. B., SHAILENDER, M., SARMAL, K. & KISHOR, B. 2012. Effects of temperature and salinity on growth, hatching rate and survival of the giant freshwater prawn, *Macrobrachium rosenbergii* (de Man) under captive conditions. *International Journal of Bioassays,* 1**,** 150-155.

CHAITANAWISUTI, N., SANTHAWEESUK, W. & WATTAYAKORN, G. 2013. The combined effects of temperature and salinity on survival of postlarvae tiger prawn *Penaeus monodon* under laboratory conditions. *Agricultural Sciences,* 4**,** 53.

CHASSOT, E., BONHOMMEAU, S., DULVY, N. K., MÉLIN, F., WATSON, R., GASCUEL, D. & LE PAPE, O. 2010. Global marine primary production constrains fisheries catches. *Ecology letters,* 13**,** 495-505.

CHATTERJEE, N., PAL, A., MANUSH, S., DAS, T. & MUKHERJEE, S. 2004. Thermal tolerance and oxygen consumption of (*Labeo rohita)* and (*Cyprinus carpio*) early fingerlings acclimated to three different temperatures. *Journal of Thermal Biology,* 29**,** 265-270.

CHEN, J., ZHU, X., VOGELMANN, J. E., GAO, F. & JIN, S. 2011. A simple and effective method for filling gaps in Landsat ETM+ SLC-off images. *Remote Sensing of Environment,* 115**,** 1053-1064.

CHEN, Y., HUANG, C., TICEHURST, C., MERRIN, L. & THEW, P. 2013. An evaluation of MODIS daily and 8-day composite products for floodplain and wetland inundation mapping. *Wetlands,* 33**,** 823-835.

CHERVINSKI, J. 1982. Environmental physiology of tilapias. *In:* PULLIN, R. S. V. & LOWE-MCCONNELL, R. H. (eds.) *The biology and culture of tilapias.* International Center for Living Aquatic Resources Management: Manila, Philippines.

CHIPMAN, J. & LILLESAND, T. 2007. Satellite-based assessment of the dynamics of new lakes in southern Egypt. *International Journal of Remote Sensing,* 28**,** 4365-4379.

CIESIN n.d. Global Rural-Urban Mapping Project (GRUMP). *In:* CENTER FOR INTERNATIONAL EARTH SCIENCE INFORMATION NETWORK (CIESIN), C. U. (ed.).

COCHE, A. G. 1985. Simple methods for aquaculture: Soil and freshwater fish culture. *FAO Training Series (FAO)*.

COCHRANE, K., DE YOUNG, C., SOTO, D. & BAHRI, T. 2009. Climate change implications for fisheries and aquaculture. *FAO Fisheries and aquaculture technical paper,* 530**,** 212.

COLT, J. 1984. Computation of dissolved gas concentrations in water as functions of temperature, salinity, and pressure. *American Fisheries Society special publication (USA)*.

CONGALTON, R. G. & GREEN, K. 2009. *Assessing the accuracy of remotely sensed data: principles and practices (2nd ed.),* Boca Raton, FL, CRC press.

COOK, J., NUCCITELLI, D., GREEN, S. A., RICHARDSON, M., WINKLER, B., PAINTING, R., WAY, R., JACOBS, P. & SKUCE, A. 2013. Quantifying the consensus on anthropogenic global warming in the scientific literature. *Environmental Research Letters,* 8**,** 024024.

COOLEY, S. R., LUCEY, N., KITE-POWELL, H. & DONEY, S. C. 2012. Nutrition and income from molluscs today imply vulnerability to ocean acidification tomorrow. *Fish and Fisheries,* 13**,** 182-215.

CULBERSON, S. D. & PIEDRAHITA, R. H. 1996. Aquaculture pond ecosystem model: temperature and dissolved oxygen prediction—mechanism and application. *Ecological modelling,* 89**,** 231-258.

DAS, T., PAL, A., CHAKRABORTY, S., MANUSH, S., CHATTERJEE, N. & MUKHERJEE, S. 2004. Thermal tolerance and oxygen consumption of Indian Major Carps acclimated to four temperatures. *Journal of Thermal Biology,* 29**,** 157-163.

DAS, T., PAL, A., CHAKRABORTY, S., MANUSH, S., SAHU, N. & MUKHERJEE, S. 2005. Thermal tolerance, growth and oxygen consumption of *Labeo rohita* fry (Hamilton, 1822) acclimated to four temperatures. *Journal of Thermal Biology,* 30**,** 378-383.

DASGUPTA, S., HUQ, M., KHAN, Z. H., AHMED, M. M. Z., MUKHERJEE, N., KHAN, M. F. & PANDEY, K. D. 2010. Vulnerability of Bangladesh to cyclones in a changing climate: potential damages and adaptation cost. *World Bank Policy Research Working Paper number 5280*.

DE SILVA, S. S. & SOTO, D. 2009. Climate change and aquaculture: potential impacts, adaptation and mitigation. FAO Fisheries and Aquaculture Technical Paper 530.

DEWAN, A. M., ISLAM, M. M., KUMAMOTO, T. & NISHIGAKI, M. 2007. Evaluating flood hazard for land-use planning in Greater Dhaka of Bangladesh using remote sensing and GIS techniques. *Water resources management,* 21**,** 1601-1612.

DEWAN, A. M., KUMAMOTO, T. & NISHIGAKI, M. 2006. Flood hazard delineation in Greater Dhaka, Bangladesh using an integrated GIS and remote sensing approach. *Geocarto International,* 21**,** 33-38.

DEWAN, A. M. & YAMAGUCHI, Y. 2009a. Land use and land cover change in Greater Dhaka, Bangladesh: using remote sensing to promote sustainable urbanization. *Applied Geography,* 29**,** 390-401.

DEWAN, A. M. & YAMAGUCHI, Y. 2009b. Using remote sensing and GIS to detect and monitor land use and land cover change in Dhaka Metropolitan of Bangladesh during 1960–2005. *Environmental monitoring and assessment,* 150**,** 237-249.

DEY, M. M., BOSE, M. L. & ALAM, M. F. 2008. *Country Case Study: Development and Status of Freshwater Aquaculture in Bangladesh*, WorldFish.

DíAZ HERRERA, F., SIERRA URIBE, E., FERNANDO BÜCKLE RAMIREZ, L. & GARRIDO MORA, A. 1998. Critical thermal maxima and minima of *Macrobrachium rosenbergii* (Decapoda: Palaemonidae). *Journal of thermal biology,* 23**,** 381-385.

DONEY, S. C., FABRY, V. J., FEELY, R. A. & KLEYPAS, J. A. 2009. Ocean acidification: the other CO2 problem. *Marine Science,* 1.

DOUBLEDAY, Z. A., CLARKE, S. M., LI, X., PECL, G. T., WARD, T. M., BATTAGLENE, S., FRUSHER, S., GIBBS, P. J., HOBDAY, A. J. & HUTCHINSON, N. 2013. Assessing the risk of climate change to aquaculture: a case study from south-east Australia. *Aquaculture Environment Interactions,* 3**,** 163–175.

DROBNE, S. & LISEC, A. 2009. Multi-attribute decision analysis in GIS: Weighted linear combination and ordered weighted averaging. *Informatica (Ljubljana),* 33**,** 459-474.

DUFRESNE, J.-L. & BONY, S. 2008. An assessment of the primary sources of spread of global warming estimates from coupled atmosphere-ocean models. *Journal of Climate,* 21**,** 5135-5144.

DUGAN, P., SUGUNAN, V., WELCOMME, R., BÉNÉ, C., BRUMMETT, R., BEVERIDGE, M., ABBAN, K., AMERASINGHE, U., ARTHINGTON, A., BLIXT, M., SLOANS, C., PRADEEP, K., JACKIE, K., JEPPE, K., SOPHIE, N. K. & JANE, T. 2007. Inland fisheries and aquaculture. *In:* MOLDEN, D. (ed.) *Water for Life: A Comprehensive Assessment of Water Management in Agriculture.* Washington D.C., USA: Earthscan and International Water Management Institute.

EASTMAN, J. 1999. Multi-criteria evaluation and GIS. *In:* LONGLEY, P. A., GOODCHILD, M. F., MAGUIRE, D. J. & RHIND, D. W. (eds.) *Geographical information systems.* Wiley, New York.

EASTMAN, J. R. 2012. Idrisi Selva Manual. Clark University, Worcester.

EGNA, H. S. & BOYD, C. E. 1997. *Dynamics of pond aquaculture*, CRC press.

ELVIDGE, C. D., TUTTLE, B. T., SUTTON, P. C., BAUGH, K. E., HOWARD, A. T., MILESI, C., BHADURI, B. & NEMANI, R. 2007. Global distribution and density of constructed impervious surfaces. *Sensors,* 7**,** 1962-1979.

EMELYANOVA, I., MCVICAR, T., VAN NIEL, T., LI, L. & VAN DIJK, A. 2012. On blending Landsat-MODIS surface reflectances in two landscapes with contrasting spectral, spatial and temporal dynamics. WIRADA Project 3.4: Technical Report, CSIRO Water for a Healthy Country Flagship, Australia, 72 pages, https://publications. csiro. au/rpr/pub.

ERICSON, J. P., VÖRÖSMARTY, C. J., DINGMAN, S. L., WARD, L. G. & MEYBECK, M. 2006. Effective sea-level rise and deltas: causes of change and human dimension implications. *Global and Planetary Change,* 50**,** 63-82.

ERNST, D. H., WATANABE, W. O., ELLINGSON, L. J., WICKLUND, R. I. & OLLA, B. L. 1991. Commercial-Scale Production of Florida Red Tilapia Seed in Low-and Brackish-Salinity Tanks. *Journal of the World Aquaculture Society,* 22**,** 36-44.

ESRI 1984. Final Report UNEP/FAO world and Africa data base. Redlands, California

FAO 1976. *A framework for land evaluation. Soils Bulletin, vol. 32,* Rome, Italy, Food and Agriculture Organization of the United Nations.

FAO 2012. *The State of World Fisheries and Aquaculture 2012*, FOOD & AGRICULTURE ORGN.

FAO 2014. The State of World Fisheries and Aquaculture. Food and Agriculture Organization of the United Nations, Rome, Italy.

FAO/IIASA/ISRIC/ISS-CAS/JRC 2012. Harmonized World Soil Database (version 1.2). *In:* FOOD AND AGRICULTURE ORGANIZATION OF THE UNITED NATIONS, R., ITALY (ed.).

FAOSTAT. 2014. *FOOD AND AGRICULTURE ORGANIZATION OF THE UNITED NATIONS STATISTICS DIVISION* [Online]. [Accessed 23-09-2014.

FENG, L., HU, C., CHEN, X., CAI, X., TIAN, L. & GAN, W. 2012. Assessment of inundation changes of Poyang Lake using MODIS observations between 2000 and 2010. *Remote Sensing of Environment,* 121**,** 80-92.

FERREIRA, J., HAWKINS, A., MONTEIRO, P., MOORE, H., SERVICE, M., PASCOE, P., RAMOS, L. & SEQUEIRA, A. 2008. Integrated assessment of ecosystem-scale carrying capacity in shellfish growing areas. *Aquaculture,* 275**,** 138-151.

FICKE, A. D., MYRICK, C. A. & HANSEN, L. J. 2007. Potential impacts of global climate change on freshwater fisheries. *Reviews in Fish Biology and Fisheries,* 17**,** 581-613.

FIELDS, R., LOWE, S. S., KAMINSKI, C., WHITT, G. S. & PHILIPP, D. P. 1987. Critical and chronic thermal maxima of northern and Florida largemouth bass and their reciprocal F1 and F2 hybrids. *Transactions of the American Fisheries Society,* 116**,** 856-863.

FISHER, J. B., TU, K. P. & BALDOCCHI, D. D. 2008. Global estimates of the land–atmosphere water flux based on monthly AVHRR and ISLSCP-II data, validated at 16 FLUXNET sites. *Remote Sensing of Environment,* 112**,** 901-919.

FISHSTATJ. 2013. *FishStatJ. FAO, Rome.* [Online]. Available: http://www.fao.org/fishery/statistics/software/fishstatj/en [Accessed 07-06-13.

FISHSTATJ. 2014. *FishStatJ* [Online]. Available: http://www.fao.org/fishery/statistics/software/fishstatj/en [Accessed 20-08-2014.

FLINT, L. E. & FLINT, A. L. 2008. A basin-scale approach to estimating stream temperatures of tributaries to the Lower Klamath River, California. *Journal of environmental quality,* 37**,** 57-68.

FOODY, G. M. 2002. Status of land cover classification accuracy assessment. *Remote sensing of environment,* 80**,** 185-201.

FORDHAM, D. A., WIGLEY, T. M. & BROOK, B. W. 2011. Multi-model climate projections for biodiversity risk assessments. *Ecological Applications,* 21**,** 3317-3331.

FRIEDL, M. A., SULLA-MENASHE, D., TAN, B., SCHNEIDER, A., RAMANKUTTY, N., SIBLEY, A. & HUANG, X. 2010. MODIS Collection 5 global land cover: Algorithm refinements and characterization of new datasets. *Remote Sensing of Environment,* 114**,** 168-182.

FRITZ, J. J., MEREDITH, D. D. & MIDDLETON, A. C. 1980. Non-steady state bulk temperature determination for stabilization ponds. *Water Research,* 14**,** 413-420.

FRITZ, S., SEE, L., MCCALLUM, I., SCHILL, C., OBERSTEINER, M., VAN DER VELDE, M., BOETTCHER, H., HAVLÍK, P. & ACHARD, F. 2011. Highlighting continued uncertainty in global land cover maps for the user community. *Environmental Research Letters,* 6**,** 044005.

FÜSSEL, H.-M. 2010. Review and quantitative analysis of indices of climate change exposure, adaptive capacity, sensitivity, and impacts. Washington, DC: World Bank.

GALL, M. 2007. *Indices of Social Vulnerabililty to Natural Hazards: A Comparative Evaluation.* PhD, University of South Carolina.

GALLEGO, F. J. 2010. A population density grid of the European Union. *Population and Environment,* 31**,** 460-473.

GAO, F., MASEK, J., SCHWALLER, M. & HALL, F. 2006. On the blending of the Landsat and MODIS surface reflectance: Predicting daily Landsat surface reflectance. *Geoscience and Remote Sensing, IEEE Transactions on,* 44**,** 2207-2218.

GASSERT, F., LANDIS, M., LUCK, M., REIG, P. & SHIAO, T. 2013. Aqueduct global maps 2.0. *Water Resources Institute (WRI): Washington, DC*.

GAZEAU, F., QUIBLIER, C., JANSEN, J. M., GATTUSO, J. P., MIDDELBURG, J. J. & HEIP, C. H. 2007. Impact of elevated CO2 on shellfish calcification. *Geophysical Research Letters,* 34.

GIAP, D. H., YI, Y., CUONG, N. X., LUU, L. T., DINH BANG, T. S., PROVINCE, B. N., LIN, V. C. K. & DIANA, J. S. 2004. AQUACULTURE CRSP 21ST ANNUAL TECHNICAL REPORT.

GIAP, D. H., YI, Y. & YAKUPITIYAGE, A. 2005. GIS for land evaluation for shrimp farming in Haiphong of Vietnam. *Ocean & coastal management,* 48**,** 51-63.

GIRI, C., PENGRA, B., ZHU, Z., SINGH, A. & TIESZEN, L. L. 2007. Monitoring mangrove forest dynamics of the Sundarbans in Bangladesh and India using multi-temporal satellite data from 1973 to 2000. *Estuarine, Coastal and Shelf Science,* 73**,** 91-100.

GIRI, C. & SHRESTHA, S. 1996. Land cover mapping and monitoring from NOAA AVHRR data in Bangladesh. *International Journal of Remote Sensing,* 17**,** 2749-2759.

GONG, P., WANG, J., YU, L., ZHAO, Y., ZHAO, Y., LIANG, L., NIU, Z., HUANG, X., FU, H. & LIU, S. 2013. Finer resolution observation and monitoring of global land cover: first mapping results with Landsat TM and ETM+ data. *International Journal of Remote Sensing,* 34**,** 2607-2654.

GREEN, B. W. & BOYD, C. E. 1995. Water budgets for fish ponds in the dry tropics. *Aquacultural engineering,* 14**,** 347-356.

GREGORY, R., TOUFIQUE, K. A. & NURUZZAMAN, M. 2007. Common interests, private gains: a study of co-operative floodplain aquaculture. The WorldFish Center.

GRIFFITHS, D., VAN KHANH, P. & TRONG, T. Q. 2010. *Cultured Aquatic Species Information Programme. Pangasius hypophthalmus.* [Online]. Available: http://www.fao.org/fishery/culturedspecies/Pangasius_hypophthalmus/en [Accessed 05-08-2014.

GUERSCHMAN, J. P., WARREN, G., BYRNE, G., LYMBURNER, L., MUELLER, N. & VAN DIJK, A. I. 2011. *MODIS-based standing water detection for flood and large reservoir mapping: algorithm development and applications for the Australian continent*, CSIRO.

GUTH, P. Geomorphometric comparison of ASTER GDEM and SRTM. A special joint symposium of ISPRS Technical Commission IV & AutoCarto in conjunction with ASPRS/CaGIS, 2010.

HABASHY, M. M. & HASSAN, M. M. S. 2011. Effects of temperature and salinity on growth and reproduction of the freshwater prawn, *Macrobrachium rosenbergii* (Crustacea- Decapoda) in Egypt. *International journal of environmental science and engineering,* 1**,** 83-90.

HAIDER, M. Z. & HOSSAIN, M. Z. 2013. Impact of salinity on livelihood strategies of farmers. *Journal of soil science and plant nutrition,* 13**,** 417-431.

HAJEK, B. F. & BOYD, C. E. 1994. Rating soil and water information for aquaculture. *Aquacultural engineering,* 13**,** 115-128.

HALL, O., STROH, E. & PAYA, F. 2012. From census to grids: comparing gridded population of the world with Swedish census records. *The Open Geogr J,* 5**,** 1-5.

HALLS, A., PAYNE, A., ALAM, S. & BARMAN, S. 2008. Impacts of flood control schemes on inland fisheries in Bangladesh: guidelines for mitigation. *Hydrobiologia,* 609**,** 45-58.

HANDISYDE, N., LACALLE, D. S., ARRANZ, S. & ROSS, L. G. 2014. Modelling the flood cycle, aquaculture development potential and risk using MODIS data: A case study for the floodplain of the Rio Paraná, Argentina. *Aquaculture,* 422**,** 18-24.

HANDISYDE, N. T., ROSS, L. G., BADJECK, M.-C. & ALLISON, E. H. 2006. The effects of climate change on world aquaculture: a global perspective. Final Technical Report. Stirling, U.K.: Stirling Institute of Aquaculture.

HANSEN, J., SATO, M. & RUEDY, R. 2012. Perception of climate change. *Proceedings of the National Academy of Sciences,* 109**,** E2415-E2423.

HANSEN, M., DEFRIES, R., TOWNSHEND, J. R. & SOHLBERG, R. 2000. Global land cover classification at 1 km spatial resolution using a classification tree approach. *International Journal of Remote Sensing,* 21**,** 1331-1364.

HANSEN, M. & REED, B. 2000. A comparison of the IGBP DISCover and University of Maryland 1 km global land cover products. *International Journal of Remote Sensing,* 21**,** 1365-1373.

HANSON, K. C. & PETERSON, D. P. 2014. Modeling the Potential Impacts of Climate Change on Pacific Salmon Culture Programs: An Example at Winthrop National Fish Hatchery. *Environmental management,* 54**,** 433-448.

HARRIS, I., JONES, P., OSBORN, T. & LISTER, D. 2014. Updated high-resolution grids of monthly climatic observations–the CRU TS3. 10 Dataset. *International Journal of Climatology,* 34**,** 623-642.

HASANUZZAMAN, A. M., RAHMAN, M. & ISLAM, S. 2011. Practice and Economics of Freshwater Prawn Farming in Seasonally Saline Rice Field in Bangladesh. *Mesopot. J. Mar. Sci,* 26**,** 69-78.

HASSAN, B., EL-SALHIA, M., KHALIFA, A., ASSEM, H., AL BASOMY, A. & EL-SAYED, M. 2013. Environmental isotonicity improves cold tolerance of Nile tilapia, *Oreochromis niloticus,* in Egypt. *The Egyptian Journal of Aquatic Research,* 39**,** 59-65.

HASSON, S., LUCARINI, V., PASCALE, S. & BÖHNER, J. 2013. Seasonality of the hydrological cycle in major South and Southeast Asian River Basins as simulated by PCMDI/CMIP3 experiments. *Earth System Dynamics Discussions,* 4**,** 627-675.

HAWKINS, A., DUARTE, P., FANG, J., PASCOE, P., ZHANG, J., ZHANG, X. & ZHU, M. 2002. A functional model of responsive suspension-feeding and growth in bivalve shellfish, configured and validated for the scallop *Chlamys farreri* during culture in China. *Journal of Experimental Marine Biology and Ecology,* 281**,** 13-40.

HENDERSON-SELLERS, B. 1984. *Engineering limnology*, Pitman Advanced Pub. Program Boston.

HEROLD, M., MAYAUX, P., WOODCOCK, C., BACCINI, A. & SCHMULLIUS, C. 2008. Some challenges in global land cover mapping: An assessment of agreement and accuracy in existing 1 km datasets. *Remote Sensing of Environment,* 112**,** 2538-2556.

HIJMANS, R. J., CAMERON, S. E., PARRA, J. L., JONES, P. G. & JARVIS, A. 2005. Very high resolution interpolated climate surfaces for global land areas. *International journal of climatology,* 25**,** 1965-1978.

HOQUE, R., NAKAYAMA, D., MATSUYAMA, H. & MATSUMOTO, J. 2011. Flood monitoring, mapping and assessing capabilities using RADARSAT remote sensing, GIS and ground data for Bangladesh. *Natural Hazards,* 57**,** 525-548.

HOSSAIN, M., LIN, C., DEMAINE, H., TOKUNAGA, M. & HUSSAIN, M. 2003a. Land use zoning for solar salt production in Cox's Bazar coast of Bangladesh: A Remote Sensing and GIS analysis. *Asian Journal of Geoinformatics,* 3**,** 69-77.

HOSSAIN, M. S., CHOWDHURY, S. R., DAS, N. G. & RAHAMAN, M. M. 2007. Multi-criteria evaluation approach to GIS-based land-suitability classification for tilapia farming in Bangladesh. *Aquaculture International,* 15**,** 425-443.

HOSSAIN, M. S., CHOWDHURY, S. R., DAS, N. G., SHARIFUZZAMAN, S. & SULTANA, A. 2009. Integration of GIS and multicriteria decision analysis for urban aquaculture development in Bangladesh. *Landscape and Urban Planning,* 90**,** 119-133.

HOSSAIN, M. S. & DAS, N. G. 2010. GIS-based multi-criteria evaluation to land suitability modelling for giant prawn *Macrobrachium rosenbergii* farming in Companigonj Upazila of Noakhali, Bangladesh. *Computers and electronics in agriculture,* 70**,** 172-186.

HOSSAIN, M. S. & LIN, C. K. 2001. Land Use Zoning for Integrated Coastal Zone Management. *ITCZM monograph***,** 24.

HOSSAIN, M. S., LIN, C. K. & HUSSAIN, M. Z. 2003b. Remote sensing and GIS applications for suitable mangrove afforestation area selection in the coastal zone of Bangladesh. *Geocarto International,* 18**,** 61-65.

HOUGHTON, J. 2009. *Global warming: the complete briefing*, Cambridge University Press.

HUANG, C., CHEN, Y. & WU, J. 2014. Mapping spatio-temporal flood inundation dynamics at large river basin scale using time-series flow data and MODIS imagery. *International Journal of Applied Earth Observation and Geoinformation,* 26**,** 350-362.

HUANG, S., LI, J. & XU, M. 2012. Water surface variations monitoring and flood hazard analysis in Dongting Lake area using long-term Terra/MODIS data time series. *Natural hazards,* 62**,** 93-100.

HUNTINGFORD, C., JONES, P. D., LIVINA, V. N., LENTON, T. M. & COX, P. M. 2013. No increase in global temperature variability despite changing regional patterns. *Nature,* 500**,** 327-330.

ICLARM_AND_GTZ 1991. The context of small-scale integrated agriculture-aquaculture systems in Africa: a case study of Malawi. ICLARM Stud. Rev. 18.

IFN. 2009. *International Flood Network* [Online]. Available: http://www.internationalfloodnetwork.org/aila.htm [Accessed 07-08-2014.

IPCC 2007a. *Climate Change 2007: impacts, adaptation and vulnerability: contribution of Working Group II to the fourth assessment report of the Intergovernmental Panel on Climate Change,* Cambridge, UK, Cambridge University Press.

IPCC 2007b. *IPCC, 2007: climate change 2007: the physical science basis*.

IPCC 2013. *Climate change 2013: The physical science basis. Intergovernmental Panel on Climate Change, Working Group I Contribution to the IPCC Fifth Assessment Report (AR5)(Cambridge Univ Press, New York)*.

ISLAM, A., BALA, S. & HAQUE, M. 2010. Flood inundation map of Bangladesh using MODIS time-series images. *Journal of Flood Risk Management,* 3**,** 210-222.

ISLAM, M. & SADO, K. 2000a. Flood hazard assessment in Bangladesh using NOAA AVHRR data with geographical information system. *Hydrological Processes,* 14**,** 605-620.

ISLAM, M. M. & SADO, K. 2000b. Development of flood hazard maps of Bangladesh using NOAA-AVHRR images with GIS. *Hydrological Sciences Journal,* 45**,** 337-355.

ISLAM, M. S., OKI, T., KANAE, S., HANASAKI, N., AGATA, Y. & YOSHIMURA, K. 2007. A grid-based assessment of global water scarcity including virtual water trading. *Integrated Assessment of Water Resources and Global Change.* Springer.

JABAR, A., SADIQ, A., SULONG, G. & GEORGE, L. E. 2014. SURVEY ON GAP FILLING ALGORITHMS IN LANDSAT 7 ETM+ IMAGES. *Journal of Theoretical & Applied Information Technology,* 63.

JAHAN, K. M., AHMED, M. & BELTON, B. 2010. The impacts of aquaculture development on food security: Lessons from Bangladesh. *Aquaculture Research,* 41**,** 481-495.

JARVIS, A., REUTER, H. I., NELSON, A. & GUEVARA, E. 2008. Hole-filled SRTM for the globe Version 4. *available from the CGIAR-CSI SRTM 90m Database (http://srtm. csi. cgiar. org)*.

JENSEN, J. R. 2006. *Remote Sensing of the Environment: An Earth Resource Perspective,* Upper Saddle River, NJ, Prentice Hall.

JI, L., ZHANG, L. & WYLIE, B. 2009. Analysis of dynamic thresholds for the normalized difference water index. *Photogrammetric Engineering & Remote Sensing,* 75**,** 1307-1317.

JIN, S., HOMER, C., YANG, L., XIAN, G., FRY, J., DANIELSON, P. & TOWNSEND, P. A. 2013. Automated cloud and shadow detection and filling using two-date Landsat imagery in the USA. *International Journal of Remote Sensing,* 34**,** 1540-1560.

JONES, P., LISTER, D., OSBORN, T., HARPHAM, C., SALMON, M. & MORICE, C. 2012. Hemispheric and large-scale land-surface air temperature variations: An extensive revision and an update to 2010. *Journal of Geophysical Research: Atmospheres (1984–2012),* 117.

JONES, P. G. & THORNTON, P. K. 2003. The potential impacts of climate change on maize production in Africa and Latin America in 2055. *Global environmental change,* 13**,** 51-59.

KAPETSKY, J. M. 1994. *A strategic assessment of warm-water fish farming potential in Africa*, Food & Agriculture Org.

KAPETSKY, J. M. 2000. Present applications and future needs of meteorological and climatological data in inland fisheries and aquaculture. *Agricultural and Forest meteorology,* 103**,** 109-117.

KAPETSKY, J. M. & NATH, S. S. 1997. *A strategic assessment of the potential for freshwater fish farming in Latin America*, Food & Agriculture Org.

KAPTUÉ TCHUENTÉ, A. T., ROUJEAN, J.-L. & DE JONG, S. M. 2011. Comparison and relative quality assessment of the GLC2000, GLOBCOVER, MODIS and ECOCLIMAP land cover data sets at the African continental scale. *International Journal of Applied Earth Observation and Geoinformation,* 13**,** 207-219.

KARIM, F., PETHERAM, C., MARVANEK, S., TICEHURST, C., WALLACE, J., GOUWELEEUW, B., CHAN, F., MARINOVA, D. & ANDERSSON, R. The use of hydrodynamic modelling and remote sensing to estimate floodplain inundation and flood discharge in a large tropical catchment. 19th International Congress on Modelling and Simulation (MODSIM), Perth, Australia, 2011.

KARIM, M., AHMED, M., TALUKDER, R. K., TASLIM, M. A. & RAHMAN, H. Z. 2006. Policy working paper : dynamic agribusiness-focused aquaculture for poverty reduction and economic growth in Bangladesh. The WorldFish Center.

KARIM, M., CASTINE, S., BROOKS, A., BEARE, D., BEVERIDGE, M. & PHILLIPS, M. 2014. Asset or liability? Aquaculture in a natural disaster prone area. *Ocean & Coastal Management,* 96**,** 188-197.

KARIM, M. F. & MIMURA, N. 2008. Impacts of climate change and sea-level rise on cyclonic storm surge floods in Bangladesh. *Global Environmental Change,* 18**,** 490-500.

KARTHIK, M., SURI, J., SAHARAN, N. & BIRADAR, R. 2005. Brackish water aquaculture site selection in Palghar Taluk, Thane district of Maharashtra, India, using the techniques of remote sensing and geographical information system. *Aquacultural engineering,* 32**,** 285-302.

KAWARAZUKA, N. 2010. The contribution of fish intake, aquaculture, and small-scale fisheries to improving food and nutrition security: a literature review. *WorldFish Center Working Paper.*

KELLY, A. M. & KOHLER, C. C. 1997. Climate, site, and pond design. *In:* EGNA, H. S. & BOYD, C. E. (eds.) *Dynamics of Pond Aquaculture.*

KENNEDY, J., RAYNER, N., SMITH, R., PARKER, D. & SAUNBY, M. 2011a. Reassessing biases and other uncertainties in sea surface temperature observations measured in situ since 1850: 1. Measurement and sampling uncertainties. *Journal of Geophysical Research: Atmospheres (1984–2012),* 116.

KENNEDY, J., RAYNER, N., SMITH, R., PARKER, D. & SAUNBY, M. 2011b. Reassessing biases and other uncertainties in sea surface temperature observations measured in situ since 1850: 2. Biases and homogenization. *Journal of Geophysical Research: Atmospheres (1984–2012),* 116.

KHAN, S. I., HONG, Y., WANG, J., YILMAZ, K. K., GOURLEY, J. J., ADLER, R. F., BRAKENRIDGE, G. R., POLICELL, F., HABIB, S. & IRWIN, D. 2011. Satellite remote sensing and hydrologic modeling for flood inundation mapping in Lake Victoria Basin: Implications for hydrologic prediction in ungauged basins. *Geoscience and Remote Sensing, IEEE Transactions on,* 49**,** 85-95.

KIRUI, K., KAIRO, J., BOSIRE, J., VIERGEVER, K. M., RUDRA, S., HUXHAM, M. & BRIERS, R. A. 2013. Mapping of mangrove forest land cover change along the Kenya coastline using Landsat imagery. *Ocean & Coastal Management,* 83**,** 19-24.

KLEMETSON, S. L. & ROGERS, G. L. 1985. Aquaculture pond temperature modeling. *Aquacultural Engineering,* 4**,** 191-208.

KNAPP, K. R., KRUK, M. C., LEVINSON, D. H., DIAMOND, H. J. & NEUMANN, C. J. 2010. The international best track archive for climate stewardship (IBTrACS) unifying tropical cyclone data. *Bulletin of the American Meteorological Society,* 91**,** 363-376.

KOCH, H. & GRÜNEWALD, U. 2010. Regression models for daily stream temperature simulation: case studies for the river Elbe, Germany. *Hydrological Processes,* 24**,** 3826-3836.

KONGKEO, H. 2005. *Cultured Aquatic Species Information Programme. Penaeus monodon.* [Online]. Available: http://www.fao.org/fishery/culturedspecies/Penaeus_monodon/en [Accessed 15-08-2014.

KRANT, J., MOTZKIN, F. & GORDIN, H. 1982. Modelling temperatures and salinities of mixed seawater fish ponds. *Aquaculture,* 27**,** 377-388.

KUNDA, M., AZIM, M. E., WAHAB, M. A., DEWAN, S., ROOS, N. & THILSTED, S. H. 2008. Potential of mixed culture of freshwater prawn (*Macrobrachium rosenbergii*) and self-recruiting small species mola (*Amblypharyngodon mola*) in rotational rice-fish/prawn culture systems in Bangladesh. *Aquaculture Research,* 39**,** 506-517.

KUTTY 1987. Site Selection For Aquaculture: Physical Features of Water. United Nations Development Program. Food and Agriculture Organisation of the United Nations. Nigerian Institute for Oceanography and Marine Research. Project RAF/82/009.

LANDSCAN. 2008. Available: http://web.ornl.gov/sci/landscan/landscan_documentation.shtml.

LEWIS, M., BATES, P., HORSBURGH, K., NEAL, J. & SCHUMANN, G. 2013. A storm surge inundation model of the northern Bay of Bengal using publicly available data. *Quarterly Journal of the Royal Meteorological Society,* 139**,** 358-369.

LI, B., YAN, Q. & ZHANG, L. Flood monitoring and analysis over the middle reaches of Yangtze River basin using MODIS time-series imagery. Geoscience and Remote Sensing Symposium (IGARSS), 2011 IEEE International, 2011. IEEE, 807-810.

LINACRE, E. T. 1993. Data-sparse estimation of lake evaporation, using a simplified Penman equation. *Agricultural and Forest Meteorology,* 64**,** 237-256.

LIVINGSTONE, D. M. & LOTTER, A. F. 1998. The relationship between air and water temperatures in lakes of the Swiss Plateau: a case study with paleolimnological implications. *Journal of Paleolimnology,* 19**,** 181-198.

LONGDILL, P. C., HEALY, T. R. & BLACK, K. P. 2008. An integrated GIS approach for sustainable aquaculture management area site selection. *Ocean & Coastal Management,* 51**,** 612-624.

LORENTZEN, T. 2008. Modeling climate change and the effect on the Norwegian salmon farming industry. *Natural Resource Modeling,* 21**,** 416-435.

LOSORDO, T. M. 1998. *The characterization and modeling of thermal and oxygen stratification in aquaculture ponds.* University of California, Davis.

LOSORDO, T. M. & PIEDRAHITA, R. H. 1991. Modelling temperature variation and thermal stratification in shallow aquaculture ponds. *Ecological modelling,* 54**,** 189-226.
LOVELAND, T., REED, B., BROWN, J., OHLEN, D., ZHU, Z., YANG, L. & MERCHANT, J. 2000. Development of a global land cover characteristics database and IGBP DISCover from 1 km AVHRR data. *International Journal of Remote Sensing,* 21**,** 1303-1330.
LU, D. & WENG, Q. 2007. A survey of image classification methods and techniques for improving classification performance. *International journal of Remote sensing,* 28**,** 823-870.
LUTZ, A., IMMERZEEL, W., SHRESTHA, A. & BIERKENS, M. 2014. Consistent increase in High Asia's runoff due to increasing glacier melt and precipitation. *Nature Climate Change*.
MALIK, K. 2013. Human development report 2013. The rise of the South: Human progress in a diverse world.
MANANDHAR, R., ODEH, I. O. & ANCEV, T. 2009. Improving the accuracy of land use and land cover classification of Landsat data using post-classification enhancement. *Remote Sensing,* 1**,** 330-344.
MANSON, P. W., SCHWARTZ, E. R. & ALLRED, E. R. 1968. Some aspects of the hydrology of ponds and small lakes. University of Minnesota Agricultural Experiment Station Technical Bulletin 257. .
MANUSH, S., PAL, A., CHATTERJEE, N., DAS, T. & MUKHERJEE, S. 2004. Thermal tolerance and oxygen consumption of *Macrobrachium rosenbergii* acclimated to three temperatures. *Journal of Thermal Biology,* 29**,** 15-19.
MARINE_REGIONS. 2013. *Exclusive Economic Zones Boundaries (EEZ)* [Online]. Available: http://www.marineregions.org/downloads.php [Accessed 09-05-2013.
MARKHAM, B. L., STOREY, J. C., WILLIAMS, D. L. & IRONS, J. R. 2004. Landsat sensor performance: history and current status. *Geoscience and Remote Sensing, IEEE Transactions on,* 42**,** 2691-2694.
MARTINUZZI, S., GOULD, W. A. & GONZÁLEZ, O. M. R. 2007. Creating cloud-free Landsat ETM+ data sets in tropical landscapes: cloud and cloud-shadow removal. General Technical Report IITF-GTR-32. United States Department of Agriculture Forest Service International Institute of Tropical Forestry.
MASOOD, M. & TAKEUCHI, K. 2012. Assessment of flood hazard, vulnerability and risk of mid-eastern Dhaka using DEM and 1D hydrodynamic model. *Natural hazards,* 61**,** 757-770.
MAXWELL, S., SCHMIDT, G. & STOREY, J. 2007. A multi-scale segmentation approach to filling gaps in Landsat ETM+ SLC-off images. *International Journal of Remote Sensing,* 28**,** 5339-5356.
MAYAUX, P., EVA, H., GALLEGO, J., STRAHLER, A. H., HEROLD, M., AGRAWAL, S., NAUMOV, S., DE MIRANDA, E. E., DI BELLA, C. M. & ORDOYNE, C. 2006. Validation of the global land cover 2000 map. *Geoscience and Remote Sensing, IEEE Transactions on,* 44**,** 1728-1739.
MCCARTY, D. F. 1998. *Essentials of Soil Mechanics and Foundations,* Upper Saddle River, New Jersey, Prentice Hall.
MCCARTY, J., CANZIANI, O., LEARY, N., DOKKEN, D. & WHITE, K. 2001. Climate Change 2001. Impacts, Adaptation, and vulnerability (Contribution of Working Group II to the Third Assessment Report of the Intergovernmental Panel on Climate Change). Cambridge University Press, Cambridge.
MCCAULEY, R. & BEITINGER, T. 1992. Predicted effects of climate warming on the commercial culture of the channel catfish, *Ictalurus punctatus*. *Geojournal,* 28**,** 61-66.
MEEHL, G. A., COVEY, C., TAYLOR, K. E., DELWORTH, T., STOUFFER, R. J., LATIF, M., MCAVANEY, B. & MITCHELL, J. F. 2007. The WCRP CMIP3 multimodel dataset: A new era in climate change research. *Bulletin of the American Meteorological Society,* 88**,** 1383-1394.

METZGER, M. J., LEEMANS, R. & SCHRÖTER, D. 2005. A multidisciplinary multi-scale framework for assessing vulnerabilities to global change. *International Journal of Applied Earth Observation and Geoinformation,* 7**,** 253-267.

MINGWEI, Z., QINGBO, Z., ZHONGXIN, C., JIA, L., YONG, Z. & CHONGFA, C. 2008. Crop discrimination in Northern China with double cropping systems using Fourier analysis of time-series MODIS data. *International Journal of Applied Earth Observation and Geoinformation,* 10**,** 476-485.

MIRZA, M. 2002. Global warming and changes in the probability of occurrence of floods in Bangladesh and implications. *Global environmental change,* 12**,** 127-138.

MIRZA, M. M. Q. 2011. Climate change, flooding in South Asia and implications. *Regional Environmental Change,* 11**,** 95-107.

MIRZA, M. M. Q., WARRICK, R. & ERICKSEN, N. 2003. The implications of climate change on floods of the Ganges, Brahmaputra and Meghna rivers in Bangladesh. *Climatic Change,* 57**,** 287-318.

MIRZA, M. Q., WARRICK, R., ERICKSEN, N. & KENNY, G. 2001. Are floods getting worse in the Ganges, Brahmaputra and Meghna basins? *Global Environmental Change Part B: Environmental Hazards,* 3**,** 37-48.

MODIS_LAND_COVER_TEAM 2003. Validation of the consistent year 2003 V003 MODIS land cover product.

MOHSENI, O. & STEFAN, H. 1999. Stream temperature/air temperature relationship: a physical interpretation. *Journal of Hydrology,* 218**,** 128-141.

MORICE, C. P., KENNEDY, J. J., RAYNER, N. A. & JONES, P. D. 2012. Quantifying uncertainties in global and regional temperature change using an ensemble of observational estimates: The HadCRUT4 data set. *Journal of Geophysical Research: Atmospheres (1984–2012),* 117.

MORRILL, J. C., BALES, R. C. & CONKLIN, M. H. 2005. Estimating stream temperature from air temperature: implications for future water quality. *Journal of Environmental Engineering,* 131**,** 139-146.

MOSNER, M. S. & AULENBACH, B. T. 2003. Comparison of methods used to estimate lake evaporation for a water budget of Lake Seminole, southwestern Georgia and northwestern Florida. *Proc., 2003 Georgia Water Resources Conf.*

MURRAY-HUDSON, M., WOLSKI, P., CASSIDY, L., BROWN, M., THITO, K., KASHE, K. & MOSIMANYANA, E. 2014. Remote Sensing-derived hydroperiod as a predictor of floodplain vegetation composition. *Wetlands Ecology and Management***,** 1-14.

MURRAY, S., FOSTER, P. & PRENTICE, I. 2012. Future global water resources with respect to climate change and water withdrawals as estimated by a dynamic global vegetation model. *Journal of Hydrology,* 448**,** 14-29.

MYINT, S. W., GOBER, P., BRAZEL, A., GROSSMAN-CLARKE, S. & WENG, Q. 2011. Per-pixel vs. object-based classification of urban land cover extraction using high spatial resolution imagery. *Remote Sensing of Environment,* 115**,** 1145-1161.

NAKAEGAWA, T. 2011. Uncertainty in land cover datasets for global land-surface models derived from 1-km global land cover datasets. *Hydrological Processes,* 25**,** 2703-2714.

NAKICENOVIC, N. & SWART, R. 2000. Special report on emissions scenarios. *Special Report on Emissions Scenarios, Edited by Nebojsa Nakicenovic and Robert Swart, pp. 612. ISBN 0521804930. Cambridge, UK: Cambridge University Press, July 2000.,* 1.

NARITA, D., REHDANZ, K. & TOL, R. S. 2012. Economic costs of ocean acidification: a look into the impacts on global shellfish production. *Climatic Change,* 113**,** 1049-1063.

NASA., U. 2004. Gap-fill Algorithm Methodology: Phase 2.

NASA_SSE_6.0 n.d. NASA Surface meteorology and Solar Energy: Global Data Sets.

NATH, S. S. 1996. *Development of a decision support system for pond aquaculture.* PhD, Oregon State University.

NATH, S. S., BOLTE, J. P., ROSS, L. G. & AGUILAR-MANJARREZ, J. 2000. Applications of geographical information systems (GIS) for spatial decision support in aquaculture. *Aquacultural Engineering,* 23**,** 233-278.

NEUMANN, D. W., RAJAGOPALAN, B. & ZAGONA, E. A. 2003. Regression model for daily maximum stream temperature. *Journal of Environmental Engineering,* 129**,** 667-674.

NEW, M., LISTER, D., HULME, M. & MAKIN, I. 2002. A high-resolution data set of surface climate over global land areas. *Climate research,* 21**,** 1-25.

NEW, M. B. 2002. *Farming Freshwater Prawns: A Manual for the Culture of the Giant River Prawn (Macrobrachium Rosenbergii)*, Food & Agriculture Org.

NGUYEN, A. L., DANG, V. H., BOSMA, R. H., VERRETH, J. A., LEEMANS, R. & DE SILVA, S. S. 2014. Simulated Impacts of Climate Change on Current Farming Locations of Striped Catfish (*Pangasianodon hypophthalmus*; Sauvage) in the Mekong Delta, Vietnam. *Ambio***,** 1-10.

NOWREEN, S., MURSHED, S. B., ISLAM, A. S., BHASKARAN, B. & HASAN, M. A. 2014. Changes of rainfall extremes around the haor basin areas of Bangladesh using multi-member ensemble RCM. *Theoretical and Applied Climatology***,** 1-15.

O'BRIEN, K., LEICHENKO, R., KELKAR, U., VENEMA, H., AANDAHL, G., TOMPKINS, H., JAVED, A., BHADWAL, S., BARG, S. & NYGAARD, L. 2004. Mapping vulnerability to multiple stressors: climate change and globalization in India. *Global environmental change,* 14**,** 303-313.

OKI, T., AGATA, Y., KANAE, S., SARUHASHI, T. & MUSIAKE, K. 2003. Global water resources assessment under climatic change in 2050 using TRIP. *International Association of Hydrological Sciences, Publication***,** 124-133.

ONOGI, K., TSUTSUI, J., KOIDE, H., SAKAMOTO, M., KOBAYASHI, S., HATSUSHIKA, H., MATSUMOTO, T., YAMAZAKI, N., KAMAHORI, H. & TAKAHASHI, K. 2007. The JRA-25 reanalysis. *J. Meteor. Soc. Japan,* 85**,** 369-432.

OSBORN, T. J. & BRIFFA, K. R. 2006. The spatial extent of 20th-century warmth in the context of the past 1200 years. *Science,* 311**,** 841-844.

OUMA, Y. O. & TATEISHI, R. 2006. A water index for rapid mapping of shoreline changes of five East African Rift Valley lakes: an empirical analysis using Landsat TM and ETM+ data. *International Journal of Remote Sensing,* 27**,** 3153-3181.

PANT, J., BARMAN, B. K., MURSHED-E-JAHAN, K., BELTON, B. & BEVERIDGE, M. 2014. Can aquaculture benefit the extreme poor? A case study of landless and socially marginalized Adivasi (ethnic) communities in Bangladesh. *Aquaculture,* 418-419**,** 1-10.

PARISH, E. S., KODRA, E., STEINHAEUSER, K. & GANGULY, A. R. 2012. Estimating future global per capita water availability based on changes in climate and population. *Computers & Geosciences,* 42**,** 79-86.

PARSONS, D. 1949. The hydrology of a small area near Auburn, Alabama, United States Soil Conservation Service. SCS-TP-85, Washington, District of Columbia, USA.

PETHICK, J. & ORFORD, J. D. 2013. Rapid rise in effective sea-level in southwest Bangladesh: Its causes and contemporary rates. *Global and Planetary Change,* 111**,** 237-245.

PHILIPPART, J.-C. & RUWET, J.-C. Ecology and distribution of tilapias. *In:* PULLIN, R. S. V. & LOWE-MCCONNELL, R. H., eds. The biology and culture of tilapias, 1982 Manila, Philippines. 15-60.

PIERCE, D. W., BARNETT, T. P., SANTER, B. D. & GLECKLER, P. J. 2009. Selecting global climate models for regional climate change studies. *Proceedings of the National Academy of Sciences,* 106**,** 8441-8446.

PONCE-PALAFOX, J., MARTINEZ-PALACIOS, C. A. & ROSS, L. G. 1997. The effects of salinity and temperature on the growth and survival rates of juvenile white shrimp, *Penaeus vannamei,* Boone, 1931. *Aquaculture,* 157**,** 107-115.

POULIOTTE, J., SMIT, B. & WESTERHOFF, L. 2009. Adaptation and development: Livelihoods and climate change in Subarnabad, Bangladesh. *Climate and Development,* 1**,** 31-46.

PRIESTLEY, C. & TAYLOR, R. 1972. On the assessment of surface heat flux and evaporation using large-scale parameters. *Monthly weather review,* 100**,** 81-92.

PRINGLE, M., SCHMIDT, M. & MUIR, J. 2009. Geostatistical interpolation of SLC-off Landsat ETM+ images. *ISPRS Journal of Photogrammetry and Remote Sensing,* 64**,** 654-664.

PURKIS, S. J. & KLEMAS, V. V. 2011. *Remote sensing and global environmental change*, John Wiley & Sons.

RAGBIRSINGH, Y. & DE SOUZA, G. 2005. Site Suitability for Aquaculture Development on the Caroni River Basin, Trinidad West Indies Using GIS. *Proceedings of the Gulf and Caribbean Fisheries Institute,* 56**,** 661-674.

RAHMAN, A. F., DRAGONI, D., DIDAN, K., BARRETO-MUNOZ, A. & HUTABARAT, J. A. 2013. Detecting large scale conversion of mangroves to aquaculture with change point and mixed-pixel analyses of high-fidelity MODIS data. *Remote Sensing of Environment,* 130**,** 96-107.

RAHMAN, M., LUND, T. & BRYCESON, I. 2011. Salinity impacts on agro-biodiversity in three coastal, rural villages of Bangladesh. *Ocean & Coastal Management,* 54**,** 455-468.

RAJITHA, K., MUKHERJEE, C. & VINU CHANDRAN, R. 2007. Applications of remote sensing and GIS for sustainable management of shrimp culture in India. *Aquacultural Engineering,* 36**,** 1-17.

RAKOCY, J. E. 2005. *Cultured Aquatic Species Information Programme. Oreochromis niloticus.* [Online]. Available: http://www.fao.org/fishery/culturedspecies/Oreochromis_niloticus/en [Accessed 02-08-2014.

RAMIREZ-VILLEGAS, J., CHALLINOR, A. J., THORNTON, P. K. & JARVIS, A. 2013. Implications of regional improvement in global climate models for agricultural impact research. *Environmental Research Letters,* 8**,** 024018.

REDOWAN, M., AKTER, S. & ISLAM, N. 2014. Analysis of forest cover change at Khadimnagar National Park, Sylhet, Bangladesh, using Landsat TM and GIS data. *Journal of Forestry Research,* 25**,** 393-400.

REICHLER, T. & KIM, J. 2008. How well do coupled models simulate today's climate? *Bulletin of the American Meteorological Society,* 89**,** 303-311.

ROHDE, R., MULLER, R. A., JACOBSEN, R., MULLER, E. & WICKHAM, C. 2013. A New Estimate of the Average Earth Surface Land Temperature Spanning 1753 to 2011. *Geoinformatics & Geostatistics: An Overview,* 01.

ROSA, R., MARQUES, A. & NUNES, M. L. 2012. Impact of climate change in Mediterranean aquaculture. *Reviews in Aquaculture,* 4**,** 163-177.

ROSS, L., TELFER, T., FALCONER, L., SOTO, D., AGUILAR-MANJARREZ, J., ASMAH, R., BERMÚDEZ, J., BEVERIDGE, M., BYRON, C., CLÉMENT, A., CORNER, R., COSTA-PIERCE, B. A., CROSS, S., DE WIT, M., DONG, S., FERREIRA, J. G., KAPETSKY, J. M., KARAKASSIS, I., LESCHEN, W., LITTLE, D., LUNDEBYE, A. K., MURRAY, F. J., PHILLIPS, M., RAMOS, L., SADEK, S., SCOTT, P. C., VALLE-LEVINSON, A., WALEY, D., WHITE, P. G. & ZHU, C. 2013. Carrying capacities and site selection within the ecosystem approach to aquaculture. *In:* ROSS, L. G., TELFER, T., FALCONER, L., SOTO, D. & AGUILAR-MANJARREZ, J. (eds.) *Site selection and carrying capacities for inland and coastal aquaculture.*

ROSS, L. G., FALCONER, L. L., CAMPOS MENDOZA, A. & MARTINEZ PALACIOS, C. A. 2011. Spatial modelling for freshwater cage location in the Presa Adolfo Mateos Lopez (El Infiernillo), Michoacán, México. *Aquaculture Research,* 42**,** 797-807.

ROSS, L. G., HANDISYDE, N. & NIMMO, D.-C. 2009. Spatial decision support in aquaculture: the role of geographical information systems and remote sensing. *In:* BURNELL, G. & ALLAN, G. (eds.) *New technologies in aquaculture: improving production efficiency, quality and environmental management.*

ROY, D. P., BORAK, J. S., DEVADIGA, S., WOLFE, R. E., ZHENG, M. & DESCLOITRES, J. 2002. The MODIS land product quality assessment approach. *Remote Sensing of Environment,* 83**,** 62-76.

ROY, D. P., JU, J., LEWIS, P., SCHAAF, C., GAO, F., HANSEN, M. & LINDQUIST, E. 2008. Multi-temporal MODIS–Landsat data fusion for relative radiometric normalization, gap filling, and prediction of Landsat data. *Remote Sensing of Environment,* 112**,** 3112-3130.

ROZENSTEIN, O. & KARNIELI, A. 2011. Comparison of methods for land-use classification incorporating remote sensing and GIS inputs. *Applied Geography,* 31**,** 533-544.

RYAN, P. J., HARLEMAN, D. R. & STOLZENBACH, K. D. 1974. Surface heat loss from cooling ponds. *Water Resources Research,* 10**,** 930-938.

SAKAMOTO, T., VAN NGUYEN, N., KOTERA, A., OHNO, H., ISHITSUKA, N. & YOKOZAWA, M. 2007. Detecting temporal changes in the extent of annual flooding within the Cambodia and the Vietnamese Mekong Delta from MODIS time-series imagery. *Remote sensing of environment,* 109**,** 295-313.

SALAM, M., KHATUN, N. & ALI, M. 2005. Carp farming potential in Barhatta Upazilla, Bangladesh: a GIS methodological perspective. *Aquaculture,* 245**,** 75-87.

SALAM, M. A. & ROSS, L. G. Optimising site selection for development of shrimp (*Penaeus monodon*) and mud crab (*Scylla serrata*) culture in South-western Bangladesh. 14th Annual Conference on Geographic Information Systems, Proceedings of the GIS, 2000. 13-16.

SALAM, M. A., ROSS, L. G. & BEVERIDGE, C. 2003. A comparison of development opportunities for crab and shrimp aquaculture in southwestern Bangladesh, using GIS modelling. *Aquaculture,* 220**,** 477-494.

SANDERS, B. F. 2007. Evaluation of on-line DEMs for flood inundation modeling. *Advances in Water Resources,* 30**,** 1831-1843.

SCARAMUZZA, P., MICIJEVIC, E. & CHANDER, G. 2004. SLC gap-filled products phase one methodology. *Landsat Technical Notes*.

SCEPAN, J. 1999. Thematic validation of high-resolution global land-cover data sets. *Photogrammetric Engineering and Remote Sensing,* 65**,** 1051-1060.

SCHIERMEIER, Q. 2006. The costs of global warming. *Nature,* 439**,** 374-375.

SCHNEIDER, A., FRIEDL, M. A. & POTERE, D. 2009. A new map of global urban extent from MODIS satellite data. *Environmental Research Letters,* 4**,** 044003.

SCHNEIDER, A., FRIEDL, M. A. & POTERE, D. 2010. Mapping global urban areas using MODIS 500-m data: New methods and datasets based on 'urban ecoregions'. *Remote Sensing of Environment,* 114**,** 1733-1746.

SCHRÖTER, D., POLSKY, C. & PATT, A. G. 2005. Assessing vulnerabilities to the effects of global change: an eight step approach. *Mitigation and Adaptation Strategies for Global Change,* 10**,** 573-595.

SEDAC/CIESIN n.d. Gridded Population of the World

SESNIE, S. E., GESSLER, P. E., FINEGAN, B. & THESSLER, S. 2008. Integrating Landsat TM and SRTM-DEM derived variables with decision trees for habitat classification and change detection in complex neotropical environments. *Remote Sensing of Environment,* 112**,** 2145-2159.

SEXTON, J. O., SONG, X.-P., FENG, M., NOOJIPADY, P., ANAND, A., HUANG, C., KIM, D.-H., COLLINS, K. M., CHANNAN, S. & DIMICELI, C. 2013. Global, 30-m resolution continuous fields of tree cover: Landsat-based rescaling of MODIS vegetation continuous fields with lidar-based estimates of error. *International Journal of Digital Earth,* 6**,** 427-448.

SHALABY, A. & TATEISHI, R. 2007. Remote sensing and GIS for mapping and monitoring land cover and land-use changes in the Northwestern coastal zone of Egypt. *Applied Geography,* 27**,** 28-41.

SHARMA, K., MOHAPATRA, B., DAS, P., SARKAR, B. & CHAND, S. 2013. Water budgets for freshwater aquaculture ponds with reference to effluent volume. *Agricultural Sciences,* 2013.

SHARMA, S., WALKER, S. C. & JACKSON, D. A. 2008. Empirical modelling of lake water-temperature relationships: a comparison of approaches. *Freshwater biology,* 53**,** 897-911.

SIFA, L., CHENHONG, L., DEY, M., GAGALAC, F. & DUNHAM, R. 2002. Cold tolerance of three strains of Nile tilapia, *Oreochromis niloticus*, in China. *Aquaculture,* 213**,** 123-129.

SINGH, O. P., KHAN, T. M. A. & RAHMAN, M. S. 2000. The vulnerability assessment of the SAARC coastal region due to sea level rise: Bangladesh case. SMRC-No.3 ed.

SPERNA WEILAND, F., VAN BEEK, L., KWADIJK, J. & BIERKENS, M. 2012. Global patterns of change in discharge regimes for 2100. *Hydrology and Earth System Sciences,* 16**,** 1047-1062.

STEHMAN, S. V. & CZAPLEWSKI, R. L. 1998. Design and analysis for thematic map accuracy assessment: fundamental principles. *Remote Sensing of Environment,* 64**,** 331-344.

STONE, N. M. & BOYD, C. E. 1989. *Seepage from fishponds*, Alabama Agricultural Experiment Station.

STURROCK, A., WINTER, T. & ROSENBERRY, D. 1992. Energy budget evaporation from Williams Lake: A closed lake in north central Minnesota. *Water Resources Research,* 28**,** 1605-1617.

SUGIYAMA, S., STAPLES, D. J. & FUNGE-SMITH, S. 2004. *Status and potential of fisheries and aquaculture in Asia and the Pacific*, Food and Agriculture organization of the United Nations, Regional Office for Asia and the Pacific.

SWINBANK, W. C. 1963. Long-wave radiation from clear skies. *Quarterly Journal of the Royal Meteorological Society,* 89**,** 339-348.

TATEM, A. J., CAMPIZ, N., GETHING, P. W., SNOW, R. W. & LINARD, C. 2011. The effects of spatial population dataset choice on estimates of population at risk of disease. *Population health metrics,* 9**,** 4.

TAYLOR, K. E., STOUFFER, R. J. & MEEHL, G. A. 2012. An overview of CMIP5 and the experiment design. *Bulletin of the American Meteorological Society,* 93**,** 485-498.

TEICHERT-CODDINGTON, D., STONE, N. & PHELPS, R. 1988. Hydrology of fish culture ponds in Gualaca, Panama. *Aquacultural Engineering,* 7**,** 309-320.

THEMATICMAPPING.ORG. 2013. *World Borders Dataset. Available under a Creative Commons Attribution-Share Alike License.* [Online]. Available: http://thematicmapping.org/downloads/world_borders.php [Accessed 21-11-13.

THILSTED, S. The potential of nutrient-rich small fish species in aquaculture to improve human nutrition and health. *In:* SUBASINGHE, R., ARTHUR, J., BARTLEY, D., DE SILVA, S., HALWART, M., HISHAMUNDA, N., MOHAN, C. & SORGELOOS, P., eds. Proceedings of the Global Conference on Aquaculture 2010. Farming the waters for people and food., 2013. FAO/NACA, 57-73.

THONING, K., KITZIS, D. & CROTWELL, A. 2013. Atmospheric Carbon Dioxide Dry Air Mole Fractions from Quasi-Continuous Measurements at Barrow, Alaska; Mauna Loa, Hawaii; American Samoa; and South Pole, 1973–2012; National Oceanic and Atmospheric Administration.

TRABUCCO, A. & ZOMER, R. 2010. Global soil water balance geospatial database. *CGIAR Consortium for Spatial Information. Published online, available from the CGIAR-CSI GeoPortal at: http://www. cgiar-csi. org*.

TROXLER, R. W. & THACKSTON, E. L. 1977. Predicting the rate of warming of rivers below hydroelectric installations. *Journal (Water Pollution Control Federation)*, 1902-1912.
TUCK, G., GLENDINING, M. J., SMITH, P., HOUSE, J. I. & WATTENBACH, M. 2006. The potential distribution of bioenergy crops in Europe under present and future climate. *Biomass and Bioenergy,* 30, 183-197.
TUCKER, C. S. & HARGREAVES, J. A. 2008. *Environmental best management practices for aquaculture,* Oxford, Blackwell Publishing Ltd.
TURKER, M. & ARIKAN, M. 2004. Field-Based Crop Mapping through Sequential Masking Classification of Multi-temporal LANDSAT-7 ETM+ Images in Karacabey, Turkey. *Int. Arch. Ph. RS,* 35, 192-197.
UDEL_AIRT_PRECIP n.d. University of Delaware Air Temperature & Precipitation.
UN_POPULATION. 2013. *United Nations, Department of Economic and Social Affairs, Population Division (2013). World Population prospects: The 2012 Revision, DVD Edition* [Online]. Available: http://esa.un.org/unpd/wpp/Excel-Data/population.htm.
UNITED_NATIONS 2014. Probabilistic Population Projections based on the World Population Prospects: The 2012 Revision. Population Division, DESA. ST/ESA/SER.A/353. .
VAN BRAKEL, M. L. & ROSS, L. G. 2011. Aquaculture development and scenarios of change in fish trade and market access for the poor in Cambodia. *Aquaculture Research,* 42, 931-942.
VAN NIEL, T. G. & MCVICAR, T. R. 2004. Determining temporal windows for crop discrimination with remote sensing: a case study in south-eastern Australia. *Computers and Electronics in Agriculture,* 45, 91-108.
VAN WART, J., VAN BUSSEL, L. G., WOLF, J., LICKER, R., GRASSINI, P., NELSON, A., BOOGAARD, H., GERBER, J., MUELLER, N. D. & CLAESSENS, L. 2013. Use of agro-climatic zones to upscale simulated crop yield potential. *Field crops research,* 143, 44-55.
VERMOTE, E., KOTCHENOVA, S. & RAY, J. 2011. MODIS Surface Reflectance User's Guide, MODIS Land Surface Reflectance Science Computing Facility, 40.
VILLANUEVA, R. R., ARANEDA, M. E., VELA, M. & SEIJO, J. 2013. Selecting stocking density in different climatic seasons: A decision theory approach to intensive aquaculture. *Aquaculture,* 384, 25-34.
VINCENT, K. 2004. Creating an index of social vulnerability to climate change for Africa. *Tyndall Center for Climate Change Research. Working Paper,* 56, 41.
VÖRÖSMARTY, C. J., MCINTYRE, P., GESSNER, M. O., DUDGEON, D., PRUSEVICH, A., GREEN, P., GLIDDEN, S., BUNN, S. E., SULLIVAN, C. A. & LIERMANN, C. R. 2010. Global threats to human water security and river biodiversity. *Nature,* 467, 555-561.
WAHAB, M. A., AHMAD-AL-NAHID, S., AHMED, N., HAQUE, M. M. & KARIM, M. 2012. Current status and prospects of farming the giant river prawn *Macrobrachium rosenbergii* (De Man) in Bangladesh. *Aquaculture Research,* 43, 970-983.
WAN, Z. 2008. New refinements and validation of the MODIS land-surface temperature/emissivity products. *Remote Sensing of Environment,* 112, 59-74.
WANG, Y., COLBY, J. & MULCAHY, K. 2002. An efficient method for mapping flood extent in a coastal floodplain using Landsat TM and DEM data. *International Journal of Remote Sensing,* 23, 3681-3696.
WARDLOW, B. D. & EGBERT, S. L. 2008. Large-area crop mapping using time-series MODIS 250 m NDVI data: An assessment for the US Central Great Plains. *Remote Sensing of Environment,* 112, 1096-1116.

WARDLOW, B. D., EGBERT, S. L. & KASTENS, J. H. 2007. Analysis of time-series MODIS 250 m vegetation index data for crop classification in the US Central Great Plains. *Remote Sensing of Environment,* 108**,** 290-310.

WAX, C. L. & POTE, J. W. 1990. A derived climatology of water temperatures for the Mississippi catfish industry. *Journal of the World Aquaculture Society,* 21**,** 25-34.

WEBB, M., SENIOR, C., SEXTON, D., INGRAM, W., WILLIAMS, K., RINGER, M., MCAVANEY, B., COLMAN, R., SODEN, B. & GUDGEL, R. 2006. On the contribution of local feedback mechanisms to the range of climate sensitivity in two GCM ensembles. *Climate Dynamics,* 27**,** 17-38.

WESTRA, T. & DE WULF, R. Monitoring floodplain dynamics in the Sahel region to detect land degradation processes. Proceedings of the 1st International Conference on Remote Sensing and Geoinformation Processing in the Assessement and Monitoring of Land Degradation and Desertification, 2006. University of Trier.

WHITESIDE, T. G., BOGGS, G. S. & MAIER, S. W. 2011. Comparing object-based and pixel-based classifications for mapping savannas. *International Journal of Applied Earth Observation and Geoinformation,* 13**,** 884-893.

WIGLEY, T. M. L. 2008. *MAGICC/SCENGEN 5.3: User Manual.* [Online]. Available: http://www.cgd.ucar.edu/cas/wigley/magicc/UserMan5.3.v2.pdf.

WIGLEY, T. M. L., CLARKE, L. E., EDMONDS, J. A., JACOBY, H. D., PALTSEV, S., PITCHER, H., REILLY, J. M., RICHELS, R., SAROFIM, M. C. & SMITH, S. J. 2009. Uncertainties in climate stabilization. *Climatic Change,* 97**,** 85-121.

WILLIAMS, K. & WEBB, M. 2009. A quantitative performance assessment of cloud regimes in climate models. *Climate dynamics,* 33**,** 141-157.

WINTER, T., ROSENBERRY, D. & STURROCK, A. 1995. Evaluation of 11 equations for determining evaporation for a small lake in the north central United States. *Water Resources Research,* 31**,** 983-993.

WORKAGEGN, K. B. 2012. Evaluation of growth performance, feed utilization efficiency and survival rate of juvenile Nile tilapia, *Oreochromis niloticus* (Linnaeus, 1758) reared at different water temperature. *International Journal of Aquaculture,* 2.

WORLD_BANK. 2013. *GDP data* [Online]. Available: http://data.worldbank.org/indicator/NY.GDP.MKTP.CD.

WORLD_BANK. 2014a. *GDP data* [Online]. Available: http://data.worldbank.org/indicator/NY.GDP.MKTP.CD [Accessed 23-09-2014.

WORLD_BANK. 2014b. *Population data* [Online]. Available: http://data.worldbank.org/indicator/EN.POP.DNST [Accessed 02-10-2014.

WORLD_BANK. 2014c. *Poverty indicators* [Online]. Available: http://povertydata.worldbank.org/poverty/country/BGD [Accessed 30-09-2014.

WUNDERLICH, W. O. 1972. *Heat and mass transfer between a water surface and the atmosphere*, Tennessee Valley Authority, Office of Natural Resources and Economic Development, Division of Air and Water Resources, Water Systems Development Branch.

XIAO, X., BOLES, S., FROLKING, S., LI, C., BABU, J. Y., SALAS, W. & MOORE III, B. 2006. Mapping paddy rice agriculture in South and Southeast Asia using multi-temporal MODIS images. *Remote Sensing of Environment,* 100**,** 95-113.

XIE, S., ZHENG, K., CHEN, J., ZHANG, Z., ZHU, X. & YANG, Y. 2011. Effect of water temperature on energy budget of Nile tilapia, *Oreochromis niloticus*. *Aquaculture Nutrition,* 17**,** e683-e690.

YOO, K. & BOYD, C. 1994. *Hydrology and water supply for aquaculture*, Chapman and Hall, New York, New York, USA.

YU, L., WANG, J. & GONG, P. 2013. Improving 30 m global land-cover map FROM-GLC with time series MODIS and auxiliary data sets: a segmentation-based approach. *International Journal of Remote Sensing,* 34**,** 5851-5867.

YU, L., WANG, J., LI, X., LI, C., ZHAO, Y. & GONG, P. 2014. A multi-resolution global land cover dataset through multisource data aggregation. *Science China Earth Sciences,* 57**,** 2317-2329.

YU, W. H., ALAM, M., HASSAN, A., KHAN, A. S., RUANE, A. C., ROSENZWEIG, C., MAJOR, D. C. & THURLOW, J. 2010. *Climate change risks and food security in Bangladesh,* London, UK., Earthscan.

ZELEDON, E. B. & KELLY, N. M. 2009. Understanding large-scale deforestation in southern Jinotega, Nicaragua from 1978 to 1999 through the examination of changes in land use and land cover. *Journal of Environmental Management,* 90**,** 2866-2872.

ZHANG, C., LI, W. & TRAVIS, D. 2007. Gaps-fill of SLC-off Landsat ETM+ satellite image using a geostatistical approach. *International Journal of Remote Sensing,* 28**,** 5103-5122.

ZHANG, X., SUN, R., ZHANG, B. & TONG, Q. 2008. Land cover classification of the North China Plain using MODIS_EVI time series. *ISPRS Journal of Photogrammetry and Remote Sensing,* 63**,** 476-484.

ZHU, X., CHEN, J., GAO, F., CHEN, X. & MASEK, J. G. 2010. An enhanced spatial and temporal adaptive reflectance fusion model for complex heterogeneous regions. *Remote Sensing of Environment,* 114**,** 2610-2623.

ZHU, X., GAO, F., LIU, D. & CHEN, J. 2012. A modified neighborhood similar pixel interpolator approach for removing thick clouds in Landsat images. *Geoscience and Remote Sensing Letters, IEEE,* 9**,** 521-525.

ZOMER, R. J. 2007. *Trees and water: smallholder agroforestry on irrigated lands in Northern India*, IWMI.

ZOMER, R. J., TRABUCCO, A., BOSSIO, D. A. & VERCHOT, L. V. 2008. Climate change mitigation: A spatial analysis of global land suitability for clean development mechanism afforestation and reforestation. *Agriculture, ecosystems & environment,* 126**,** 67-80.

8 APPENDIX 1

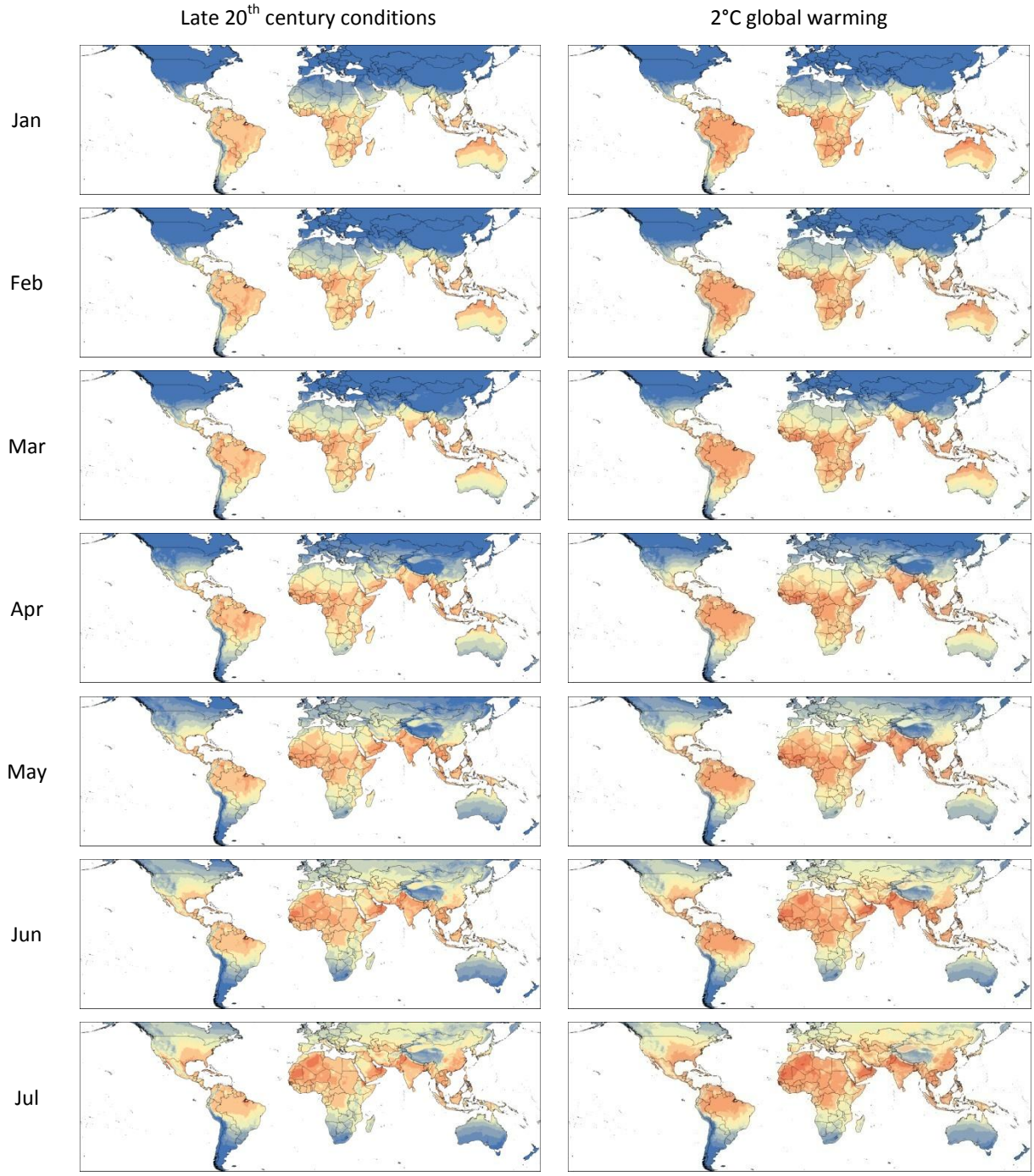
Late 20th century conditions
2°C global warming
Jan
Feb
Mar
Apr
May
Jun
Jul

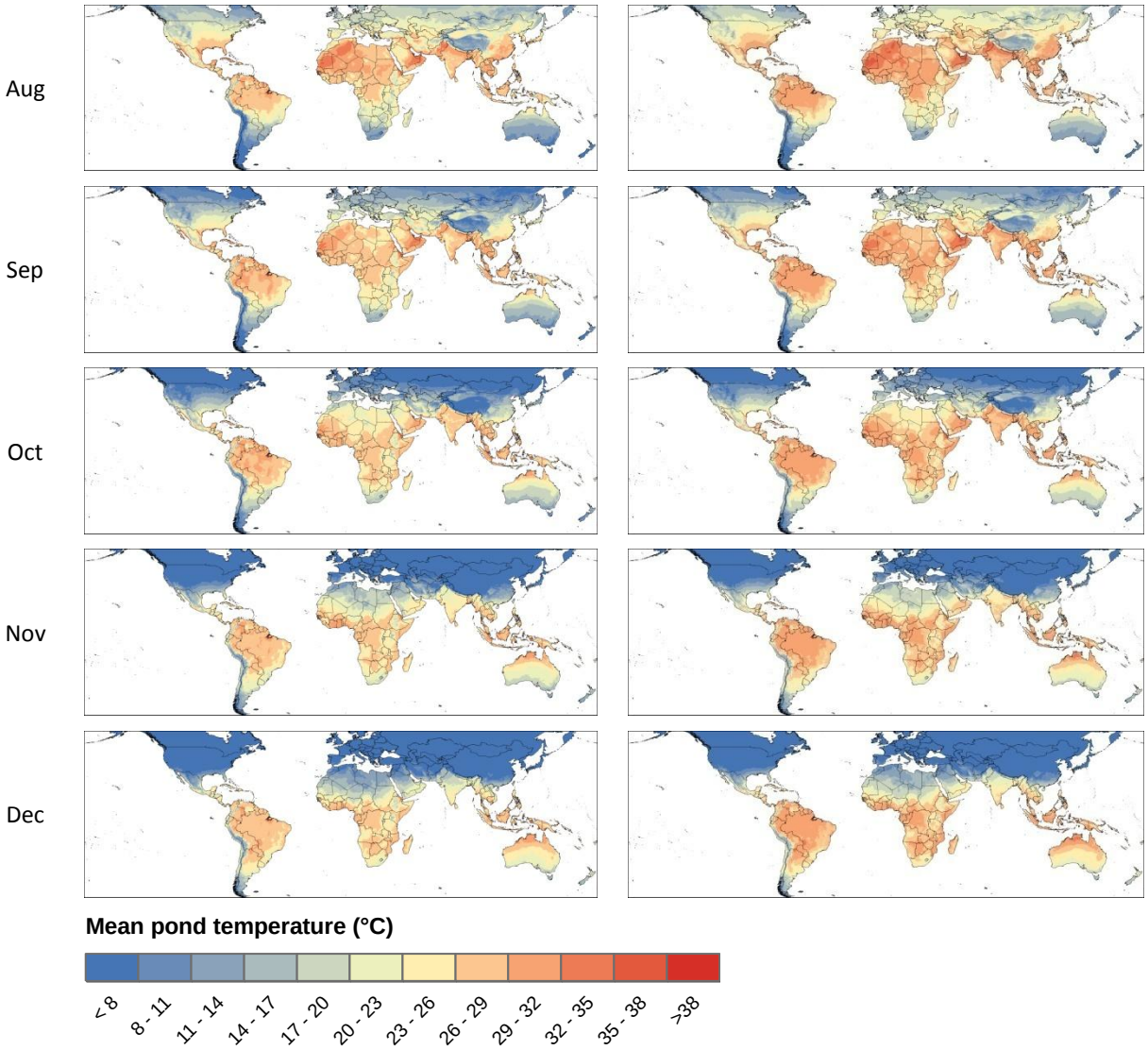

Figure 8-1: Modelled mean pond temperature under late 20th century conditions and for a 2°C warmer world.

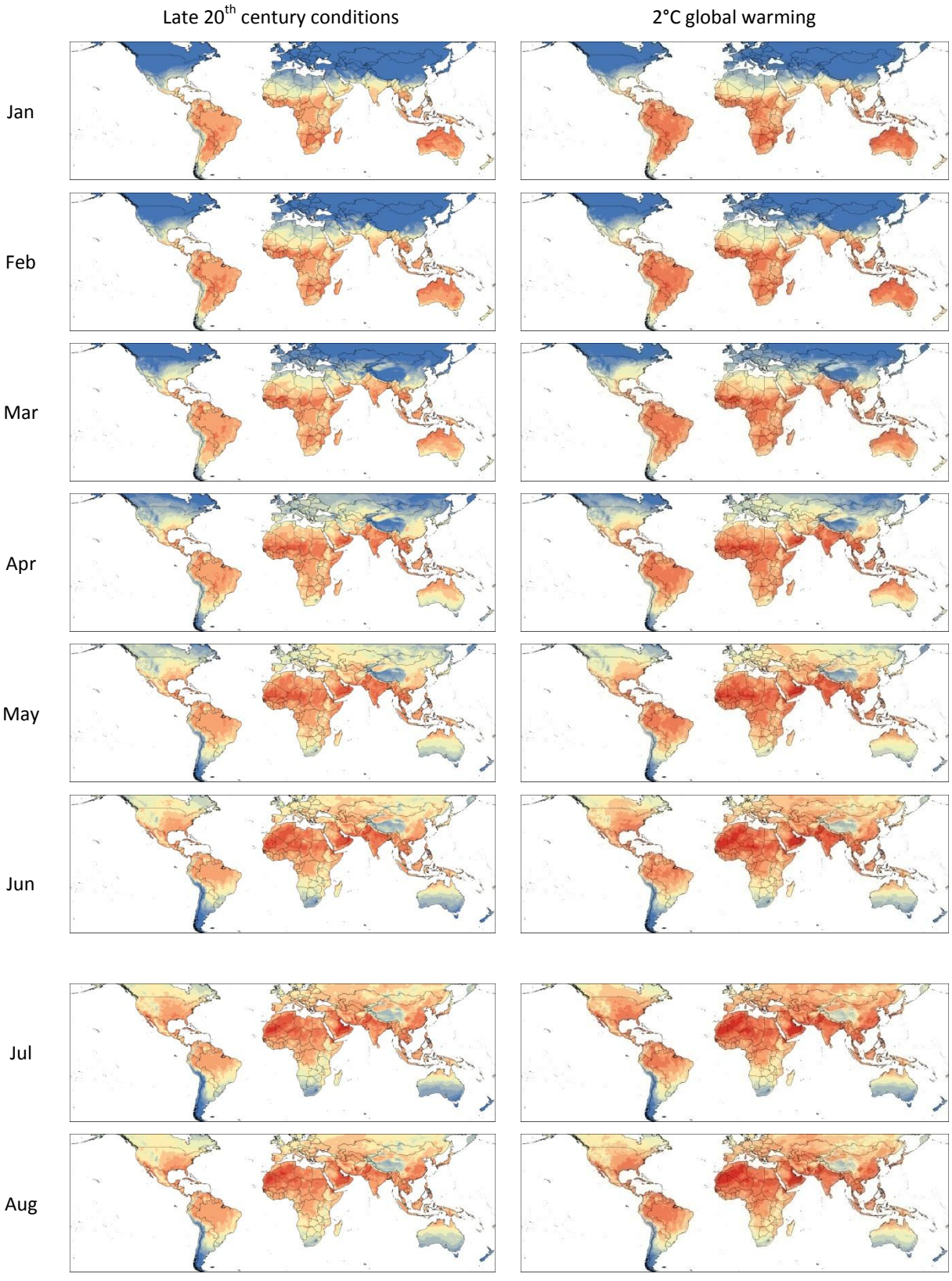
Late 20th century conditions
2°C global warming
Jan
Feb
Mar
Apr
May
Jun
Jul
Aug

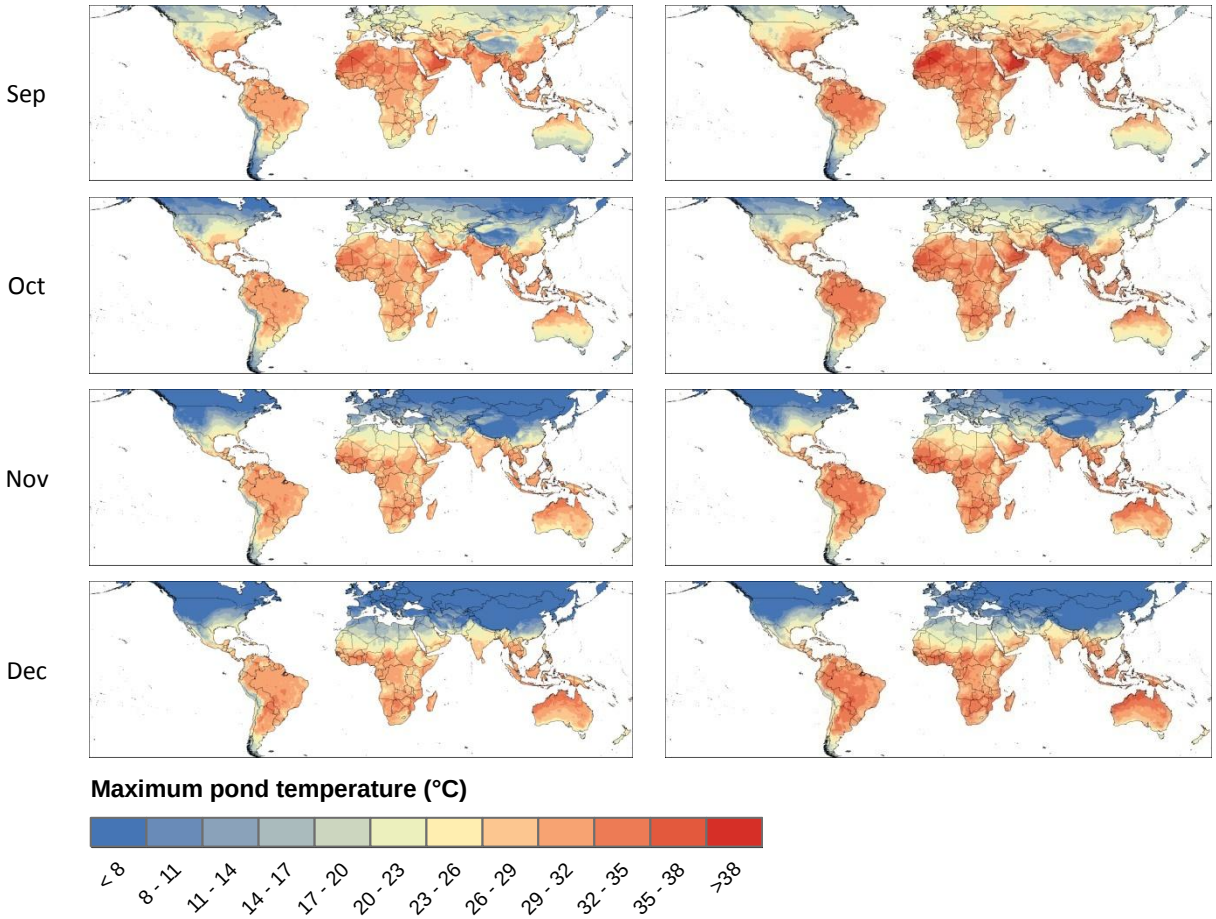

Figure 8-2: Modelled maximum pond temperature under late 20th century conditions and for a 2°C warmer world.

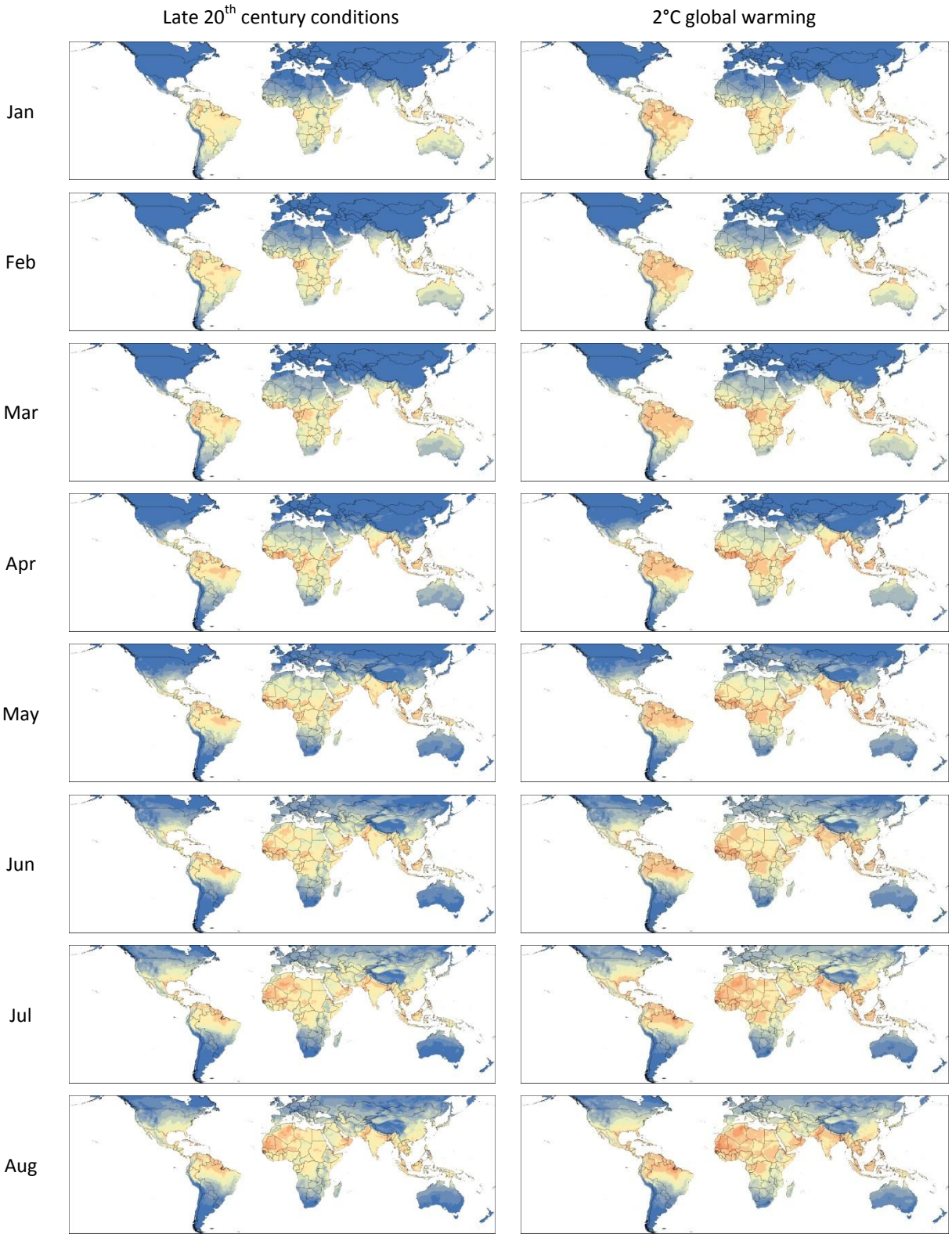
Late 20th century conditions
2°C global warming
Jan
Feb
Mar
Apr
May
Jun
Jul
Aug

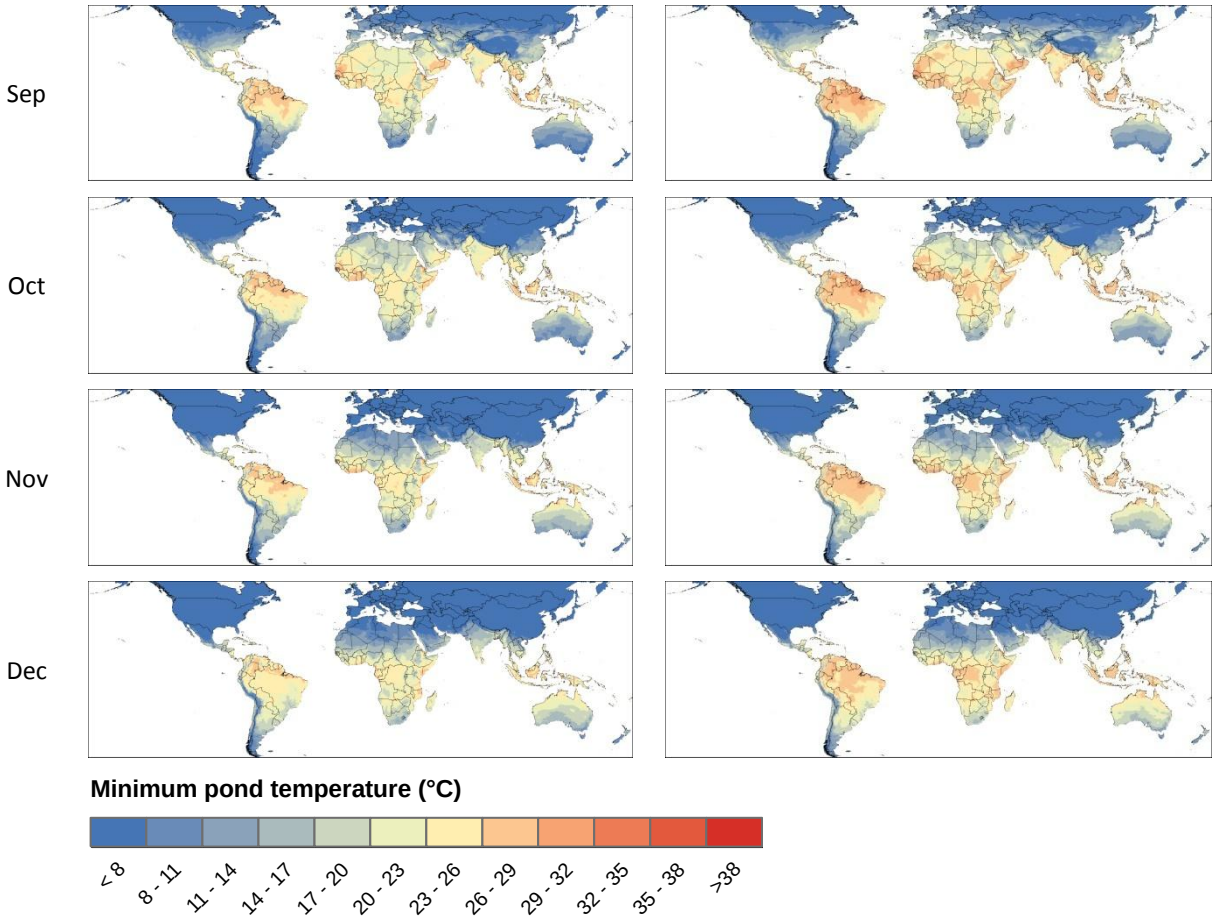

Figure 8-3: Modelled minimum pond temperature under late 20th century conditions and for a 2°C warmer world.

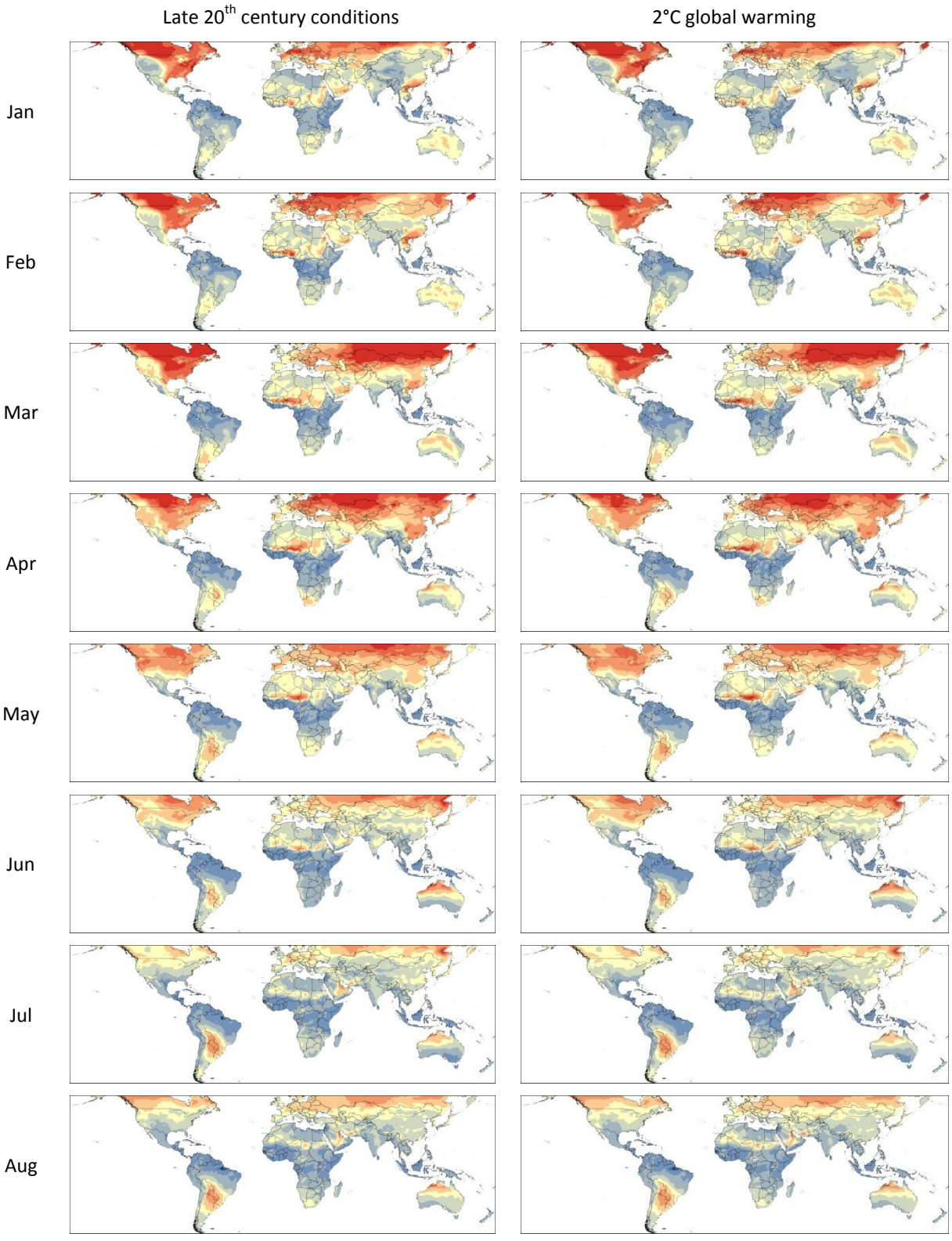
Late 20th century conditions
2°C global warming
Jan
Feb
Mar
Apr
May
Jun
Jul
Aug

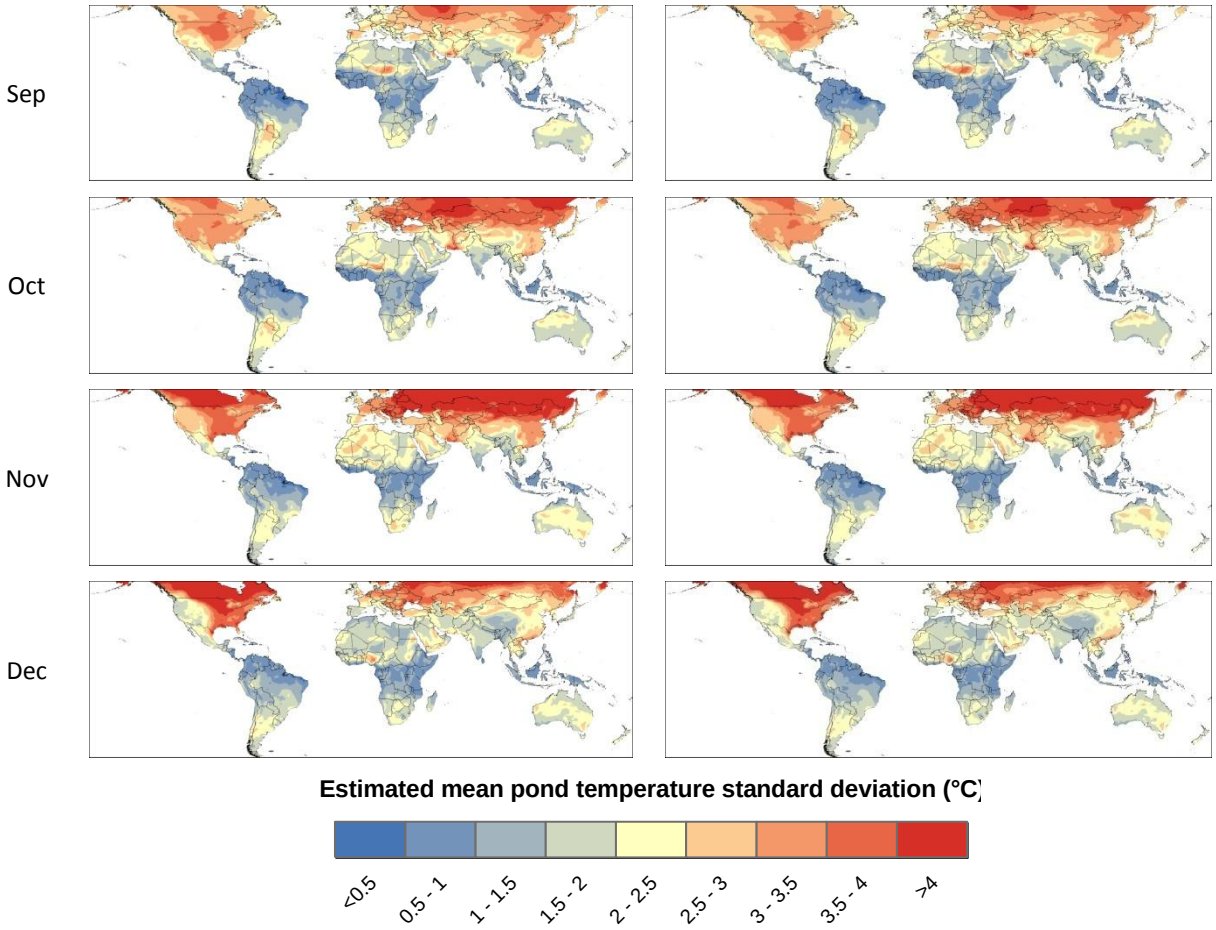

Figure 8-4: Modelled standard deviation of pond temperature (°C) under late 20th century conditions and for a 2°C warmer world.

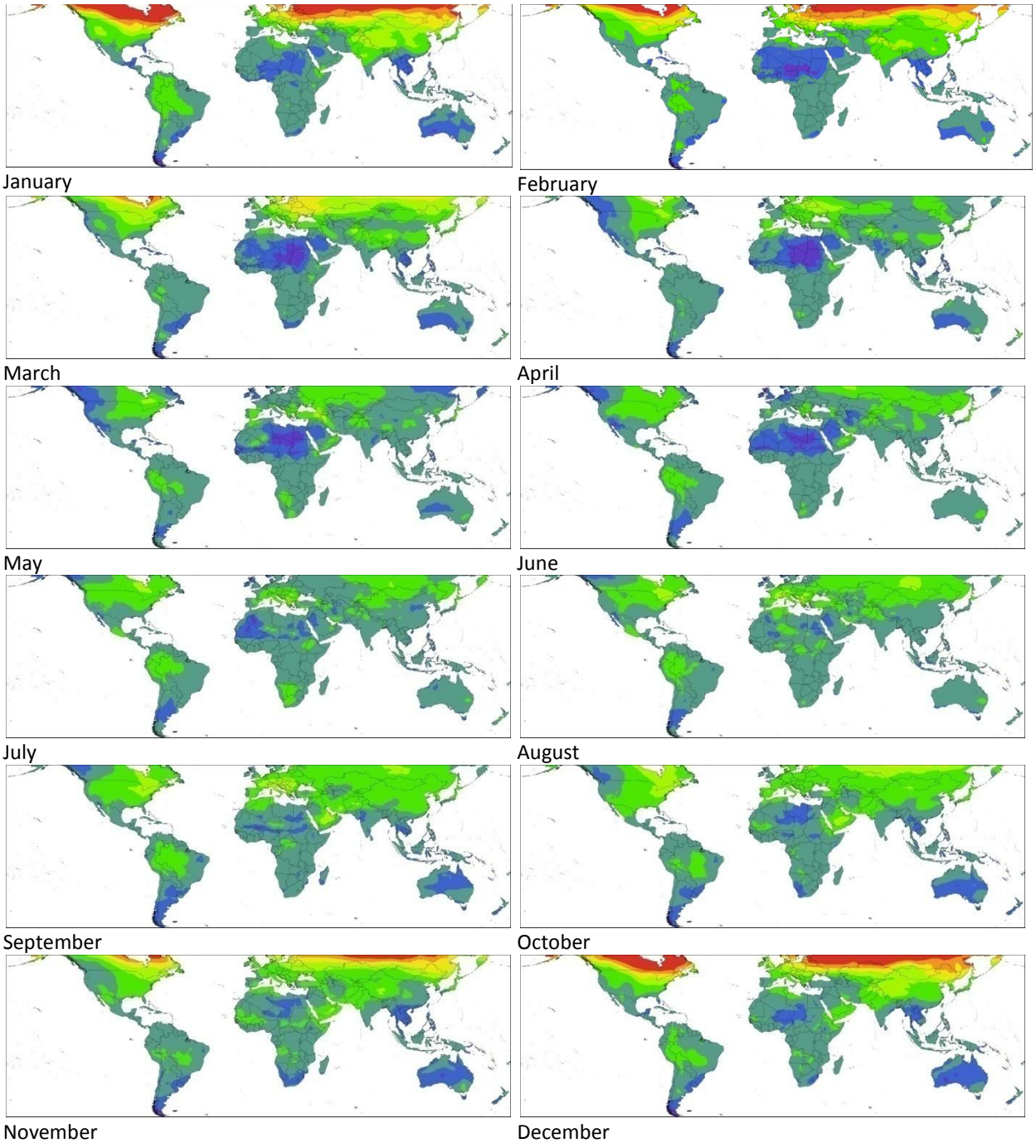

Figure 8-5: Modelled pond temperature difference under late 20th century and 2°C Global warming.

9 APPENDIX 2

Table 9-1: Error matrix for accuracy assessment of Landsat ETM+ data classified using the adapted Sakamoto method. Accuracy assessed against GCPs excluding areas of floating vegetation.

	Land	Mixed	Water	Total	ErrorC	KIA
Land	654	14	0	668	0.0210	0.9494
Mixed	2	110	0	112	0.0179	0.9800
Water	77	9	325	411	0.2092	0.7291
Total	733	133	325	1191		
ErrorO	0.1078	0.1729	0.0000			
KIA	0.7546	0.8091	1.0000			
Total Error (95% Confidence Interval) = 0.0856 (0.0159) Overall Kappa = 0.8443						

Table 9-2: Error matrix for accuracy assessment of Landsat ETM+ data classified using the adapted Sakamoto method. Accuracy assessed against GCPs including areas of floating vegetation.

	Land	Mixed	Water	Total	ErrorC	KIA
Land	654	120	0	774	0.1550	0.6435
Mixed	2	110	0	112	0.0179	0.9781
Water	77	9	325	411	0.2092	0.7208
Total	733	239	325	1297		
ErrorO	0.1078	0.5397	0.0000			
KIA	0.7327	0.4092	1.0000			
Total Error (95% Confidence Interval) = 0.1604 (0.0200) Overall Kappa = 0.7174						

Table 9-3: Error matrix for accuracy assessment of Landsat ETM+ data classified using the adapted Sakamoto method. Accuracy assessed against GCPs excluding areas of floating vegetation and urban areas.

	Land	Mixed	Water	Total	ErrorC	KIA
Land	450	14	0	464	0.0302	0.9400
Mixed	2	110	0	112	0.0179	0.9791
Water	1	9	325	335	0.0299	0.9536
Total	453	133	325	911		
ErrorO	0.0066	0.1729	0.0000			
KIA	0.9865	0.8028	1.0000			
Total Error (95% Confidence Interval) = 0.0285 (0.0108) Overall Kappa = 0.9522						

Table 9-4: Error matrix for accuracy assessment of Landsat ETM+ data classified using the ISOCLUST routine. Accuracy assessed against GCPs excluding areas of floating vegetation.

	Land	Mixed	Water	Total	ErrorC	KIA
Land	732	13	0	745	0.0174	0.9546
Mixed	1	111	19	131	0.1527	0.8281
Water	0	9	306	306	0.0286	0.9607
Total	733	133	325	1191		
ErrorO	0.0014	0.1654	0.0585			
KIA	0.9964	0.8141	0.9205			
Total Error (95% Confidence Interval) = 0.0353 (0.0105) Overall Kappa = 0.9335						

Table 9-5: Error matrix for accuracy assessment of Landsat ETM+ data classified using the ISOCLUST routine. Accuracy assessed against GCPs including areas of floating vegetation.

	Land	Mixed	Water	Total	ErrorC	KIA
Land	714	19	0	733	0.0259	0.9404
Mixed	19	211	19	249	0.1526	0.8129
Water	0	9	306	315	0.0286	0.9619
Total	733	239	325	1297		
ErrorO	0.0259	0.1172	0.0585			
KIA	0.9404	0.8550	0.9228			
Total Error (95% Confidence Interval) = 0.0509 (0.0120) Overall Kappa = 0.9129						

Table 9-6: Error matrix for accuracy assessment of Landsat ETM+ data classified using a single NDSI from bands 2 and 7. Accuracy assessed against GCPs excluding areas of floating vegetation.

	Land	Mixed	Water	Total	ErrorC	KIA
Land	730	3	0	733	0.0041	0.9894
Mixed	3	123	6	132	0.0682	0.9232
Water	0	7	319	326	0.0215	0.9705
Total	733	133	325	1191		
ErrorO	0.0041	0.0752	0.0185			
KIA	0.9894	0.9154	0.9746			
Total Error (95% Confidence Interval) = 0.0160 (0.0071) Overall Kappa = 0.9701						

Table 9-7: Error matrix for accuracy assessment of Landsat ETM+ data classified using a single NDSI from bands 2 and 7. Accuracy assessed against GCPs including areas of floating vegetation.

	Land	Mixed	Water	Total	ErrorC	KIA
Land	730	14	0	744	0.0188	0.9567
Mixed	3	218	6	227	0.0396	0.9514
Water	0	7	319	326	0.0215	0.9713
Total	733	239	325	1297		
ErrorO	0.0041	0.0879	0.0185			
KIA	0.9904	0.8935	0.9753			
Total Error (95% Confidence Interval) = 0.0231 (0.0082) Overall Kappa = 0.9602						

Table 9-8: Error matrix for accuracy assessment of Landsat ETM+ data classified using the two stage process with NDSIs from from bands 2 and 7, and 3 and 4. Accuracy assessed against GCPs excluding areas of floating vegetation.

	Land	Mixed	Water	Total	ErrorC	KIA
Land	730	3	0	733	0.0041	0.9894
Mixed	3	128	0	131	0.0229	0.9742
Water	0	2	325	327	0.0061	0.9916
Total	733	133	325	1191		
ErrorO	0.0041	0.0376	0.0000			
KIA	0.9894	0.9578	1.0000			
Total Error (95% Confidence Interval) = 0.0067 (0.0046) Overall Kappa = 0.9874						

Table 9-9: Error matrix for accuracy assessment of Landsat ETM+ data classified using the two stage process with NDSIs from from bands 2 and 7, and 3 and 4. Accuracy assessed against GCPs including areas of floating vegetation.

	Land	Mixed	Water	Total	ErrorC	KIA
Land	730	14	0	744	0.0188	0.9567
Mixed	3	223	0	226	0.0133	0.9837
Water	0	2	325	327	0.0061	0.9918
Total	733	239	325	1297		
ErrorO	0.0041	0.0669	0.0000			
KIA	0.9904	0.9189	1.0000			
Total Error (95% Confidence Interval) = 0.0146 (0.0065) Overall Kappa = 0.9748						

Table 9-10: Error matrix for accuracy assessment of land, mixed, water map created at approximately 500m resolution using the method adapted from Sakamoto et al. (2007) and data from MOD09A1. Accuracy assessed against GCPs designated for accuracy assessment.

	Land	Mixed	Water	Total	ErrorC	KIA
Land	700	56	47	803	0.1283	0.6664
Mixed	7	75	126	208	0.6394	0.2802
Water	26	2	152	180	0.1556	0.7861
Total	733	133	325			
ErrorO	0.0450	0.4361	0.5323			
KIA	0.8618	0.4716	0.3729			
Total Error (95% Confidence Interval) = 0.2217 (0.0236) Overall Kappa = 0.5772						

Table 9-11: Error matrix for accuracy assessment of land, mixed, water map created at approximately 500m resolution using the method adapted from Sakamoto et al. (2007) and data from MOD09A1. Accuracy assessed against the most accurate map obtained from classification of Landsat ETM+ data (two step process with NDSIs of bands 2 and 7, and 3 and 4).

	Land	Mixed	Water	Total	ErrorC	KIA
Land	77916142	8929845	1700386	88546373	0.1201	0.5244
Mixed	4862957	5054315	2382423	12299695	0.5891	0.3213
Water	1581513	923375	9494470	11999358	0.2088	0.7627
Total	84360612	14907535	13577279	112845426		
ErrorO	0.0764	0.6610	0.3007			
KIA	0.6452	0.2582	0.6635			
Total Error (95% Confidence Interval) = 0.1806 (0.0001) Overall Kappa = 0.5324						

Table 9-12: Error matrix for accuracy assessment of land, mixed, water map created at approximately 250m resolution using the method adapted from Sakamoto et al. (2007) and data from MOD09A1 (bands 3 and 6), and MOD09Q1 (bands 1 and 2). Accuracy assessed against GCPs designated for accuracy assessment.

	Land	Mixed	Water	Total	ErrorC	KIA
Land	689	79	79	847	0.1865	0.5149
Mixed	26	52	51	129	0.5969	0.3281
Water	18	2	195	215	0.0930	0.8721
Total	733	133	325			
ErrorO	0.0600	0.6090	0.4000			
KIA	0.7922	0.3170	0.5119			
Total Error (95% Confidence Interval) = 0.2141 (0.0233) Overall Kappa = 0.5726						

Table 9-13: Error matrix for accuracy assessment of land, mixed, water map created at approximately 250m resolution using the method adapted from Sakamoto et al. (2007) and data from MOD09A1 (bands 3 and 6), and MOD09Q1 (bands 1 and 2). Accuracy assessed against the most accurate map obtained from classification of Landsat ETM+ data (two step process with NDSIs of bands 2 and 7, and 3 and 4).

	Land	Mixed	Water	Total	ErrorC	KIA
Land	78912940	9573037	1653986	90139963	0.1246	0.5066
Mixed	4038459	4389319	1504791	9932569	0.5581	0.3570
Water	1409213	945179	10418502	12772894	0.1843	0.7905
Total	84360612	14907535	13577279	112845426		
ErrorO	0.0646	0.7056	0.2327			
KIA	0.6791	0.2263	0.7377			
Total Error (95% Confidence Interval) = 0.1695 (0.0001) Overall Kappa = 0.5512						

Table 9-14: Error matrix for accuracy assessment of land, mixed, water map created at approximately 500m resolution through the reclassification of a single NDSI using bands 4 and 7 from MOD09A1. Accuracy assessed against GCPs designated for accuracy assessment.

	Land	Mixed	Water	Total	ErrorC	KIA
Land	723	71	99	893	0.1904	0.5050
Mixed	10	50	130	163	0.6933	0.2196
Water	0	12	123	135	0.0889	0.8778
Total	733	133	325			
ErrorO	0.0136	0.6241	0.6215			
KIA	0.9455	0.2770	0.2990			
Total Error (95% Confidence Interval) = 0.2477 (0.0245) Overall Kappa = 0.4969						

Table 9-15: Error matrix for accuracy assessment of land, mixed, water map created at approximately 500m resolution through the reclassification of a single NDSI using bands 4 and 7 from MOD09A1. Accuracy assessed against the most accurate map obtained from classification of Landsat ETM+ data (two step process with NDSIs of bands 2 and 7, and 3 and 4).

	Land	Mixed	Water	Total	ErrorC	KIA
Land	78106230	7369018	2017282	87492530	0.1073	0.5750
Mixed	5324852	6045154	2751392	14121398	0.5719	0.3410
Water	929530	1493363	8808605	11231498	0.2157	0.7548
Total	84360612	14907535	13577279	112845426		
ErrorO	0.0741	0.5945	0.3512			
KIA	0.6700	0.3205	0.6100			
Total Error (95% Confidence Interval) = 0.1762 (0.0001) Overall Kappa = 0.5503						

Table 9-16: Error matrix for accuracy assessment of land, mixed, water map created at approximately 250m resolution based on a two stage reclassification using NDSIs from bands 4 and 7 (MOD09A1), and 1 and 2 (MOD09Q1). Accuracy assessed against GCPs designated for accuracy assessment.

	Land	Mixed	Water	Total	ErrorC	KIA
	723	71	99	893	0.1904	0.5050
	8	60	46	114	0.4737	0.4668
	2	2	180	184	0.0217	0.9701
Total	733	133	325	1191		
ErrorO	0.0136	0.5489	0.4462			
KIA	0.9455	0.3930	0.4723			
Total Error (95% Confidence Interval) = 0.1914 (0.0223) Overall Kappa = 0.6059						

Table 9-17: Error matrix for accuracy assessment of land, mixed, water map created at approximately 250m resolution based on a two stage reclassification using NDSIs from bands 4 and 7 (MOD09A1), and 1 and 2 (MOD09Q1). Accuracy assessed against the most accurate map obtained from classification of Landsat ETM+ data (two step process with NDSIs of bands 2 and 7, and 3 and 4).

	Land	Mixed	Water	Total	ErrorC	KIA
Land	78106230	7369018	2017282	87492530	0.1073	0.5750
Mixed	4779117	6238354	1113717	12131188	0.4858	0.4403
Water	1475265	1300163	10446280	13221708	0.2099	0.7614
Total	84360612	14907535	13577279	112845426		
ErrorO	0.0741	0.5815	0.2306			
KIA	0.6700	0.3484	0.7388			
Total Error (95% Confidence Interval) = 0.1600 (0.0001) Overall Kappa = 0.5919						

10 APPENDIX 3

Table 10-1: Error matrix for accuracy assessment of the decision tree classification. Accuracy assessed against GCPs produced using a stratified random sampling approach in association with careful inspection of ETM+ composites and high resolution true colour imagery.

	Water	Bare	Trees	Crops	Mixed	Urban	Total	ErrorC	KIA
Water	117	5	0	0	9	0	131	0.1069	0.8718
Bare	0	75	2	8	4	1	90	0.1667	0.8034
Trees	0	0	100	22	0	0	122	0.1803	0.7774
Crops	0	1	23	116	1	8	149	0.2215	0.7158
Mixed	2	4	11	12	127	2	158	0.1962	0.7553
Urban	0	24	0	0	1	41	66	0.3788	0.5915
Total	119	109	137	158	142	52	716		
ErrorO	0.0168	0.3119	0.2647	0.2658	0.1056	0.2115			
KIA	0.9794	0.6432	0.6809	0.6643	0.8645	0.7670			
Total Error (95% Confidence Interval) = 0.1955 (0.0291)									
Overall Kappa = 0.7620									

Table 10-2: Error matrix for accuracy assessment of the MLP classification. Accuracy assessed against GCPs produced using a stratified random sampling approach in association with careful inspection of ETM+ composites and high resolution true colour imagery.

	Water	Bare	Trees	Crops	Mixed	Urban	Total	ErrorC	KIA
Water	115	3	0	0	6	1	125	0.0800	0.9041
Bare	2	76	3	14	8	5	108	0.2963	0.6505
Trees	0	0	93	17	0	0	110	0.1545	0.8092
Crops	0	7	37	115	1	10	170	0.3235	0.5849
Mixed	2	2	3	12	128	2	149	0.1429	0.8218
Urban	0	21	0	0	1	34	56	0.3929	0.5764
Total	119	109	137	158	142	52	716		
ErrorO	0.0336	0.3028	0.3162	0.2722	0.1127	0.3462			
KIA	0.9593	0.6435	0.6264	0.6431	0.8582	0.6245			
Total Error (95% Confidence Interval) = 0.2193 (0.0303)									
Overall Kappa = 0.7326									

Table 10-3: Error matrix for accuracy assessment of the ARTMAP classification. Accuracy assessed against GCPs produced using a stratified random sampling approach in association with careful inspection of ETM+ composites and high resolution true colour imagery.

	Water	Bare	Trees	Crops	Mixed	Urban	Total	ErrorC	KIA
Water	105	1	0	0	2	0	108	0.0278	0.9667
Bare	2	62	4	21	5	7	101	0.3861	0.5445
Trees	0	0	93	18	0	0	111	0.1622	0.7998
Crops	0	7	38	107	4	7	163	0.3436	0.5592
Mixed	11	1	1	12	129	1	155	0.1677	0.7908
Urban	1	38	0	0	2	37	78	0.5256	0.4332
Total	119	109	137	158	142	52	716		
ErrorO	0.1176	0.4312	0.3162	0.3228	0.0915	0.2885			
KIA	0.8615	0.4980	0.6258	0.5821	0.8832	0.6763			
Total Error (95% Confidence Interval) = 0.2556 (0.0320)									
Overall Kappa = 0.6894									

Table 10-4: Error matrix for accuracy assessment of the KNN classification. Accuracy assessed against GCPs produced using a stratified random sampling approach in association with careful inspection of ETM+ composites and high resolution true colour imagery.

	Water	Bare	Trees	Crops	Mixed	Urban	Total	ErrorC	KIA
Water	106	1	0	0	3	0	110	0.0364	0.9564
Bare	0	46	0	12	1	1	60	0.2333	0.7248
Trees	0	0	97	33	0	0	130	0.2538	0.6866
Crops	0	10	38	106	8	10	172	0.3837	0.5076
Mixed	10	2	1	7	125	1	146	0.1438	0.8206
Urban	3	50	0	0	5	40	98	0.5918	0.3618
Total	119	109	137	158	142	52	716		
ErrorO	0.1092	0.5780	0.2868	0.3291	0.1197	0.2308			
KIA	0.8709	0.3692	0.6496	0.5668	0.8496	0.7326			
Total Error (95% Confidence Interval) = 0.2737 (0.0327)									
Overall Kappa = 0.6677									

Table 10-5: Error matrix for accuracy assessment of the MAXLIKE classification. Accuracy assessed against GCPs produced using a stratified random sampling approach in association with careful inspection of ETM+ composites and high resolution true colour imagery.

	Water	Bare	Trees	Crops	Mixed	Urban	Total	ErrorC	KIA
Water	92	0	0	0	2	0	94	0.0213	0.9745
Bare	12	97	3	26	11	19	168	0.4226	0.5015
Trees	0	0	69	8	0	0	77	0.1039	0.8717
Crops	0	3	60	106	4	5	178	0.4045	0.4810
Mixed	15	1	4	18	125	0	163	0.2331	0.7092
Urban	0	8	0	0	0	28	36	0.2222	0.7604
Total	119	109	137	158	142	52	716		
ErrorO	0.2269	0.1101	0.4926	0.3291	0.1197	0.4615			
KIA	0.7388	0.8562	0.4480	0.5620	0.8450	0.5140			
Total Error (95% Confidence Interval) = 0.2779 (0.0328-) Overall Kappa = 0.6604									

Table 10-6: Error matrix for accuracy assessment of the LDA classification. Accuracy assessed against GCPs produced using a stratified random sampling approach in association with careful inspection of ETM+ composites and high resolution true colour imagery.

	Water	Bare	Trees	Crops	Mixed	Urban	Total	ErrorC	KIA
Water	119	8	0	0	27	1	155	0.2323	0.7214
Bare	0	38	1	8	1	0	48	0.2083	0.7543
Trees	0	0	102	32	0	0	134	0.2388	0.7052
Crops	0	7	31	105	3	8	154	0.3182	0.5917
Mixed	0	3	2	31	108	4	148	0.1496	0.8134
Urban	0	53	0	2	2	39	96	0.6020	0.3508
Total	119	109	137	158	142	52	716		
ErrorO	0.0000	0.6514	0.2500	0.3354	0.2394	0.2500			
KIA	1.0000	0.3018	0.6924	0.5726	0.7089	0.7104			
Total Error (95% Confidence Interval) = 0.2863 (0.0331) Overall Kappa = 0.6532									

Table 10-7: Error matrix for accuracy assessment of the SOM classification. Accuracy assessed against GCPs produced using a stratified random sampling approach in association with careful inspection of ETM+ composites and high resolution true colour imagery.

	Water	Bare	Trees	Crops	Mixed	Urban	Total	ErrorC	KIA
Water	100	1	0	0	9	0	110	0.0909	0.8910
Bare	0	50	2	21	1	6	80	0.3750	0.5577
Trees	0	0	95	26	0	0	121	0.2339	0.7113
Crops	0	4	33	97	2	6	142	0.3169	0.5934
Mixed	17	4	4	10	126	2	163	0.2270	0.7169
Urban	2	50	2	1	4	38	97	0.6082	0.3441
Total	119	109	137	158	142	52	716		
ErrorO	0.1597	0.5413	0.3015	0.3861	0.1127	0.2692			
KIA	0.8114	0.3906	0.6354	0.5184	0.8541	0.6886			
Total Error (95% Confidence Interval) = 0.2933 (0.0333) Overall Kappa = 0.6448									

Table 10-8: Error matrix for accuracy assessment of the MINDIST classification. Accuracy assessed against GCPs produced using a stratified random sampling approach in association with careful inspection of ETM+ composites and high resolution true colour imagery.

	Water	Bare	Trees	Crops	Mixed	Urban	Total	ErrorC	KIA
Water	112	1	0	0	17	0	130	0.1385	0.8339
Bare	0	45	1	15	1	1	63	0.2857	0.6630
Trees	0	0	94	40	0	0	134	0.2985	0.6315
Crops	0	10	40	95	7	9	161	0.4099	0.4740
Mixed	4	8	1	8	116	2	139	0.1655	0.7936
Urban	3	45	0	0	1	40	89	0.5506	0.4063
Total	119	109	137	158	142	52	716		
ErrorO	0.0588	0.5872	0.3088	0.3987	0.1831	0.2308			
KIA	0.9281	0.3562	0.6201	0.4856	0.7728	0.7365			
Total Error (95% Confidence Interval) = 0.2989 (0.0335) Overall Kappa = 0.6372									

Table 10-9: Error matrix for accuracy assessment of the CTA classification. Accuracy assessed against GCPs produced using a stratified random sampling approach in association with careful inspection of ETM+ composites and high resolution true colour imagery.

	Water	Bare	Trees	Crops	Mixed	Urban	Total	ErrorC	KIA
Water	96	0	0	0	5	0	101	0.0495	0.9406
Bare	3	73	1	18	6	16	117	0.3761	0.5564
Trees	0	0	62	15	0	0	77	0.1948	0.7595
Crops	0	8	62	113	1	7	191	0.4084	0.4760
Mixed	20	8	11	12	130	3	184	0.2935	0.6339
Urban	0	20	0	0	0	26	46	0.4348	0.5312
Total	119	109	137	158	142	52	716		
ErrorO	0.1933	0.3303	0.5441	0.2848	0.0845	0.5000			
KIA	0.7750	0.6052	0.3903	0.6116	0.8863	0.4657			
Total Error (95% Confidence Interval) = 0.3017 (0.0336) Overall Kappa = 0.6306									